



University of HUDDERSFIELD

University of Huddersfield Repository

Chadha, Marcus J.

Novel Techniques for the Characterisation of Exopolysaccharides Secreted by Lactic Acid Bacteria

Original Citation

Chadha, Marcus J. (2009) Novel Techniques for the Characterisation of Exopolysaccharides Secreted by Lactic Acid Bacteria. Doctoral thesis, University of Huddersfield.

This version is available at <http://eprints.hud.ac.uk/id/eprint/8749/>

The University Repository is a digital collection of the research output of the University, available on Open Access. Copyright and Moral Rights for the items on this site are retained by the individual author and/or other copyright owners. Users may access full items free of charge; copies of full text items generally can be reproduced, displayed or performed and given to third parties in any format or medium for personal research or study, educational or not-for-profit purposes without prior permission or charge, provided:

- The authors, title and full bibliographic details is credited in any copy;
- A hyperlink and/or URL is included for the original metadata page; and
- The content is not changed in any way.

For more information, including our policy and submission procedure, please contact the Repository Team at: E.mailbox@hud.ac.uk.

<http://eprints.hud.ac.uk/>

Novel Techniques for
the Characterisation of
Exopolysaccharides Secreted by
Lactic Acid Bacteria

Marcus Chadha BSc (Hons) MSc



University of
HUDDERSFIELD

A thesis submitted to the University of Huddersfield in partial fulfilment of the
requirements for the degree of Doctor of Philosophy

Department of Chemical and Biological Sciences
The University of Huddersfield

September 2009

ABSTRACT

This project investigated the structures and physical characteristics of exopolysaccharides (EPSs) secreted by lactic acid bacteria.

The structure of a novel exopolysaccharide (EPS) produced by *Lactobacillus acidophilus* 5e2 has been characterised. Analysis of the anomeric region of the ¹H-NMR showed that the repeating oligosaccharide contained seven monosaccharides. GC-MS showed the structure to consist of D-glucose, D-galactose and D-N-acetyl-glucosamine in a molar ratio of 3:3:1. The linkage analysis showed that there were two terminal, three di-linked and two tri-linked monosaccharides, and in collaboration with data generated from a series of 2D-NMR experiments, an overall structure was determined.

The weight-average molecular weight (M_w) of the EPS secreted by *Lactobacillus acidophilus* 5e2 when grown in skimmed milk was monitored during extended fermentation times. During the exponential growth phase, the increase in M_w closely followed the increase in yield of EPS. Under the fermentation conditions applied in this study, few if any new polysaccharide chains were formed during this growth phase despite a twenty five-fold increase in the cell count; almost the entire increase in yield can be accounted for by an increase in chain length. These results suggested that synthesis of new EPS chains is switched off during the exponential and stationary phase of fermentation. The increase in yield observed in this period is a consequence of the bacteria's ability to extend existing chains right up to the mid-stationary phase. These results raise questions about the factors that control EPS production and chain length.

Depolymerisation techniques have been shown to reduce the M_w of the polysaccharide in a controlled manner. The ¹H-NMR results have shown that the physical methods, constant pressure and ultrasonic disruption break the EPS randomly through the repeating oligosaccharide unit; polydispersity data suggests that the breakages were occurring mid-chain. A change to the peaks in the anomeric region of the ¹H-NMR spectrum showed that depolymerisation, by acid hydrolysis, was chemically modifying the EPS structure. The approximate intrinsic viscosities of the EPS produced by *Lactobacillus acidophilus* 5e2 were determined to range between 0.6–2.0 dL g⁻¹ for the M_w range of 1.59×10^5 – 4.78×10^5 g mol⁻¹.

A capillary zone electrophoresis method was developed to determine the monosaccharide composition of two EPS samples. The method successfully determined D-glucose and D-galactose, but a peak for D-N-acetyl-glucosamine was not seen. The method was sensitive compared to current techniques, but not as low as using a HP-AEC-PAD.

A novel method using LC-MS was developed for the linkage analysis of EPSs. Methylation, hydrolysis and reductive amination were used to derivatise the polysaccharide, and the fragmentation patterns were examined to determine the different linkage positions. Due to undesirable further fragmentation the method could not unequivocally differentiate between the different linkage positions, but the method was capable of resolving the monosaccharides residues with different linkage positions, at approximately the correct relative ratio.

ACKNOWLEDGMENTS

Firstly I would like to thank my director of studies Dr. Andrew Laws for his help and enthusiasm for my project. I would like to thank Dr. Neil McLay for NMR training, Dr. Richard Hughes for his help in the chromatography laboratory and Mohammed Maqsood for HP-SEC-MALLS training. I would also like to thank Shaun Leivers for his help during the Milk Fermentation studies, and the assistance of Dr. Paul Humphreys and his team of microbiologists when growing and quantifying the Lactic acid bacteria cultures. Finally I would like to thank the support of my family, in particular Helen, who has become my wife and mother of our first child during my PhD studies.

GLOSSARY

Reagents / Chemicals / Terms

AcO	Acetyl
ACN	Acetonitrile
BP	British Pharmacopoeia
d.p.	Degree of polymerisation
D ₂ O	Deuterium oxide
DMSO	Dimethylsulphoxide
EPS	Exopolysaccharide
EPSs	Exopolysaccharides
<i>f</i>	Furanose
FDA	Food and Drug Administration
Gal	Galactose
GalNAc	<i>N</i> -acetyl-galactosamine
GlcNAc	<i>N</i> -acetyl-glucosamine
Glc	Glucose
GRAS	Generally regarded as safe
ICH	International Conference on Harmonisation
IUPAC	International Union of Pure and Applied Chemistry
OH	Hydroxyl
LAB	Lactic acid bacteria
<i>Lb.</i>	Lactobacillus
Me	Methyl
MRD	Maximum recovery diluent
MRS	de Man, Rogosa and Sharpe growth media
OMe	Methoxy
<i>p</i>	Pyranose
pABN	p-aminobenzonitrile
Rha	Rhamnose
TCA	Trichloroacetic acid
TFA	Trifluoroacetic acid

Experimental terms

1D	One dimensional
2D	Two dimensional
AU	Arbitrary Unit
CID	Collision-induced Dissociation
COSY	Correlated spectroscopy
CZE	Capillary zone electrophoresis
DEPT	Distortionless enhancement by polarization transfer
dn/dc	Refractive index increment
ESI	Electrospray ionisation
FAB	Fast Atom Bombardment
GC	Gas chromatography
GC-MS	Gas chromatography – mass spectrometry
HMBC	Heteronuclear multiple bond correlation
HP	High pressure
HP-AEC-PAD	High performance–anion exchange chromatography–pulsed amperometric detection
HPLC	High Pressure Liquid Chromatography
HSQC	Heteronuclear single quantum coherence
HSQC-TOCSY	Heteronuclear single quantum coherence – total correlation spectroscopy
Hz	Hertz
RI	Refractive index
LC	Liquid chromatography
LC -MS	Liquid chromatography coupled to mass spectrometer
LC-MS-MS	Liquid chromatography coupled to a tandem mass spectrometer
M	Molar (mol dm^{-3})
M	Matrix-assisted Laser Desorption/ionization
MALLS	Multi-angle laser light scattering
MS	Mass spectrometer
M_w	Weight-average molecular weight
M_n	Number-average molecular weight
mV	Millivolt
NMR	Nuclear magnetic resonance
NOE	Nuclear overhauser effect/enhancement
mg L^{-1}	Milligrams per litre (equivalent to parts per million)
$\mu\text{g mL}^{-1}$	Micrograms per millilitre (equivalent to parts per million)
ppm	parts per million
RI	Refractive Index
SEC	Size exclusion chromatography
TOCSY	Total correlation spectroscopy
TOF	Time of flight
UV	Ultraviolet

TABLE OF CONTENTS

1.	INTRODUCTION	1
1.1	Polysaccharides.....	1
1.2	Bacteria.....	2
1.3	Lactic Acid Bacteria	6
1.3.1	Lactic Acid Bacteria in the Food Industry	11
1.4	Exopolysaccharides.....	12
1.4.1	Application of Exopolysaccharides	13
1.4.2	Spoilage	14
1.4.3	Synthesis of Exopolysaccharides	15
1.4.4	Review of EPS structures	19
1.5	Production and Isolation of Exopolysaccharides.....	21
1.5.1	Production of Exopolysaccharides during Milk Fermentation.....	22
1.5.2	Isolation of Exopolysaccharides	24
1.6	Characterisation of Exopolysaccharides	24
1.6.1	Monosaccharides.....	25
1.6.2	Linkage Analysis	29
1.6.3	NMR Analysis of Polysaccharides	32
1.6.4	Weight-average Molecular Weight (M_w) Determination.....	35
1.7	New Methods of Analysis	43
1.7.1	Depolymerisation Techniques	43
1.7.2	Derivatisation of Carbohydrates	48
1.7.3	Analytical Techniques.....	50
1.8	Research Aims	53
1.9	Appendices	56
1.9.1	EPS Structures from Lactic Acid Bacteria	56
2.	EXPERIMENTAL	64
2.1	General Regents.....	64
2.2	Fermentation of Bacterial Cultures and Isolation of the Exopolysaccharide.....	64
2.2.1	Micro-organisms	64
2.2.2	Media	65
2.2.3	Milk Fermentation Procedure.....	66
2.2.4	Bacterial Growth Measurements	67
2.2.5	Isolation of the Exopolysaccharide	68
2.2.6	Qualification and Quantification of Exopolysaccharide	69
2.3	Structural Characterisation of the EPS using Established Protocols	71
2.3.1	NMR Analysis of Exopolysaccharides	71
2.3.2	Monosaccharide Composition Analysis of Exopolysaccharides.....	71
2.3.3	Linkage Analysis of the Repeating Unit of Exopolysaccharides.....	71
2.3.4	Molecular Weight Determination of the Exopolysaccharide	72
2.4	Depolymerisation of EPS Produced by <i>Lactobacillus acidophilus</i> 5e2	74

2.4.1	Depolymerisation of an EPS using a Cell Disruptor (Application of Hydrodynamic Shear)	74
2.4.2	Ultrasonic Disruption of Exopolysaccharides	75
2.4.3	Mild Acid-catalysed Hydrolysis of Exopolysaccharides	77
2.5	Development of Novel LC-MS Methods for the Analysis of Carbohydrates.....	78
2.5.1	Reductive Amination of Carbohydrates	78
2.5.2	Isolation of pABN-glucose using Preparative HPLC.....	82
2.5.3	Acid-catalysed Hydrolysis of Carbohydrates	83
2.5.4	Monosaccharide Analysis using Capillary Zone Electrophoresis	84
2.5.5	Adaptation of the 'Hakomori Methylation Procedure'	85
2.5.6	Adaptation of the 'Ciucanu Methylation Procedure'	87
2.5.7	Deuterated Samples	88
2.6	Development of a Novel Method for the Linkage Analysis of Carbohydrates	89
2.6.1	Linkage Analysis of Carbohydrates using LC-MS-MS	90
3.	PRODUCTION AND CHARACTERISATION OF EXOPOLYSACCHARIDES	95
3.1	Introduction	95
3.2	Qualification and Quantification of the Exopolysaccharides.....	95
3.2.1	Determination of Solids Content of Exopolysaccharide	95
3.2.2	Determination of Carbohydrate Content.....	98
3.2.3	Protein Content of the Recovered Exopolysaccharides Samples	100
3.2.4	Nucleic Acid Content of the Recovered Exopolysaccharide Samples	102
3.2.5	Overall Composition of the EPS	105
3.2.6	Solubility of the EPS	106
3.3	Structural Characterisation of the EPS using Established Protocols	108
3.3.1	Structural Characterisation of <i>Lactobacillus acidophilus</i> 5e2	108
3.3.2	Determination of Weight-average Molecular Weight for Exopolysaccharides	119
3.4	Results of the Timed Fermentation Studies of <i>Lb. acidophilus</i> 5e2	129
3.4.1	Timed Fermentation of <i>Lactobacillus acidophilus</i> 5e2 - Preliminary Study.....	130
3.4.2	Timed Fermentation of <i>Lactobacillus acidophilus</i> 5e2 (Batch Xn360)	133
3.4.3	Discussion of Timed Fermentation of <i>Lactobacillus acidophilus</i> 5e2	143
4.	DEPOLYMERISATION OF EXOPOLYSACCHARIDES	146
4.1	Introduction	146
4.2	Depolymerisation of EPS Produced by <i>Lactobacillus acidophilus</i> 5e2	146
4.2.1	Depolymerisation of Exopolysaccharides Using a Constant Pressure Disruptor (Application of Hydrodynamic Shear).....	147
4.2.2	Depolymerisation of Exopolysaccharides using Ultrasonic Disruption.....	160
4.2.3	Intrinsic Viscosity Measurements of EPS Solutions	168
4.2.4	Depolymerisation Using Mild Acid-catalysed Hydrolysis.....	175
5.	NEW METHODS FOR ANALYSIS OF EXOPOLYSACCHARIDES	180
5.1	Introduction	180
5.2	Reductive Amination of Carbohydrates	180
5.2.1	Reductive Amination of Standard Monosaccharides.....	186

5.2.2	Reductive Amination of Oligosaccharides	187
5.3	Acid-Catalysed Hydrolysis of Carbohydrates	192
5.4	Capillary Zone Electrophoresis of Monosaccharides	192
5.4.1	Determination of pABN-Labelled Monosaccharide Standards by CZE	193
5.4.2	Monosaccharide Composition of EPSs Produced by Lactic Acid Bacteria	195
5.5	Methylation of Carbohydrates	199
5.5.1	Methylation – ‘Hakomori Procedure’	199
5.5.2	Methylation – ‘Ciucanu Procedure’	211
5.5.3	Comparison of the Methylation Procedures Used	218
5.6	Novel Linkage Analysis of Carbohydrates using LC-MS-MS	219
5.6.1	Disaccharide Standards	219
5.6.2	Linkage Analysis of Oligosaccharides	225
5.6.3	Linkage Analysis of Exopolysaccharides	226
5.7	Appendices	234
5.7.1	Mass Spectra of pABN-labelled Monosaccharides	234
5.7.2	Examples of the CZE Chromatograms for the pABN-labelled Monosaccharides	236
5.7.3	UV Chromatograms For Timed Methylation Reaction	239
5.7.4	MS/MS Spectra – Optimising the Methylation of pABN-maltohexanose	242
5.7.5	MS/MS Spectra – Analysis of Partially Methylated pABN-maltohexanose	246
5.7.6	MS/MS Spectra – Linkage Analysis of Disaccharide Standards	252
5.7.7	Fragmentation Masses for y- and b- Series	257
5.7.8	MS/MS Spectra – Linkage Analysis of Deuterated Disaccharide Standards	258
5.7.9	MS/MS Spectrum of Cellobiose (1,4-Linked) using Sodium Cyanoborodeuteride	263
6.	CONCLUSIONS	264
6.1	Production and Characterisation of Exopolysaccharides	264
6.1.1	Future Work	266
6.2	Depolymerisation of Exopolysaccharides	266
6.2.1	Future Work	269
6.3	Novel Methods of Analysis	269
6.3.1	Future Work	273
7.	REFERENCES	275
8.	PUBLICATIONS	284

TABLE OF FIGURES AND TABLES

Figures

Figure 1: Structure of Cellulose (Homopolysaccharide).....	1
Figure 2: Cross Sections of the Cell Wall from Gram-positive and Gram-negative Bacteria ⁹	3
Figure 3: Hypothetical Bacterial Growth Curve	4
Figure 4: Homolactic Acid Fermentation Pathway	7
Figure 5: Heterolactic Acid Fermentation Pathway	8
Figure 6: Exopolysaccharide Biosynthesis (Base on Diagram by Kleerebezem <i>et al.</i>) ⁴⁴	16
Figure 7: Structures of β -D-galactopyranose and β -D-galactofuranose	25
Figure 8: The Structures of α - and β -D-galactose.....	25
Figure 9: Chemical Derivatisation Process of Monosaccharide Analysis	27
Figure 10: D-glucose and D-galactose Borate Complexes.....	28
Figure 11: Chemical Derivatisation Process of Linkage Analysis	30
Figure 12: Newman Projection Showing the Dihedral Angles in D-glucose	33
Figure 13: Diagram of the Interaction of Molecules with the Column Particles.....	36
Figure 14: Oscillating Dipole in a Macromolecule (Adaption of Diagram from Wyatt) ¹¹⁰	37
Figure 15: Schematic of the HP-SEC-MALLS	40
Figure 16: Example of a HP-SEC-MALLS Chromatogram of an Exopolysaccharide	41
Figure 17: Diagram of Constant Pressure Disruptor (Lovitt <i>et al.</i> , 2000) ¹²⁴	44
Figure 18: Diagram of a Sonication Probe	45
Figure 19: S _N 1 and S _N 2 Reaction Mechanisms for Acid-catalysed Hydrolysis of Sugars	46
Figure 20: Reaction – Reductive Amination.....	48
Figure 21: Structure of Maltohexanose	81
Figure 22: Calibration Curve for D-glucose Standard using Phenol/Sulphuric Acid Assay	99
Figure 23: Calibration Curve for BSA Standard using Bradford Protein Assay	101
Figure 24: Example of the Chromatogram of DNA Standard (25 $\mu\text{g mL}^{-1}$)	103
Figure 25: Example of the Chromatogram of an EPS (1000 $\mu\text{g mL}^{-1}$)	103
Figure 26: Graph to Determine the Critical Solubility of EPS Produced by <i>Lb. acidophilus</i> 5e2	107
Figure 27: ¹ H NMR Spectrum of EPS from <i>Lactobacillus acidophilus</i> 5e2 in D ₂ O at 70 °C	109
Figure 28: DEPT 135 ¹³ C NMR Spectrum of EPS from <i>Lactobacillus acidophilus</i> in D ₂ O at 70 °C	110
Figure 29: COSY spectrum of EPS from <i>Lactobacillus acidophilus</i> 5e2 in D ₂ O at 70 °C.....	111
Figure 30: HSQC-TOCSY Spectrum of EPS from <i>Lactobacillus acidophilus</i> 5e2 in D ₂ O at 70 °C	112
Figure 31: ¹ H- ¹³ C HSQC Spectrum of EPS from <i>Lactobacillus acidophilus</i> 5e2 in D ₂ O at 70 °C.....	113
Figure 32: ¹ H- ¹³ C HMBC Spectrum of EPS from <i>Lactobacillus acidophilus</i> 5e2 in D ₂ O at 70 °C.....	115
Figure 33: ¹ H- ¹ H NOESY (500ms) Spectrum of EPS from <i>Lb. acidophilus</i> in D ₂ O at 70 °C.....	116
Figure 34: Structure of Exopolysaccharide Produced by <i>Lactobacillus acidophilus</i> 5e2.....	118
Figure 35: <i>dn/dc</i> Curve for the Sodium Chloride	120
Figure 36: <i>dn/dc</i> Curve for the EPS Produced by <i>Lb. Acidophilus</i> 5e2	121
Figure 37: A Chromatogram of the Pullulan Standard (800,000 <i>M_w</i>)	123
Figure 38: A Chromatogram of EPS produced by 5e2 Batch Xn341	126
Figure 39: A Chromatogram of EPS Produced by 5e2 Batch Xn342.....	126

Figure 40: A M_w vs Volume Plot for the Pullulan Standard (800,000 M_w)	127
Figure 41: A Molar Mass vs Volume Plot for EPS Produced by <i>Lb. acidophilus</i> 5e2	128
Figure 42: Graph of Molecular Weight against Time for Batch Xn356 during Fermentation	132
Figure 43: Solid Content Isolated for Each Time Point during the Fermentation Process.....	133
Figure 44: Log of cfu mL ⁻¹ for Samples Taken during the 72 hr Fermentation of <i>Lb. acidophilus</i>	136
Figure 45: Turbidity of Samples taken during the 72 hr Fermentation of <i>Lb. acidophilus</i>	137
Figure 46: Sodium Hydroxide Consumption during the Fermentation of <i>Lb. acidophilus</i> 5e2.....	139
Figure 47: Solid Content Recovered during the 72 hr Fermentation of <i>Lb. acidophilus</i> 5e2	140
Figure 48: M_w of Samples Taken during The 72 hr Fermentation of <i>Lb. acidophilus</i> 5e2	141
Figure 49: Graph - Constant Pressure Disruption at Different Pressures	149
Figure 50: Change in M_w at Different Pressures after One Pass	150
Figure 51: Inverse Square of Percentage M_w Vs Pressure.....	151
Figure 52: Polydispersity at Different Pressures for Four Passes.....	152
Figure 53: Apparent Hydrodynamic Radius at Different Pressures for Four Passes.....	154
Figure 54: Change in M_w using Different Pressures for Each Pass	155
Figure 55: Graph of Constant Pressure Disruption using Different Viscosity Solvents	158
Figure 56: ¹ H-NMR Spectrum of the Anomeric Region for EPS Produced by <i>Lb. acidophilus</i> 5e2....	159
Figure 57: Graph – Ultrasonic Disruption Results of EPS (No Temperature Control)	163
Figure 58: Polydispersity Results for Ultrasonic Disrupted EPS (No Temperature Control)	164
Figure 59: Graph – Ultrasonic Disruption Results of EPS (Using an Ice-bath).....	166
Figure 60: ¹ H-NMR Spectrum of the Anomeric Region for EPS Produced by <i>Lb. acidophilus</i> 5e2....	167
Figure 61: Determination of the Intrinsic Viscosities at Each Molecular Weight Distribution.....	171
Figure 62: Approximate Intrinsic Viscosity against Weight-average Molecular Weight	172
Figure 63: Mark–Houwink–Kuhn–Sakurada Plot of the EPS produced by <i>Lb. acidophilus</i> 5e2.....	173
Figure 64: Graph – Percentage of Initial M_w against Time for the Hydrolysis of the EPS.....	178
Figure 65: ¹ H-NMR of EPS Produced by 5e2 after Acid Hydrolysis (1500 minutes).....	179
Figure 66: Reductive Amination Reaction.....	181
Figure 67: Preparative HPLC Chromatogram of pABN-glucose using UV Detection at 280 nm.....	181
Figure 68: ¹ H-NMR Spectrum of pABN-glucose in D ₂ O	182
Figure 69: Expanded ¹ H- ¹ H-COSY Spectrum of pABN-glucose in D ₂ O	183
Figure 70: Base Peak Chromatogram of pABN-glucose with Mass Spectrum of Principal Peak.....	184
Figure 71: Structure of pABN-Labelled D-glucose	185
Figure 72: b- and y-ion Series for the Fragmentation of pABN-glucose	185
Figure 73: pABN-glucosamine	186
Figure 74: Mass Spectrum of pABN-maltohexanose	187
Figure 75: HPLC Chromatogram of pABN-maltohexanose	188
Figure 76: LC-MS Chromatogram of pABN-maltohexanose.....	189
Figure 77: MS/MS Spectrum of the [M+Na] ⁺ Peak of pABN-maltohexanose	190
Figure 78: Structure and Predicted Masses of pABN-maltohexanose.....	191
Figure 79: Diagram showing the ^{1,4} x- and ^{1,4} a-ion Cleavage of a Monosaccharide Unit	191
Figure 80: Example of a CZE Chromatogram of the EPS Produced by NCFB2074	196

Figure 81: CZE Chromatogram of the EPS Produced by <i>Lb. acidophilus</i> 5e2	197
Figure 82: CZE Chromatogram of Hydrolysed and pABN-labelled <i>N</i> -acetyl-glucosamine	198
Figure 83: Mass Spectrum of Methylated pABN-glucose	200
Figure 84: LC-MS Chromatogram of Methylated pABN-glucose	201
Figure 85: Formation of Dimethyl Ion and Methylation Reaction	202
Figure 86: Mass Spectrum of pABN-glucose Before and After Deuteration	203
Figure 87: Graph – Timed Methylation Reaction.....	205
Figure 88: Mass Spectrum of Methylated pABN-maltohexanose	206
Figure 89: Deuterated Methylated pABN-maltohexanose.....	208
Figure 90: EIC of Partially Methylated pABN-maltohexanose.....	209
Figure 91: Positions of Methylation	210
Figure 92: LC-MS Chromatogram of Methylated pABN-glucose (BPC)	212
Figure 93: LC-MS Chromatogram of Acetonitrile / Water Blank (BPC)	213
Figure 94: Deuterated Methylated pABN-maltohexanose.....	216
Figure 95: LC-MS of Methylated pABN-maltohexanose	217
Figure 96: An Overview of the Proposed Linkage Analysis Reaction.....	220
Figure 97: Deuterium Oxide Exchange of 1,6-linked Sugar Residue	222
Figure 98: Product from the Reductive Amination using Sodium Cyanoborodeuteride.....	223
Figure 99: LC-MS Chromatogram of the Linkage Analysis of Maltohexanose	225
Figure 100: Structures of the Exopolysaccharides used for the Linkage Analysis	227
Figure 101: LC-MS Chromatogram of the Linkage Analysis of the EPS produced by 5e2	230
Figure 102: LC-MS Chromatogram of the Linkage Analysis of the EPS produced by NCFB2074.....	232

Tables

Table 1: Lactic Acid Bacteria that Produce Homopolysaccharides	10
Table 2: LAB that Produce Heteropolysaccharides	11
Table 3: Steps Involved in Exopolysaccharide Biosynthesis	16
Table 4: Ultracentrifuge Methods and the Potential Information Available	42
Table 5: Table of Reported Amines used for Reductive Amination	49
Table 6: Detection Limits of the Different Techniques used for Carbohydrate Analysis	51
Table 7: Samples prepared for the viscosity study using the Cell Disruptor	75
Table 8: Sonication Times and Amplitude for Samples A – D	76
Table 9: Table of Disaccharide Standards Studied	91
Table 10: Batch Descriptions and Yield of EPS Produced by from Lactic Acid Bacteria.....	96
Table 11: Results for the Carbohydrate Analysis of EPS from Each Fermented Batch	100
Table 12: Results for the Protein Analysis of EPS from Each Fermented Batch.....	102
Table 13: Results for the Nucleic Acid Analysis of EPS from Each Fermented Batch	104
Table 14: Composition of EPS Samples	105
Table 15: Solubility of Exopolysaccharide produced by <i>Lactobacillus acidophilus</i> 5e2.....	106
Table 16: $^3J_{1,2}$ Coupling Constants	109
Table 17: 1H NMR Chemical Shifts of EPS Recorded in D_2O at 70 °C.....	114
Table 18: ^{13}C NMR Chemical Shifts of EPS Recorded in D_2O at 70 °C	114
Table 19: HP-SEC-MALLS Results for Pullulan Standard (800,000 M_w).....	122
Table 20: M_w of the EPS Produced by Two Fermentations of <i>Lb. acidophilus</i> 5e2	124
Table 21: M_w/M_n of the EPS Produced by Two Fermentations of <i>Lb. acidophilus</i>	125
Table 22: The M_w Results From EPS Isolated from Other Fermentations.....	129
Table 23: Table of Fermentation Results (Batch Xn356)	131
Table 24: Results of 72 hour Fermentation (Batch Xn360).....	135
Table 25: Results Reported by Lin and Chien ⁷³ for the M_w of EPS during Fermentation	142
Table 26: Results for the Constant Pressure Disruption Analysis of EPS Produced by 5e2.....	148
Table 27: Results of the Constant Pressure Disruption of the EPS using Water as Solvent.....	155
Table 28: Table of the Viscosities of the Solvents	156
Table 29: Results of the Constant Pressure Disruption of the EPS using Two Other Solvents	157
Table 30: Results - Ultrasonic Disruption of EPS without Temperature Control.....	162
Table 31: Results - Ultrasonic Disruption of EPS Solutions in an Ice-bath.....	165
Table 32: Viscosity Results and Determination of Approximate Intrinsic Viscosity.....	170
Table 33: Results - Intrinsic Viscosity and Weight-average Molecular Weights for Each Sample	171
Table 34: Results – Mild Acid-catalysed Hydrolysis of EPS Produced by <i>Lb. acidophilus</i> 5e2.....	177
Table 35: Optimized Mass Spectrometer Conditions for pABN-maltohexanose	190
Table 36: Retention Times of pABN-labelled Monosaccharides ($100 \mu g mL^{-1}$)	194
Table 37: Time Methylation Reaction Results.....	204
Table 38: Results – To Optimize Ciucanu Methylation Procedure.....	215
Table 39: Methylated pABN-maltohexanose Ions Analysed by LC-MS-MS	218
Table 40: Optimized MS and MS/MS Conditions for the Linkage Analysis	221

Table 41: Table of Expected Structures for the Repeating Unit of the EPS Produced by 5e2	228
Table 42: Table of Expected Structures for the Repeating Unit of the EPS from NCFB2074	229
Table 43: LC-MS Peak Area Results for the Linkage Analysis of the EPS produced by 5e2.....	231
Table 44: LC-MS Peak Areas for the Linkage Analysis of the EPS produced by NCFB2074	232

1. INTRODUCTION

1.1 Polysaccharides

Polysaccharides belong to the general class of biomolecules known as carbohydrates. Polysaccharides comprise the most abundant group of natural products in the biosphere. They are large chains of sugar units, depending on the polysaccharide the chains may be linear or branched. It is estimated that approximately 4×10^{11} tons of carbohydrates are biosynthesised each year on earth by plants and bacteria, and the majority of these carbohydrates are produced as polysaccharides ¹.

Carbohydrates are involved in a variety of biological macromolecules e.g. in isolation of carbohydrates, as glycoproteins and as glycolipids. For this project, we are only interested in polysaccharides, for information about other glycosylated macromolecules the reader is directed towards excellent reviews by Stick and Williams ² and Bhagavan ³ for glycoproteins and Furukawa *et al.* ⁴ for glycolipids. The carbohydrate portion of these glycoconjugates is referred to as glycan.

Polysaccharides are macromolecules consisting of large numbers of monosaccharide residues, and when dissolved in water they produce viscous liquids. They are natural thickeners which are abundant in nature, and have been used to supplement foods for centuries. Polysaccharides that consist of one type of monosaccharide are called homopolysaccharides (Figure 1), and when they are built up of two or more different monomeric units they are called heteropolysaccharides.

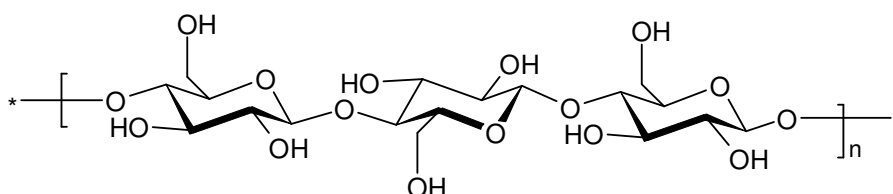


Figure 1: Structure of Cellulose (Homopolysaccharide)

Polysaccharides exist in an enormous structural diversity as they are produced by a great variety of species, including microbes, plants and animals. In animals excess D-glucose is stored as a large branched polysaccharide called glycogen, whereas in most plants, the storage form of D-glucose is called starch. Bacteria and yeasts store D-glucose as yet another type of polysaccharide called dextrans. In each case these are nutritional reserves; when required, they are broken down and the monosaccharide products are metabolised to yield energy. In contrast, cellulose is a structural polysaccharide used to make plant cell walls and has particular importance, as it is the most common organic compound on earth. These four polysaccharides are the most common, which all have repeating chains of D-glucose monosaccharide units, with some branching ¹.

Other, more complex polysaccharides are biosynthesised by bacteria; these are referred to as bacterial extracellular polysaccharides ⁵. They are biosynthesised, by bacteria, as either exopolysaccharides (EPSs), which are secreted into the surroundings during growth and are not permanently attached to the surface of the microbial cell or as capsular polysaccharides (CPS), which are permanently attached to the cell surface. This project will focus only on exopolysaccharides, monitoring their production, structure and characteristics.

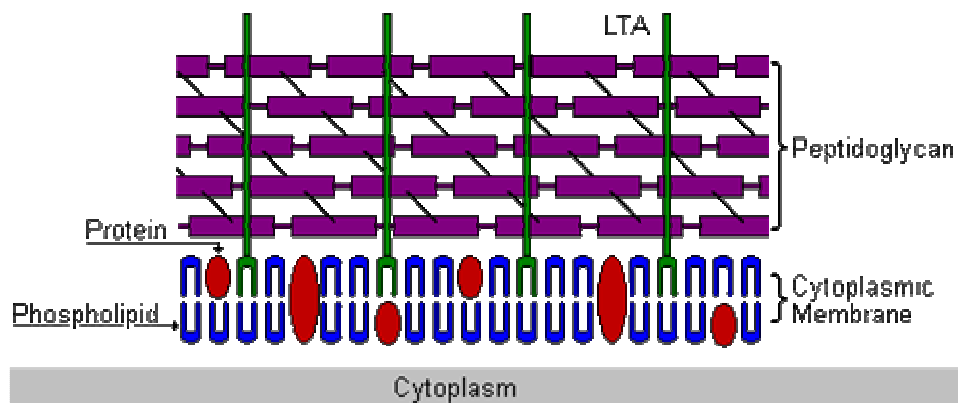
1.2 **Bacteria**

Bacteria are a large group of unicellular microorganisms, that are found in every habitat on earth, growing in soil, water, and deep in the Earth's crust, as well as in organic matter and in the live bodies of plants and animals ⁶. There are approximately 5 nonillion bacteria on this planet, accounting for much of the world's biomass ⁷.

Commercially, bacteria are important in sewage treatment, the production of cheese and yoghurt through fermentation, as well as in biotechnology, and the manufacture of antibiotics and other chemicals ⁸.

In terms of their cell structure, bacterial cells can be divided into two types: Gram-positive and Gram-negative. Gram-positive bacteria differ from Gram-negative bacteria in the structure of their cell walls. The cell walls of Gram-positive bacteria are made up of approximately twenty times as much peptidoglycan than Gram-negative bacteria. The differences between Gram-positive and Gram-negative bacteria can be seen in cross sectional diagrams (Figure 2).

Gram-positive Cell Wall



Gram-negative Cell Wall

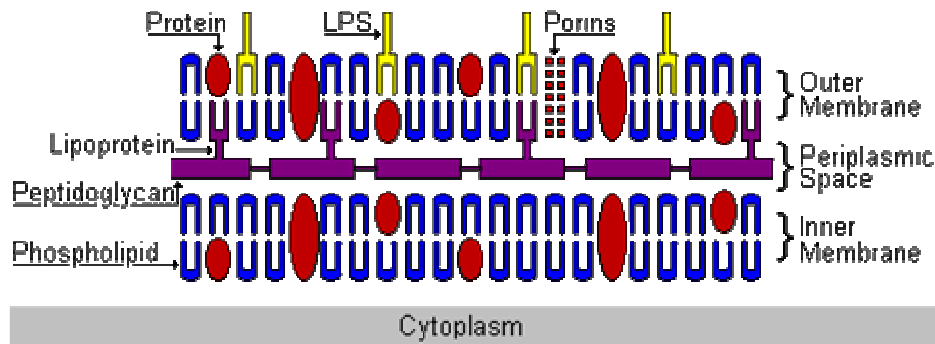


Figure 2: Cross Sections of the Cell Wall from Gram-positive and Gram-negative Bacteria⁹

The peptidoglycan consists of complex cross-links of polysaccharides and amino acids, which layer the cell wall. The polysaccharide component consists of alternating residues of β -1,4-linked *N*-acetyl-glucosamine and *N*-acetyl-muramic acid residues. The thick outer matrix of peptidoglycan serves a number of purposes, including membrane transport regulation, cell expansion, and shape formation. Other differences between the two types

of cells are that Gram-negative cell walls possess a lipid outer membrane consisting of various lipid complexes and porins.

The classification relies on the positive or negative results from Gram's staining method¹⁰ which uses complex purple dye and iodine. The Gram-positive bacteria have more layers of peptidoglycan in their cell walls than Gram-negative, which results in them retaining the dye, giving a positive result.

The growth of bacteria can be measured when a culture of bacteria is inoculated to fresh medium. The cell concentration can be periodically measured, and a curve plotted, that shows the change in cell number against time. The growth curve for bacteria has four distinct phases; lag, exponential, stationary and death shown in Figure 3.

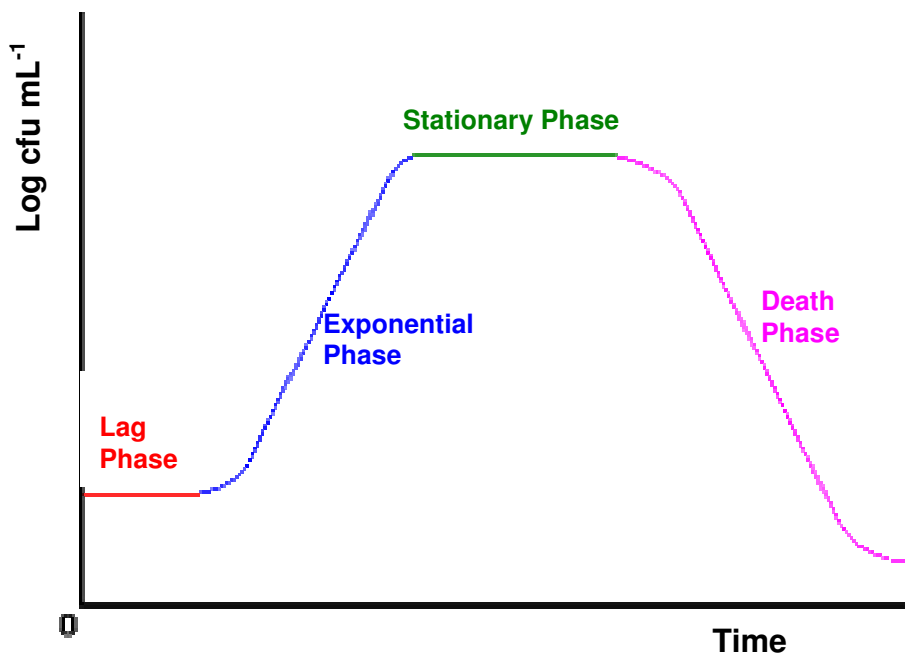


Figure 3: Hypothetical Bacterial Growth Curve

Typically growth starts with the lag phase, where there is little increase in cell numbers. At this point the bacteria are transporting nutrients from the medium into the cell, preparing for reproduction.

The exponential phase is next, where the bacterial cell division begins and proceeds as a geometric progression. During the exponential phase bacterial reproduction occurs at the maximum rate, the number of cells increases as an exponential function of time.

The growing bacterial culture eventually reaches a phase during which there is no further net increase in bacterial cell numbers. This is called the stationary growth phase, the growth rate equals the death rate. The stationary phase is usually reached when a required nutrient is exhausted.

The final phase is the death phase, where the number of viable bacterial cells begins to decline. The kinetics of bacterial death, like those of growth, is exponential because the death phase really represents the result of the inability of the bacteria to carry out further reproduction. The rate of death is not necessarily equal to the rate of growth during the exponential phase; it is simply dependent on the number of surviving cells.

As discussed earlier, bacteria are found in live bodies of plants and animals. The effects that bacteria have on these host organisms can be divided into three sections: probiotic, pathogenic and commensal.

Probiotic bacteria are known to have beneficial effects on their host, where as pathogenic bacteria are the bacteria that cause infectious diseases. The term commensal is used to group all other bacteria that provide neither benefit nor harm to their host. Commensal bacteria account for the vast majority of all bacteria, with very few being beneficial or harmful¹¹.

Probiotic bacteria are being used as dietary supplements. Fuller¹², once referred to probiotic bacteria as 'a live microbial feed supplement which beneficially affects the host animal by improving its intestinal microbial balance'. The main type of bacteria used as a probiotic is

lactic acid bacteria (LAB). Recently, foods containing probiotic bacteria have become widely available, which will be discussed in a later section.

1.3 Lactic Acid Bacteria

LAB are widespread in nature, and are found primarily in the environments where there are high levels of carbohydrates, peptides, amino acids and vitamins. They are classified as Gram-positive and consequently have a thick peptidoglycan layer, as explained in section 1.2. LAB are usually rod-shaped and present in a regular morphology. LAB are known to produce lactic acid as the major metabolic end-product of carbohydrate (D-glucose) fermentation¹³. In the lactic acid fermentation pathway, pyruvate is reduced to lactic acid, with the coupled oxidation of NADH to NAD⁺. This fermentation pathway is carried out by bacteria that are classified as LAB in response to the end product that is produced (lactic acid). This happens by two pathways, homolactic fermentation and heterolactic fermentation.

Homolactic fermentation is carried out by *Streptococcus*, *Pediococcus*, *Lactococcus*, *Enterococcus* and various *Lactobacillus* species. This pathway is important in the dairy industry, where it is responsible for souring milk, and is used in the production of cheeses, yoghurts and various other dairy products¹⁴.

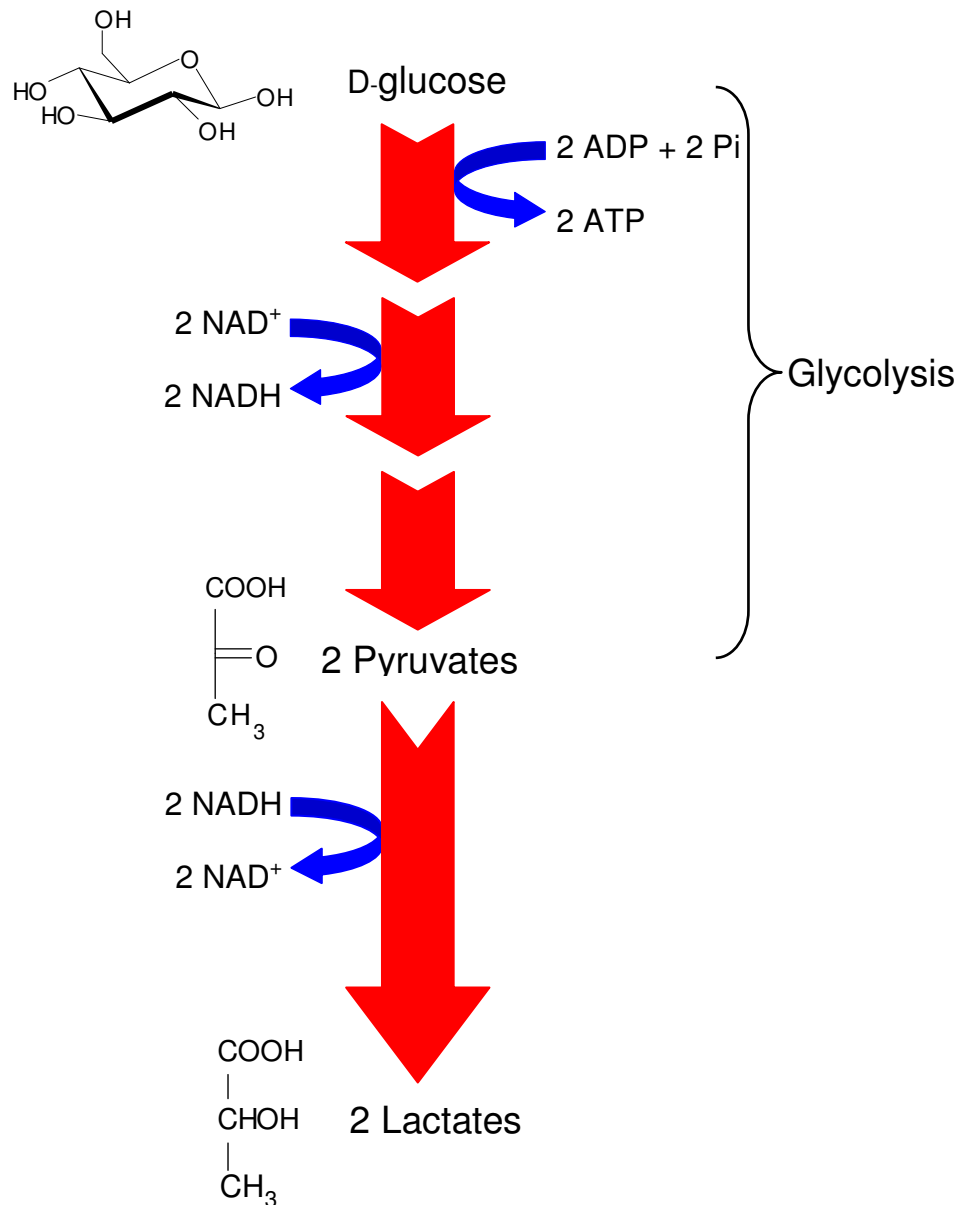


Figure 4: Homolactic Acid Fermentation Pathway

A schematic of homolactic fermentation is shown in Figure 4. The glycolysis involves glucose being broken down into two pyruvates (or pyruvic acids), two adenosine diphosphates (ADP) and two inorganic phosphates (Pi) being converted to two adenosine triphosphates (ATP) and the reduction of Nicotinamide adenine dinucleotide (NAD⁺) to NADH. Most cells will regenerate the used NAD⁺ by further converting the two pyruvates to two lactates (or Lactic acids) as the NADH is oxidised back to NAD⁺. The overall reaction can be thought of as D-glucose (1 mole), reacting with ADP (2 moles) and Pi (2 mole) to

produce lactic acid (2 mole) and ATP (2 mole). The structures are shown on the left hand side of the schematic (Figure 4).

In heterolactic fermentation, lactic acid, ethanol and carbon dioxide are all produced.

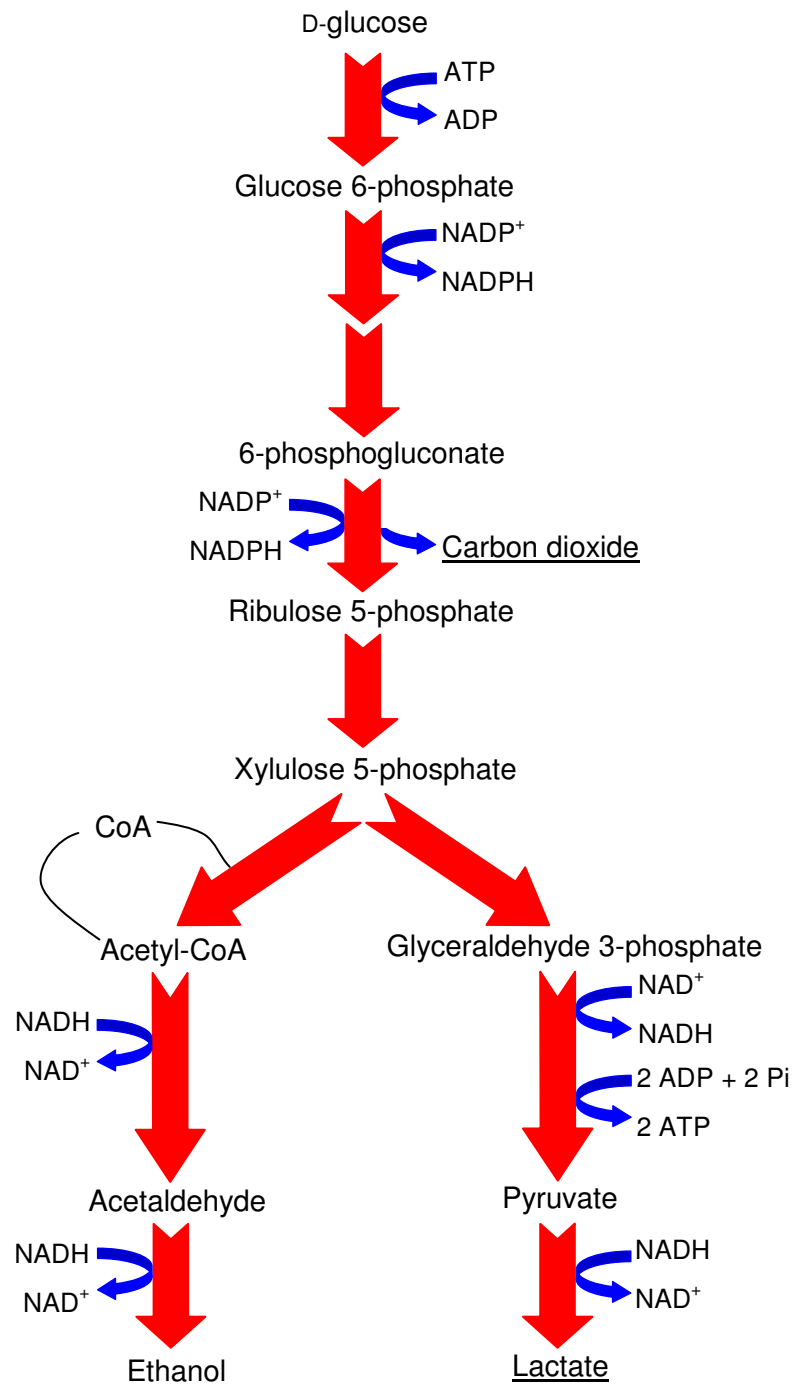


Figure 5: Heterolactic Acid Fermentation Pathway

At the start of the heterolactic pathway a phosphate, which has been removed from ATP to form ADP, is substituted onto the glucose molecule at carbon C6. The energy released as Nicotinamide adenine dinucleotide (NAD⁺) is reduced to NADH ring opens the glucose-6-phosphate to produce 6-phosphogluconate. At the next stage more NAD⁺ is reduced to NADH, which removes carbon dioxide to leave ribulose 5-phosphate. Xylulose 5-phosphate then forms two products, whereas glyceraldehyde 3-phosphate results in the production of lactate, and acetyl-CoA results in the production of ethanol. The overall reaction, yields lactic acid (1 mole), ethanol (1 mole), carbon dioxide (1 mole) and ATP (1 mole), from D-glucose (1 mole), ADP (1 mole) and Pi (1 mole). This fermentation pathway is carried out by *Leuconostoc* and various *Lactobacillus* species.

Species of *Lactobacillus* produce lactic acid by either homolactic or heterolactic fermentation. Measuring the ethanol and carbon dioxide produced can determine which pathway is occurring.

A large variety of bacterial systems can produce complex polysaccharides. It is not just probiotic bacteria, pathogenic strains can also biosynthesise polysaccharides. Our research focuses only on probiotic systems, in particular LAB that secrete polysaccharides.

As discussed briefly in section 1.1, bacterial extracellular polysaccharides are biosynthesised as either exopolysaccharides or as capsular polysaccharides. The main focus of this project will be on exopolysaccharides. Exopolysaccharides can be divided into two groups; those that produce homopolysaccharides, and those that produce heteropolysaccharides. The homopolysaccharides can be further divided into subgroups, where different strains of LAB have been found to produce unique classes of polysaccharides; α -D-glucans, β -D-glucans and fructans⁵.

Table 1: Lactic Acid Bacteria that Produce Homopolysaccharides

Subgroups	Lactic Acid Bacterial Strains	Polysaccharide
α -D-glucans	<i>Leuconostoc mesenteroides</i> subsp. <i>mesenteroides</i> <i>Leuconostoc mesenteroides</i> subsp. <i>Dextranicum</i>	α -1,6-linked D-glucose, variable degree of branching at position 3, sometimes positions 3 and 4 (Strain Specific)
	<i>Leuconostoc Mesenteroides</i> <i>Streptococcus mutans</i> <i>Streptococcus sobrinus</i>	α -1,6-linked and α -1,3-linked D-glucose
β -D-glucans	<i>Pediococcus</i> spp. <i>Streptococcus</i> spp	β -D-glucans, β -1,3-linked D-glucose, with β -1,2-branches
Fructans	<i>Streptococcus salivarius</i>	β -2,6-linked D-fructose, with some β -1,2-branches

LAB that produces heteropolysaccharides can be subdivided into two groups, mesophilic strains and thermophilic strains. Mesophilic strains are organisms that grow best at moderate temperature, 15 – 40 °C for example. Whereas thermophilic organisms thrive at relatively high temperatures, greater than 40 °C. Mesophilic and thermophilic LAB that produce heteropolysaccharides are given in Table 2.

Table 2: LAB that Produce Heteropolysaccharides

Subgroups	Lactic Acid Bacterial Strains
Mesophilic	<i>Lactococcus lactis</i> subsp. <i>lactis</i> <i>Lactococcus lactis</i> subsp. <i>cremoris</i> <i>Lactobacillus casei</i> <i>Lactobacillus sake</i> <i>Lactobacillus rhamnosus</i>
Thermophilic	<i>Lactobacillus acidophilus</i> <i>Lactobacillus delbrueckii</i> subsp. <i>bulgaricus</i> <i>Lactobacillus helveticus</i> <i>Streptococcus thermophilus</i>

Recently, exopolysaccharides biosynthesised from the thermophilic group have received the most interest because of their important role in the rheology, texture and mouth feel of fermented milk drinks and products ⁵.

1.3.1 Lactic Acid Bacteria in the Food Industry

LAB are associated with natural food fermentations such as milks, meat, beverages and bakery products ¹⁵, one example of their exploitation is the Scandinavian Dairy Industry which commercially utilizes their characteristics in the production of their buttermilk products ¹⁴. Some of the LAB used in the food industry include: *Streptococcus*, *Lactobacillus*, *Enterococcus*, *Lactococcus*, *Leuconostoc*, *Pedidococcus* and *Aerococcus* genera. They secrete EPS into the growth medium but also produce lactic acid during fermentation.

LAB are widely used as starter cultures in fermented products. Their growth lowers both the carbohydrate content and the pH of foods they ferment. It is this acidification process which is one of the most desirable side-effects of their growth. During fermentation, the production of lactic acid can reduce the pH to as low as 4.0, which has been reported to be low enough

to inhibit the growth of most other microorganisms, including the most common human pathogens, which can increase the shelf life of foods ¹⁶.

Lactobacillus acidophilus is also added to various commercial milk products (Acidophilus Milk), as a probiotic, to aid individuals who are unable to digest milk products adequately ¹⁷, where enzymes produced by *Lactobacillus acidophilus* convert milk sugars to products that do not accumulate and cause gastrointestinal problems.

LAB have a useful role in winemaking, converting malic acid to lactic acid in malolactic fermentation. Unfortunately, after this conversion has completed the bacteria may still be present within the wine, where they can metabolise other compounds leading to spoilage. Wines that have not undergone malolactic fermentation may be contaminated with LAB; leading to re-fermentation of the wine so that it becomes turbid and slightly effervescent. This can be avoided by sterile filtering of wine directly before bottling or the use of phenolic compounds to control LAB growth ¹⁸.

Other benefits of 'probiotic' LAB are that they have anti-hypercholesteremic effects ¹⁹, anti-carcinogenic effects ²⁰, immunopotentiality ²¹ and the ability to control intestinal pathogens ²². In addition, there have been claims for the use of products containing LAB in alleviating hypertension ²³, allergies ²⁴, heart disease, urogenital infection ²⁵ and hepatic encephalopathy ²⁶.

1.4 Exopolysaccharides

Microbial exopolysaccharides are extracellular polysaccharides that are secreted into the extracellular environment in the form of slime. There is no definitive understanding of why EPSs are produced by bacteria, they are not used as a feedstock for the bacteria but are thought to provide a defensive barrier. The secretion of exopolysaccharides often envelopes the bacteria in a biofilm that enables them to survive and prosper in a range of hostile

environments²⁷. A biofilm is a complex aggregation of microorganisms that grows on a solid substrate. They are held together and protected by a matrix of excreted polymeric compounds, where the main component is a polysaccharide, referred to as an exopolysaccharide. The biofilm matrix traps required nutrients and water and offers bacteria a way to adhere to surfaces which they otherwise would be unable to inhabit, surrounding the bacteria and reducing and often eliminating the effects of antibacterial agents²⁸. It is also known that EPSs aid the protection of bacteria against bacteriophage attack, phagocytosis, predation by protozoa, antibiotics and desiccation²⁹.

Our interest in bacterial exopolysaccharides has two main focuses, an interest in beneficial application of EPSs and also in the spoilage of foods caused by biofilm formation.

1.4.1 Application of Exopolysaccharides

Polysaccharides are indispensable tools in food product formulation due to their thickening and gelling properties. They are also used as emulsifiers, stabilizers, and in the inhibition of syneresis, which is the release of water from processed foods⁵. Most polysaccharides used by the food industry as bio-thickeners are derived from plants, such as starch, pectin, guar and seaweed (carrageenan, alginate). These are not always readily available, and their rheological properties often do not match those required, hence, most polysaccharides of plant origin require chemical modifications to improve their structure and rheological properties³⁰. The consequence of these chemical modifications is that the polysaccharides carry heavy restrictions over their usage in food products, being labelled with an E-number classification⁵.

Due to the concerns with established biothickeners, microbial exopolysaccharides are becoming widely applied as natural thickening, gelling and stabilizing agents in the food industry³¹. They are water soluble and become viscous when hydrated which gives them

thickening and gelling properties. This has made them very attractive to the food industry as replacements for plant and animal derived polysaccharides.

Exopolysaccharides produced by lactic acid bacteria (LAB) carry the 'generally recognised as safe' (GRAS) status because the microorganisms are food grade, which make them much more favourable compared to their synthetic counterparts. Examples in industry of important microbial polysaccharides are dextrans, xanthan, pullulan, and bacterial alginates⁵. Once developed, it is envisaged that novel microbial biopolymers will eventually replace the synthetic polysaccharides, improving both the rheology and stability of foods³². The main problem when using EPSs has been the variable consistency and an inability to produce them on a scale suitable for industrial use. This means that novel polysaccharides of bacterial origin, which can be prepared in large quantity, are of significant interest. The production of Xanthan, from *Xanthomonas campestris*, has been reviewed by Rosalam and England³³, as mentioned above, it is an industrial thickening agent, but because the strain is phytopathogenic it is not given GRAS status, despite having gained Food and Drug Administration (FDA) approval. In the search for a new generation of 'green' food thickeners, much attention is currently being given to exopolysaccharides; the application of the excreted EPSs into food products is expected to have great commercial potential. Where there is further need of food thickening, with a move to low fat dairy products, LAB are of interest as they are currently used in the production of many fermented foods such as yoghurts, cheeses and butters as thickening agents to improve the rheological properties of the products, such as texture, mouth feel and viscosity¹⁴. A study by Folkenberg *et al.*³⁴ into the textural effects of EPSs in yoghurt, reported that EPS-protein interaction was extremely important, benefiting mouth feel, ropiness and low serum separation.

1.4.2 Spoilage

The negative attributes of EPS synthesis are associated with their spoilage properties. The synthesis of EPSs by LAB during wine^{35 36} and cider³⁷ production leads to products having

undesirable rheological properties. The formation of dental plaques is related to EPS synthesis by LAB^{38 39}. The exopolysaccharides for LAB are responsible for biofilm formation^{40 41} that can lead to biofouling⁴². The most notable examples of biofouling are associated with biofilm formation in equipment used for processing in the dairy industry e.g. pipe blockages⁴¹.

1.4.3 Synthesis of Exopolysaccharides

The synthesis of the great majority of bacterial homopolysaccharides, and of all heteropolysaccharides is a complex intracellular process, in which sugar nucleotides provide activated forms of the monosaccharides²⁸. Whilst the exact biosynthetic mechanism for heteropolysaccharide production in LAB is not known, important details have been identified. The mechanism is similar to that proposed for Gram-negative bacteria, as both systems require the polymerisation of reducing sugar units. Heteropolysaccharides are constructed from multiple copies of an oligosaccharide (a repeating unit). The oligosaccharide can contain between three and seven residues, possessing a variety of two or more different types of monosaccharides, and often a range of different linkage patterns⁴³. The varieties of monosaccharides are produced through epimerization, dehydrogenation, and decarboxylation reactions at the sugar nucleotide level, where D-glucose and D-mannose can be converted to D-galactose, uronic acids or pentoses. The stages of EPS synthesis can be summarised into five steps, based on Kleerebezem *et al.*⁴⁴. A general overview of the pathways involved in the synthesis of EPSs is provided in Figure 6.

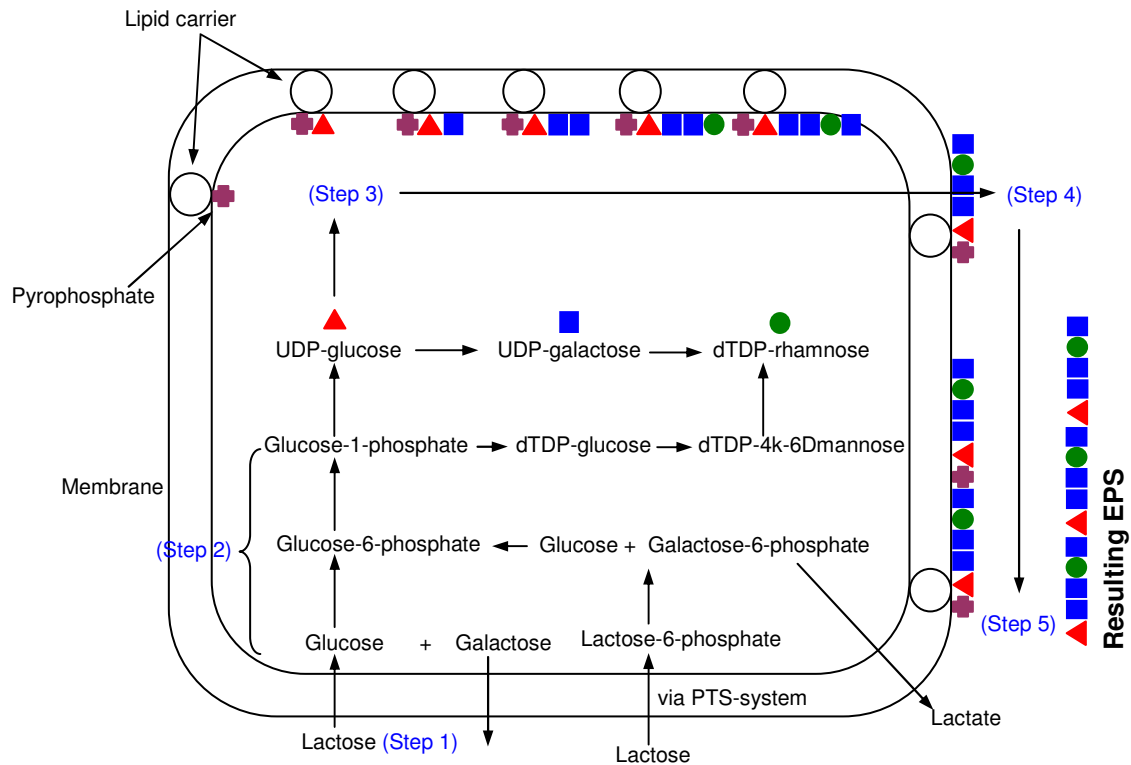


Figure 6: Exopolysaccharide Biosynthesis (Base on Diagram by Kleerebezem *et al.*)⁴⁴

The steps involved are given in Table 3, where the repeating units of heteropolysaccharides are synthesised as lipid soluble components to which acyl groups are also attached.

Table 3: Steps Involved in Exopolysaccharide Biosynthesis

Steps	Action
Step 1	Sugar transport into the cytoplasm
Step 2	Synthesis of glucose-1-phosphate
Step 3	Synthesis of sugar nucleotides and polymerisation into EPS subunit
Step 4	Export out of the cytoplasm
Step 5	EPS polymerisation and detachment

As shown in Figure 6, there are two systems for uptake of lactose, via the phosphotransferase (PTS)-system or via a non-PTS-system. The best established system is the PTS-system⁴⁵, which transfers a high-energy phosphate group from

phosphoenolpyruvate to an incoming carbohydrate. The PTS-system is energy conserving as fermentation yields very few ATP molecules in comparison to respiration, and this low energy yield from fermentation would not support active transport. This is why it is found predominantly associated with fermentative organisms. Some bacteria have been shown to lack a PTS for lactose and grow significantly more slowly than cells with PTS. Thompson and Thomas⁴⁶ have shown this to be true of *thermophilus*. Detailed work on EPS biosynthesis in LAB has focused on *Lactococcus lactis* subsp *cremoris* by Oba *et al.*⁴⁷. They suggest that lactose is taken in via a PTS-system and subsequently hydrolysed by the phospho- β -galactosidase enzyme. The D-glucose moiety is converted to glucose-6-phosphate by glucokinase then to glucose-1-phosphate by phosphoglucomutase. Qian *et al.*⁴⁸ proposed that the action of α - and β -phosphoglucomutase is the limiting step in EPS biosynthesis as it regulates the flux between metabolism and EPS production in *Lactococcus lactis* subsp *cremoris*.

As can be seen in Figure 6, the biosynthesis of glucose-1-phosphate generally results in the production of UDP-glucose, UDP-galactose, and dTDP-rhamnose nucleotide sugars. These activated nucleotide sugars attach to phospholipids on the lipid carrier and assemble into sugar units. Construction of the basic repeat unit occurs by the transfer of sugar nucleotides diphospho-precursors to a carrier lipid. The lipid carrier plays a central role, acting as an anchor to which assembly of the repeating unit takes place. Oba *et al.*⁴⁷ have analysed the lipid linked oligosaccharides by conventional compositional and methylation analysis (discussed in section 1.6.2). The structure of the isolated lipid linked oligosaccharide was in agreement with the structure of the secreted polysaccharide.

The repeating units are then polymerised and the polysaccharides are excreted into the extracellular environment, where they can be found attached to the cell surface, or as cell-free colloidal masses or sometimes both. The EPS produced is usually of distinct weight-average molecular weight, and the method by which the chain length of the EPS is dictated

is still unknown, although genes purporting to control chain length of EPSs have been suggested in many exopolysaccharide-synthesised bacteria ⁴⁹. Groot and Kleerebezem ⁵⁰ have studied the genes that are thought to be responsible for controlling EPS production, *epsA*, *epsB*, *epsC* and *epsD*. They investigated the effect of deletion and mutation of each gene, working out that *epsA* and *epsB* appeared to be essential in the biosynthesis of EPSs. The deletion of *epsC* had only a minor effect, while phosphorylation of *epsB* indicated that the EPS synthesis is driven by the presence of a non-phosphorylated form of *epsB*.

Studies on genetic control of EPS production in LAB have shown that the genes encoding synthesis of the polymers may be located either on plasmids for mesophilic species, such as *Lactobacillus lactis* and *Lactobacillus casei*, or on the chromosome, as in thermophilic LAB species ⁴⁹. The substrate specificity of the glycosyltransferases controls the sequence of the repeating unit, the polymerisation and export ⁵¹. De Vuyst *et al.* ⁵², has suggested that there are four functional regions of the polysaccharide synthetic cluster in LAB. The central region contains the gene for glycosyltransferases and is sandwiched by two regions, each involved in chain-length determination and export. The final region is situated at one end of the gene cluster and is responsible for regulation of biosynthesis of EPSs. The *esp* clusters are thought to be very similar for different LAB, implying there is a common mechanism for all EPS biosynthesis ⁵¹.

The mechanism for secretion of EPSs is still unclear; it is thought that EPS subunits are transported across the membrane by either proton motive forces ⁵³ or translocated from membrane embedded lipid carriers by a translocase enzyme ⁵⁴.

Biosynthesis of polysaccharides is considered to be energy dependant, requiring one mole of ATP for the conversion of each hexose substrate molecule to hexose phosphate and a further high-energy phosphate bond is needed for the synthesis of each sugar nucleotide. Also one mole of ATP is required for the phosphorylation of the lipid carrier and energy will

then be required for the polymerisation and transport of the polysaccharide. De Vuyst (1999)⁵ states energy generation in LAB is limited, which will limit polysaccharide production. EPSs are produced in relatively small amounts and its production may compete with cellular growth⁵⁵, this could explain the close relationship between cell growth and EPS synthesis⁵⁶.

1.4.4 Review of EPS structures

Exopolysaccharides from LAB can have many different characteristic properties, as well as having distinct chemical structures.

1.4.4.1 Subgroups of Exopolysaccharides

As explained in section 1.1, EPSs that consist of one type of monosaccharide are called homopolysaccharides, however heteropolysaccharides, produced by mesophilic and thermophilic LAB strains (shown in Table 1 and Table 2) can be composed of many different monomeric units, as the α - or β - anomer and in the pyranose or furanose form⁵. The range of monosaccharides and the number of possible linkages between each sugar unit lead to a wide range of structures and properties in EPSs from LAB.

1.4.4.2 Chemical Composition of Exopolysaccharides

The chemical composition and structure of their EPSs varies widely, even from different strains within the same species. The chemical composition of heteropolysaccharides from LAB has been investigated and there is agreement that EPSs from LAB are polysaccharides with D-glucose and D-galactose as the main sugar constituents and the ratio of the two components varies (Laws *et al.*, 2001)⁴³. Incorporation of other neutral sugars has been reported, for example, D-mannose, L-rhamnose, L-fucose, *N*-acetyl-D-glucosamine and *N*-acetyl-D-galactosamine and to a smaller extent D-glucuronic acid and D-galacturonic acid, which both carry a formal negative charge, and are also found in a small number of EPS structures.

A list of all the reported EPS structures from lactic acid bacteria are given in the Appendix section 1.9. The structures are presented using the rules of nomenclature detailed by Laws *et al.*⁴³, which are loosely derived from the guidelines presented by the International Union of Pure and Applied Chemistry (IUPAC) for the nomenclature of polysaccharides composed of more than one kind of residue. Inspection of the reported EPS structures from lactic acid bacteria show that the monosaccharide present in the highest frequency is galactose, closely followed by glucose. Each of these is always present in the D-absolute configuration, whereas rhamnose is always present in the L-absolute configuration. There are a small number of structures that contain, D-GalNAc, D-GlcNAc and phosphor-diester, acetyl-ester, phosphate-ester, pyruvate-acetal substitutions. The structures show slight preference for the β -anomer, however, there is a definite preference for the α -anomer for rhamnose. The only sugar found to adopt the furanose ring was galactose. In terms of the different linkages, anomeric configuration and linkage type, some general observations can be made. A large number of branches are terminated by D-galactose. β -D-galactose is preferentially attached either as branch terminus or via a 3-, 4- or 6-hydroxyl group. α -D-glucose shows a strong preference for attachment via its 3-hydroxyl group. β -D-glucose is preferentially attached via its 3-, 4- or 6- hydroxyl group, where as α -D-glucose is preferentially attached via its 3- or 6-hydroxyl group. And finally, L-rhamnose is frequently used as a branch junction.

It has also been reported that certain strains of LAB can secrete more than one EPS, for example, Grobber *et al.*^{57 58} reported different monosaccharide compositions of EPS material from the thermophilic LAB strain *Lactobacillus delbrueckii* subsp. *bulgaricus* NCFB 2772. Also, Marshall *et al.*⁵⁹ isolated two different EPSs from the mesophilic LAB strain *Lactococcus lactis* subsp. *cremoris* LC330, where the two EPSs showed different monomeric composition and weight-average molecular weight. High and low molecular weight material was also found from fermentations with the *Lactobacillus delbrueckii* subsp. *bulgaricus* NCFB 2772 strain⁵⁸ and the *Streptococcus thermophilus* LY03 strain⁶⁰. However, the high and low

molecular mass material from both of these species did not differ in monosaccharide composition.

1.4.4.3 Structure of Exopolysaccharides

The monosaccharides in EPSs are found in repeat units; the monosaccharides are connected by α - or β - glycosidic linkages and have D- and L- configurations, which are present in the pyranose and furanose forms. The repeating units range from trisaccharides to heptasaccharides. One exopolysaccharide was reported to consist of a repeating unit of eight monosaccharides ⁶¹. This was produced by *Streptococcus thermophilus* MR-1C but this was shown to be a capsular polysaccharide.

According to De Vuyst and Degeest ⁵ EPSs produced by LAB have a molecular mass range from 40 kDa – 6000 kDa. Care must be taken when determining the molecular mass of EPSs, as the material measured is often presumed to be EPS, but may just be due to impurities present from the fermentation process. There is a possibility of mis-assignment of residual D-glucose, lactose, proteins and salts or perhaps a glycoprotein or protein-carbohydrate complex, as has been reported by Al *et al.* ⁶², where chemical composition analysis showed that the low molecular weight material that was isolated was due to protein.

1.5 Production and Isolation of Exopolysaccharides

LAB can be grown on plates, where those that, when contacted with a toothpick, generate aropy strand are believed to be EPS producing. LAB have been shown to be able to biosynthesize exopolysaccharides that are secreted into their environment when they are used to ferment large working volumes of milk ⁵. These fermentation conditions must be optimised in order to produce exopolysaccharides in a large enough quantity to isolate and structurally characterise. There have been many studies carried out to both optimise and

improve the fermentation conditions and EPS isolation procedure, these developments are detailed below.

1.5.1 Production of Exopolysaccharides during Milk Fermentation

LAB cultures have been shown to thrive during the fermentation of milk, where the optimal fermentation conditions differ for each LAB subgroup. Cerning *et al.*⁵⁶ has suggested that there is a close relationship between LAB cell growth and EPS synthesis, therefore the milk fermentation process has been developed as a technique for producing exopolysaccharides in a large enough amount to allow their isolation and characterisation. Individual LAB cultures can be inoculated and grown in milk. To grow an individual culture, the preparation of the milk is critical, prior heat treatment of milk is essential as it destroys pathogens and other microorganisms which may interfere with the fermentation process. Once sterile, the milk is then inoculated with the LAB culture, and the fermentation proceeds.

The fermentation temperature influences the growth of LAB, which subsequently affects the biosynthesis of EPSs. It has been reported that temperature above and below the optimum growth temperature for the LAB have resulted in greater EPS production. Results demonstrating increased EPS production at low incubation temperatures have been published by Cerning *et al.*⁵⁶, Marshall *et al.*⁵⁹ and Looijesteijn and Hugenholtz⁶³. Their reasoning for this is explained by the fact that slowly growing bacterial cells exhibit a much slower cell wall polymer biosynthesis, making more lipid carriers available for EPS biosynthesis. In contrast, De Vuyst *et al.*⁶⁴ and Kimmel *et al.*⁶⁵, found higher EPS yield by fermenting LAB at higher growth temperatures than the optimal value.

The optimal pH conditions found for production of EPSs are often close to pH 6.0, however, some authors (Gamar-Nourani *et al.*, 1998⁶⁶ and Dupont *et al.*, 2000⁶⁷) do not find significant differences in the amount of EPS produced under pH controlled conditions when compared to the acidic conditions produced by the LAB generating lactic acid during

fermentations. De Vuyst *et al.*⁶⁴ carried out fermentation experiments under constant pH conditions, using automatic addition of sodium hydroxide to maintain the pH at 5.5.

There have also been reports that EPS degradation can occur upon prolonged incubation Gassem *et al.*⁶⁸, De Vuyst *et al.*⁶⁴, Petry *et al.*⁶⁹, which they suggest could be due to glycohydrolase activity, although the presence of glycohydrolase has only been demonstrated in *Lactobacillus rhamnosus* R by Pham *et al.*⁷⁰.

To be able to characterise the structures of EPSs, a significant amount of EPS material is required. Work carried out at the University of Huddersfield has developed a procedure to produce exopolysaccharide, at an adequate level, during milk fermentations. The procedure involves inoculating sterile milk with LAB, and then fermenting the milk to grow the LAB. As the culture of LAB grows, it synthesises and secretes EPS. Studies into the fermentation procedure have optimized the temperature, pH conditions, supplementation, and length of fermentation^{71 72}.

Although the mechanism of the biosynthesis of exopolysaccharides is moderately understood, the actual time course of the production of exopolysaccharides during the fermentation process requires further investigation. During fermentation the yields of LAB have been monitored to determine the phase of growth. Some workers have identified an increase in EPS production during the exponential phase. Lin and Chang Chien⁷³ have attempted to monitor the yield and weight-average molecular weight of EPSs during the fermentation of milk, produced from cultures of *Lactobacillus helveticus*. They have reported that the molecular weight significantly increases throughout the fermentation, then decreases during the death phase of the bacterial culture. Their conclusions were drawn from a study that had limited data, sampling at only nine intervals over an 84 hour experiment.

1.5.2 Isolation of Exopolysaccharides

The synthesis and excretion of exopolysaccharides from LAB into the growth medium has been described above, the difficulty then lies with isolating and purifying the EPS. There have been many publications that have developed the procedure for isolating EPSs. Most of these methods commonly use solvent such as acetone^{74 75 76} or ethanol^{77 78 79} to precipitate the EPS. Since 2001, ethanol appears to be the solvent of choice and has been used in the majority of EPS precipitations.

When EPS is isolated from milk cultures a de-proteination step prior to EPS precipitation is required. This can be achieved in one of two ways: using a proteinase enzyme or using acid to precipitate the protein. Doco *et al.*⁸⁰ used proteinase initially to break down the caseins, followed by the addition of trichloroacetic acid (TCA). Using proteinase removes the majority of proteins but small proteins may remain in the supernatant liquid following centrifugation. Studies into the addition of TCA⁷¹ have shown a concentration of TCA (14% w/v) to be optimal for precipitation of proteins, although De Vuyst *et al.*⁶⁴ has published a method that included two rounds of TCA addition and EPS precipitation.

Once protein has been precipitated, the separated cells and proteins are then removed by centrifugation which is followed by the addition of chilled ethanol to re-precipitate the EPS. The precipitated EPS is collected and dissolved in water and dialysed to remove the small neutral sugars, salts and small proteins. The dialysed EPS solution is then freeze dried to produce a pure EPS solid that is white in colour and has a soft spongy texture.

1.6 Characterisation of Exopolysaccharides

The structures of exopolysaccharides have been discussed in section 1.4.4, they consist of monosaccharide units, which are attached together through α - and β - glycosidic linkages to form repeating oligosaccharide units. The two most important elements of the structural characterisation of exopolysaccharides are, firstly, to determine the monosaccharide

composition, in terms of identification of monomers and their relative ratio, in the repeating unit. Then secondly, to determine how each monosaccharide is arranged (linked) in the repeating unit. The overall configuration of the repeating oligosaccharide sequence can then be deduced.

1.6.1 Monosaccharides

The most basic carbohydrate units are called monosaccharides, which when linked together form more complex carbohydrates, such as di-, oligo- and polysaccharides. The monosaccharide components, can have D- or L- configurations, and be present in both furanose and pyranose forms. The monosaccharides present in exopolysaccharides are normally aldohexoses and exist in either the pyranose or furanose forms.

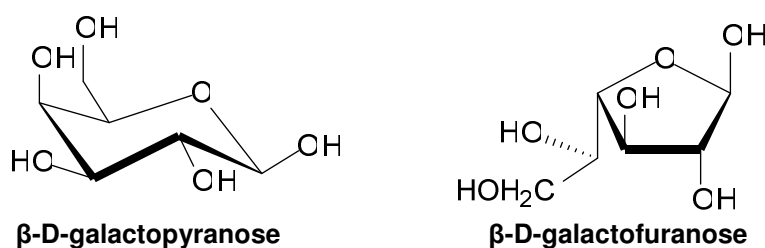


Figure 7: Structures of β -D-galactopyranose and β -D-galactofuranose

In an aldohexose, the sixth carbon is attached equatorially as $-\text{CH}_2\text{OH}$ to the carbon C5.

The anomeric proton is situated on carbon C1, which has been labelled in Figure 8.

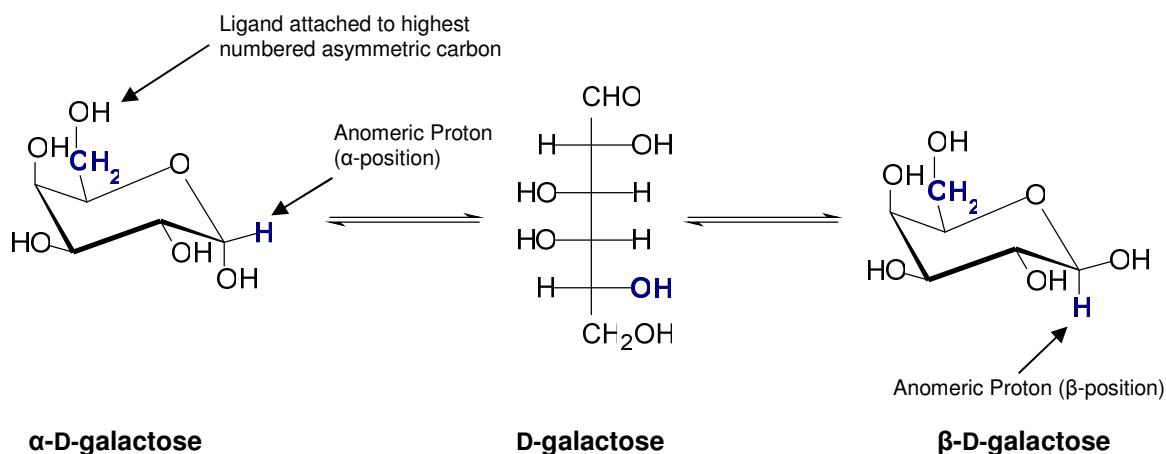


Figure 8: The Structures of α - and β -D-galactose

In solution, D-glucose is present in the open-chain form (acyclic) and ring (cyclic) form in equilibrium.

The anomeric configuration of a monosaccharide unit is assigned by the position of the ligand attached at the highest numbered asymmetric carbon (within the ring) with the anomeric proton. Therefore determining the position of the anomeric proton on the C1 carbon in relation to the highest numbered chiral carbon, which for a cyclic aldohexose, is carbon C5. The alpha (α -) anomeric configuration occurs when the anomeric proton is positioned on the same side of the ring as the ligand attached to the highest numbered asymmetric carbon, and in the beta (β -) anomeric configuration the anomeric proton is positioned on the opposite side of the ring as the highest numbered asymmetric carbon. This is illustrated in Figure 8, where the groups of interest are labelled. Nuclear magnetic resonance is used to distinguish between the two configurations and this will be discussed further in section 1.6.3.

Glycosidic linkages are defined as bonds between monosaccharides, where a bond forms between a hemiacetal or hemiketal, at carbon C1 and an alcohol, which is usually another carbohydrate. Glycosidic linkages between carbohydrates can lead to linkages between carbon C1 and hydroxyl groups attached to carbons C2, C3, C4 or C6 of another pyranose based monosaccharide. A monosaccharide can have up to four linkages; therefore complicated branched structures are possible. The rules are different when looking at furanoses.

1.6.1.1 Monosaccharide Analysis

Polysaccharides are polymers made up of many monosaccharides joined together by glycosidic linkages. There are several methods that can be used to determine the monosaccharide composition of a polysaccharide.

The majority of published exopolysaccharide structures have used the procedure described by Gerwig *et al.*⁸¹ to determine the monosaccharide composition. The analytical procedure involves hydrolysis of the exopolysaccharide to monosaccharides, using an acid to catalyse the reaction. The monosaccharide units are then reduced, using sodium borohydride and acetylated using acetic anhydride. The volatile derivatised alditol acetates are assayed by GC and their identity confirmed by comparison to alditol acetate standards.

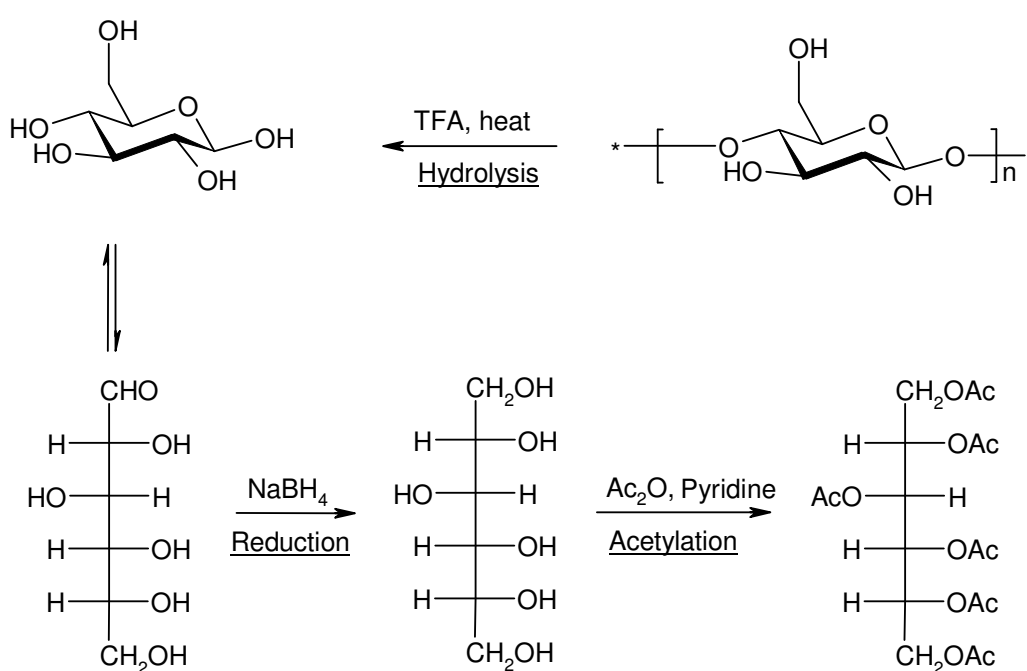


Figure 9: Chemical Derivatization Process of Monosaccharide Analysis

The derivatization process is illustrated in Figure 9, which shows trifluoroacetic acid (TFA) used as a catalyst for the hydrolysis. The aldehyde is then reduced, and the hydroxyl groups are acetylated to provide the alditol acetate of the monosaccharide. This method is time consuming, and difficulties associated with the thermal decomposition of amino sugars have been well documented⁸². The method cannot detect *N*-acetyl amino sugars because the acetyl group is removed during hydrolysis leaving only the amino sugar residue⁸³.

1.6.1.2 Alternative Methods for Monosaccharide Analysis

More recent methods that have been developed for monosaccharide analysis of polysaccharides use high pressure anion exchange chromatography with pulsed amperometric detection (HP-AEC-PAD) ^{84 85}. This method does not require monosaccharide derivatisation as alditol acetates, the polysaccharide is simply hydrolysed into monosaccharides. As with the gas chromatography method described above, this technique also compares the retention times and relative intensities of monosaccharide standards to identify and quantify the monosaccharide composition of polysaccharides. Again, due to the requirement for a hydrolysis step, this method cannot distinguish between *N*-acetyl amino sugars and amino sugars ⁸³.

The detection of carbohydrates using capillary zone electrophoresis (CZE) has been well documented, in particular by Paulus and Klockow ⁸⁶. The detection of underivatised neutral carbohydrates is difficult and carbohydrates need to be labelled to improve their detection. Neutral carbohydrates lack a conjugated π -system and the absence of a chromophore restricts the use of UV detection. Hofstetter-Kuhn *et al.* ⁸⁷, managed to increase the UV detection of neutral carbohydrates, by forming on-column complexes with borates, which could be detected. Although the detection levels are still not attractive, the potential of borate complexation for sugar analysis was clearly demonstrated. In formation of borate complexes, neutral carbohydrates acquire a partial negative charge as they form a complex with the tetrahydroxyborate ion ⁸⁸, this is illustrated in Figure 10.

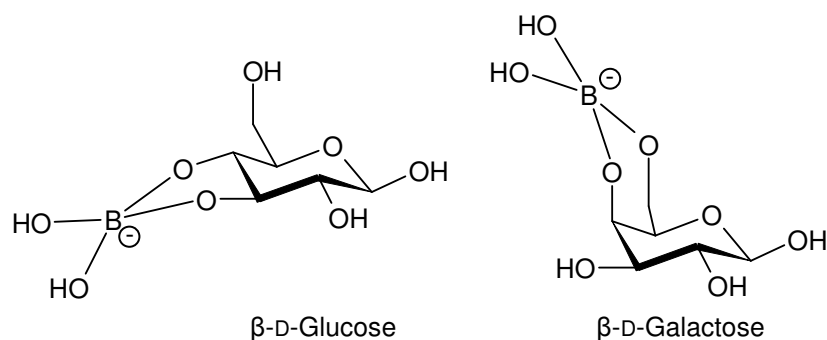


Figure 10: D-glucose and D-galactose Borate Complexes

The formation of borate complexes magnifies the small steric differences between closely related isomers, based on the tendency of borate to form more stable complexes with *cis*- rather than *trans*-oriented pairs of hydroxyl groups on adjacent or alternate carbon atoms⁸⁹. More recently this methodology has been used for monosaccharide analysis by Xioa *et al.*⁹⁰, who have reported baseline resolution greater than one minute between D-glucose and D-galactose using a borate buffering system.

1.6.2 Linkage Analysis

For determination of the linkage patterns in the repeating oligosaccharide, the majority of reported structures use the method developed by Stellner *et al.*⁹¹. This procedure has similarities to the monosaccharide analysis developed by Gerwig *et al.*⁸¹; before hydrolysis, all the unsubstituted hydroxyl groups are methylated. The methylated polysaccharide is then hydrolysed to monosaccharides using trifluoroacetic acid (TFA). The partially methylated monosaccharides are subsequently converted to alditols by reduction with sodium borodeuteride and the products acetylated with acetic anhydride. The derivatisation process is provided in Figure 11, which shows that the end product contains both methoxy (-OMe) and acetyl (-OAc) groups.

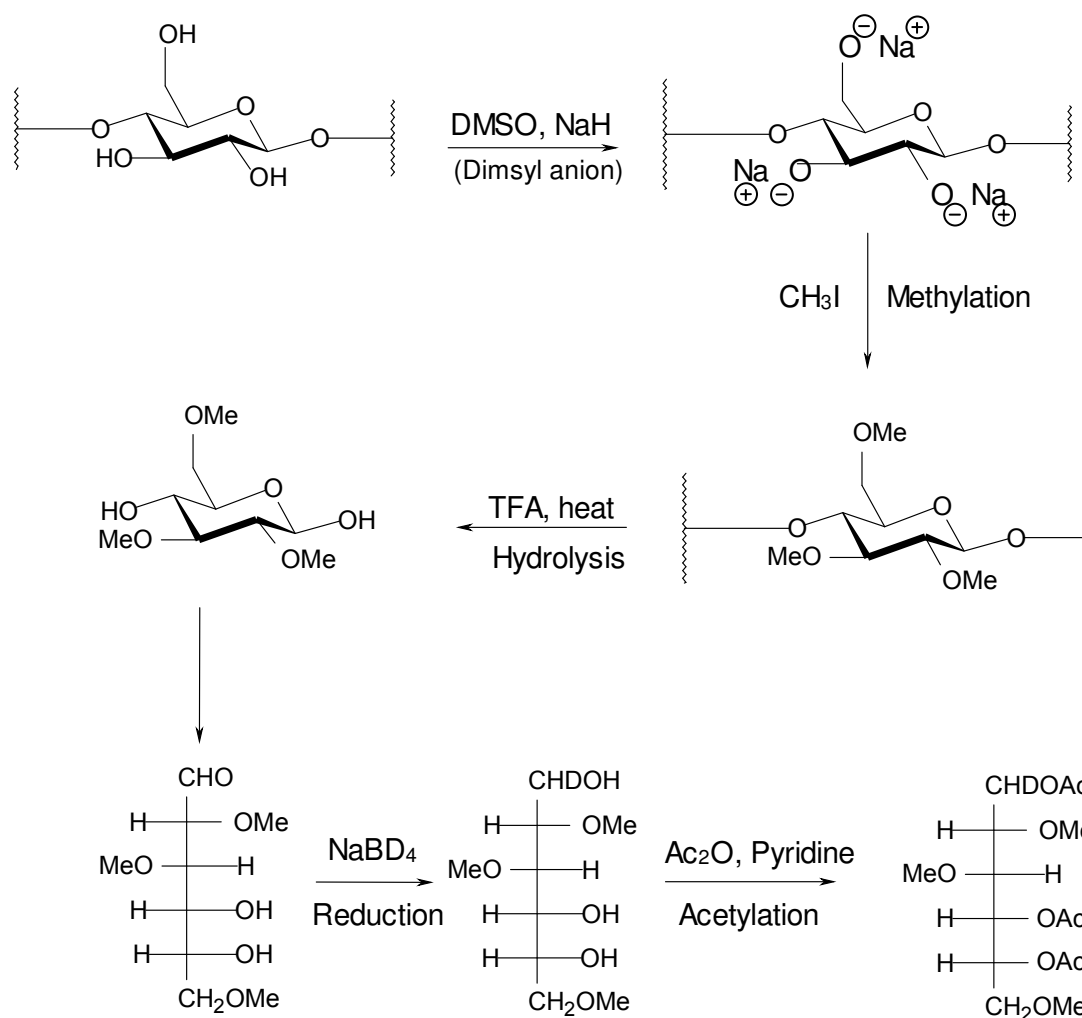


Figure 11: Chemical Derivatization Process of Linkage Analysis

The methoxy groups identify where a free hydroxyl group was present and the acetylated sites show where there was a glycosidic linkage to another monosaccharide. There are several different methods for the methylation; the most commonly used is the Hakomori method⁹², where dimethylsulfoniyl anion acts as a base and removes the free hydroxyl protons on the monosaccharide and then methyl iodide is added to form methoxy groups. The methylated alditol acetates are then analysed using GC-MS, and the fragmentation patterns are used to identify the positions of linkages.

An alternative procedure for the methylation of carbohydrates was developed by Ciucanu and Kerek⁹³. Their methylation procedure uses sodium hydroxide for base-catalysed ionisation of the hydroxyl groups, which is then followed by methylation using methyl iodide.

Ciucanu and Kerek report that this methylation procedure provides short reaction times, high yields and clean gas chromatograms. The procedure has been recently modified to use an excess amount of powdered sodium hydroxide to scavenge any water present in the sample. The absence of water means that per-*O*-methylation with methyl iodide was more feasible⁹⁴.

In recent publications, the 'Ciucanu methylation procedure' seems to be the preferred choice for the methylation of carbohydrates; Rodriguez-Carvajal *et al.*⁷⁹ have used the 'Ciucanu methylation procedure' to methylate a high-molecular weight EPS isolated from *Lactobasillus pentosus* LPS26. Kohno *et al.*⁹⁵ have used the 'Ciucanu methylation procedure' to characterise an extracellular polysaccharide produced by *Bifidobacterium longum* JBL05. The Micshnick Group (Institut für Lebensmittelchemie, Germany) have also been using this methylation procedure in their recent work^{96 97}, where they report the fragmentation patterns of regioselectively *O*-methylated malto-oligosaccharides and the substitution patterns of *O*-methyl- α - and β -1,4-glucans.

Other methylation procedures exist and they have recently been reviewed by Ciucanu⁹⁸. Highlighted methods include the use of metal oxide, where the carbohydrate is dissolved in methanol and then treated with silver oxide and methyl iodide^{99 100} or barium oxide and methyl iodide¹⁰¹. The drawbacks of these methods are that a suitable solvent cannot be found for polysaccharides. Other methods include using aqueous solution of metal hydroxide as the basic agent. This was first introduced by Denham and Woodhouse¹⁰², unfortunately this method gives a mixture of partially and fully methylated monosaccharides. None of these other methods has been successfully used to per-*O*-methylate carbohydrates. The two most successful are those developed by Hakomori⁹² and Ciucanu⁹³ described above.

1.6.3 NMR Analysis of Polysaccharides

Nuclear magnetic resonance spectroscopy (NMR) can be used to determine the anomeric configuration of the monosaccharides, and also how the monosaccharides are linked together in the repeating oligosaccharide unit of the EPS. Doco *et al.*⁸⁰, were the first to determine the structure of the repeating unit from an EPS, produced by *Streptococcus thermophilus* CNCMI 733 using NMR spectroscopy. Since this first publication, many structures have been published, that have utilised the advances in 1D- and 2D- NMR spectroscopy^{103 104 105}.

1.6.3.1 ¹H-NMR Spectra for Carbohydrates

In analysing NMR spectra, spectra are split into two separate regions, the anomeric region and the bulk region. The anomeric region is situated downfield from the ring protons due to the electron-withdrawing effects of the neighbouring ring oxygen atoms. Particular attention is placed on the anomeric region (4.4 – 5.6 ppm); the integration and number of signals in this region identifies how many monosaccharides are in the repeating oligosaccharide unit.

The configuration of the anomeric proton can be deduced from the ¹H-NMR spectra by using a combination of the ³J_{1,2H-H} and ¹J_{C-H} coupling constants. For monosaccharides adopting the ⁴C₁ chair conformation where the proton attached to carbon C2 is axial, the following rules apply: a monosaccharide has an α-anomeric configuration when the ³J_{1,2} coupling constant is less than 4Hz and β-anomeric configuration when greater than 7.5Hz. These figures are based on the values obtained from the Karplus curve, as described by Tafazzoli and Ghiasi¹⁰⁶, which shows the relationship between dihedral angle and the ³J_{1,2} coupling constants.

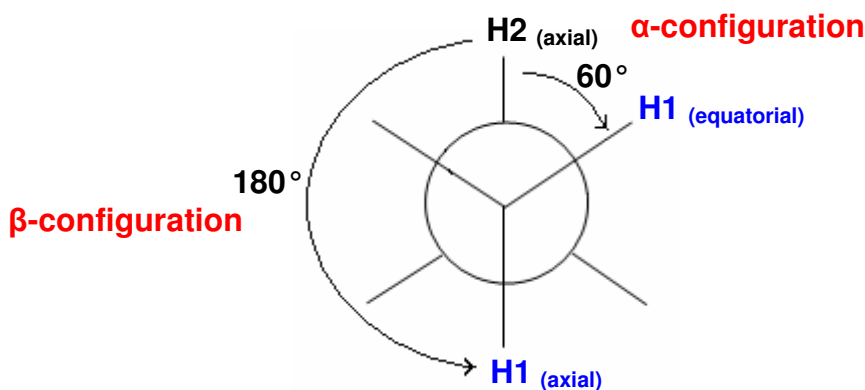


Figure 12: Newman Projection Showing the Dihedral Angles in D-glucose

It must be stressed that the Karplus curve can only be applied to sugars which have the hydrogen attached to carbon C2 in the axial position e.g. D-glucose and D-galactose. For these sugars an α -configuration is when the hydrogen, attached to carbon C1, is in an equatorial position and the hydrogen, attached to carbon C2, is in an axial position, therefore a dihedral bond angle of 60° . For a β -configuration both hydrogens are axial, so the dihedral bond angle is 180° . The angles for each configuration are shown in Figure 12, which shows the anomeric protons in blue.

The configuration can be visually assessed, where the peaks in the $^1\text{H-NMR}$ spectrum are observed as singlets for an α -configuration and doublets for a β -configuration. This can be inaccurate as it assumes adsorption of the $^4\text{C}_1$ conformation and often requires confirmation using the $^3\text{J}_{1,2}$ coupling constants. Also the $^1\text{J}_{\text{C-H}}$ coupling constants can discriminate between the two configurations, where a value of approximately 160Hz confirms the assignment of the β -configuration and a value exceeding 170Hz confirms the assignment of the α -configuration ¹⁰⁷.

1.6.3.2 DEPT135 $^{13}\text{C-NMR}$ spectra for Carbohydrates

The DEPT 135 $^{13}\text{C-NMR}$ spectrum shows all carbons present that are attached to a hydrogen ($-\text{CH}$, $-\text{CH}_2$ and $-\text{CH}_3$) in the analyte. The $-\text{CH}_3$ and $-\text{CH}$ signals are shown as positive peaks, where as the $-\text{CH}_2$ signals are negative. In aldohexoses, there are specific

regions of the DEPT 135 spectra in which certain carbons are observed. The $-\text{CH}$ signals from carbons C2 – C5 are generally located between 65 – 85 ppm, providing they have $-\text{OH}$ substitution. Carbons substituted with amino sugars or methyl groups give signals at a lower chemical shift. The carbon C1 signals are generally located between 95 – 105 ppm due to the adjacent electron withdrawing oxygen in the heterocyclic ring. The signals for carbon C6, are observed as $-\text{CH}_2$, therefore seen as negative peaks, which are generally located between 60 – 70 ppm. Any $-\text{CH}_3$ groups, such as from rhamnose, or *N*-acetyl-amino sugars are observed at a lower ppm, which can be used to quickly identify them.

1.6.3.3 Data from two-dimensional experiments

Using specific 2D- experiments which show the environment in which each carbon / hydrogen is positioned, the structure of complex oligosaccharide repeating units of EPSs can be determined.

These experiments are:-

2D-COSY	-	Two dimensional correlated spectroscopy
2D-TOCSY	-	Two dimensional total correlation spectroscopy
2D-HSQC	-	Two dimensional heteronuclear single quantum coherence
2D-HMBC	-	Two dimensional heteronuclear multiple bond correlation
2D-HSQC-TOCSY	-	Two dimensional heteronuclear single quantum coherence total correlation spectroscopy
2D-NOESY	-	Two dimensional nuclear overhauser effect-enhancement spectroscopy

An explanation of each experiment is given during the data interpretation, discussed in section 3.3.1.1.

1.6.3.4 Choice of solvent

Polysaccharides are insoluble in common NMR solvents such as CDCl_3 and d_6 -DMSO, therefore deuterium oxide (D_2O) is used. Unfortunately, D_2O gives a signal from the HOD in

the solvent which can mask important signals from the polysaccharide. This signal can be shifted when the samples are recorded different temperatures.

1.6.4 Weight-average Molecular Weight (M_w) Determination

The molecular weight determination of a polysaccharide is not rudimentary, because it cannot be attributed to one distinctive molecular weight as with monodispersed molecules. Polysaccharides have a range of molecular weights, therefore they are polydispersed molecules. They are generally characterised by using weight-average (M_w) or number-average (M_n) molecular weights. The polydispersity (M_w/M_n) is a ratio of weight-average molecular weight divided by the number-average molecular weight. A polymer is monodispersed if the M_w/M_n is equal to one,

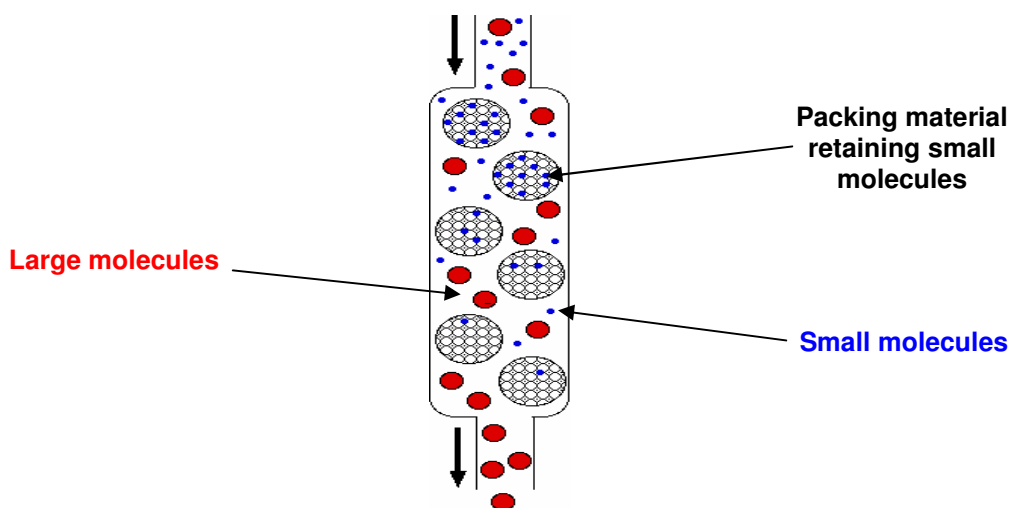
The size of a polysaccharide can be expressed by the number of monosaccharide units it contains. This is termed the degree of polymerisation (d.p).

High performance size exclusion chromatography with multi-angle laser light scatter detection (HP-SEC-MALLS) can determine the weight-average molecular weights (M_w) of macromolecules¹⁰⁸. This high performance chromatography system has begun to replace the older technique of separating polysaccharides, which used gel permeation chromatography (GPC). GPC is now mostly used for sample purification because of the large volumes that can be loaded onto the column. The HP-SEC-MALLS uses columns which provide greater resolution and they can withstand much greater back pressure, which results in greatly improved chromatography in terms of speed and separation capability.

1.6.4.1 Size Exclusion Chromatography

Size exclusion chromatography (SEC) is used to analyse molecules such as polysaccharides, proteins, and industrial polymers. SEC is the simplest chromatographic method, which is based on separation of particles with respect to their size¹⁰⁹.

The column packing consists of particles containing various size pores and pore networks, so that molecules are retained or excluded on the basis of their size and shape. The sample is introduced into the flow of the mobile phase which passes through the column. The molecules are separated according to their size.



Large molecules elute first, small molecules are retained

Figure 13: Diagram of the Interaction of Molecules with the Column Particles

Very large molecules cannot enter many of the pores, and they also penetrate less into the comparatively open regions of the packing, thus interacting less with the stationary phase than smaller molecules do. This means that the larger molecules elute faster than the smaller molecules, because very small molecules diffuse into all or many of the pores accessible to them. Between these two extremes, intermediate-size molecules can penetrate some passages, which delays their progress down the column, and exit at intermediate times. For a comprehensive review of size exclusion chromatography the reader is directed to Barth *et al.*¹⁰⁹.

The stationary phases used for separating carbohydrates are strongly hydrophilic. The phases used in GPC are made from rigid allyl dextran / bisacrylamide matrix, such as Sephacryl™ (GE Healthcare, Piscataway, NJ, USA). The phases used for high performance size exclusion chromatography of carbohydrates are made from hydroxylated

methacrylic polymer beads. The two leading column manufacturers are Varian Inc. Corporation (Palo Alto, CA, USA) who makes the Aquagel-OH column range and Tosoh Bioscience (Tokyo, Japan) who makes the TSK-gel range of columns.

1.6.4.2 Multi-angle laser light scatter detection

Multi-angle laser light scattering (MALLS) is one of the most direct and effective ways of obtaining molar mass and size information of polymers and biopolymers ¹¹⁰. It has been used to determine the weight-average molecular weights of several bacterial exopolysaccharide structures ^{111 112,113}.

When laser light focuses on a macromolecule, the oscillating electric field of the light induces an oscillating dipole within it, which will re-radiate light ¹¹⁰.

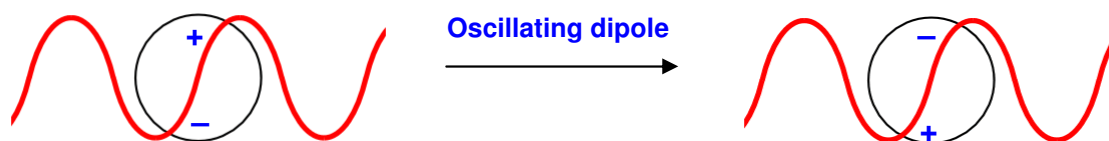


Figure 14: Oscillating Dipole in a Macromolecule (Adaption of Diagram from Wyatt) ¹¹⁰

The intensity of the radiated light depends on the magnitude of the dipole induced in the macromolecule, which depends on its polarizability. It is necessary to know the macromolecule polarizability to determine the scattering from a solution of such macromolecules. This may be determined from the measurement of the dn/dc value also referred to as the 'specific refractive index increment' ¹¹⁴.

1.6.4.3 Refractive Index Increment (dn/dc)

The dn/dc value describes how much the refractive index of a polymer solution changes with respect to the concentration of the solute. Measurement of dn/dc is essential for the absolute characterization of the molar mass, since it is a term used in the molar mass

calculation. Polymers with larger values of dn/dc scatter more light at the same mass than those having smaller values. Therefore, knowing dn/dc permits the deduction of molar masses from the light scattering data. Because dn/dc changes with wavelength, it is vital to measure it at the same wavelength as the light scattering apparatus.

The refractive index detector requires a calibration constant so that the software can convert the signals to Rayleigh ratios and refractive index differences respectively. The calibration constant must be determined before the instrument can measure dn/dc values. The calibration constant is measured using a suitable solvent, such as toluene, due to its high and accurately determined Rayleigh ratio and also its refractive index is similar to the cell windows in the refractive index detector ¹¹⁰.

1.6.4.4 Differential Refractive Index

Differential refractive index detection is a process whereby solvent passes through one half of the cell and the sample passes through the other half of the cell. The two compartments are separated by a glass plate positioned at an angle such that bending of the incident beam occurs if the two solutions differ in refractive index. This resulting displacement of the beam causes variation in the output signal, which, when amplified and recorded, provides the chromatogram that can be used to measure the concentration of macromolecules, such as polysaccharides. Differential refractive index detectors are used on HPLC instruments, providing signals for chromophore and non-chromophore containing analytes. Refractive index detection is not as sensitive as UV detection, therefore are normally only used for analysis of compounds with poor UV absorption.

Refractive index detectors are also used for the calculation of dn/dc , refractive index detectors respond to nearly all solutes. A list of dn/dc values was published by Theisen *et al.* ¹¹⁵, which shows that in aqueous systems most dn/dc values of macromolecules lie between 0.14 – 0.16 mL g⁻¹.

An older technique that was used to determine M_w of polysaccharides was to use SEC with a differential refractometer to compare the retention times of the analyte to a calibration curve generated from a series of different M_w standards. An example of this has been reported by Beer and co-workers, who used a series of pullulan and dextran standards to determine the M_w of guar gum. This approach is acceptable for simple homopolysaccharides that have similar structures to the standards, but for exopolysaccharides that can be complex heteropolysaccharides the M_w determined are inaccurate, which is why M_w determination using dn/dc values is now the preferred technique. The use of light scattering can more accurately determine the M_w of polysaccharides compared to this older technique, especially when a dn/dc value that is specific for the particular polysaccharides is used.

1.6.4.5 UV Detection of Proteins and Nucleic acid

Ultra-violet (UV) detection is another well established method; this detector technique measures the UV absorption of the sample. The sample is passed through an incident UV beam and the amount of UV light absorbed is measured. As neutral carbohydrates are poorly detected by a UV detector, due to the lack of conjugated π -bonds, the purpose of the UV detector, in the analysis of EPS samples, is to detect residual protein and nucleic acids. The UV detectors are set to 260 nm to detect any nucleic acids impurities and set to 280nm to detect any protein impurities. Protein absorbs UV light due to the presence of three amino acids, phenylalanine, tyrosine and tryptophan, which all give a strong UV response at 280nm.

1.6.4.6 HP-SEC-MALLS System

In HP-SEC-MALLS, the light scattering and other detectors are connected in series after the size-exclusion columns. The detectors are usually set up with the ultra-violet (UV) detector first, then the laser light scatter detector and finally the refractive index (RI), as shown in Figure 15.

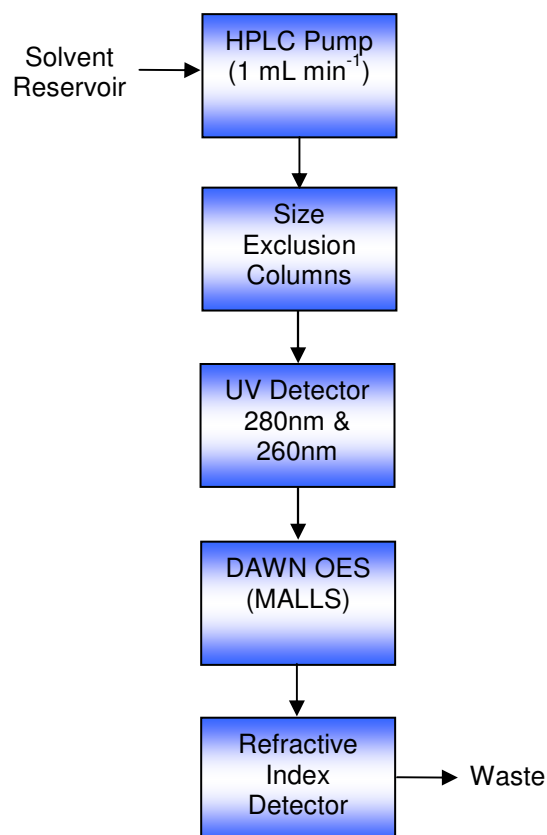
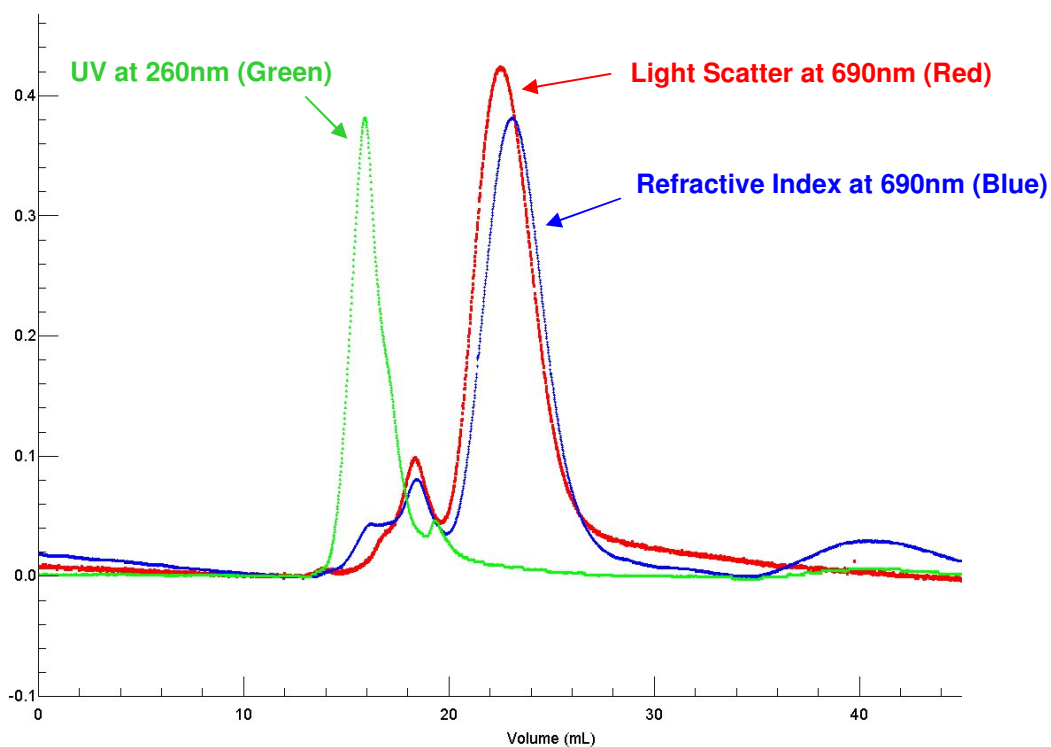


Figure 15: Schematic of the HP-SEC-MALLS

The molecular weight is calculated by applying measurements from the laser light scatter detector and the refractive index detector to a series of equations that are reviewed by Phillip Wyatt ¹¹⁰.

The analysis of light scattering data can be processed using different mathematical equations. The most common equation used to derive M_w is using the Debye plot; other equations available are the Zimm and Berry plots. By applying these different types of plots, more accurate results can be generated for different types of macromolecules. Andersson *et al.* ¹¹⁶, reviews each equation, and suggests that the Berry method is superior, in terms of accuracy and robustness. They also conclude that errors in the different equations are less than 1% for molecules with low root-mean square radius of <50nm. All the macromolecules measured in this thesis had radius <50nm. Therefore, any of the three different mathematical equations could be used, without significantly altering the results.

The responses from each of the three detectors are plotted on the same chromatogram. An example of a plot obtained for an exopolysaccharide solution can be seen in Figure 16, which shows that for this particular sample, there is a 260nm UV signal (green) corresponding to the first peak, showing that it is probably due to nucleic acid.



- Major peak due to Exopolysaccharide
- Secondary peak due to Nucleic acids

Figure 16: Example of a HP-SEC-MALLS Chromatogram of an Exopolysaccharide

The major peak has a large light scatter (red) and refractive index (blue), and no UV response, this is characteristic of a polysaccharide.

1.6.4.7 Sedimentation Analysis

Another technique that is used for the determination of the size and shape of polysaccharides is sedimentation analysis. Sedimentation analysis is a type of ultracentrifugation analysis developed as early as 1920s by Svedberg¹¹⁷. The type of information that can be obtained from ultracentrifugation analysis depends on the particular technique used. There are four ultracentrifuge methods which can provide information about

polysaccharides. These are sedimentation velocity, sedimentation equilibrium, isopycnic density gradient analysis and diffusion analysis. The potential information available is provided in Table 4 ¹¹⁸.

Table 4: Ultracentrifuge Methods and the Potential Information Available

Ultracentrifuge method	Potential information available
Sedimentation velocity	Sample homogeneity / purity
	Shape information
	Interaction information
Sedimentation equilibrium	Size (molar mass)
	Size / molar mass distribution
	Interaction information
Isopycnic density gradient analysis	Sample Purity
Diffusion analysis	Small molecules through polysaccharide matrix
	Interface transport

Sedimentation equilibrium provides similar information to the MALLS system described in section 1.6.4.2. For sedimentation equilibrium, a much lower rotor speed is used, less than 10,000 rpm. The distribution of equilibrated solute concentrations of polysaccharides are recorded using sensitive refractive index detectors.

The advantages of using sedimentation equilibrium analysis are that reliable molar mass measurements can be made for polysaccharides with no problem of interference with dust particles or supramolecular contamination, which can be one of the problems encountered when using light scattering techniques. Sedimentation analysis is also better for measuring the distribution analysis. Also the natural ability of sedimentation analysis to separate, means there is no need for separating columns or membranes ¹¹⁸.

1.7 New Methods of Analysis

The methods described in section 1.6 have been applied to the analysis of polysaccharides, and in most cases have been used to characterise the chemical and physical structures of exopolysaccharides. This section describes proposed novel approaches for measuring the physical characteristics and structures of exopolysaccharides, and serves to provide the Carbohydrate community with novel analytical approaches for the structural analysis of exopolysaccharides. In terms of monosaccharide composition and linkages present in the oligosaccharide repeating structure, the methods are faster and more sensitive than those currently available.

1.7.1 *Depolymerisation Techniques*

As described previously exopolysaccharides are composed of repeating oligosaccharide units joined together to form a large polysaccharide chain which, when present in an aqueous environment, provides a viscous solution^{119 120 121 122}. The viscosity of the exopolysaccharide solution is related to their degree of polymerisation; for polysaccharides having the same repeating unit the viscosity increases with the degree of polymerisation¹²³. There are a number of areas where it would be beneficial to manipulate the degree of polymerisation of exopolysaccharides: to reduce the peak broadening of viscous solutions in NMR; to monitor the relationship between the exopolysaccharide chain length and solution viscosity.

There are several techniques that have been reported to depolymerise macromolecules. These are constant pressure disruption (application of hydrodynamic shear), ultrasonic disruption and mild-acid catalysed hydrolysis. Constant pressure and ultrasonic disruption use physical forces to affect the polysaccharide, whereas acid hydrolysis uses chemical reaction.

1.7.1.1 Constant Pressure Disruption (Application of Hydrodynamic Shear)

Constant pressure disruption uses physical force to break open cells. This is a device predominantly used by microbiologists to break open cell membranes to extract DNA and enzymes. It is thought that the hydrodynamic behaviour of the fluid in the disruptor is important when considering the mechanics of this disruption process (Lovitt *et al.*, 2000)¹²⁴.

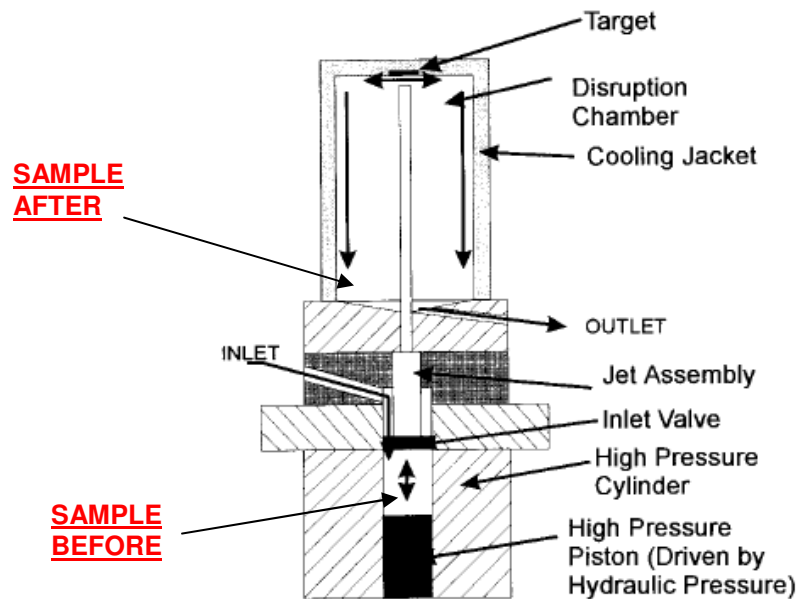


Figure 17: Diagram of Constant Pressure Disruptor (Lovitt *et al.*, 2000)¹²⁴

This mechanical disruptor works by forcing a solution through a small orifice at a specified pressure and the solution is then collected in the top chamber. If required the disrupted solution can then be repeatedly disrupted at the same or different pressures. Lovitt *et al.* (2000)¹²⁴ used a constant pressure disruptor to release enzymes from bakers' yeast. From their studies they changed two experimental variables that affected the extent of the disruption. The two variables were the pressure applied and viscosity of solvent. The solvent viscosity will alter the hydrodynamic behaviour, which will change forces exerted through the sample. It was envisaged that the forces created by this technique would be enough to break the structure of polysaccharides.

1.7.1.2 Ultrasonic Disruption

Ultrasonic disruption is another technique used to open cell membranes. Ultrasonic disruption can also be used to cleave DNA, or other macromolecules, and uses high frequency sound waves. It is usually applied to biological materials, but can also be used to speed up the rates of chemical reactions.

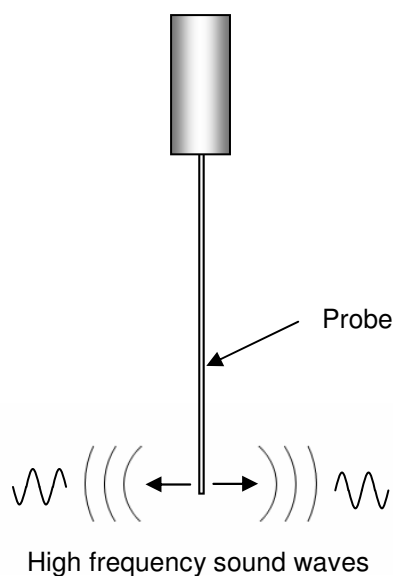


Figure 18: Diagram of a Sonication Probe

The principle of ultrasonic disruption is that it converts 50-60 Hz line voltage to high frequency electrical energy which is then converted to mechanical vibrations via a piezoelectric transducer. These vibrations are intensified by the probe creating waves through the liquid. The action forms millions of microscopic bubbles, which expand during the negative pressure excursion, and implode violently during the positive excursion; as the bubbles implode they cause millions of shock waves and eddies to radiate outwardly from the site of collapse. This effect, referred to as 'cavitation', generates extreme pressures and temperatures at the implosion sites ¹²⁵.

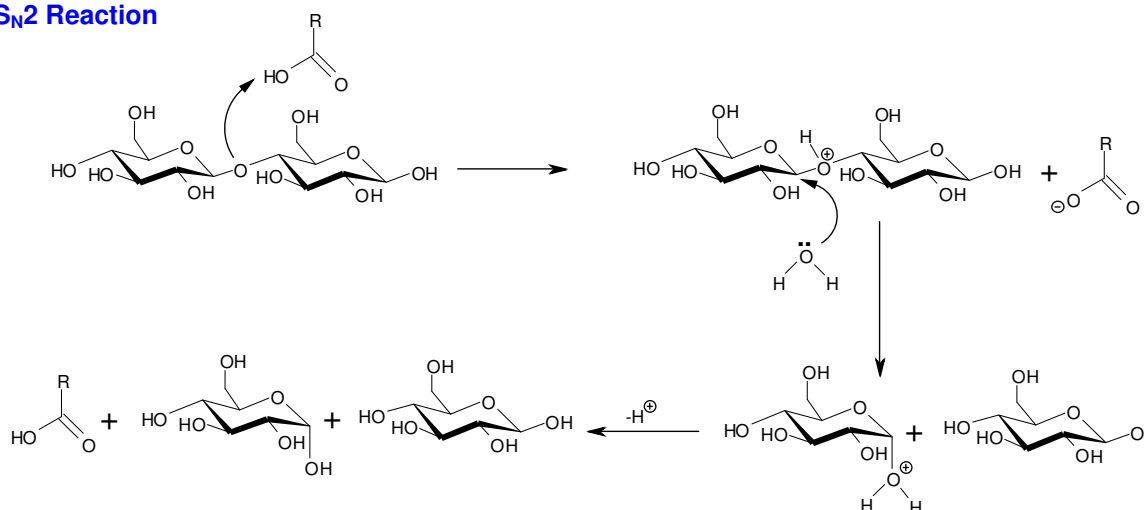
The effect of ultrasonic disruption can be altered by changing the amplitude, pulse time and probe size ¹²⁵.

This technique has been used to successfully depolymerise polysaccharides^{126 127}, although there has been no work reported that has used ultrasonic disruption to depolymerise exopolysaccharides produced by LAB.

1.7.1.3 Acid-catalysed Hydrolysis

Acid-catalysed hydrolysis can be used as a depolymerisation technique, but this time a chemical reaction is responsible for breaking the bonds. The reaction can proceed as either an S_N1 or an S_N2 reaction, which are shown in Figure 19.

S_N2 Reaction



S_N1 Reaction

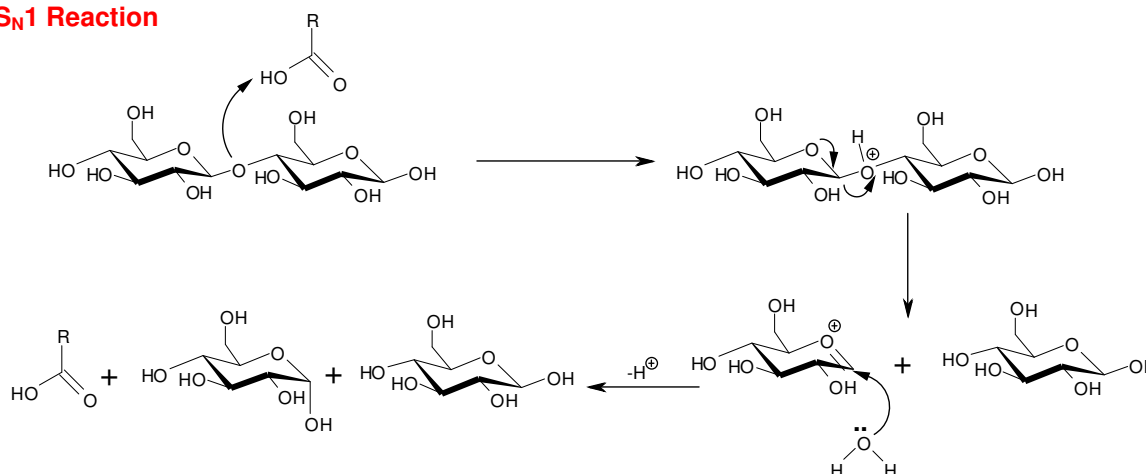


Figure 19: S_N1 and S_N2 Reaction Mechanisms for Acid-catalysed Hydrolysis of Sugars

The hydrolysis reaction is catalysed by acid, and it is an old established technique first reported by Hakomori⁹², where the polysaccharides were fully hydrolysed to

monosaccharides, the first stage of the monosaccharide analysis described earlier in section 1.6.1.

1.7.1.4 Mild-Acid Catalysed Hydrolysis

To provide structural information during depolymerisation only partial acid-catalysed hydrolysis is required. This can be carried out using mild acid conditions at low temperatures. Due to the nature of this particular reaction, other, unwanted, reactions may take place, such as the removal of functional groups attached to monosaccharides, in particular, removal of the *N*-acetyl groups in *N*-acetyl-amino sugars⁸³. Any chemical modification would be observed in NMR and GC analysis.

1.7.1.5 Other Depolymerisation Techniques

Two other depolymerisation techniques recently reported are the use of microwave-assisted depolymerisation and enzymic hydrolysis.

Microwave-assisted depolymerisation has been carried out on hyaluronan by Drimalova *et al.*¹²⁸ and Bezakova *et al.*¹²⁹. They monitored the change in molecular and structural properties of hyaluronan, which is a polysaccharide made up of alternating β -1,4- and β -1,3-linked disaccharides of D-glucuronic acid and D-*N*-acetyl-glucosamine. They reported a reduction in chain length, but no change to the primary structure.

Enzymic hydrolysis can be applied differently for structural analysis of polysaccharides. It has been used by Rinaudo and Milas¹³⁰ in an investigation of enzymic hydrolysis of xanthan using cellulase. They used enzymic hydrolysis to reduce the exopolysaccharide chain length, they reported that in salt-free solution there is a random breakdown in the polysaccharide chain. Similar findings were reported by Sutherland¹³¹ who used a fungal cellulase to hydrolyse xanthan.

Enzymic hydrolysis can also be used to cleave branches from the repeating unit of exopolysaccharides. The removal of branches from the repeating unit can be used to simplify complicated NMR spectra and can be used to confirm the structure. This technique has been successfully employed by van Casteren *et al.*¹³² who removed a terminal D-galactose, using an unnamed enzyme, from the EPS produced by *Lactococcus lactis* subsp. *cremoris* B891. Others, Nankai *et al.*¹³³, Jansson *et al.*¹³⁴ have also used this methodology to reduce exopolysaccharides to heptasaccharides by cleaving a specific glycosidic linkage.

1.7.2 Derivatisation of Carbohydrates

Neutral carbohydrates contain no conjugated π -bonds and carry no formal charge. This makes their detection and analysis challenging. For many years neutral carbohydrates have been detected by refractive index detection, but this technique has poor sensitivity and is prone to large inaccuracies when compared to other popular forms of detection, such as UV. To provide greater precision, accuracy and sensitivity, derivatisation of neutral carbohydrates is required. The established derivatisation method for monosaccharide and linkage analysis of exopolysaccharides has previously been described in sections 1.6.1 and 1.6.2, where hydrolysis, reduction, acetylation and methylation have all been discussed. An alternative method is to use reductive amination to label carbohydrates.

1.7.2.1 Reductive Amination

Reductive amination is where an amine first reacts with a carbonyl group to form an iminol, which subsequently loses one molecule of water in a reversible reaction to form an imine.

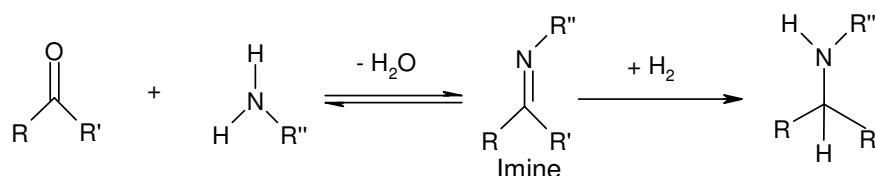
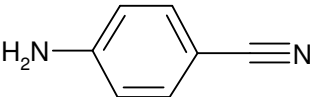
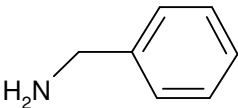
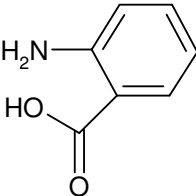
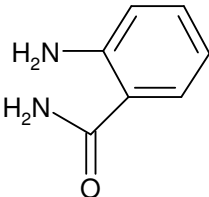


Figure 20: Reaction – Reductive Amination

The equilibrium between aldehyde / ketone and imine can be shifted toward imine formation by removal of water. This intermediate imine can then be isolated and reduced with a suitable reducing agent (e.g. sodium borohydride).

It is possible to carry out both reactions at the same time, with the imine formation and reduction occurring simultaneously¹³⁵. This is carried out with reducing agents that are more reactive toward imines than ketones, such as sodium cyanoborohydride (NaCNBH_3) or sodium triacetoxyborohydride ($\text{NaBH}(\text{OCOCH}_3)_3$). The use of several different amines has been reported, including: benzylamine¹³⁶, 2-aminobenzoic acid¹³⁷, 2-aminobenzamide¹³⁷; structures are given in Table 5.

Table 5: Table of Reported Amines used for Reductive Amination

Amine	Structure	Formula Weight (g mol^{-1})
p-Aminobenzonitrile		118.14
Benzylamine		107.16
2-Aminobenzoic acid		137.14
2-Aminobenzamide		136.15

The use of p-aminobenzonitrile (pABN) has been reported by several research groups most notably by Suzuki *et al.*¹³⁸.

1.7.2.2 Reductive Amination of Carbohydrates

As explained in earlier sections, exopolysaccharides usually contain neutral sugars which carry no formal charge or chromophore. This makes them difficult to detect using conventional HPLC (using UV detection or mass spectrometry). By carrying out the reductive amination with an amine species that contains an aromatic ring the derivatised sugars will contain a chromophore and when in an acidic environment carry a formal positive charge, hence increasing the sensitivity to both UV and electrospray mass spectrometry detection.

1.7.3 Analytical Techniques

One of the main aims of this project was to provide the 'Carbohydrate community' with novel analytical approaches for the structural analysis of exopolysaccharides. Ideally, any new method should be faster and more sensitive than the current methods. This section will describe different analytical techniques that will be used to conduct the proposed research.

1.7.3.1 Capillary Zone Electrophoresis

The application of capillary zone electrophoresis for the analysis of carbohydrates has been discussed previously in section 1.6.1.2, which describes a review by Paulus and Klockow⁸⁶ about the separation and detection of monosaccharides. Paulus and Klockow discuss different methods of detection (using UV, amperometric and RI detectors) for derivatised and non-derivatised carbohydrates. The review provides the detection limits of each technique, which are given in Table 6.

Table 6: Detection Limits of the Different Techniques used for Carbohydrate Analysis

Detection Technique	Details	Detection Limit	Reference
UV Detection	Non-derivatised carbohydrate at 195nm (Optimum wavelength)	10^{-3} M	Hoffstetter-kuhn <i>et al.</i> (1991) ¹³⁹
Amperometric	Non-derivatised carbohydrate using a gold wire electrode	10^{-6} M	O'Shea <i>et al.</i> (1993) ¹⁴⁰
RI Detection	Non-derivatised carbohydrate	10^{-4} M	Bruno <i>et al.</i> (1991) ¹⁴¹
UV Detection	Derivatised carbohydrate using reductive amination (pABN) at 285nm (Optimum wavelength)	10^{-7} M	Schwaiger <i>et al.</i> (1994) ¹⁴²

Although the review by Paulus and Klockow is more than 10 years old, the comparisons between the different detection techniques are useful. The methods show that non-derivatised carbohydrates can be detected using UV, RI and amperometric detectors, with differing sensitivity. The use of amperometric detection is very sensitive, and close to the sensitivity of methods using derivatised carbohydrates that use UV detection. The combination of derivatising the carbohydrates and detecting them using UV will be developed further in this project.

1.7.3.2 Chromatography and LC-MS

Chromatography is an essential component for the monosaccharide composition and linkage analysis of carbohydrates. The separation of carbohydrates can be extremely difficult, as the majority of them contain the same functional groups and are often of the same mass. Separation of isomeric species is required, which has been made possible using

chromatography techniques such as gas chromatography (GC), high performance anion exchange chromatography (HP-AEC) and size exclusion chromatography (SEC). Each of these methods has limitations. With the development of new hyphenated LC-MS methods there is scope for the use of this technology to produce new analytical methods for analysing monosaccharide composition and linkages in carbohydrates.

As discussed in section 1.6.2, GC-MS has been used for many years to determine the glycosyl linkages analysis of oligo- and polysaccharides. Until the beginning of the 1990s the analysis of carbohydrates by mass spectrometry was limited to the use of electron impact (EI) and the fast-atom bombardment mass spectrometry (FAB). Recently there have been a number of mass spectrometry techniques developed, in particular, the development of desorption/ionization techniques like matrix assisted laser desorption/ionisation (MALDI) and electrospray (ESI), which in the past 10 years has allowed the application of liquid chromatography coupled to mass spectrometry to structurally characterise carbohydrates. Some of the earliest LC-MS work on carbohydrates has been reported by Reinhold *et al.*,¹⁴². Using a LC coupled to CID-MS, they successfully determined sequence, linkage and branching data of carbohydrates. Since the publication by Reinhold *et al.*¹⁴², mass spectrometers have developed, in particular in the area of mass spectrometry detection, with the development of ion-trap (IT), time-of-flight (TOF) and fourier transform ion cyclotron resonance (FT-ICR) mass analysers. Recently, each of these types of mass spectrometer has been used to determine the structures of carbohydrates by IT-MS¹³⁶, TOF-MS¹³⁷ and FT-ICR-MS¹⁴³.

To provide the 'Carbohydrate community' with novel analytical approaches for the structural analysis of exopolysaccharides, this project will utilise certain aspects of other workers' results to produce oligosaccharides which, when charged, can be analysed using LC-MS-MS to determine their monosaccharide make up. To some extent other groups have initiated work in this area:

Anumula and Dhume ¹⁴⁴ have separated reductively aminated oligosaccharides using amide columns under normal phase chromatographic conditions. The structures were confirmed using MALDI-TOF-MS. The oligosaccharides that were analysed were not novel.

Stephens' group at the University of Cambridge have reductively aminated oligosaccharides with 2-aminobenzoic acid and 2-aminobenzamide. The labelled oligosaccharide was then successfully analysed by normal-phase liquid chromatography coupled to MALDI-TOF-MS

¹³⁷.

Work has been reported identifying oligosaccharides in milk using LC-ESI-ITMS ¹⁴⁵. Broberg used reductive amination with benzylamine followed by *N,N*-dimethylation to produce DMBA-oligosaccharides with fixed positive charge at the former reducing terminus. The derivatised oligosaccharide was then analysed using LC-ESI-ITMS.

Even though the developments in LC-MS have progressed, there have been no publications using this technique to characterise the repeating structure of exopolysaccharides. The work carried out during this report will attempt to develop methods that incorporate methylation of EPS to aid the analysis of the intact oligosaccharide repeating unit or the glycosidic linkage positions of the individual monosaccharides residues of the repeating EPS oligosaccharide unit.

1.8 Research Aims

The research aims of this project were divided into three distinctive sections:

The first aim of this project will be directed at using spectrometry (NMR and MS) to characterise bacterial polysaccharides. A number of novel exopolysaccharides have been produced from LAB by the group of Prof. V. Marshall and Dr. A. Laws in the department of Chemical and Biological Sciences at the University of Huddersfield. The molecular structure

of the EPS produced by *Lactobacillus acidophilus* 5e2 has yet to be determined. Using current techniques, such as NMR and GC-MS the monosaccharide and linkage analysis of the repeating oligosaccharide structure will be determined. HP-SEC-MALLS will be used to determine the M_w of EPS produced from *Lactobacillus acidophilus* 5e2. An accurate weight-average molecular weight will be determined by measuring the specific refractive increment (dn/dc value) for this EPS. This value will be used in the calculation to provide a more accurate representation of M_w . The production of the EPS during fermentation will be periodically monitored, in particular the yield and M_w of the EPS will be evaluated. A thorough study of EPS production has never been reported before, this study could potentially resolve many uncertainties surrounding the physical aspects of EPS production by LAB during milk fermentation.

The second aim of this project will be to study the depolymerisation of the EPS produced by *Lactobacillus acidophilus* 5e2; using both established and novel approaches, the change in weight-average molecular weight will be closely monitored. This will provide a greater understanding of how chain length varies during depolymerisation using several different techniques. The rheological properties will also be examined, in particular, the intrinsic viscosity will be calculated for EPS samples that have differing M_w distributions.

The final aim of this project will be to develop a novel approach to determine the structures of the oligosaccharide repeating units of EPSs. This will involve designing a method capable of determining the structure of intact oligosaccharides, and also a method that will provide the linkage analysis between each monosaccharide in the repeating oligosaccharide units of EPSs. The methods will utilise the recent developments in CZE and LC-MS, providing greater sensitivity and faster analysis times than current methods used for characterising exopolysaccharides.

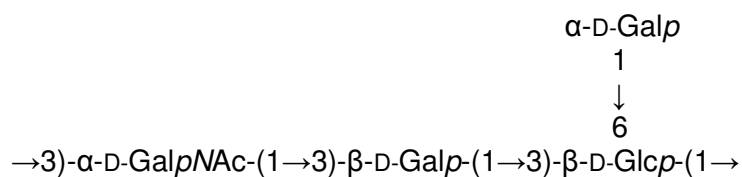
The overarching objective of the programme of work is to provide the Bioorganic / Carbohydrate community with new and more sensitive methods for the analysis of bacterial polysaccharides, in terms of their chemical structures and physical properties when in solution.

1.9 Appendices

1.9.1 EPS Structures from Lactic Acid Bacteria

1.9.1.1 EPS Structures from *Str. thermophilus* (A-F)

(A)

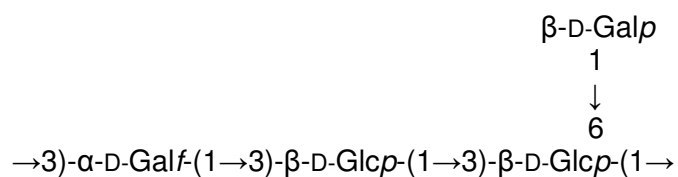


Str. thermophilus CNCCMI 733, 734, 735⁸⁰

Str. thermophilus Sfi6¹⁴⁶

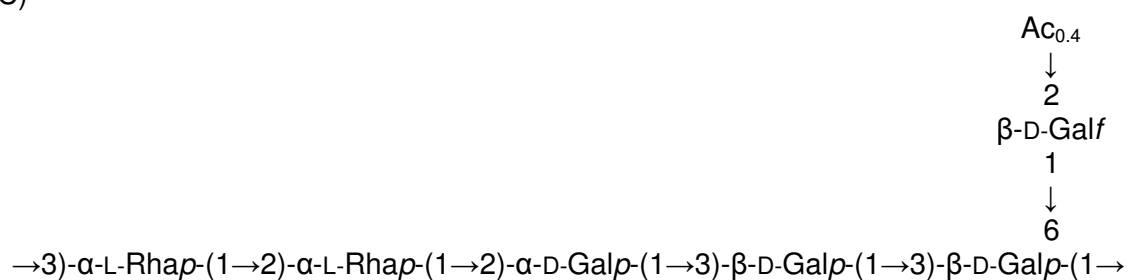
Str. thermophilus Sfi20¹⁴⁷

(B)



Str. thermophilus Sfi39¹⁴⁶

(C)

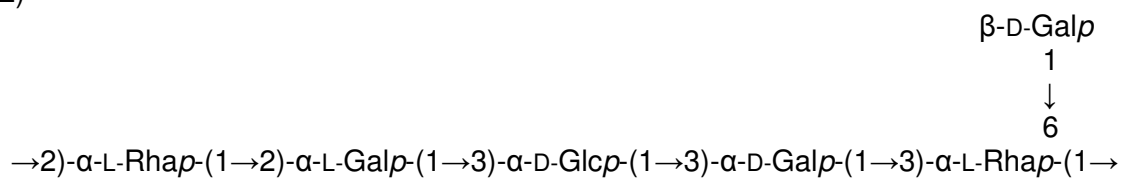


Str. thermophilus S3¹⁴⁸

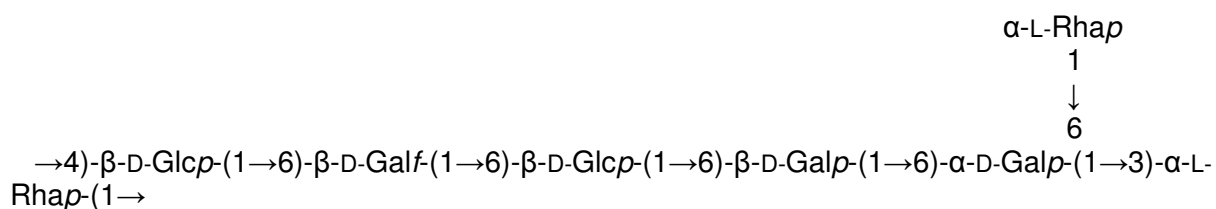
(D)

*Str. thermophilus* OR901¹⁴⁹*Str. thermophilus* Rs¹⁵⁰*Str. thermophilus* Sts¹⁵⁰

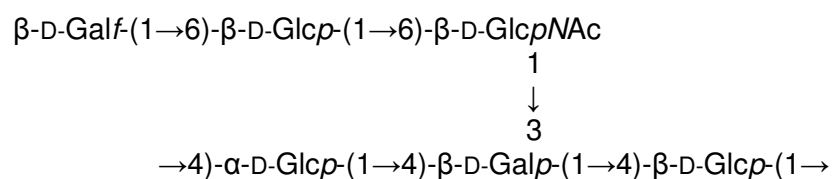
(E)

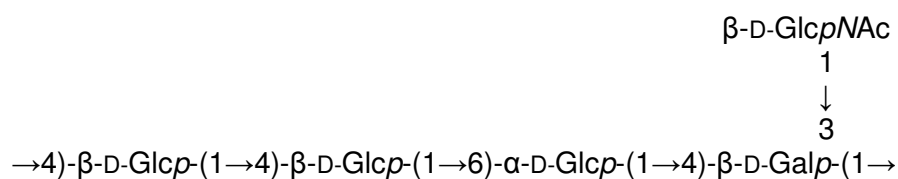
*Str. thermophilus* Sti12⁷⁵

(F)

*Str. thermophilus* EU20¹⁵¹

1.9.1.2 EPS Structures from *Str. macedonicus*

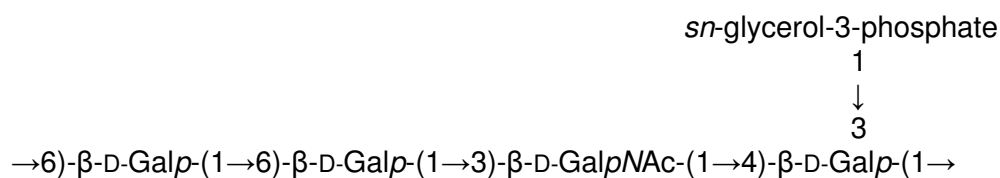
*Str. macedonicus* Sc136⁷⁴

1.9.1.3 EPS Structures from *Lactobacillus acidophilus*

Lactobacillus acidophilus LMG9433 ¹⁵²

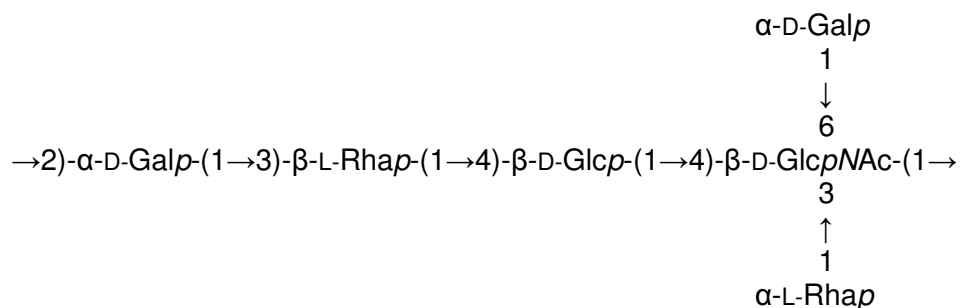
1.9.1.4 EPS Structure from *Lactobacillus paracasei* (A-B)

(A)



Lactobacillus paracasei 34-1 ¹⁵³

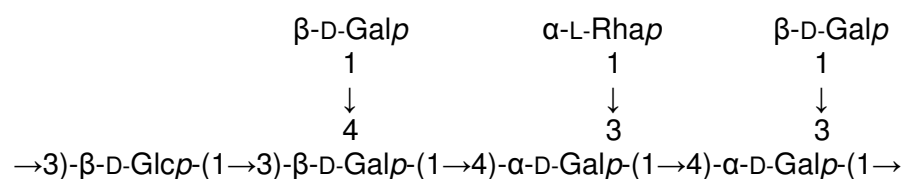
(B)



Lactobacillus paracasei Type V ¹⁵⁴

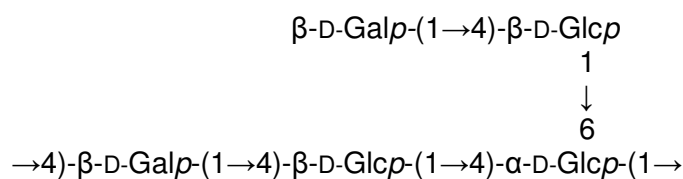
1.9.1.5 EPS Structures from *Lactobacillus delbrueckii* subsp. *bulgaricus* (A-D)

(A)

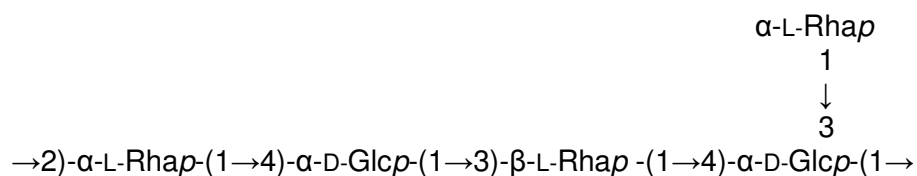


Lactobacillus delbrueckii subsp. *bulgaricus* rr ⁷⁶

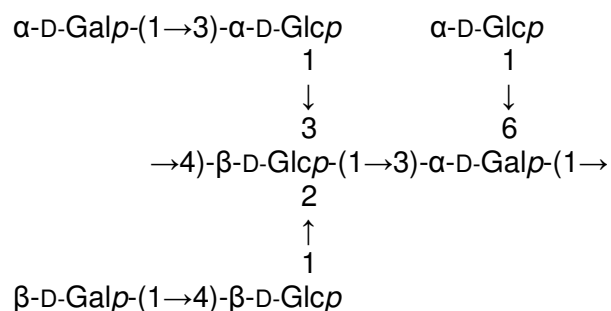
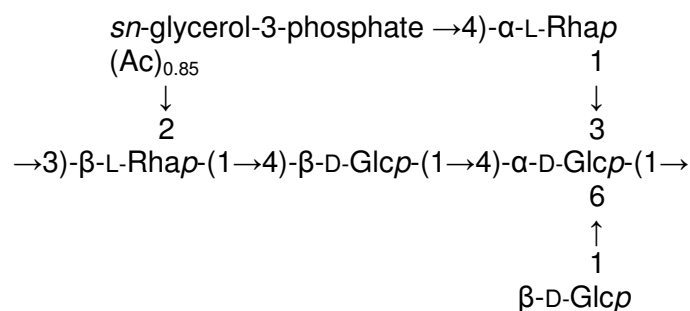
(B)

*Lactobacillus delbrueckii* subsp. *bulgaricus* 291¹⁵⁵

(C)

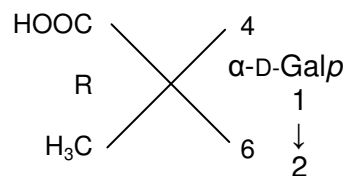
*Lactobacillus delbrueckii* subsp. *bulgaricus* EU23¹⁰⁴

(D)

*Lactobacillus delbrueckii* subsp. *bulgaricus* NCFB2074⁷⁸1.9.1.6 EPS Structures from *Lactobacillus sakei**Lactobacillus sakei* 0-1¹⁵⁶

1.9.1.7 EPS Structures from *Lactobacillus rhamnosus* (A-C)

(A)



→3)-α-L-Rhap-(1→3)-β-L-Rhap-(1→2)-α-D-Glcp-(1→3)-α-L-Rhap-(1→3)-α-D-Glcp-(1→3)-α-L-Rhap-(1→

Lactobacillus rhamnosus R W 9595 M and R ¹⁵⁴

(B)

→6)-α-D-Galp-(1→6)-α-D-Glcp-(1→3)-β-D-Galf-(1→3)-α-D-Glcp-(1→2)-β-D-Galf-(1→

Lactobacillus rhamnosus C83 ¹⁵⁷

(C)

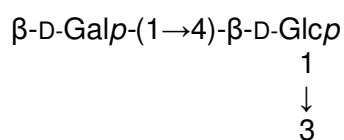


→3)-α-L-Rhap-(1→3)-α-D-Galp-(1→3)-β-D-Galf-(1→3)-β-D-Galp-(1→4)-α-D-GlcfNAc-(1→

Lactobacillus rhamnosus GG (ATCC 53103) ¹⁵⁸

1.9.1.8 EPS Structures from *Lactobacillus helveticus* (A-F)

(A)

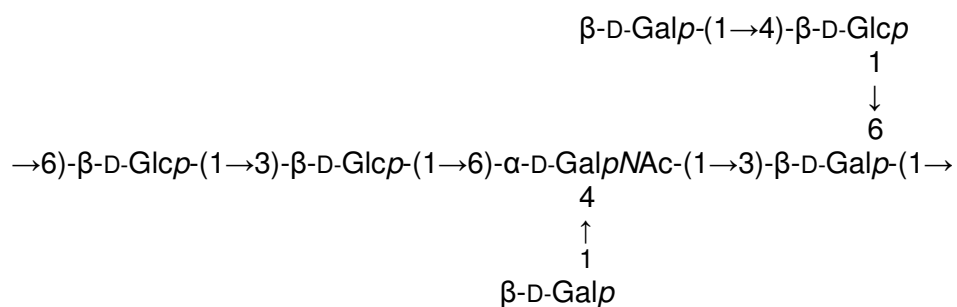


→3)-α-D-Galp-(1→3)-α-D-Glcp-(1→3)-β-D-Glcp-(1→5)-β-D-Galf-(1→

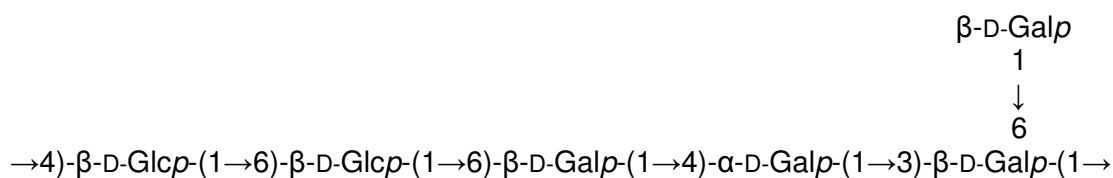
Lactobacillus helveticus TN-4 ¹⁵⁹

Lactobacillus helveticus Lh59 ¹⁶⁰

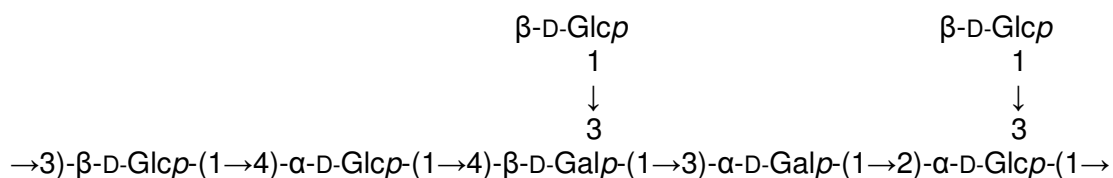
(B)

*Lactobacillus helveticus* TY 1-2 ¹⁶¹

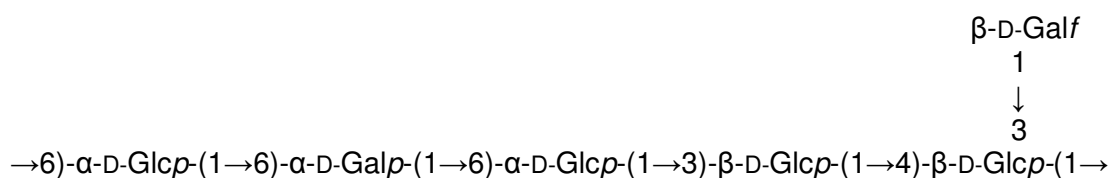
(C)

*Lactobacillus helveticus* 2091 ¹⁶²

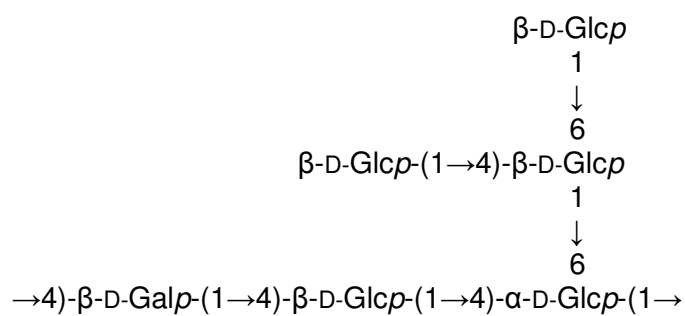
(D)

*Lactobacillus helveticus* Lb161 ¹⁶³

(E)

*Lactobacillus helveticus* NCDO 766 ¹⁶⁴

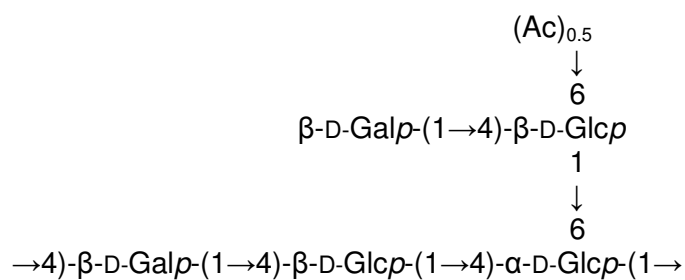
(F)



Lactobacillus helveticus K16 ¹⁶⁵

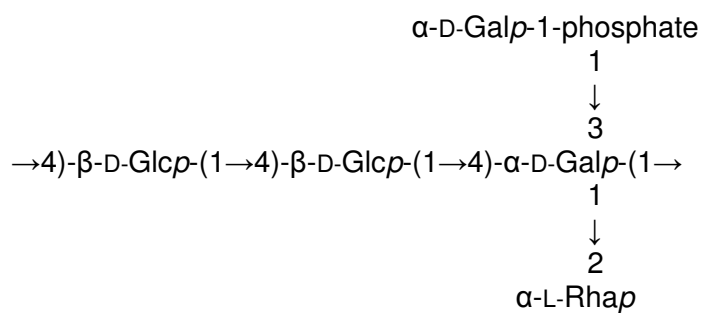
1.9.1.9 EPS Structures from *Lactococcus lactis* subsp. *cremoris* (A-E)

(A)



Lactococcus lactis subsp. *cremoris* NIZO B891 ¹³²

(B)



Lactococcus lactis subsp. *cremoris* SBT0495 ¹⁶⁶

Lactococcus lactis subsp. *cremoris* NIZO B40 ¹⁶⁷

Lactococcus lactis subsp. *cremoris* ARH74 ¹⁶⁸

2. EXPERIMENTAL

2.1 General Regents

The general reagents described throughout the experimental section were all purchased from either Sigma-Aldrich Co. Ltd (Gillingham, Dorset, UK), Fisher Scientific UK (Loughborough, Leicestershire, UK), Avocado Research Chemicals Ltd (Heysham, Lancashire, UK) or VWR International Ltd (Lutterworth, Leicestershire, UK) unless otherwise stated.

2.2 Fermentation of Bacterial Cultures and Isolation of the Exopolysaccharide

2.2.1 *Micro-organisms*

2.2.1.1 *Bacterial Cultures*

The bacterial cultures *Lactobacillus acidophilus* 5e2 and *Lactobacillus helveticus* Rosyjski were obtained from an industrial partner (Rhodia Food Biolacta, Poland) on slants (MRS).

2.2.1.2 *Maintenance of Bacterial Cultures*

All cultures were resuscitated in skimmed milk (42 °C) and streaked onto MRS agar. Single well isolated colonies were grown in skimmed milk and maintained as a frozen stock in a cryoprotectant (10 % glycerol) on glass beads at -80 °C according to the method described by Jones *et al.*¹⁷¹.

2.2.1.3 *Preparation of Inoculum*

Prior to inoculation into skimmed milk, the cultures were grown from a bead in MRS¹⁷² in static cultures at 42 °C. A pure working culture (1 mL) was inoculated into reconstituted skimmed milk powder (20 mL, 10% w/v supplied by St. Ivel Ltd, Swindon, UK) supplemented

with D-glucose (0.166 M, 3 %w/v) to create, after incubation for 24 hours at 42 °C a master culture. This amount of master culture was used to inoculate a two litre working volume.

2.2.2 Media

2.2.2.1 Skimmed Milk

Skimmed milk (St. Ivel Ltd, Swindon, UK) was used as the growth medium for both the pH controlled fermentation batches and to prepare the inoculums for each bacterial culture.

An amount of skimmed milk powder (10 %w/v) was added to deionised water to make the desired working volume (typically two litres). The milk was agitated to make a homogenous suspension and then heated to 70 °C for 20 minutes. The milk was then left to stand at room temperature for 24 hours before being poured into the fermentation vessel and autoclaved at 121 °C for 5 minutes.

2.2.2.2 Preparation of D-glucose Supplemented Media

To increase the yield of EPS produced, the skimmed milk medium was supplemented using D-glucose (0.166 M). A solution of D-glucose monohydrate (0.166 M, 3 %w/v) was prepared using deionised water (100 mL). This was autoclaved at 121 °C for 5 minutes and then added to the skimmed milk in the fermentation vessel prior to inoculation.

2.2.2.3 Preparation of MRS agar

MRS agar (Oxoid Ltd, Basingstoke, UK) was prepared by dispensing MRS powder (52.0 g) into a one litre Schott bottle. The contents of the bottle were diluted to one litre with deionised water. The MRS agar was then autoclaved at 121 °C for 15 minutes and stored at 50 °C until required.

2.2.2.4 Preparation of MRS Supplemented with Cysteine (MRS-C)

The MRS agar was supplemented with cysteine (0.5 g) to optimise the growth of the bacterial cultures under anaerobic conditions. The contents of the bottle were diluted to one litre with deionised water. The MRS-C agar was then autoclaved at 121 °C for 15 minutes and stored at 50 °C until required.

2.2.2.5 Preparation of the Maximum Recovery Diluent (MRD)

Maximum Recovery Diluent (Oxoid Ltd, Basingstoke, UK) solution was used as the solvent for the serial dilutions of the milk cultures for the viable count assays (discussed in section 2.2.4.2) and turbidity analysis. To prepare, MRD (9.5 g) was diluted to one litre with deionised water and autoclaved at 121 °C for 15 minutes. The MRD solution was allowed to cool to room temperature before being dispensed (9 mL) into sterile glass bottles (20 mL).

2.2.3 Milk Fermentation Procedure

2.2.3.1 Fermentation Conditions

The bacteria were grown in a stirred fermentation vessel; the temperature was maintained at 42 °C with a thermostatically controlled heating jacket. The pH was set at 5.82 and controlled by the addition of sodium hydroxide (4 M). The sodium hydroxide was delivered using a peristaltic pump (BioFlo 110 liquid addition, New Brunswick Scientific Co. Edison, NJ, USA) which is an integral part of the fermenter. The batch was continuously agitated at 100 rpm and samples were removed using a syringe attached to a stainless-steel sampler. All the conditions were controlled and monitored using a BioFlo 110 Fermentor (New Brunswick Scientific Co. Edison, NJ, USA).

2.2.3.2 Fermentation

The fermentation vessel, containing the skimmed milk medium and D-glucose, was left to equilibrate at the conditions described in section 2.2.3.1. The inoculum was added aseptically to the fermentation vessel using a peristaltic pump (Bioflo 110 liquid addition, New Brunswick Scientific Co, Edison, NJ, USA).

Samples were taken periodically into sterile glass bottles (30 mL) using a syringe attached to a stainless-steel sampling port. The consumption of sodium hydroxide (4 M) was monitored throughout the entire fermentation.

The fermentation time depended on the particular type of investigation, typically 24 – 48 hours for a standard fermentation and up to 72 hours for a timed fermentation.

2.2.4 Bacterial Growth Measurements

2.2.4.1 Turbidity

The turbidity of the milk cultures (10^{-1} and 10^{-2} dilution in MRD solution) was measured spectrophotometrically (Cary 50 Bio UV, Varian Inc. Corporation, Palo Alto, CA, USA), at 650nm, in 1cm glass cuvettes.

2.2.4.2 Viable Count

The viable counts were estimated using the pour plate technique described by Messer *et al.* (2004)¹⁷³ in which samples were serially diluted in MRD solution and then the diluted samples (1mL) were placed onto individual plates. The samples were covered with molten MRS-C agar and the plates were swirled in a figure of eight motion, and left at room temperature until the agar had set. The plates were then stored in a BugBox (Ruskinn Technology Ltd, Bridgend, UK) at 37 °C for 72 hours. The colonies were counted manually and the results were expressed as colony forming units per mL (cfu mL⁻¹).

2.2.5 Isolation of the Exopolysaccharide

The procedure used for EPS extraction was developed in the laboratories at the University of Huddersfield ¹⁷⁴.

2.2.5.1 Exopolysaccharide Extraction from Milk using Ethanol Precipitation

Samples were heated to 80 °C and then left to cool to room temperature, trichloroacetic acid (TCA) was added until the TCA concentration of each sample reached 14 %v/v and they were then left at 4 °C overnight. The samples were then centrifuged at 25000g (Avanti J-26 XPI centrifuge, Beckman Coulter Ltd UK, High Wycombe, UK) for 35 minutes at 4 °C to remove cells and proteins. The crude EPS was then precipitated out by the addition of an equal volume of chilled absolute ethanol to the supernatant liquid. After overnight precipitation at 4 °C the sample was centrifuged, as above, and the pellet retained. The pellet was re-dissolved in water (10 mL) with heating at 45 °C if required, until it had completely dissolved. The resulting solution was dialysed to remove small neutral sugars, for 72 hours at 4 °C, with three changes of water per day.

2.2.5.2 Preparation of Dialysis Tubing

Dialysis tubing was prepared by boiling deionised water (500 mL) containing ethylenediaminetetraacetic acid (EDTA) (0.186 g) and sodium carbonate (10 g) for 10 minutes. The tubing was then rinsed before boiling again with deionised water (500 mL) for a further 10 minutes. Finally the tubing was rinsed with deionised water and stored at 4 °C in deionised water.

2.2.6 Qualification and Quantification of Exopolysaccharide

2.2.6.1 Determination of Solids Content

After dialysis (described in section 2.2.5.1) the exopolysaccharide solutions were frozen and lyophilised (freeze-dried) in a pre-weighed round-bottom flask overnight using an Edwards Freeze-drier (Northern Scientific, York, UK). The dry weight was determined.

2.2.6.2 Determination of Carbohydrate Content

The procedure used for EPS quantitation was based on that described by Dubois *et al.*¹⁷⁵. The total carbohydrate of a sample solution (250 $\mu\text{g mL}^{-1}$, 1 mL) was measured colourimetrically, after addition of phenol solution (5 %w/v, 1 mL) and concentrated sulphuric acid (5 mL). This was left at 70 °C for 20 minutes, mixed then placed in a cool water bath at 10 °C for a further 10 minutes. The absorbance was measured spectrophotometrically (Cary 50 Bio UV, Varian Inc., Palo Alto, CA, USA) at 490 nm against a blank (deionised water) and compared to a graph generated from the results obtained for a series of D-glucose standards (50 – 300 $\mu\text{g mL}^{-1}$, 1 mL).

2.2.6.3 Determination of Protein Content

The amount of protein in the EPS sample was estimated using the Bradford assay¹⁷⁶. The assay is based on the interaction between coomassie brilliant blue with protein under acidic conditions. The chromophore formed has a maximum absorbance at 595 nm and the absorbance is proportional to the amount of protein present in the sample. The protein assay was performed using the following procedure.

In a volumetric flask (200 mL), coomassie brilliant blue (20 mg) was dissolved in ethanol (95 %v/v, 10 mL). Phosphoric acid (85 %w/w, 20 mL) was also added, and the solution made up to 200 mL by the addition of deionised water. The solution was shaken vigorously, and labelled Bradford solution.

A series of bovine serum albumin (BSA) standards ($10 - 1000 \mu\text{g mL}^{-1}$) were made, from a stock solution (2 mg mL^{-1}). Each BSA standard ($100 \mu\text{l}$) was added to a portion of Bradford solution (3 mL) and left at room temperature for 20 minutes. The absorbance was measured spectrophotometrically (Cary 50 Bio UV, Varian Inc., Palo Alto, CA, USA) at 595 nm against a blank (Bradford solution) and a calibration curve was generated. A solution of EPS ($250 \mu\text{g mL}^{-1}$, $100 \mu\text{l}$) was added to a portion of Bradford solution (3 mL) and was left at room temperature for 20 minutes. The absorbance was measured spectrophotometrically at 595 nm and the amount of protein present in the sample was determined from the calibration curve. The protein content of the EPS was then expressed in %w/w of EPS.

2.2.6.4 Determination of Nucleic Acid Content

The amount of nucleic acid present in the EPS was determined using HP-SEC (procedure described in section 2.3.4). The amount of nucleic acid present was separated from the carbohydrate using size exclusion chromatography and then quantified spectrophotometrically (UV detector, Shimadzu, Milton Keynes, UK) at 260 nm , which is the optimum wavelength for nucleic acid. The peak area of the DNA was then measured and compared to that of a DNA standard (Promega UK, Southampton, UK) (1800 bp) ($25 \mu\text{g mL}^{-1}$). The DNA content of the EPS was then expressed in %w/w of EPS.

2.2.6.5 Measuring the Solubility of Exopolysaccharides

To measure the solubility of the EPS, suspensions / solutions of known concentrations were left to equilibrate at $25 \text{ }^\circ\text{C}$ for 15 hours. An accurate amount of each suspension / solution was freeze dried in a pre-weighed flask to determine the solid residue. The suspensions / solutions (5 mL) were then filtered through $0.2 \mu\text{m}$ nylon membranes and an accurate amount of the filtrate (1 mL) was then freeze-dried in a pre-weight flask and the weight of the dry residue determined. The concentration of a saturated solution could then be calculated.

This procedure was carried out on a range of concentrations (300 – 4700 $\mu\text{g mL}^{-1}$) to determine the maximum solubility.

2.3 Structural Characterisation of the EPS using Established Protocols

The experimental details of the NMR and GC-MS techniques used for the analysis of the EPS are given in this section.

2.3.1 NMR Analysis of Exopolysaccharides

NMR spectra of the exopolysaccharide produced by *Lactobacillus acidophilus* 5e2 were recorded on a Bruker Avance DPX400 400.13 MHz spectrometer by Dr. Neil McLay.

^1H and ^{13}C DEPT 135 (one-dimensional experiments) and COSY, TOCSY, HSQC, HMBC, HSQC-TOCSY and NOESY (two-dimensional experiments) were all run on different batches of the exopolysaccharide produced from *Lactobacillus acidophilus* 5e2. Saturated samples of EPS were prepared in deuterium dioxide (D_2O) (GOSS Scientific Instruments Ltd, Nantwich, UK) and left overnight. The NMR experiments were all acquired at a temperature of 70 °C.

2.3.2 Monosaccharide Composition Analysis of Exopolysaccharides

This work was carried out by Mr. Mohammed Maqsood, the experimental details are given in Laws *et al.*¹⁷⁷.

2.3.3 Linkage Analysis of the Repeating Unit of Exopolysaccharides

This work was carried out by Mr. Mohammed Maqsood, the experimental details are given in Laws *et al.*¹⁷⁷.

2.3.4 Molecular Weight Determination of the Exopolysaccharide

The experimental detail for the HP-SEC-MALLS analysis is given in this section. Note only the exopolysaccharide produced by *Lactobacillus acidophilus* 5e2 was analysed by HP-SEC-MALLS during this study.

*2.3.4.1 Measuring the Refractive Index Increment (dn/dc) of the EPS from *Lb. acidophilus**

The dn/dc value was required for the determination of the weight-average molecular weight (M_w) of the exopolysaccharide produced by *Lactobacillus acidophilus* 5e2. Refractive index increments (dn/dc) were measured, using a differential refractometer (Optilab rEX, Wyatt Technology, Santa Barbara, USA). A HPLC pump (118 Solvent Module, Beckman Coulter Ltd, California, USA) delivered deionised water at 1 mL min^{-1} and a 2 mL injection loop was used on the injection port (7125i port, Rheodyne LLC, California, USA). Initially the instrument was calibrated by determining the dn/dc value for standard solutions of sodium chloride.

To determine the instrument constant a sodium chloride solution ($1000 \text{ } \mu\text{g mL}^{-1}$) was diluted to a series of dilutions ranging from $25 \text{ } \mu\text{g mL}^{-1}$ to $1000 \text{ } \mu\text{g mL}^{-1}$. The first standard (2 mL of $25 \text{ } \mu\text{g mL}^{-1}$) was injected, giving a rise in the output signal, as the response fell back to zero the next standard in the sequence was injected, this continued until all standards were measured. A graph of the signal response (mV) against concentration was then plotted and the results generated were used to calculate optical constant for the instrument, this was used in subsequent measurements of the dn/dc value for EPS samples.

To measure the dn/dc value of the exopolysaccharide produced by *Lactobacillus acidophilus* 5e2 the same procedure was carried out using dilutions of the EPS ranging from $25 \text{ } \mu\text{g mL}^{-1}$ to $1000 \text{ } \mu\text{g mL}^{-1}$. The calculated dn/dc result for the EPS was then used to find the M_w for all EPS samples prepared as part of this work.

Chromatographic conditions

Pump	-	Quaternary Pump, 118 Solvent Module
Flow rate	-	1 mL min ⁻¹
Mobile Phase	-	Water HPLC grade
Injection volume	-	2 mL
Detector	-	Refractive index (690nm)

*2.3.4.2 Determination of the M_w of Exopolysaccharides using Multi-Angle Laser Light**Scatter Analysis*

Solutions of EPS (1 mg mL⁻¹) in deionised water were prepared and left for 24 hours to completely dissolve. Samples (200 μ L) were injected (using a 7125i injection port, Rheodyne LLC, California, USA) onto an analytical size exclusion system comprising three columns connected in series (Aquagel-OH 40, 50 and 60, 15 μ m particle size, 25 cm x 4 mm, Polymer Laboratories UK). A HPLC pump (Prominence LC-20AD, Shimadzu, Milton Keynes, UK) delivered HPLC grade water (Sigma-Aldrich Co. Ltd, Poole, UK) at 1 mL min⁻¹ and the neutral analytes were eluted into a series of detectors. First, a UV detector (Prominence SPD-20A, Shimadzu, Milton Keynes, UK) set to 260 nm was used to determine the DNA content of the EPS (method discussed in section 2.2.6.4). Then the concentrations of the EPS fractions eluting from the column were determined by a differential refractometer (Optilab rEX, Wyatt technology, Santa Barbara, USA) and then finally, the weight average molecular weights of each peak of the chromatogram were measured using a multi-angle light scattering photometer with the laser set to 690 nm (Dawn EOS, Wyatt technology, Santa Barbara, USA).

Chromatographic conditions

Pump	-	Prominence LC-20AD, Shimadzu, Milton Keynes, UK
Flow rate	-	1 mL min ⁻¹
Mobile Phase	-	Water HPLC grade (Sigma-Aldrich Co. Ltd, Poole, UK)
Injection volume	-	200 μ L

Calibration constant	-	$2.000 \times 10^{-5} \text{ (V}^{-1}\text{)}$
dn/dc value	-	0.198
Columns	-	Aquagel-OH 15 μm 40, low molecular weight
	-	Aquagel-OH 15 μm 50, medium molecular weight
	-	Aquagel-OH 15 μm 60, high molecular weight
		(Polymer Laboratories Ltd, Shropshire, UK)
Detectors	-	UV, MALLS and RI detectors (in series)
Run time	-	45 minutes

These optimised conditions were used for all HP-SEC-MALLS analysis of the EPS produced by 5e2 in this work.

2.4 Depolymerisation of EPS Produced by *Lactobacillus acidophilus* 5e2

As explained previously (in section 1.7.1), depolymerisation techniques were employed to provide structural information about the exopolysaccharide, and to create oligosaccharides which would be used for LC-MS analysis. Depolymerisation was carried out using three methods: using a cell disruptor; using ultrasonic disruption and using acid-catalysed hydrolysis.

2.4.1 *Depolymerisation of an EPS using a Cell Disruptor (Application of Hydrodynamic Shear)*

A solution of the EPS was prepared in deionised water (1 mg mL^{-1} , 10 mL) and the solution was charged to the sample chamber of a cell disruptor (Constant Cell Disruption system, Daventry, UK). Once the samples had been disrupted an aliquot (1 mL) was removed and the sample was charged to the sample chamber for a second pass. For the first investigation a fixed pressure was used for each pass in the series. For the second investigation the pressure was increased for each pass (2 – 40 kpsi). The second investigation was carried

out to study the effect of the solvents' viscosity on the depolymerisation of EPS. The solvents and viscosities are given in Table 7.

Table 7: Samples prepared for the viscosity study using the Cell Disruptor

Sample	Solvent	Kinematic Viscosity of Solvent at 20 °C ¹⁷⁸	Concentration of EPS
A	Water	1.01 cSt	500 µg mL ⁻¹
B	Glycerol: Water	5.26 cSt	500 µg mL ⁻¹
C	Glycerol	1160 cSt	500 µg mL ⁻¹

Samples were taken after each pass and diluted to 250 µg mL⁻¹. The diluted samples were subjected to HP-SEC-MALLS analysis using the chromatographic conditions described in section 2.3.4.2 to determine the weight-average molecular weight (M_w).

A cell disrupted sample was freeze-dried and 5 mg were dissolved in D₂O (0.75 mL). A 1D-¹H NMR spectrum was recorded and the anomeric region inspected, which would detect any structural alterations to the repeating oligosaccharide unit.

2.4.2 Ultrasonic Disruption of Exopolysaccharides

The EPS (10mg) was diluted to 1000 µg mL⁻¹ using a sample diluent composed of aqueous acetone (1 %v/v, acting as a radical scavenger) ¹⁷⁹ with added sodium chloride to 0.1 M. The solution (10 mL) was poured into a glass bottle (30 mL) and placed in an ice-bath. Once the sample had cooled the tip of an ultrasonic probe (VCX130, Sonics and Materials Inc, Connecticut, USA) was lowered into the centre of the solution until the end was situated 2 mm from the bottom of the glass bottle. The solution was sonicated and aliquots (0.5 mL) were removed periodically and subjected to HP-SEC-MALLS analysis using the chromatographic conditions described in section 2.3.4.2. The change in average molecular weight during sonication was determined.

Initially three different amplitudes of ultrasonic power were applied (25 %, 45 % and 85 %) each for a duration of 50 minutes using the small probe (3 mm) and operating without any temperature control. The initial results showed that the sonication conditions were too intense; therefore the experiment was repeated with the sample submerged in an ice-bath.

A sonicated sample was freeze-dried and 5 mg was dissolved in D₂O (0.75 mL). A ¹D-¹H NMR spectrum was recorded and the anomeric region inspected, which would detect any structural alterations to the repeating oligosaccharide unit.

2.4.2.1 Study of the Effect of Ultrasonic Disruption on the Intrinsic Viscosity of EPS solutions

A sample diluent was prepared as described in section 2.4.2. The EPS produced by *Lb. acidophilus* 5e2 (80 mg) was added to sample diluent (80 mL), to make a concentration of 1000 µg mL⁻¹. This solution was left to fully dissolve over 24 hours, the sample was inspected to ensure that there were no solid particles remaining which could potentially block the viscometer. The solution was split equally into four glass bottles (30 mL) labelled A – D.

Table 8: Sonication Times and Amplitude for Samples A – D

Sample	Sonication time (using the 3mm probe on a 5 second pulse cycle)	Amplitude
A	0 minutes	-
B	10 minutes	50 %
C	20 minutes	50 %
D	40 minutes	50 %

The bottles were placed in an ice-bath and once the sample had cooled the probe was lowered into the centre of the solution until the end was situated 2 mm from the bottom of the glass bottle. The sample solutions (B – D) were sonicated individually and aliquots (0.5 mL)

were removed and subjected to HP-SEC-MALLS analysis using the chromatographic conditions described in section 2.3.4.2. Sample solution A was also subjected to HP-SEC-MALLS analysis. A proportion of the remaining solution (15 mL) was poured into a glass capillary viscometer (Rheotek BS/U tube viscometer size A, Poulten Selfe & Lee Ltd, Burnham on Crouch, UK). The viscometer was submerged in a water bath (20 ± 1 °C) and left to equilibrate until the samples had reached 20 °C. The time taken for the solution to travel down the viscometer was measured (in seconds).

Each sample solution (A – D) was then diluted firstly to $500 \mu\text{g mL}^{-1}$, and then to $250 \mu\text{g mL}^{-1}$, and the time taken for these sample solutions to travel down the viscometer was measured. A measurement was also taken for the sample diluent. The densities (20 ± 1 °C) of all of the solutions were measured and used to calculate the intrinsic viscosity.

2.4.3 Mild Acid-catalysed Hydrolysis of Exopolysaccharides

EPS (10mg) was dissolved in trifluoroacetic acid (0.2 M) and held at 30 °C in a heating block for 24 hours. Aliquots (0.5 mL) were taken every 30 minutes for the first 7.5 hours, further aliquots were taken after 21 and 25 hours. Once the aliquots were taken they were neutralised immediately to pH 7 using sodium carbonate (0.5 M).

The resulting solutions were subjected to HP-SEC-MALLS analysis using the chromatographic conditions described in section 2.3.4.2. The change in average molecular weight during hydrolysis was determined.

The 25 hour sample was freeze-dried and 5 mg were dissolved in D_2O (0.75 mL). A $1\text{D}^{-1}\text{H}$ NMR spectrum was recorded and the anomeric region examined which would detect any structural alterations to the repeating oligosaccharide unit.

2.5 Development of Novel LC-MS Methods for the Analysis of Carbohydrates

One aim of this project was to provide the Carbohydrate Community with novel methods of analysis that are more sensitive and less time consuming than are currently available.

2.5.1 *Reductive Amination of Carbohydrates*

The process of reductive amination is explained in section 1.7.2.1, where an amine reacts with a carbonyl group to form an aminol species, which subsequently loses one molecule of water in a reversible reaction to form an imine. The imine is then reduced to a secondary amine. This can be done successfully using the following procedure, that is based on a method described by Suzuki *et al.*¹³⁸.

A reducible carbohydrate (0.1 mmol) was added to a 25 mL round bottom flask containing a magnetic flea and was dissolved in water (400 μ L). In a glass vial p-aminobenzonitrile (0.60 g, 5.08 mmol) and acetic acid (200 μ L) were dissolved in methanol (1.0 mL). In a second glass vial, sodium cyanoborohydride (175 mg) was dissolved in methanol (Fisher Scientific UK, Loughborough, UK) (0.75 mL). The contents of the first and second vials were added to the round bottom flask. A water cooled reflux condenser was attached and the flask was lowered into an oil bath at 80 °C. The reaction was stirred constantly and maintained at 80 °C for 45 minutes.

The solution was cooled to room temperature and transferred to a separating funnel. Water (5 mL) was added and the excess reagents were extracted with ethyl acetate (3 x 5 mL). The ethyl acetate extracts were discarded and the aqueous phase was freeze dried overnight to produce a white/yellow solid.

The samples were dissolved in with water before LC-MS analysis or stored as a solid in an air-tight container until required.

2.5.1.1 Reductive Amination of Carbohydrates using 1:1 Ratio of pABN

The method described in section 2.5.1.2 uses approximately a 50 times excess of p-aminobenzonitrile, this is the amount that was used by Suzuki *et al.*¹³⁸. In an attempt to reduce the excess, the same reaction described in section 2.5.1 was carried out using a 1:1 ratio of pABN to monosaccharide.

2.5.1.2 Reductive Amination of Monosaccharides

The reductive amination reaction procedure described in section 2.5.1 was first carried out on a series of five monosaccharides; α -D-glucose, α -D-galactose, α -D-mannose, α -D-glucosamine and α -D-N-acetyl-glucosamine. These were to be used as standards for the monosaccharide analysis of the EPS using CZE (see section 2.5.4).

LC-MS Analysis

The p-ABN-labelled monosaccharides (1 mg) were diluted with water (1 mL) to provide a concentration of $1000 \mu\text{g mL}^{-1}$, and further diluted to $100 \mu\text{g mL}^{-1}$. The solutions were then subjected to LC-MS analysis using the following chromatographic and mass spectrometry conditions.

Chromatographic Conditions – Old Capillary HPLC System

Instrument	-	Ultimate Capillary LC, Camberley, UK
Mobile Phase	-	Gradient: 10-90 % acetonitrile (for 33 minutes)
UV wavelength	-	280 nm
Injection volume	-	5 μL
Column	-	Hypercarb 100 mm x 0.32 mm, 5 μm particle size, pore size 250 A (P/N: 35005-100365)
Flow rate	-	0.4 mL min^{-1} (split to column flow of 8 $\mu\text{L min}^{-1}$ before entering the ESI interface)
Run Time	-	35 minutes (including 2 minutes equilibration)

Chromatographic Conditions – New UPLC System

Instrument	-	Prominence UFLC-XR, Shimadzu, Milton Keynes, UK
Mobile Phase	-	Gradient: 10-90 % acetonitrile (for 18 minutes)
UV wavelength	-	280 nm
Injection volume	-	5 μ L
Column	-	Shim-pack XR-ODS II, 7.5 cm x 2.0 mm, 2.2 μ m particle size (P/N: 228-41623-91)
Flow rate	-	0.4 mL min ⁻¹ (split 1:3 before entering the ESI interface)
Run Time	-	20 minutes (including 2 minutes equilibration)

Mass Spectrometry Conditions

Instrument	-	MicrOTOF-q with ESI interface, Bruker Daltonics, Coventry, UK)
Capillary Voltage	-	-4500 V
Dry Gas	-	4.0 L min ⁻¹
Nebulizer	-	0.4 bar
Mass Range	-	50 – 3000m/z
Collision Energy	-	4.0 eV
Collision RF	-	200 Vpp
PrePulse Storage	-	6.0 μ s

MS/MS Conditions

Isolation width	-	1 m/z
Collision Energy	-	15 eV
Isolation Mass	-	[M+H] ⁺

2.5.1.3 Reductive Amination of Oligosaccharide

The method developed for monosaccharides in section 2.5.1.2 was then applied to an oligosaccharide. Maltohexanose (Sigma-Aldrich Co. Ltd, Poole, UK), a neutral six unit oligosaccharide (shown in Figure 21) was used to trial the method.

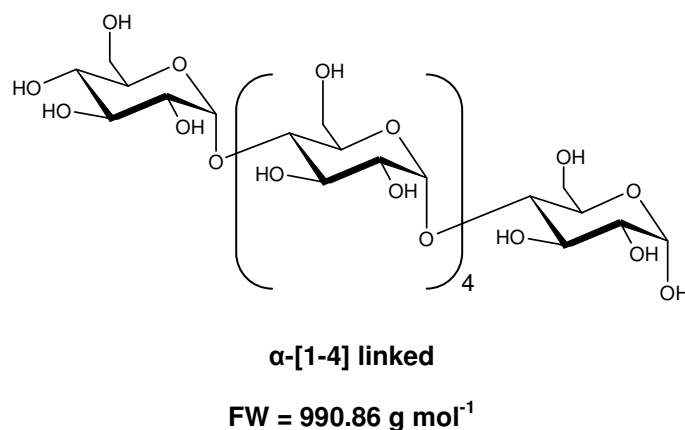


Figure 21: Structure of Maltohexanose

Maltohexanose (0.01 mmol) was added to a 25 mL round bottom flask containing a magnetic flea and was dissolved in water (400 μ L) and the procedure in section 2.5.1 was followed.

The p-ABN-labelled maltohexanose (1 mg) was diluted with water (1 mL) to provide a solution of concentration of 1000 μ g mL⁻¹, and further diluted to 100 μ g mL⁻¹. The solutions were then subjected to LC-MS analysis using the same chromatographic and mass spectrometry conditions as described in section 2.5.1.2 but with the following modifications.

MS Conditions

Mass Range	-	50 – 5000m/z
Collision Energy	-	10.0 eV
Collision RF	-	500 Vpp
PrePulse Storage	-	10.0 μ s

MS/MS Conditions

Isolation width	-	1 m/z
Collision Energy	-	85 eV
Isolation Mass	-	[M+Na] ⁺

2.5.2 Isolation of pABN-glucose using Preparative HPLC

The pABN-labelling of D-glucose was carried out at a larger scale to provide enough material to perform 1D- and 2D-NMR analysis.

D-glucose (1.0 g) (5.6 mol) was transferred into a 250 mL round bottom flask containing a magnetic flea. p-aminobenzonitrile (33.0 g) was added to a conical flask (100 mL) and was then dissolved in acetic acid (11 mL) and methanol (25 mL). In a second conical flask 100 mL sodium cyanoborohydride (9.63 g) was dissolved in methanol (30 mL).

The contents of the two flasks were mixed in a round bottom flask, a reflux condenser was attached and the flask was lowered into an oil bath at 80 °C and stirred constantly for 45 minutes.

The solution was transferred to a separating funnel. Water was added (~50 mL) and the excess reagents were extracted with ethyl acetate (3 x 50 mL). The ethyl acetate extracts were discarded and the aqueous phase was retained.

Preparative HPLC was used to isolate the pABN-labelled D-glucose from the excess reagents. The crude solution was injected into the Rheodyne 7125 injection port and the product was separated using the conditions described below. The pABN-labelled D-glucose was collected between 6.8 – 8.4 minutes (16.0 mL) from the outlet of the UV detector. Fractions were collected from eight separate chromatographic runs.

Chromatographic Conditions

Instrument	-	Gilson 303 and 303 pump with Holochrome UV detector, Gilson Inc., Middleton, WI, USA
Mobile Phase	-	85:15 (Acetonitrile: Water)
UV wavelength	-	280 nm
Injection volume	-	5 mL
Column	-	C18 Dynamax column, 21.4 mm ID, 8 μ m PS, 250 mm length
Flow rate	-	10.0 mL min ⁻¹ pump
Chart recorder	-	5 mm min ⁻¹ , 10 mV

Fractions containing the desired product were collected and combined, and then freeze-dried overnight. The collected pABN-labelled D-glucose (5 mg) was dissolved in D₂O and subjected to ¹H-NMR analysis and compared to literature results of pABN-labelled D-glucose to confirm the identity and to check purity.

2.5.3 Acid-catalysed Hydrolysis of Carbohydrates

To break down oligosaccharides and exopolysaccharides a method was developed which used a similar procedure to that reported by Hakomori in 1964⁹². The procedure was carried out as follows:

Trifluoroacetic acid (TFA, 4M, 1 mL) was added to the dry residue and the solution was heated at 120 °C for 2 hours in a pressure tube. After 2 hours the solution was evaporated to dryness under a stream of nitrogen gas at 50 °C. The residue was then dissolved in distilled water (200 μ L). This procedure was later applied both to methylated oligosaccharides and to exopolysaccharides (discussed in section 2.6).

2.5.4 Monosaccharide Analysis using Capillary Zone Electrophoresis

The procedure used for the monomer analysis of EPSs was based on that described by Xioa *et al.*⁹⁰. Five pABN-labelled monosaccharides were analysed by CZE to determine their relative migration times.

2.5.4.1 Mobile Phase and CZE Conditions

The mobile phase was prepared as follows: disodium tetraborate (Sigma-Aldrich Co. Ltd, Poole, UK) (1.91 g) was added to a volumetric flask (100 mL) and made to volume with ultra pure water. The pH was adjusted to 9.3 using dilute hydrochloric acid (2 M) (Fisher Scientific UK, Loughborough, UK) and then the solution was filtered.

A solution of acetone (1 %v/v) was prepared by diluting acetone (50 μ L) with water (5 mL). This solution was used to measure the electroosmotic flow. The samples and standards were evaluated on the CZE using the following conditions:

Chromatographic Conditions

Instrument	-	P/ACE™ MDQ, Beckman Coulter, High Wycombe, UK
Column	-	Capillary length 50 cm, 75 μ m ID and 375 μ m OD
Mobile Phase	-	50 mM disodium tetraborate, adjusted to pH 9.3 with HCl
UV wavelength	-	254 nm and 280 nm
Injection type	-	Pressure injection
Voltage	-	20 kV
Temperature	-	30 °C
Run Time	-	15 minutes

2.5.4.2 Identification of the Retention Times of pABN-labelled Monosaccharide Standards

The standards were prepared using the procedure described in section 2.5.1.2 with a final concentration of 100 μ g mL⁻¹ and the samples were run on the CZE using the procedure described in section 2.5.4.1.

2.5.4.3 Analysis of the Monosaccharide Composition of Exopolysaccharides using CZE

The monosaccharide analysis was carried out on two known exopolysaccharides produced by LAB that have been previously characterised at the University of Huddersfield. The two published structures were cultures from *Lactobacillus acidophilus* 5e2¹⁷⁷ and *Lactobacillus delbrueckii subsp. bulgaricus* NCFB2074⁷⁸. They first had to be hydrolysed into monosaccharides using the following procedure:

EPS (10 mg) was placed into a pressure tube and the acid-catalysed hydrolysis was performed as stated in section 2.5.3. The hydrolysed EPS samples were then pABN-labelled using the method described in section 2.5.1.1. The EPS samples (1 mg) were diluted to 1ml with ultra pure water to make a final concentration of 100 $\mu\text{g mL}^{-1}$. The samples and standards were analysed on the CZE using the conditions described in section 2.5.4.1.

2.5.5 Adaptation of the 'Hakomori Methylation Procedure'

Out of the various methylation reactions discussed in section 1.6.2, the two most applicable were evaluated for the analysis of EPS samples using LC-MS. The first methylation procedure used was based on that described by Hakomori in 1964⁹², where dimethylsulfinyl anion acts as a base and removes the free hydroxyl protons on the monosaccharide and then methyl iodide is added to form methoxy- groups. Methylation was carried out on both pABN-derivatised and non-derivatised carbohydrates depending on the application.

An amount of carbohydrate (10 mg) was placed into a pressure tube and anhydrous dimethylsulphoxide (1.5 mL) was added, the tube was capped and the solution heated in an oil bath at 65 °C for one hour (Tube A).

Sodium hydride (30 mg) was weighed into a pressure tube and anhydrous dimethylsulphoxide (1.5 mL) was added, the tube was capped and the solution heated in an oil bath at 65 °C for one hour (Tube B).

The contents of the two pressure tubes were combined and methyl iodide (CH₃I) (Sigma-Aldrich Co., Poole, UK) (0.7 mL) was added. The pressure tube was heated at 40 °C for 3 hours. After 3 hours the solution was transferred into a separating funnel and chloroform (10 mL) and water (5 mL) were added, and then the flask was gently shaken. The two layers were separated and the aqueous layer was placed in the separating funnel and extracted a further two more times, combining the organic layers. The combined organic layer was dried using anhydrous sodium sulphate (Fisher Scientific UK, Loughborough, UK), filtered into a pressure tube and evaporated to dryness under a stream of nitrogen gas at 40 °C to give the methylated carbohydrate. This was stored in an air-tight container until required.

2.5.5.1 '*Hakomori Methylation Procedure*' for pABN-glucose

The adapted Hakomori methylation procedure (described in section 2.5.5) was first carried out on a sample of pure pABN-labelled D-glucose produced in section 2.5.2.

This sample was used to evaluate the methylation procedure, in particular the time required for per-*O*-methylation to occur. This was achieved by repeating the experiment several times and varying the time which the methyl iodide had to react before the extraction. This time was varied between 30 – 210 minutes.

Methylated p-ABN-glucose (1 mg) was dissolved in acetonitrile (1 mL, 50 % in water) and further diluted to give a final concentration of 250 µg mL⁻¹. The solution was then subjected to LC-MS analysis using the chromatographic and mass spectrometry conditions described in section 2.5.1.2

2.5.5.2 'Hakomori Methylation Procedure' for Oligosaccharides

The adapted Hakomori methylation procedure (described in section 2.5.5) was then applied to the pABN-maltohexanose which had been produced using the method described in section 2.5.1.3.

Methylated pABN-maltohexanose (1 mg) was dissolved in acetonitrile (1 mL, 50 % in water) and further diluted to give a final concentration of 250 $\mu\text{g mL}^{-1}$. The solution was then subjected to LC-MS analysis using the chromatographic and mass spectrometry conditions described in section 2.5.1.3.

2.5.6 Adaptation of the 'Ciucanu Methylation Procedure'

The second methylation procedure investigated was based on that described by Ciucanu and Caprita⁹⁴.

An amount of carbohydrate (0.01 mmol) was added to a pressure tube and was dissolved in water (10 μL) and DMSO (0.7 mL). Sodium hydroxide was heated (100 – 120 °C) and then added to a pestle and mortar where the sodium hydroxide was ground to a fine powder. The hot powder was poured into a screw top vial and kept in a dessicator until required.

The sodium hydroxide (fine powder, 70 mg) was added to the pressure tube containing the carbohydrate. The sample solution was stirred to achieve a suspension. Then methyl iodide (300 μL) was added using a syringe and the mixture was stirred vigorously for 60 minutes at 25 °C.

The per-*O*-methylated carbohydrate was extracted by adding water (1 mL) and dichloromethane (1 mL) to the reaction mixture. The organic layer was washed with 3 x 5 mL of water and then dried with a stream of nitrogen at 40 °C to give a residue of methylated carbohydrate. This was stored in an air-tight container until required.

2.5.6.1 'Ciucanu Methylation Procedure' for Mono- and Disaccharides

The methylation procedure based on that described by Ciucanu (described in section 2.5.6) was carried out on pABN-labelled mono- and disaccharides (2 mg, 0.01 mmol).

The methylated pABN-labelled mono- and disaccharides (1 mg) was dissolved in acetonitrile (1 mL, 50 %v/v in water) and further diluted to give a final concentration of 250 $\mu\text{g mL}^{-1}$. The solution was then subjected to LC-MS analysis using the chromatographic and mass spectrometry conditions described in section 2.5.1.2

2.5.6.2 'Ciucanu Methylation Procedure' for Oligosaccharides

The Ciucanu methylation procedure (described in section 2.5.6) was also carried out on pABN-maltohexanose (9.9 mg, 0.01 mmol) prepared using the method described in section 2.5.1.3.

This method was repeated in an attempt to optimize the amount of carbohydrate being per-O-methylated; the reaction time (10 – 60 minutes) and excess of methyl iodide (3 – 15 times excess) was altered in an attempt to fully methylate all 20 hydroxyl groups (plus the 2° amine) of pABN-maltohexanose. The results for each sample were then expressed as a percentage of full methylation.

All the methylated pABN-maltohexanose samples (1mg) were dissolved in acetonitrile (1 mL, 50 %v/v in water) and further diluted to give a final concentration of 250 $\mu\text{g mL}^{-1}$. The solution was then subjected to LC-MS analysis using the chromatographic and mass spectrometry conditions described in section 2.5.1.3.

2.5.7 Deuterated Samples

The exchangeable proton on the hydroxyl groups can be deuterated by simply shaking an anhydrous solution with deuterium hydroxide (D_2O) (GOSS Scientific Instruments Ltd,

Nantwich, UK). This test identifies how many hydroxyl groups are present in the sample, which is particularly useful when monitoring the completion of the methylation of a carbohydrate.

2.5.7.1 Deuteration of Methylated Mono- and Disaccharides

Methylated pABN-labelled mono- and disaccharides (1 mg) were freeze-dried overnight and the solid residue was re-dissolved in D₂O:ACN (50:50, 1 mL). After a further dilution to 250 µg mL⁻¹ with D₂O, the samples were then infused into the mass spectrometer using the same conditions that are described in section 2.5.1.2.

2.5.7.2 Deuteration of Methylated Oligosaccharides

Methylated pABN-maltohexanose (1 mg) was freeze dried overnight and the solid residue was re-dissolved in D₂O:ACN (50:50, 1 mL). After a further dilution to 250 µg mL⁻¹ with D₂O, the sample was then infused into the mass spectrometer using the same conditions that are described in section 2.5.1.3.

2.6 Development of a Novel Method for the Linkage Analysis of Carbohydrates

The methodology developed (in section 2.5) for mono- and oligosaccharides was used to design a novel approach to determine the linkages of the monosaccharides in complex carbohydrates.

This new approach uses the methylation procedure described in section 2.5.6 followed by the acid-catalysed hydrolysis given in section 2.5.3 and finally the reductive amination procedure in detailed section 2.5.1.

2.6.1 Linkage Analysis of Carbohydrates using LC-MS-MS

Carbohydrate (0.01 mmol) was added to a pressure tube and was dissolved in water (10 μ L) and DMSO (0.7 mL). Sodium hydroxide was heated (100 – 120 $^{\circ}$ C) in pestle and mortar and the sodium hydroxide was ground to a fine powder. The hot powder was poured into a screw top vial and kept in a dessicator until required. The sodium hydroxide (fine powder, 70 mg) was added to the pressure tube containing the carbohydrate. The sample solution was stirred vigorously for 2 minutes in order to generate a suspension. Methyl iodide (300 μ L) was added with a syringe and the mixture was stirred vigorously for 60 minutes. The per-*O*-methylated maltohexanose was extracted by adding water (1 mL) and dichloromethane (1 mL) to the reaction mixture. The organic layer was washed with 3 x 5 mL of water and then dried with a stream of nitrogen at 40 $^{\circ}$ C to give a crude sample of the methylated carbohydrate.

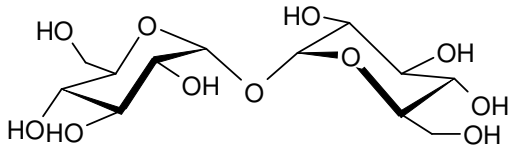
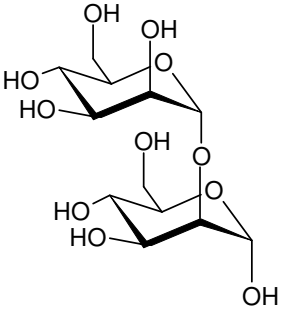
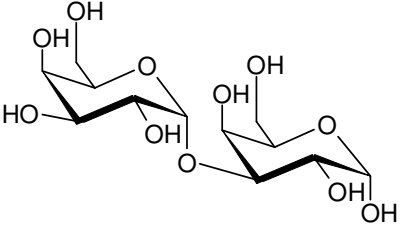
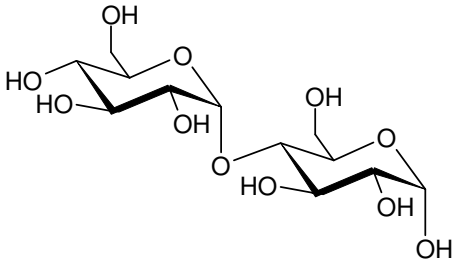
TFA (4 M, 1 mL) was added to the dry residue and the solution was heated at 120 $^{\circ}$ C for 2 hours in a pressure tube. After 2 hours the solution was evaporated to dryness under a stream of nitrogen gas at 40 $^{\circ}$ C. The residue was then dissolved in distilled water (200 μ L) and subjected to the reductive amination procedure (using 1:1 ratio of pABN) reported in section 2.5.1.1 but without the extraction procedure.

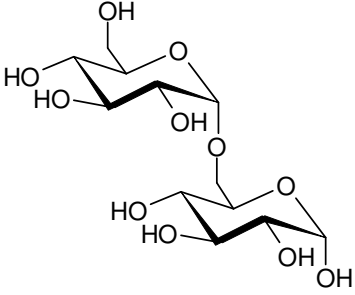
2.6.1.1 Linkage Analysis of Disaccharide Standards

The linkage analysis described in section 2.6.1 was first carried out on a series of five disaccharide standards (0.01 mmol) listed in

Table 9.

Table 9: Table of Disaccharide Standards Studied

Disaccharides	Structure	Formula Weight (g mol ⁻¹)
Trehalose α-[1-1]-linked		342.30
2-α-Mannobiose α-[1-2]-linked		342.30
3-α-Galactobiose α-[1-3]-linked		342.30
Cellobiose α-[1-4]-linked		342.30

Gentibiose α -[1-6]-linked		342.30
--------------------------------------	---	--------

Each solution was further diluted with acetonitrile to $250 \mu\text{g mL}^{-1}$ and subjected to LC-MS and

LC-MS-MS analysis using the chromatographic and mass spectrometry conditions described in section 2.5.1.2.

2.6.1.2 Application of the Novel Linkage Analysis Method to Oligosaccharides

The linkage analysis procedure described in section 2.6.1 was carried out on maltohexanose (shown in Figure 21) (9.9 mg, 0.01 mmol).

The sample solution was further diluted with acetonitrile to $250 \mu\text{g mL}^{-1}$ and subjected to LC-MS and LC-MS-MS analysis using the chromatographic and mass spectrometry conditions described in section 2.5.1.2.

2.6.1.3 Application of the Novel Linkage Analysis Method to Exopolysaccharides

The linkage analysis, described in section 2.6.1, was finally carried out on two known exopolysaccharides produced by LAB that have been characterised at the University of Huddersfield. The two published cultures were *Lactobacillus acidophilus* 5e2¹⁷⁷ and *Lactobacillus delbrueckii subsp. bulgaricus* NCFB2074⁷⁸.

The sample solution was further diluted with acetonitrile to $250 \mu\text{g mL}^{-1}$ and subjected to LC-MS and LC-MS-MS analysis using the chromatographic and mass spectrometry conditions described in section 2.5.1.2.

2.6.1.4 Linkage Analysis in a Deuterated Exchange System

The linkage analysis of the standard disaccharides described in section 2.6.1.1 was repeated but this time the samples were first deuterated as described in section 2.5.7.1 and then subjected to LC-MS-MS analysis, as described in section 2.5.1.2, but using D₂O in the mobile phase instead of water.

2.6.1.5 Linkage Analysis of Sodium Cyanoborodeuteride

The linkage analysis of a standard disaccharide (cellobiose) was carried out as described in section 2.6.1.1, but during the reductive amination reaction sodium cyanoborodeuteride was used instead of sodium cyanoborohydride. The sample solution was further diluted with acetonitrile to 250 µg mL⁻¹ and subjected to LC-MS and LC-MS-MS analysis using the chromatographic and mass spectrometry conditions described in section 2.5.1.2.

RESULT & DISCUSSION SECTIONS

3. Production and Characterisation of Exopolysaccharides

4. Depolymerisation of Exopolysaccharides

5. New Methods for Analysis of Exopolysaccharides

3. PRODUCTION AND CHARACTERISATION OF EXOPOLYSACCHARIDES

3.1 Introduction

This chapter discusses the production of exopolysaccharide from LAB cultures; *Lactobacillus acidophilus* 5e2 and *Lactobacillus helveticus* Rosyjski. Firstly the quantity and purity of the isolated EPS will be analysed, then the full structural characterisations of the isolated EPS will be discussed. Finally a study designed to monitor the EPS production and measure the change in M_w of the EPS throughout fermentation will be examined and rationalised.

3.2 Qualification and Quantification of the Exopolysaccharides

Using the experimental protocols described in section 2.2.6, the isolated exopolysaccharides were analysed to establish their quantity and composition using different fermentation conditions.

3.2.1 Determination of Solids Content of Exopolysaccharide

The solid content was determined by the lyophilisation of a dialysed solution of exopolysaccharide. The solids content of each fermentation batch was expressed in mg L^{-1} , so the yields of each batch could be compared. The results are given in Table 10.

Table 10: Batch Descriptions and Yield of EPS Produced by from Lactic Acid Bacteria

Batch Number	Batch Description	Yield (Solid Content, mg L ⁻¹)
Xn341	-Culture: <i>Lb. acidophilus</i> 5e2 -10 %w/w skimmed milk -1.5 L batch -2 % inoculum -D-glucose 0.166 M -pH 5.82 -100 rpm -37 °C -29 hr Prepared by Mariana Chacon-Romero	124.1
Xn342	-Culture: <i>Lb. acidophilus</i> 5e2 -10 %w/w skimmed milk -1.5 L batch -2 % inoculum -D-glucose 0.166 M -pH 5.82 -100 rpm -37 °C -24 hr Prepared by Mariana Chacon-Romero	133.4
Xn358	-Culture: <i>Lb. acidophilus</i> 5e2 -10 %w/w skimmed milk -2 L batch -2 % inoculum -D-glucose 0.166 M -pH 5.82 -100 rpm -42 °C -46 hr	281.5
Xn359	-Culture: <i>Lb. helveticus</i> Rosyjski -10 %w/w skimmed milk -2 L batch -2 % inoculum -D-glucose 0.166 M -pH 5.82 -100 rpm -42 °C -46 hr	237.0

The yield of the timed fermentation batches Xn356 and Xn360 are given in sections 3.4.1 and 3.4.2.4 respectively.

The yields from each batch differ significantly, This may be because the biosynthesis of EPSs is complex and involves a large number of gene products (Laws *et al.*, 2001)⁴³. The genes coding for the enzyme and regulatory proteins required for EPS synthesis are of plasmid origin. It is thought that the decreased EPS production can be attributed to the reduction in gene coding due to the loss of these plasmids (van Kranenburg *et al.*, 2000)¹⁸⁰.

Other reasons may also contribute; firstly the growth of bacterial cultures is often not reproducible, even when identical fermentation conditions are maintained (Cerning, 1990)¹⁸¹. This would account for the variability of solid content observed from batch to batch. Secondly, the recovery process for isolation of EPSs is not very accurate, the EPS recovery is significantly dependent on its solubility, there would be a reduction in recovery of EPS as the solubility reduces. EPS remaining as a solid would be removed during the isolation process with the precipitated proteins, cells and DNA.

Work carried out at the University of Huddersfield by Elvin⁷² and Dunn⁷¹ has attempted to improve the isolation procedure, but their work mainly focused on producing purer exopolysaccharides, by reducing the protein contamination. Research into improving the overall yield was carried out by Chacon-Romero¹⁸², also at the University of Huddersfield, she attempted to improve the yield of EPS by supplementing the fermentation media with different carbon feeds and through use of controlled pH (5.82). The results for her work on *Lactobacillus acidophilus* 5e2 can be found in Laws *et al.*¹⁷⁷. Historically, the yields of EPSs produced by LAB are modest, previously reported EPS yields for batches fermented without pH control or D-glucose supplemented growth media for *Lactobacillus acidophilus* 5e2 were $74.6 \pm 15 \text{ mg L}^{-1}$. Similar results were observed for *Lactobacillus helveticus* Rosyjski where the yield varies by $\pm 50 \%$ ⁷¹.

The solids content results reported in Table 10 are significantly greater than those previously reported by Dunn⁷¹, this is probably due to the supplementation with glucose increasing the yield of batches: Xn341 and Xn342 to 124.1 mg L^{-1} and 133.4 mg L^{-1} respectively. These batches used growth media supplemented with D-glucose (0.166 M) and were pH controlled at 5.82. In the current work, by increasing the length of time of fermentations, it has been possible to increase yields further. *Lactobacillus acidophilus* 5e2 batch Xn358 was fermented for 46 hours providing a 281.5 mg L^{-1} yield (cf. 124.1 mg L^{-1} for batch Xn341),

batch Xn359 of *Lactobacillus helveticus* Rosyjski was fermented for 46 hours and gave a yield of 237.0 mg L⁻¹.

Historically, the solids content was used as a value for the amount of EPS produced by LAB during fermentation. To obtain a more accurate assessment the carbohydrate, protein and nucleic acid content of EPS were determined.

3.2.2 Determination of Carbohydrate Content

The carbohydrate content of the dried exopolysaccharide for each batch was determined using a procedure based on that described by Dubois *et al.*¹⁷⁵. The method used was a colourmetric test for sugars and polysaccharides, where an orange colour was produced when carbohydrates were treated with a phenol/sulphuric acid solution. The intensity of this colouration is directly proportional to the amount of sugar present. The carbohydrate content of the EPS from each fermented batch was evaluated against a series of D-glucose standards. A calibration curve was plotted using the absorbance readings at 490 nm of the D-glucose standards (1 mL, 25 – 300 µg mL⁻¹, Figure 22).

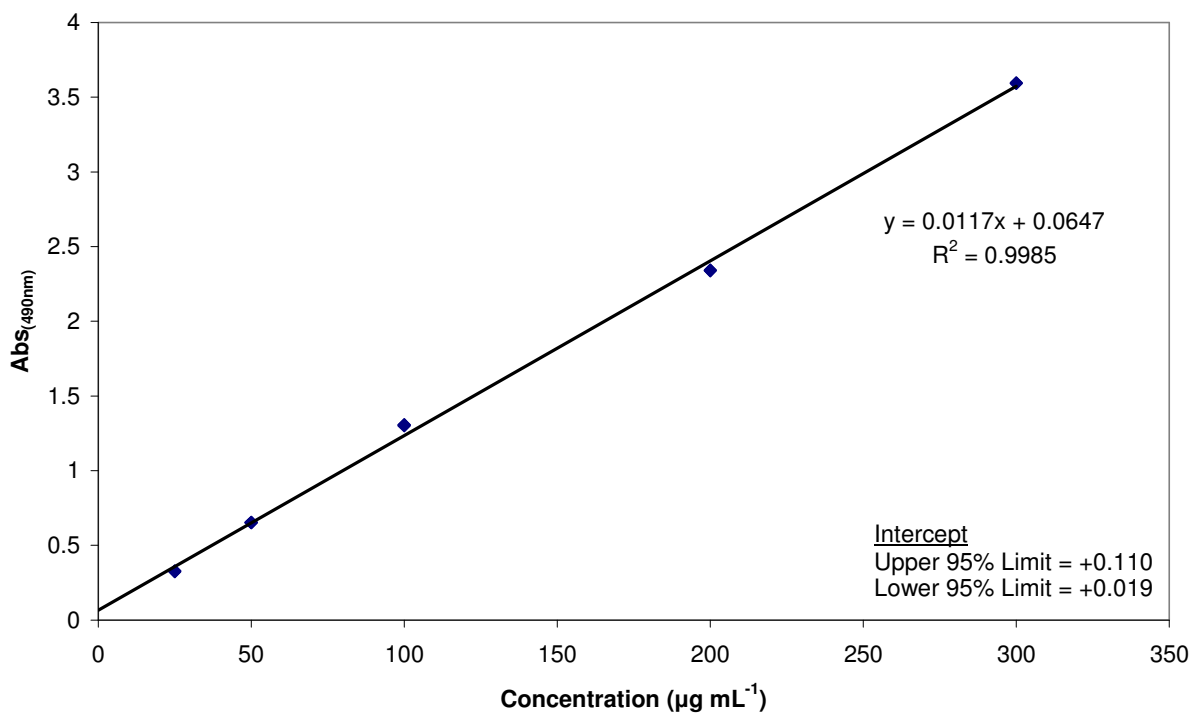


Figure 22: Calibration Curve for D-glucose Standard using Phenol/Sulphuric Acid Assay

The absorbance measurements for each concentration of D-glucose standard showed satisfactory correlation, $R^2 = 0.9985$. The trendline shows a slight positive bias, both the upper and lower 95 % confidence limits are positive values, therefore the bias is significant. Although significant, the carbohydrate determination for each EPS sample would not be affected as the expected carbohydrate concentrations were towards the top end of the calibration curve. The equation of the trendline was used to calculate the carbohydrate content of each batch; the results are shown in Table 11.

Table 11: Results for the Carbohydrate Analysis of EPS from Each Fermented Batch

Batch Number	Abs _{490 nm}	Calculated Amount ($\mu\text{g mL}^{-1}$)	Carbohydrate content of EPS (%w/w)
Xn341	2.5217	210.0	84.00
Xn342	2.4351	202.6	81.03
Xn356	2.3368	194.2	77.66
Xn358	2.5088	208.9	83.54
Xn359	2.2924	190.4	76.14
Xn360	2.6135	217.9	87.14

The amounts of carbohydrate present for each batch are lower than expected, comparisons from literature were difficult to find, but Ai *et al.*⁶² describe similar results which will be discussed in section 3.2.5. Tuiner *et al.*¹⁸³ also reported low carbohydrate content (after purification) of the EPS produced by *Lactococcus lactis* subsp. *cremoris* NIZO B40. They detailed the breakdown as; EPS (72 %), protein (6 %), inorganic material (9 %), mannan (7 %) and water (6 %). The results show that the solid content is not only due to carbohydrate and other material must be present. The EPS samples were tested for their protein and DNA content in an attempt to identify any non-carbohydrate components.

3.2.3 Protein Content of the Recovered Exopolysaccharides Samples

The protein content was determined using the Bradford protein assay¹⁷⁶, which used the interaction between coomassie brilliant blue dye and protein under acidic conditions. Coomassie brilliant blue dye has three charge forms, red, blue and green which have absorbance maxima at 470, 590 and 650 nm respectively. The blue charge form is the one that binds to protein forming a complex that intensely absorbs light at 590 nm. This intensity is proportional to the amount of protein present in the sample.

A series of BSA standards ($10 - 100 \mu\text{g mL}^{-1}$) were analysed and the absorbances were plotted against concentration to create a calibration curve, given in Figure 23.

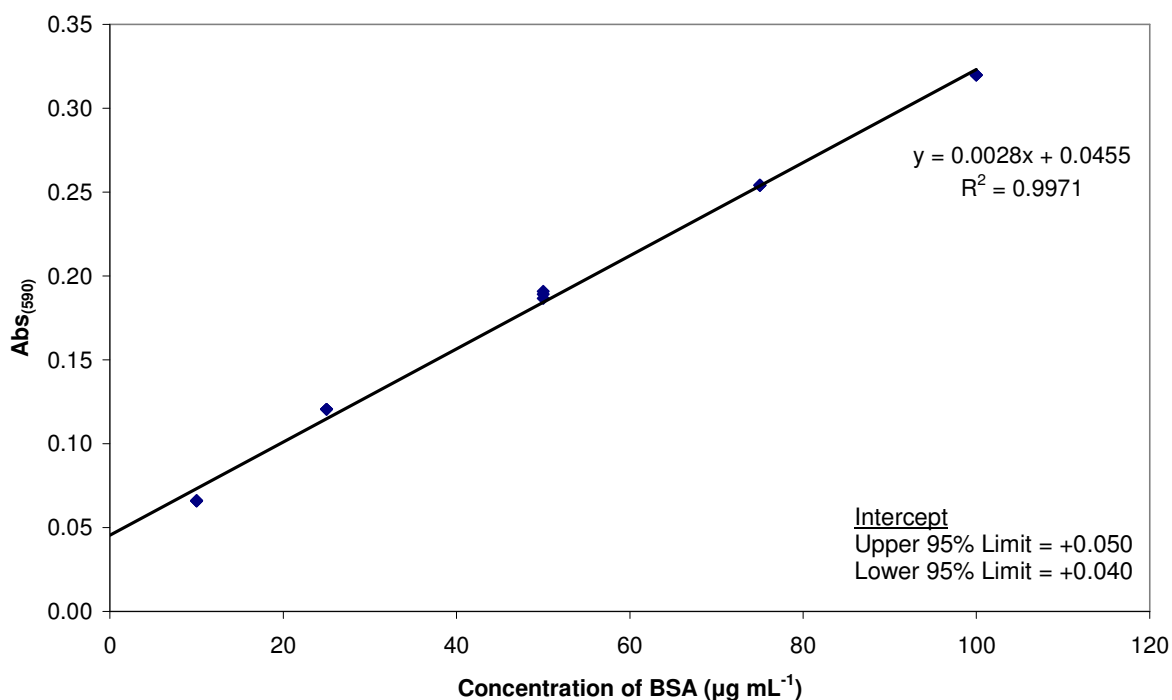


Figure 23: Calibration Curve for BSA Standard using Bradford Protein Assay

The calibration curve appears to be linear over the concentrations tested. It has been reported that the linear range of this method is narrow due to the overlapping spectrum of two of the different colour forms of the dye¹⁸⁴. This source suggests that the linear range is only $2 - 10 \mu\text{g mL}^{-1}$. The possible non-linearity of the calibration curve could also account for the large positive intercept ($+0.0455$). The positive upper and lower 95 % confidence limits confirm that the intercept has significant bias. This had to be considered when calculating the protein content of the EPS samples. The calibration curve (Figure 23) is comparable to that described by Zor and Selinger¹⁸⁴, who also reported a positive intercept.

The intensity of the absorptions of the EPS samples were measured at 590 nm and the amount of protein was calculated using the equation of the trendline given. The protein

content was then expressed as a percentage of the solid content of each EPS sample (see Table 12).

Table 12: Results for the Protein Analysis of EPS from Each Fermented Batch

Batch Number	Abs _{590 nm}	Calculated Amount ($\mu\text{g mL}^{-1}$)	Protein content of EPS (%w/w)
Xn341	0.0457	0.07	0.03
Xn342	0.0461	0.21	0.09
Xn356	0.0590	4.81	1.92
Xn358	0.0564	3.89	1.56
Xn359	0.0486	1.12	0.45
Xn360	0.0471	0.57	0.23

The amount of protein present in all EPS samples was low, showing that the isolation sufficiently removes residual protein, which is probably from the growth media and bacterial cultures. The greatest amount detected was <2 %, found in batch Xn356.

Protein accounted for only a small proportion of the non-carbohydrate content of the isolated EPS samples. The determination of nucleic acids was then performed.

3.2.4 Nucleic Acid Content of the Recovered Exopolysaccharide Samples

The nucleic acid content of the EPS samples was determined using a method developed by the author that used HP-SEC with UV detection. The EPS samples were separated using size exclusion chromatography and the nucleic acid content measured using a UV detector at 260 nm. The peak area of the nucleic acids in the EPS sample was quantified against the peak area of a DNA standard.

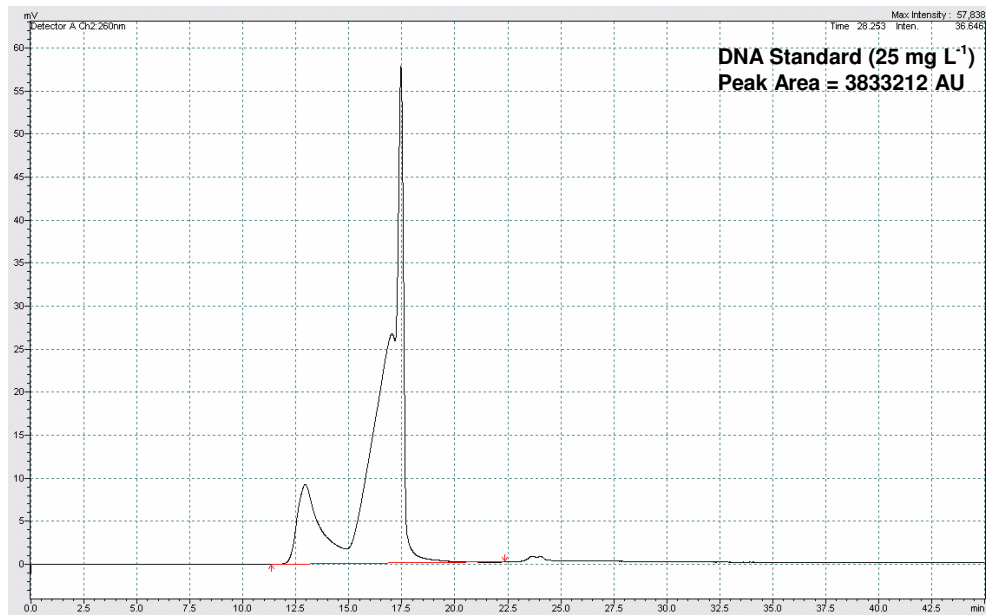


Figure 24: Example of the Chromatogram of DNA Standard (25 µg mL⁻¹)

The chromatogram for the DNA standard is shown in Figure 24, the sample contained a mixture of DNA strands ranging from 50 – 1800 bp. The total peak area at 260 nm was found to be 3.83×10^6 AU.

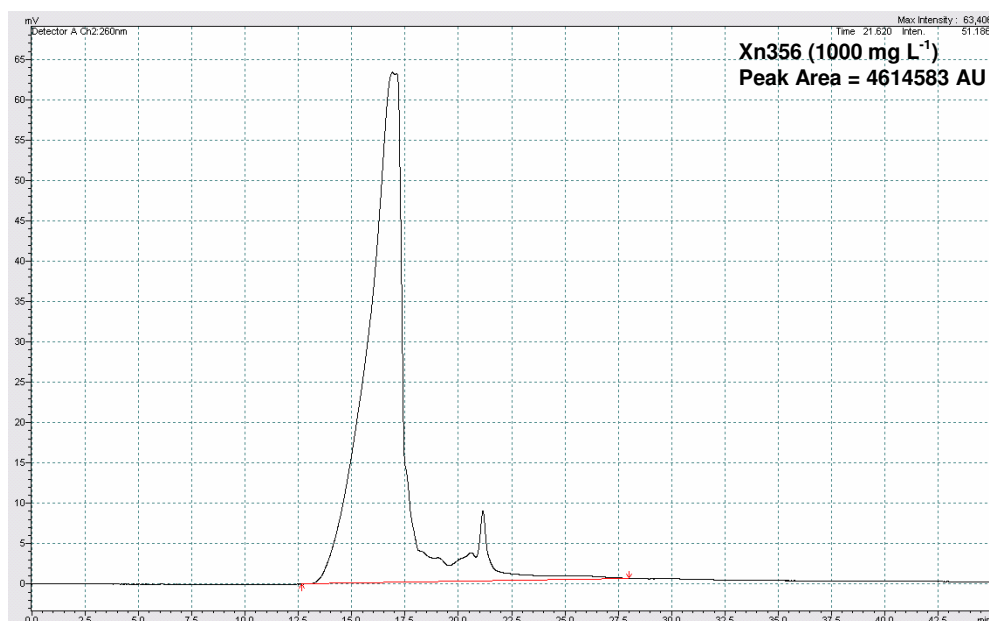


Figure 25: Example of the Chromatogram of an EPS (1000 µg mL⁻¹)

An example of a chromatogram obtained for one of the EPS samples is shown in Figure 25; the peak appears to be different, this is due to the molecular weight distribution of DNA present. The standard has two distinct molecular weight distributions, whereas the EPS sample has one.

The peak areas measured at 260 nm were recorded for each batch of EPS sample and then compared to the standard ($25 \mu\text{g mL}^{-1}$). The results for each batch are shown in Table 13, as with the protein, the results were expressed as a percentage of the solid content of the EPS.

Table 13: Results for the Nucleic Acid Analysis of EPS from Each Fermented Batch

Sample	Concentration ($\mu\text{g mL}^{-1}$)	Peak Area	Nucleic acid content of EPS (%w/w)
Xn341	1000	4026800	0.42
Xn342	1000	4025962	0.42
Xn356	1000	4614583	0.48
Xn358	1000	7305496	0.76
Xn359	1000	4799396	0.50
Xn360	1000	3833212	0.42
DNA Standard	25	3833212	-

The nucleic acid content for each EPS sample isolated from the fermentations of *Lb. acidophilus* 5e2 is low, in each case it accounted for less than 1 % of the solid content. This shows that the isolation process is satisfactory but that small amounts of nucleic acids remain.

3.2.5 Overall Composition of the EPS

The overall composition of each EPS sample was determined using the results from the carbohydrate, protein and nucleic acid analysis. The amount of remaining solid from each EPS sample is shown in Table 14.

Table 14: Composition of EPS Samples

Batch Number	Carbohydrate Content (%w/w)	Protein Content (%w/w)	Nucleic Acid Content (%w/w)	Remaining Amount (%w/w)
Xn341	84.00	0.03	0.42	15.55
Xn342	81.03	0.09	0.42	18.46
Xn356	77.66	1.92	0.48	19.94
Xn358	83.54	1.56	0.50	14.40
Xn359	76.14	0.45	0.76	22.65
Xn360	87.14	0.23	0.42	12.21

As can be seen from the results generated, each EPS sample contained a large amount of remaining material that was not due to carbohydrate, nucleic acid or protein. Ai *et al.*⁶² describe the chemical composition of an EPS isolated from a fermentation of *Lactobacillus casei* LC2W, their EPS was isolated using the same methodology as was used to isolate all the EPS sample in the current project. They measured the carbohydrate, protein, inorganic material and moisture content of their EPS. They state that their EPS has three distinct molecular weight distributions; one around 1,236 kDa, and two more at 21 and 17 kDa. The largest EPS fraction, which is the most comparable to the EPS samples in Table 14 (see M_w results in section 3.3.2), contains approximately 90 % carbohydrate and a trace amount of protein. The remaining 10 % was attributed to the moisture and inorganic material content. The remaining amounts in the above EPS samples may also be due to moisture, even though the samples have been lyophilized, trapped water could be present.

Due to the limited amounts of EPS available investigation of the moisture content was not determined, but it seems a plausible explanation that the remaining material is due to trapped water and inorganic incombustible materials.

3.2.6 Solubility of the EPS

The solubility of EPS in water at 25°C was assessed using the protocol described in section 2.2.6.5. The solubility was determined by measuring the amount of EPS dissolved in suspensions / solutions of known concentration. A portion (1 mL) of each suspension was freeze dried to determine the amount of EPS. Another portion (5 mL) was filtered through a 0.2µm nylon filter and the filtrate (1mL) was then freeze dried to determine the amount of EPS. Due to non-carbohydrate material present in the EPS samples, these results only provided an approximate indication of the EPS solubility.

Table 15: Solubility of Exopolysaccharide produced by *Lactobacillus acidophilus* 5e2

EPS Solution	Solid weight of 1 mL of initial suspension/ solution (mg)	Concentration of suspension/solution ($\mu\text{g mL}^{-1}$)	Solid weight of 1 mL of filtrate (mg)
1	0.3	300	0.3
2	0.6	600	0.6
3	1.1	1100	1.1
4	2.1	2100	1.8
5	2.8	2800	1.9
6	3.9	3900	1.8
7	4.7	4700	1.9

Due to a limited amount of sample only the solubility of batch: Xn358 was evaluated.

To determine the critical solubility at 25°C the results from Table 15 were plotted in a graph (Figure 26).

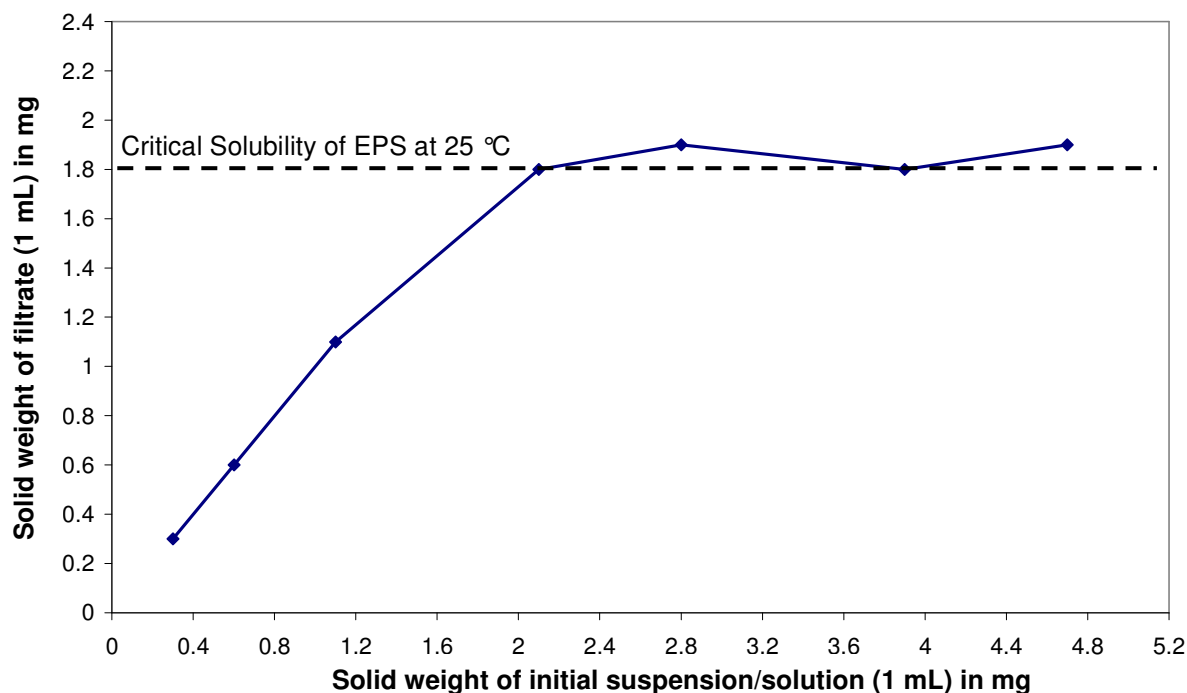


Figure 26: Graph to Determine the Critical Solubility of EPS Produced by *Lb. acidophilus* 5e2

The maximum amount of EPS recovered from the filtrate of the suspensions / solutions was approximately 1.8 mg per 1 mL ($1800 \mu\text{g mL}^{-1}$). This is the concentration of a saturated solution and the point of critical solubility at 25 °C. The dotted line on the graph (Figure 26) illustrates the critical solubility at 25 °C; above this concentration the filtration removed the undissolved EPS. Slight fluctuations can be seen for the amount of solid recovered, but the critical solubility can be clearly defined by this method.

This was the first time the solubility of the EPS produced by *Lb. acidophilus* 5e2 has been evaluated. A comparison of solubility of EPS isolated from other fermented batches of *Lb. acidophilus* 5e2 would have been informative but due to the limited amount of EPS available, this was not possible.

An alternative, and more accurate method to determine the solubility of a solute in water would be to use cloud point (turbidity) determination as described by Dinter *et al.*¹⁸⁵. This technique requires a larger amount of material therefore was not considered.

3.3 Structural Characterisation of the EPS using Established Protocols

This section discusses the structural characterisation of EPS using NMR and GC-MS. The analysis of the exopolysaccharide produced by *Lactobacillus acidophilus* 5e2 is reported in this section.

3.3.1 Structural Characterisation of Lactobacillus acidophilus 5e2

3.3.1.1 Structural Analysis using NMR

To determine the structure of the repeating oligosaccharide unit of the exopolysaccharide produced by *Lactobacillus acidophilus* 5e2 a series of 1D- and 2D- NMR experiments was carried out.

The first NMR experiment performed was the 1D-¹H NMR. The spectrum from this experiment showed a signal for every proton in the repeating oligosaccharide unit of the EPS. Particular attention was placed on the anomeric region (4.4 – 5.6 ppm); the number of signals in this region identifies how many monosaccharides are in the repeating oligosaccharide unit.

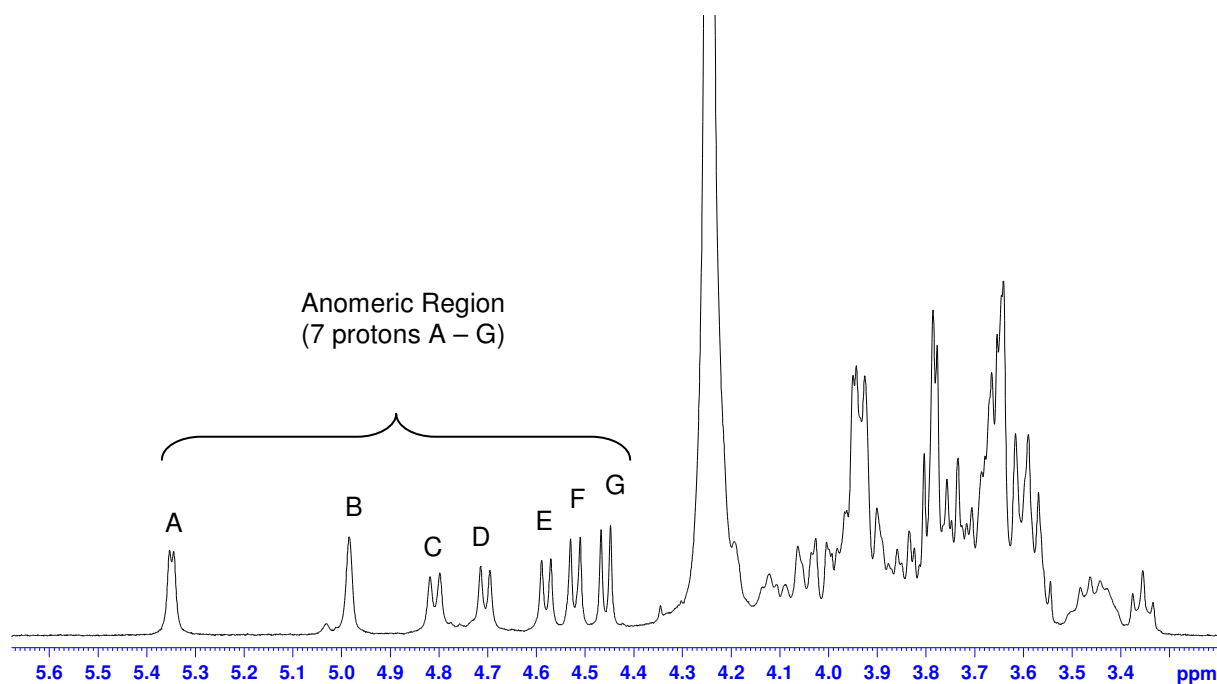


Figure 27: ^1H NMR Spectrum of EPS from *Lactobacillus acidophilus* 5e2 in D_2O at 70°C

As can be seen from the spectrum shown in Figure 27, there are seven signals in the anomeric region, which can be labelled **A – G** (from left to right). Anomeric protons **A** and **B** are unresolved doublets or single peaks. The peaks corresponding to **C**, **D**, **E**, **F** and **G** are clearly resolved doublets. The anomeric configuration of the sugars was determined by measurement of the $^3J_{1,2}$ coupling constants, where **A** and **B** are less than 4 Hz representing sugars having α -anomeric configuration. Signals **C – G** all have coupling constants greater than 7.5 Hz and are of β -anomeric configuration.

Table 16: $^3J_{1,2}$ Coupling Constants

Monosaccharide	$^3J_{1,2}$ Coupling constants	Configuration
A	3.24	α
B	0	α
C	8.04	β
D	7.72	β
E	7.52	β
F	7.92	β
G	7.68	β

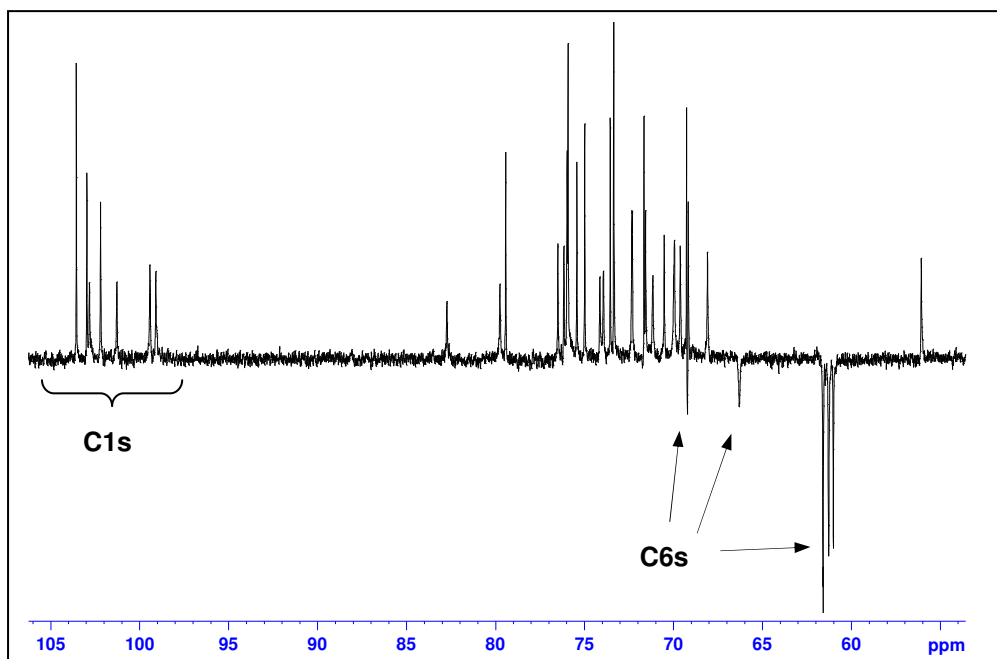


Figure 28: DEPT 135 ^{13}C NMR Spectrum of EPS from *Lactobacillus acidophilus* in D_2O at 70°C

The DEPT 135 ^{13}C spectrum (Figure 28) shows CH and CH_3 displayed as positive peaks and CH_2 (C6s) as negative peaks. The anomeric (C1) carbons are positioned downfield due to the presence of the neighbouring ring oxygen atom and the CH_2 s are typically located between 60 – 70 ppm.

Full characterisation of the structure of the EPS was achieved through inspection of a series of 2D-NMR experiments. The COSY spectrum was the first of the 2D- spectra to be examined, it showed protons attached to the adjacent carbon (linked by scalar coupling) therefore, for example, the hydrogens on C2 (H2) can be found from the scalar coupling to hydrogens on C1 (H1) of each monosaccharide.

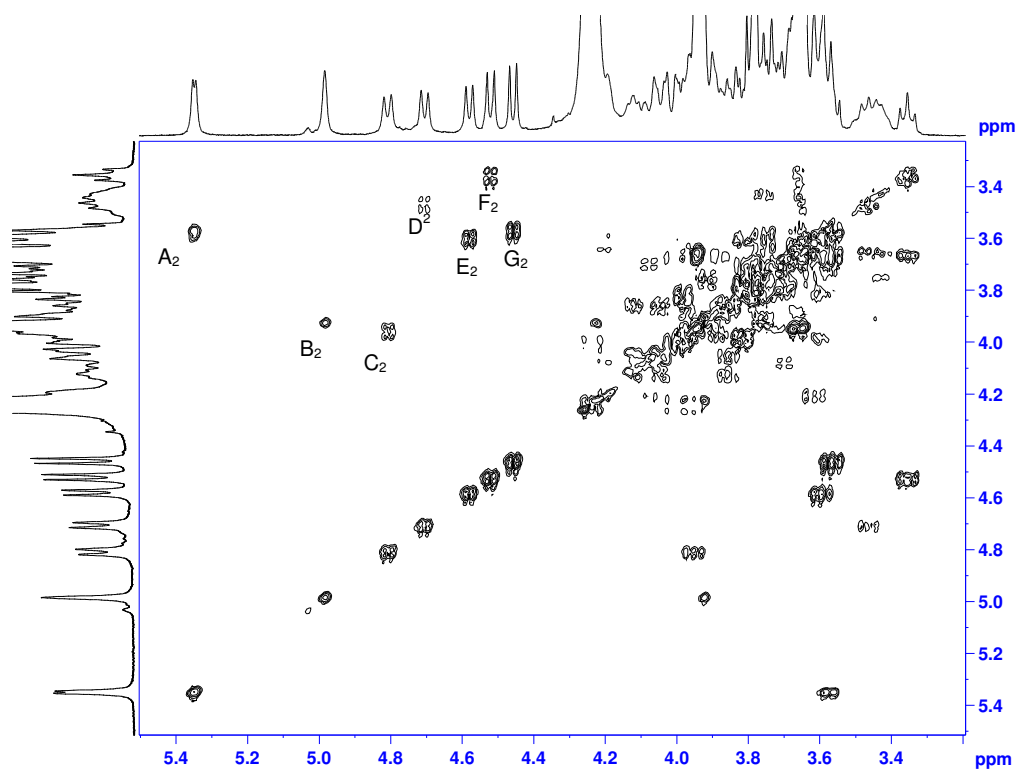


Figure 29: COSY spectrum of EPS from *Lactobacillus acidophilus* 5e2 in D₂O at 70 °C

Once the H₂ were identified (see Figure 29) then the corresponding C₂ were identified on the HSQC spectrum, which shows which protons are attached to which carbon. The HSQC spectrum of EPS from *Lactobacillus acidophilus* 5e2 is shown in Figure 31.

The most informative spectra, when determining which carbons belong to which monosaccharide, is the HSQC-TOCSY spectrum. A normal TOCSY spectrum detects contiguous protons on a carbon chain, therefore in a sugar residue a TOCSY spectrum can give a signal for every proton attached to the six carbons in the ring. When combined with the results of a HSQC experiment the carbons present in each sugar residue can be read directly under the sugar residues' anomeric proton.

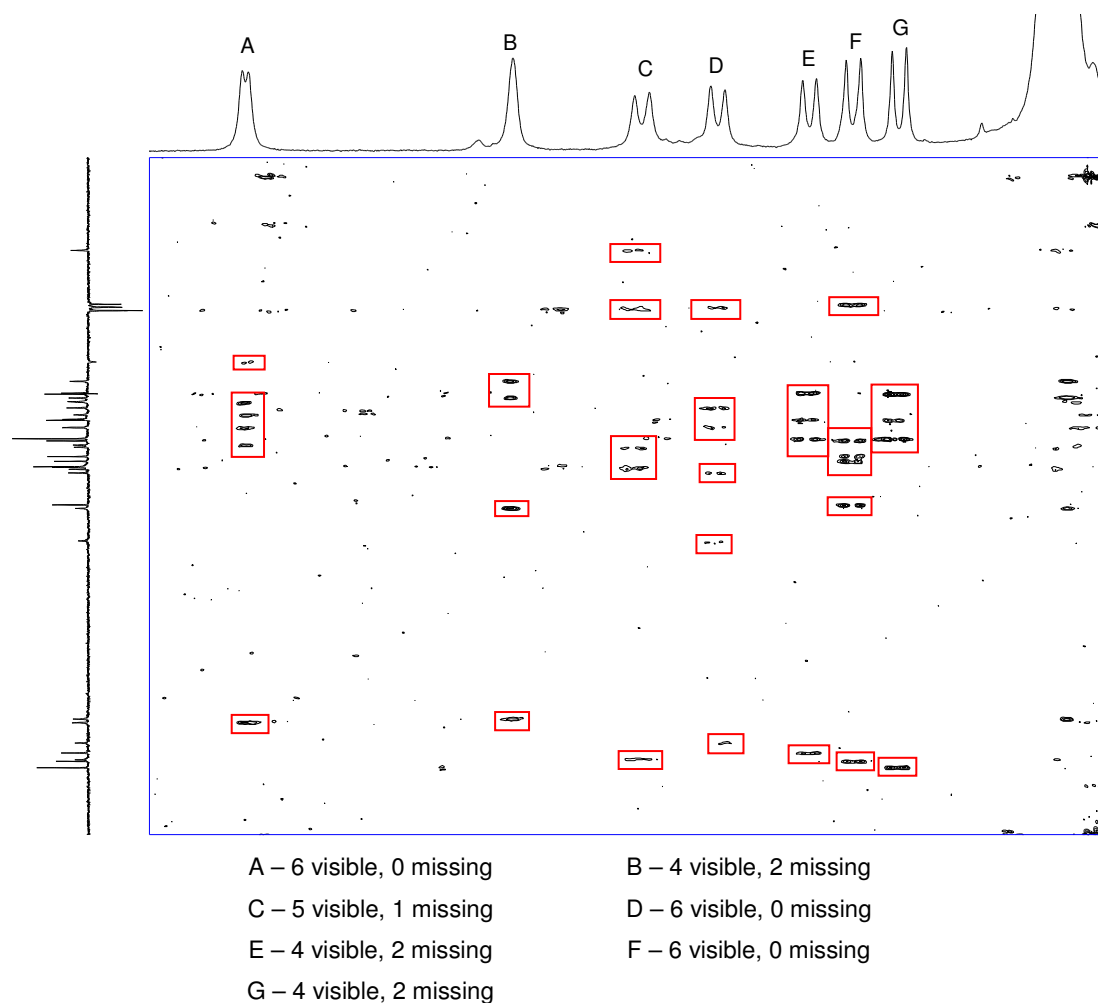


Figure 30: HSQC-TOCSY Spectrum of EPS from *Lactobacillus acidophilus* 5e2 in D₂O at 70 °C

The HSQC-TOCSY spectrum of the EPS is shown in Figure 30, where cross-peaks are visible for the protons attached to their monosaccharide. All the protons can be seen for **A**, **D** and **E**, but **B**, **C**, **E** and **G** still have missing information that must be found using the other 2D-spectra. Not all the protons are visible because the 2D-TOCSY spectrum relies on scalar coupling; if absent then no contiguous coupling is observed beyond that point. The carbon numbers in the monosaccharide ring are then assigned; the peaks at the highest ppm are the C1s (more deshielded next to the oxygen in the heterocyclic ring). Next the negative CH₂ peaks are assigned as the C6s (using Figure 28), then a combination of 2D-TOCSY and 2D-HMBC spectra is used to assign the remaining carbons.

To determine which peaks are due to C2 – C5, the 2D-TOSCY spectra can be run using different mixing times (ms). A shorter mixing time will only show the tallest, most intense peaks; which are usually due to the proton on the adjacent carbon. As the mixing times are extended, peaks of lesser intensities become visible; which are usually due to the protons on the next but one carbon. The 2D-TOCSY spectra were analysed and the results were compared to the 2D-HMBC spectra shown in Figure 32.

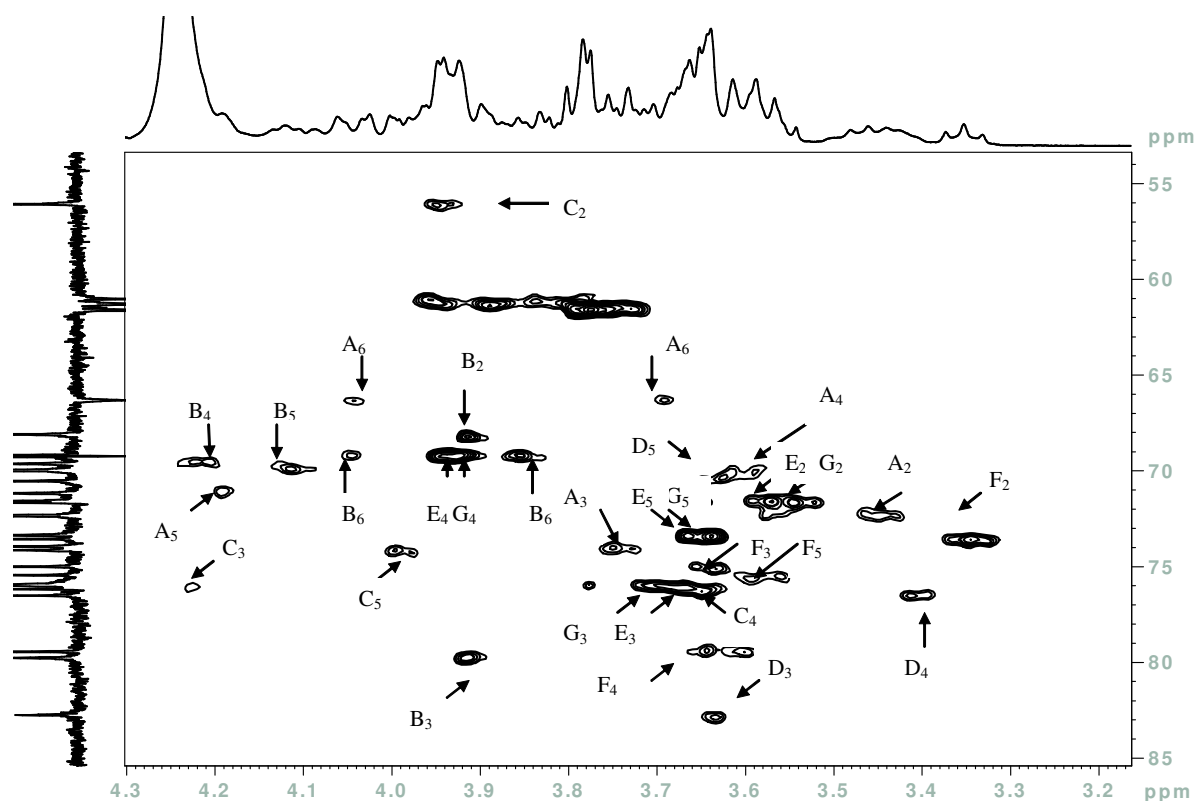


Figure 31: ^1H - ^{13}C HSQC Spectrum of EPS from *Lactobacillus acidophilus* 5e2 in D_2O at 70 °C

The identity of cross peaks is noted by the sugar residue, as **A – G**, and by identifying the location of hydrogens/carbons within the ring as **2 – 6**. The resonance positions for the non-anomeric ^1H signals and ^{13}C signals are indicated on the ^1H - ^{13}C HSQC spectrum (Figure 31), the anomeric ^1H signals are indicated on the HMBC spectrum (Figure 32) and the combined data is presented in Table 17 and Table 18.

Table 17: ^1H NMR Chemical Shifts of EPS Recorded in D_2O at 70 °C

SUGAR RESIDUE	^1H Chemical Shifts (ppm)						
	H1	H2	H3	H4	H5	H6	H6'
Glc – A	5.35	3.57	3.61	3.75	4.21	4.04	3.68
Gal – B	4.97	3.93	3.91	4.21	4.11	4.04	3.85
NAcGlc – C	4.80	3.96	4.22	3.99	3.67	4.04	3.86
Glc – D	4.71	3.46	3.63	3.42	3.66	3.87	3.74
Gal – E	4.58	3.59	3.67	3.95	3.67	3.80	3.72
Glc – F	4.52	3.36	3.67	3.62	3.60	3.97	3.83
Gal – G	4.46	3.57	3.66	3.95	3.66	3.80	3.80

The designation of monomers as either D-galactose (**B, E & G**) or as D-glucose (**A, D & F**) is based primarily on the location of the H4 resonance. The H4 resonance for a D-galactose is shifted substantially to a lower field than that of a D-glucose, regardless of the anomeric configuration and linkage: data collected from the assignments for LAB EPS structures show that the H4 resonances for a D-galactose lie in the range 4.30–3.85 ppm whilst those for D-glucose lie in the range 3.7 – 3.4 ppm ⁷⁸.

Table 18: ^{13}C NMR Chemical Shifts of EPS Recorded in D_2O at 70 °C

SUGAR RESIDUE	^{13}C Chemical Shifts (ppm)					
	C1	C2	C3	C4	C5	C6
Glc – A	99.44 (L)	72.35	69.96	73.94	71.17	66.32 (L)
Gal – B	99.08 (L)	68.10	79.76 (L)	69.63	69.96	69.23 (L)
NAcGlc – C	102.83 (L)	56.08	75.99 (L)	74.15 (L)	76.17	61.29
Glc – D	101.30 (L)	72.35	82.76 (L)	76.51	70.53	61.29
Gal – E	102.21 (L)	71.58	75.99	69.18	73.37	61.59
Glc – F	102.98 (L)	73.57	75.00	79.44 (L)	75.48	61.03
Gal – G	103.57 (L)	71.67	75.93	69.28	73.37	61.62

(L) = Glycosidic linkage

The chemical shifts data from Table 17 and Table 18 for the H5 and C5 resonances indicate that the monosaccharides are all present in their pyranose (6-membered) ring form, as furanose (5-membered) has C5 values greater than 81 ppm¹⁸⁶.

As described above the ^1H - ^{13}C HMBC spectrum is used in conjunction with the ^1H - ^{13}C HSQC spectrum to find out which carbons are next to each other within a monosaccharide and importantly, how they are linked through the glycosidic acetal bond.

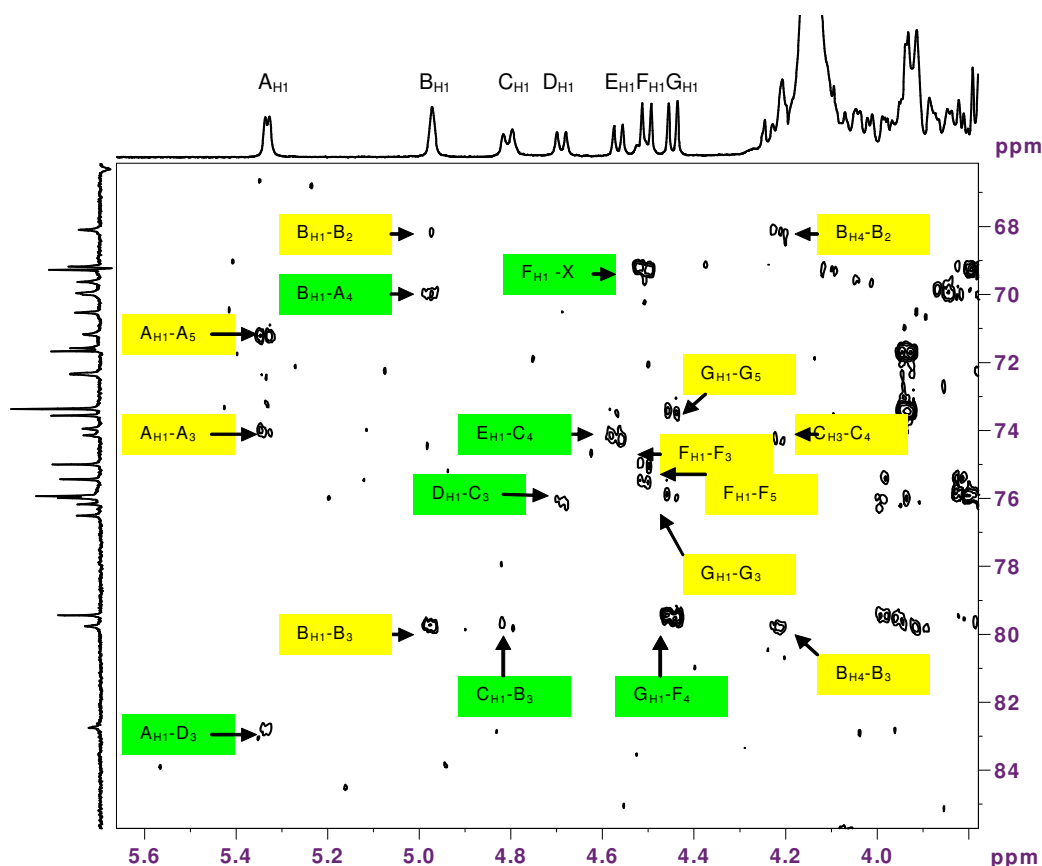


Figure 32: ^1H - ^{13}C HMBC Spectrum of EPS from *Lactobacillus acidophilus* 5e2 in D_2O at 70 °C

The ^1H - ^{13}C HMBC spectrum (Figure 32) shows intra-residue couplings highlighted in yellow and the inter-residue couplings are highlighted in green. The identity of cross peaks is noted by the sugar residue, **A – G**, and by identifying the location of coupled hydrogens/carbons within the ring as **1 – 6**. On the ^1H - ^{13}C HMBC spectrum, inter-residue cross peaks are observed between **A H1** and **D C3** confirming a **A(1→3)D** linkage; **C H1** and **B C3** confirming

a **C(1→3)B** linkage; **D** H1 and **C** C3 confirming a **D(1→3)C** linkage; **E** H1 and **C** C4 confirming a **E(1→4)C** linkage and finally **G** H1 and **F** C4 confirming a **G(1→4)F** linkage.

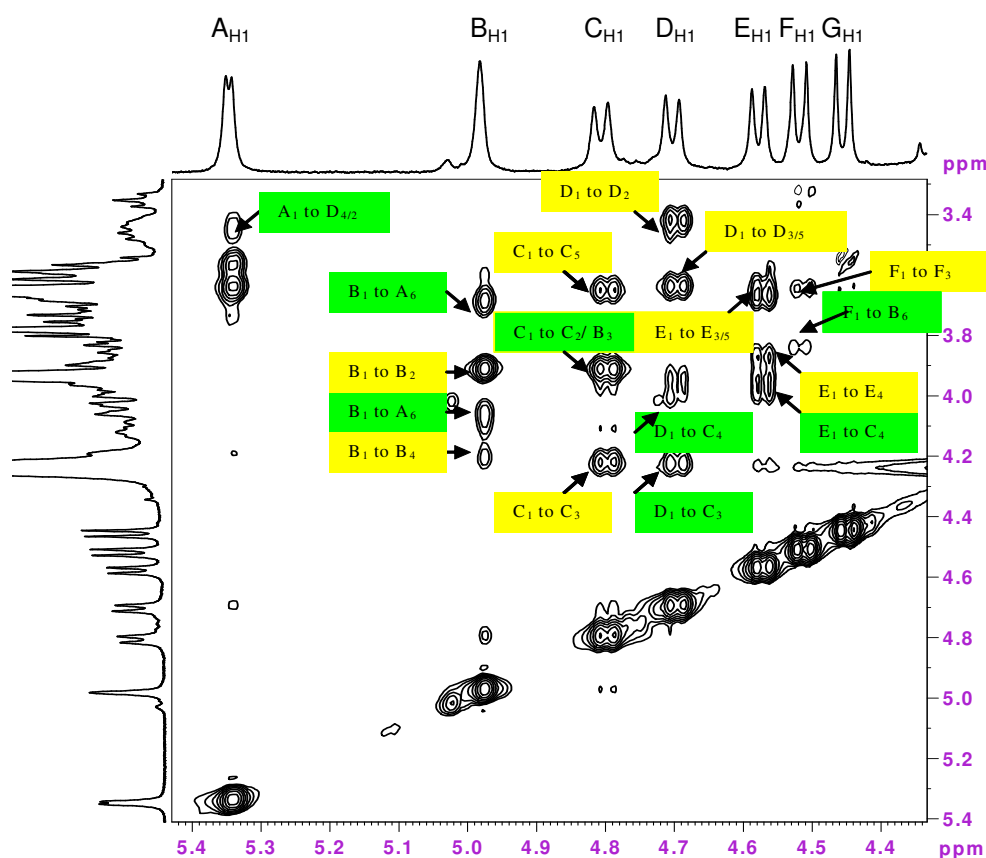


Figure 33: ^1H - ^1H NOESY (500ms) Spectrum of EPS from *Lb. acidophilus* in D_2O at $70\text{ }^\circ\text{C}$

Finally, the sequence of the monosaccharides in the oligosaccharide repeat unit was confirmed by the examination of the 2D- ^1H - ^1H NOESY spectra. This technique can detect proton interactions through space, from one sugar residue to another. These are called Nuclear Overhauser Enhancements (NOE) and give further structural information. Cross peaks linking different sugars are highlighted on the spectrum shown in Figure 33, where the intra-residue NOEs are highlighted in yellow, the inter-residue NOEs are highlighted in green. As was the case for the ^1H - ^{13}C HMBC spectrum the identity of cross peaks is noted by the sugar residue, **A – G**, and by identifying the location of coupled hydrogens within the ring as **1 – 6**.

On the ^1H - ^1H NOESY spectrum there are inter-residue cross peaks between: **A** H1 and **D** H4/2 which is consistent with a **A(1→3)D** linkage (see HMBC results for confirmation of the presence of this linkage, Figure 32); **B** H1 and **A** H6 confirming a **B(1→6)A** linkage; a strong cross peak between **D** H1 and **C** H3 confirming a **D(1→3)C** linkage; **E** H1 and **C** H4 confirming a **E(1→4)C** linkage and finally, there is a weak cross peak between **F** H1 and **B** H6 suggesting a **F(1→6)B** linkage.

3.3.1.2 Structural Analysis using GC-MS

The results for monosaccharide (GC) and linkage analysis (GC-MS) were generated at the University of Huddersfield by Mr. Mohammed Maqsood. The results were combined with data from the NMR experiments.

Monosaccharide Analysis

The results of monosaccharide analysis and determination of the absolute configuration indicate that the exopolysaccharide is composed of D-glucose, D-galactose and either *N*-acetyl-D-glucosamine or D-glucosamine in a molar ratio of 3.1 : 2.9 : 0.7. This is consistent with the EPS having a heptasaccharide repeat unit as shown in the anomeric region of the ^1H -NMR (see Figure 27).

Linkage Analysis

In the ^{13}C -NMR spectrum, the glycosidic links for the simple hexoses (**A**, **B**, **D–G**) were signalled by a shift to a lower field (by approximately 4 ppm) of the bridging carbons. When combined with the GC-MS linkage analysis, the sugar residues were identified as follows:

A as a 1,6-linked α -D-glucose; **B** as a 1,3,6- linked α -D-galactose; **C** as the 1,3,4-linked β -*N*-acetyl- D-glucosamine; **D** as a 1,3-linked β -D-glucose; **E & G** as terminal β -D-galactoses and **F** as a 1,4-linked β -D-glucose.

The results indicate that branching is present in the repeating oligosaccharide unit of the EPS and that there is a *N*-acetyl-glucosamine located at one of the branching points.

3.3.1.3 Proposed Structure of the EPS produced by *Lactobacillus acidophilus* 5e2

Using information from the NMR spectra and the GC-MS results the following structure was proposed.

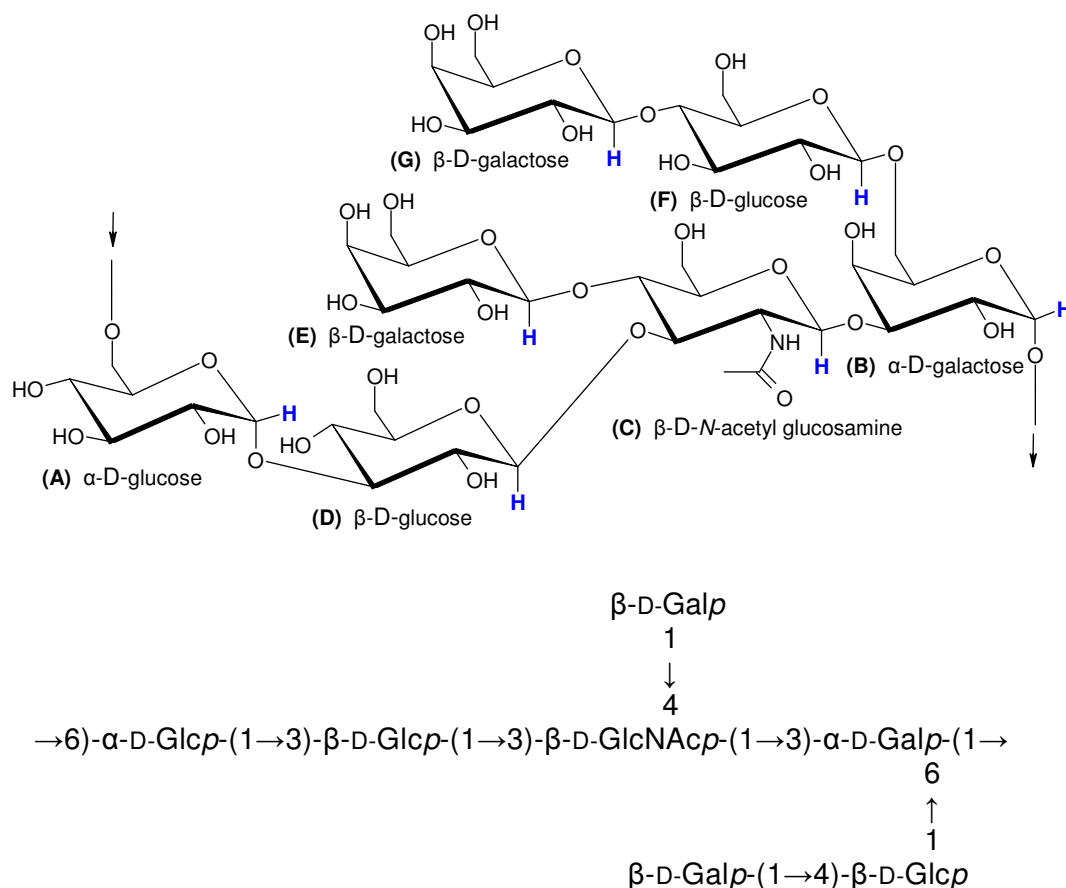


Figure 34: Structure of Exopolysaccharide Produced by *Lactobacillus acidophilus* 5e2

The anomeric protons of the proposed structure of the exopolysaccharide produced by 5e2 are shown in blue. The spine of the repeating unit consists of four monosaccharides joined by a series of 1,3-linkages, with two branches, one a D-galactose unit and the other a galactose – glucose disaccharide i.e. a lactose unit. The structures of published EPS produced from LAB can be found in the appendix section 1.9.1. The EPS structure from *Lactobacillus acidophilus* 5e2 agrees with many of the statements made for the inspection of reported EPS structures from lactic acid bacteria, discussed in section 1.4.4.2. The EPS

from *Lactobacillus acidophilus* 5e2 shows that the monosaccharide present in the highest frequency is galactose, closely followed by glucose, which are both present in the D-absolute configuration. This structure contains a GlcNAc, which has been seen in numerous EPS structures from LAB. The EPS structures showed slight preference for the β -anomer, containing only two α -anomers. The branches of the EPS structure are terminated by D-galactose, and the remaining β -D-galactoses are attached via a 3-, 4- or 6-hydroxyl group. β -D-Glucose is preferentially attached via its 3- or 4- hydroxyl group, whereas α -D-glucose is preferentially attached via its 3- hydroxyl group. This is a novel exopolysaccharide and its proposed structure has been published in Carbohydrate Research ¹⁷⁷.

3.3.2 Determination of Weight-average Molecular Weight for Exopolysaccharides

The weight-average molecular weight of the exopolysaccharides produced by *Lactobacillus acidophilus* 5e2 and *Lactobacillus helveticus* Rosyjski were determined using the HP-SEC-MALLS. Prior to the analysis of EPS the differential refractometer was calibrated by determining the refractive index increment (dn/dc) for sodium chloride and the accuracy and precision of the HP-SEC-MALLS instrument was evaluated using a pullulan standard of known M_w (800,000) and low polydispersity ($M_w/M_n = \sim 1.23$).

3.3.2.1 Measuring dn/dc Value of the EPS Produced by 5e2 using Refractive Index

HP-SEC with multi-angle laser light scattering (MALLS) detection is a technique that can be used to determine the molecular weight distribution of macromolecules (e.g. exopolysaccharides). To calculate an accurate weight-average molecular weight (M_w) the specific refractive index increment (dn/dc value) of the EPS was required.

Calculating the Refractometer Calibration Constant

Upon installation the refractometer was calibrated by a Wyatt Technology Engineer. Sodium chloride (with a known dn/dc value of 0.172 mL g^{-1} at 690 nm) was used to calculate a

calibration constant. The slope of the calibration curve plotted (change in refractive index, dn , versus phase difference between the sample and reference cells, mV) was used to calculate the instruments' calibration constant. The intercept should be close to zero since a zero voltage corresponds to zero change in refractive index. The calibration constant calculated by Wyatt Technology was $2.0000 \times 10^{-5} \text{ V}^{-1}$; this was used in all subsequent measurements of dn/dc .

Calculating dn/dc

Using the calibration constant ($2.000 \times 10^{-5} \text{ V}^{-1}$) the dn/dc value for sodium chloride at 690nm was checked and compared to the known value of 0.172 mL g^{-1} . A series of concentrations (2.5×10^{-4} to $1.0 \times 10^{-3} \text{ g mL}^{-1}$) were prepared and evaluated as described in section 2.3.4.1.

A graph of the signal response (mV) against concentration was then plotted and the calculated result was compared to the known value.

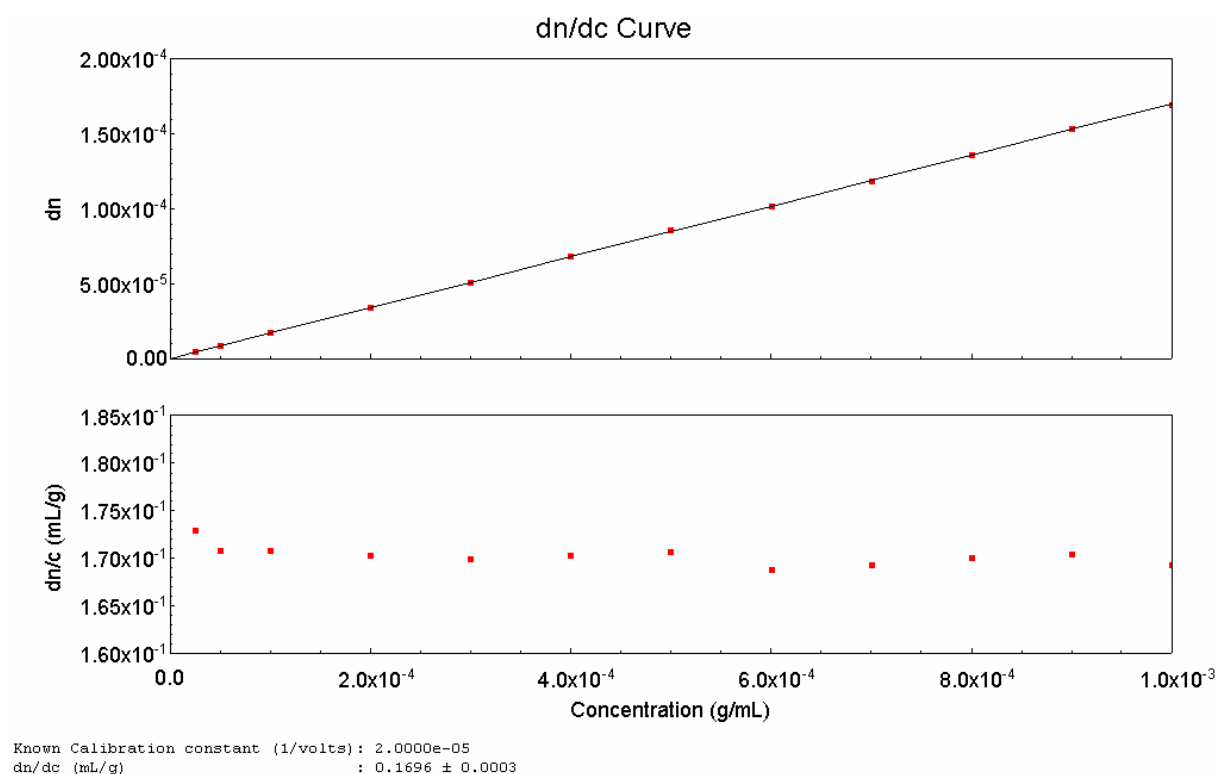


Figure 35: dn/dc Curve for the Sodium Chloride

The dn/dc was calculated to be 0.170 mL g^{-1} , this was close to the known dn/dc value for sodium chloride (at 690 nm) of 0.172 mL g^{-1} . This confirmed that the calibration constant was suitable.

Literature values for the dn/dc can be found for common polysaccharides such as dextran, pullulan, etc. The dn/dc value for the EPS produced by *Lb. acidophilus* 5e2 had never been measured before, and was therefore calculated using the same procedure as performed on sodium chloride.

A series of EPS solutions ranging from 2.5×10^{-4} to $1.0 \times 10^{-3} \text{ g mL}^{-1}$, were made and the change in signal response (dn) was measured for each concentration (g mL^{-1}). A graph was generated as is illustrated in Figure 36.

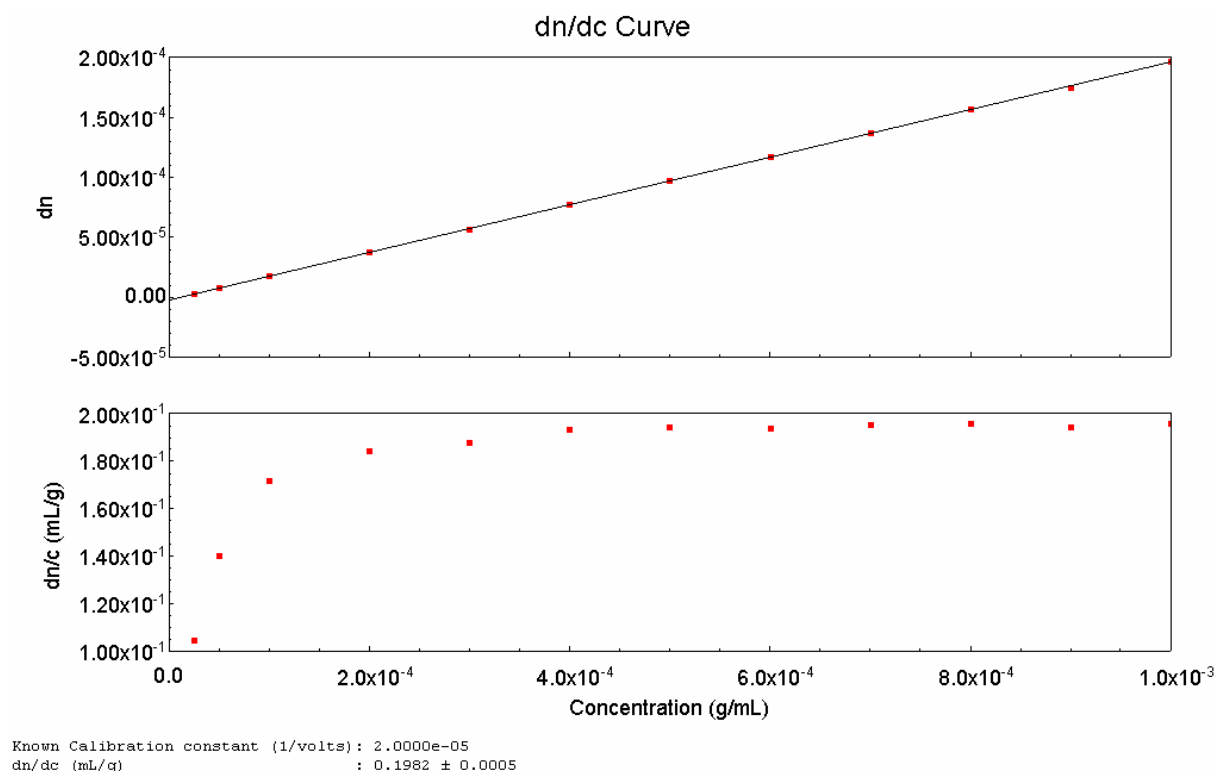


Figure 36: dn/dc Curve for the EPS Produced by *Lb. Acidophilus* 5e2

The dn/dc value was calculated to be 0.198 mL g^{-1} , which is relatively large when compared to the list of values published by Theisen *et al.* in 2000, which shows that most dn/dc values

for macromolecules, in aqueous systems, lie between 0.14 – 0.16 mL g⁻¹. The value may have been large due to the purity of the EPS, the carbohydrate content has been shown to be approximately 80 % (see section 3.2.2).

This value was used for all subsequent weight-average molecular weight (M_w) measurements of EPS produced by 5e2.

3.3.2.2 Determination of the M_w of a Pullulan Standard (800,000 M_w)

A pullulan standard of known M_w and narrow polydispersity ($M_w/M_n = \sim 1.23$) was used to evaluate the accuracy and precision of the HP-SEC-MALLS. A literature dn/dc value of 0.147 mL g⁻¹ was found for pullulan¹⁸⁷ and was used in the following measurements.

Table 19: HP-SEC-MALLS Results for Pullulan Standard (800,000 M_w)

Pullulan Standard 800,000 M_w (700 $\mu\text{g mL}^{-1}$)	Weight-average Molecular Weight (g mol⁻¹)	Polydispersity (M_w/M_n)
Run 1	795100	1.122
Run 2	793500	1.095
Run 3	792100	1.090
Mean	793567	1.102
Standard Deviation	1501.1	0.0172
RSD %	0.2	1.6

The results generated (Table 19) showed that the HP-SEC-MALLS gave good accuracy and precision for the pullulan standard. The M_w value obtained was similar to the known M_w and there was satisfactory agreement between repeat determinations.

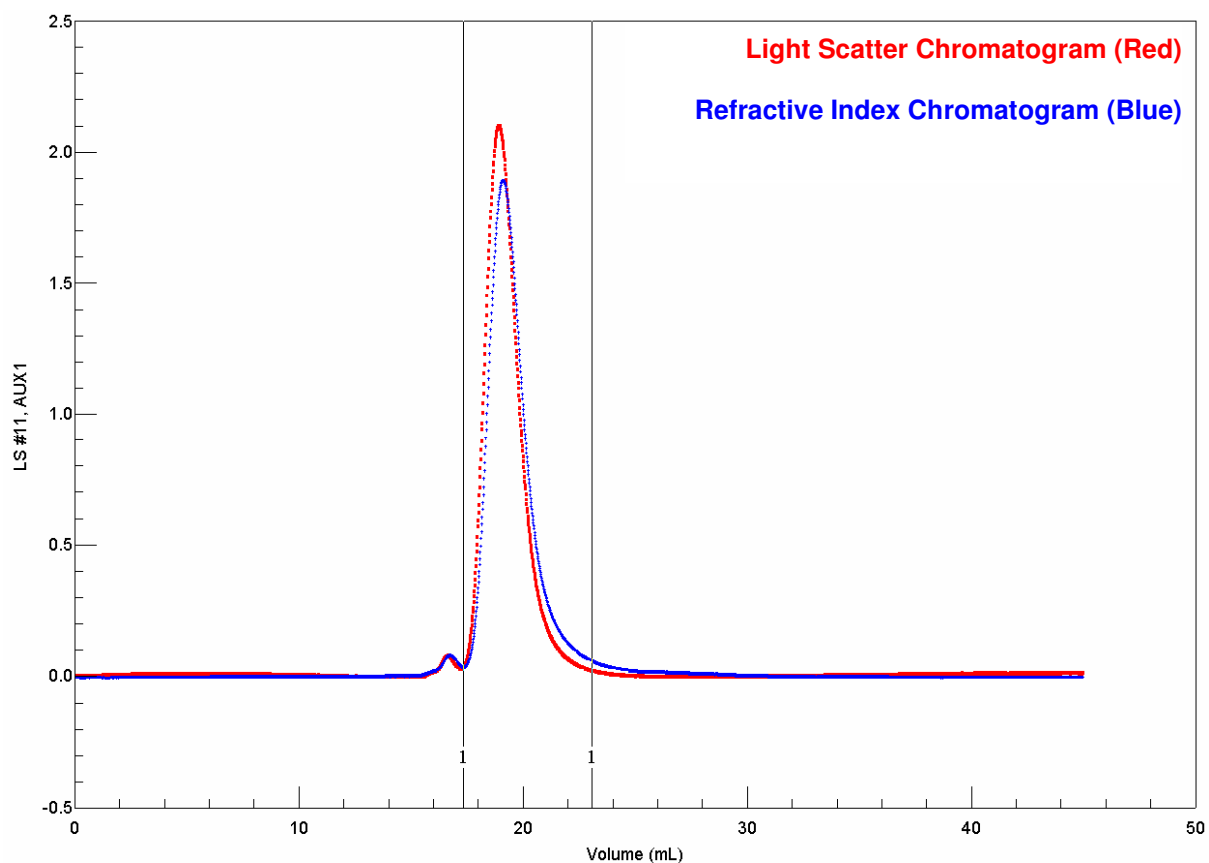


Figure 37: A Chromatogram of the Pullulan Standard (800,000 M_w)

The chromatography (example given in Figure 37) was clean with a large principal peak, which was preceded by a very much smaller peak which had a M_w of $\sim 810000 \text{ g mol}^{-1}$.

The results from the pullulan analysis showed that the HP-SEC-MALLS was capable of accurately and precisely determining the M_w of neutral polysaccharides of known dn/dc .

3.3.2.3 Determination of the Weight-average Molecular Weight for EPS produced by 5e2

After the determination of dn/dc and the successful analysis of pullulan, the HP-SEC-MALLS was used to determine the weight-average molecular weight for the EPS produced by *Lactobacillus acidophilus* 5e2. The specific dn/dc for the EPS (0.198 mL g^{-1} , calculated in section 3.3.2.1) was used to accurately work out the weight-average molecular weight of a $1000 \text{ } \mu\text{g mL}^{-1}$ sample solution (dissolved in deionised water).

Table 20: M_w of the EPS Produced by Two Fermentations of *Lb. acidophilus* 5e2

Fermentation Batch and Details	Samples (1000 $\mu\text{g mL}^{-1}$)	Weight-average Molecular Weight (M_w)[#]	Statistics
Xn341 29 Hours Fermentation	Run 1	643800	Mean = 629600 S.D = 12312 RSD = 2.0 %
	Run 2	623100	
	Run 3	621900	
Xn342 24 Hours Fermentation	Run 1	361500	Mean = 348900 S.D = 21737 RSD = 6.2 %
	Run 2	323800	
	Run 3	361400	

[#] In all cases the major peak is used for the M_w determination.

Initially two batches were analysed, Xn341 and Xn342, the fermentation conditions are shown in Table 10. The results show that even though the fermentation conditions are similar there is a distinct difference in the M_w of the EPS from each batch. Xn341 was fermented for five hours longer and has a M_w approximately double that of Xn342, this difference will be discussed in section 3.4. The results for batch Xn342 gave a RSD% of >6 % for three repeat injections of the same sample solution, compared to 2 % for batch Xn341. The differences can be explained by the polydispersity of the samples.

Table 21: M_w/M_n of the EPS Produced by Two Fermentations of *Lb. acidophilus*

Fermentation Batch	Samples (1000 $\mu\text{g mL}^{-1}$)	Polydispersity (M_w/M_n)[#]	Statistics
Xn341	Run 1	1.084	Mean = 1.106
	Run 2	1.104	S.D = 0.023
	Run 3	1.129	RSD % = 2.0
Xn342	Run 1	1.135	Mean = 1.162
	Run 2	1.225	S.D = 0.055
	Run 3	1.125	RSD % = 4.7

[#] In all cases the major peak is used for the M_w/M_n determination.

As can be seen in Table 21, batch Xn342 has a higher polydispersity, hence a broader distribution of molecular weight across the peak. Broader peaks are more difficult to integrate accurately; this may then lead to a higher overall RSD %¹⁸⁸.

A comparison of the peaks in the chromatograms from each batch (shown in Figure 38 and Figure 39) show that batch Xn342 is in fact broader, confirming the polydispersity result.

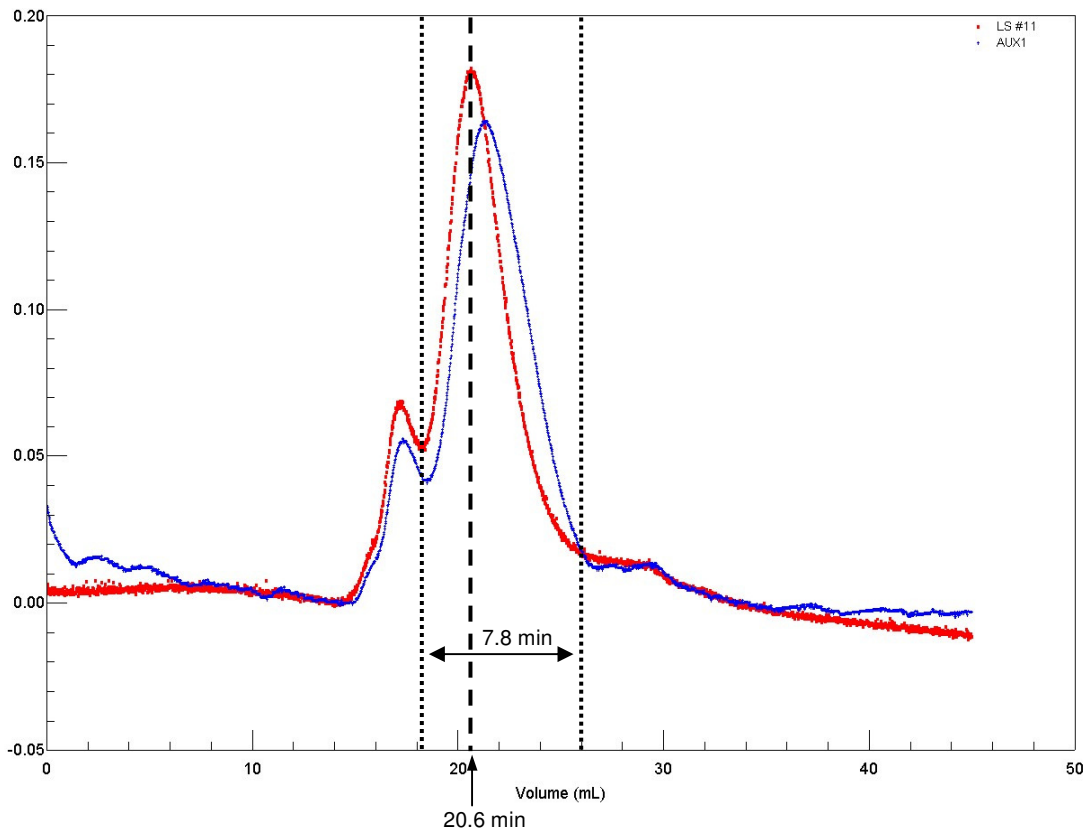


Figure 38: A Chromatogram of EPS produced by 5e2 Batch Xn341

The peak width for batch Xn341 is approximately 7.8 minutes, compared to 8.4 minutes for batch Xn342.

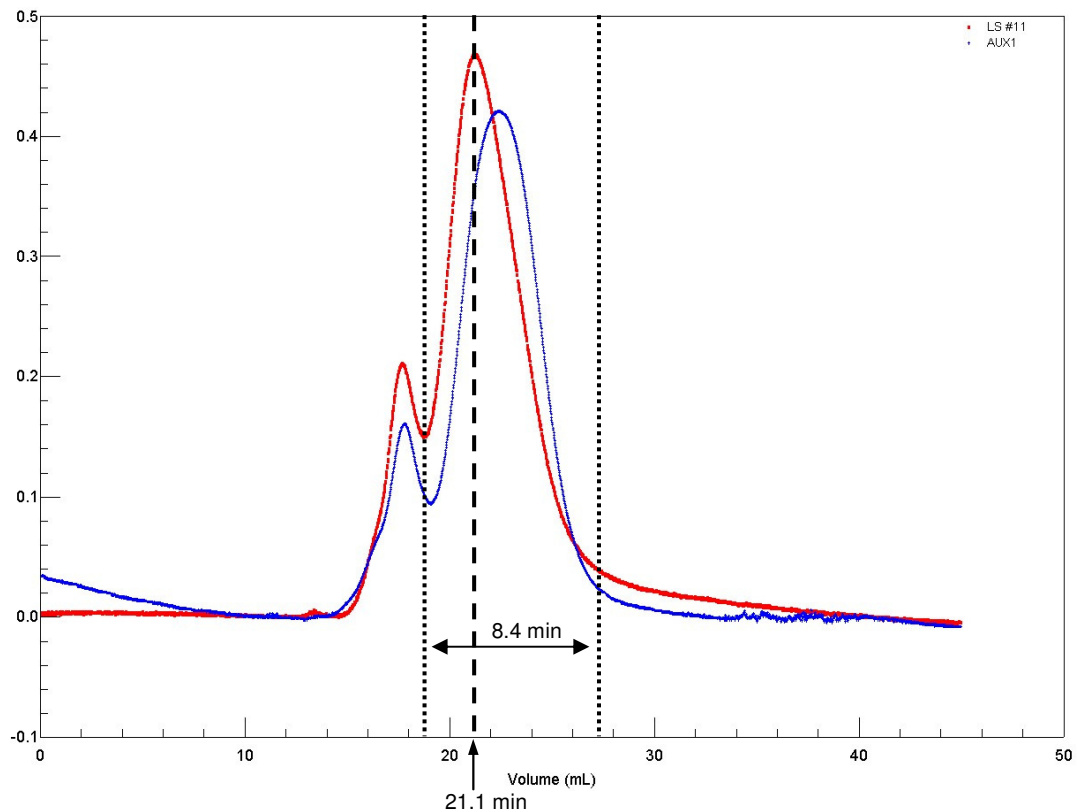


Figure 39: A Chromatogram of EPS Produced by 5e2 Batch Xn342

The volume at which the peak maxima occurred were also measured, as expected the principal peak in batch Xn341 has a smaller volume due to it having a larger weight-average molecular weight. As explained in section 1.6.4.1, larger macromolecules elute first when using size exclusion chromatography.

Both chromatograms of the EPS sample (Figure 38 and Figure 39) show that there are two peaks present; a small peak which is followed by a major peak. Both peaks are believed to be due to EPS, the smaller peak, which elutes first, is thought to be due to EPS with a larger M_w distribution. This is not unusual, many EPS structures have been published that have two or three distinct M_w distributions^{62 79 189}. For this study, the M_w of the major peak was determined for all EPS samples, this meant that comparison between different fermentation batches could be made.

The exact limits within which to integrate the peak are difficult to define, the M_w can change depending at which points the peak is integrated between. If the M_w is plotted against the volume (which is effectively the time due to the instrument delivering the mobile phase at 1.0 mL min⁻¹), the change in M_w can be observed as a negative slope.

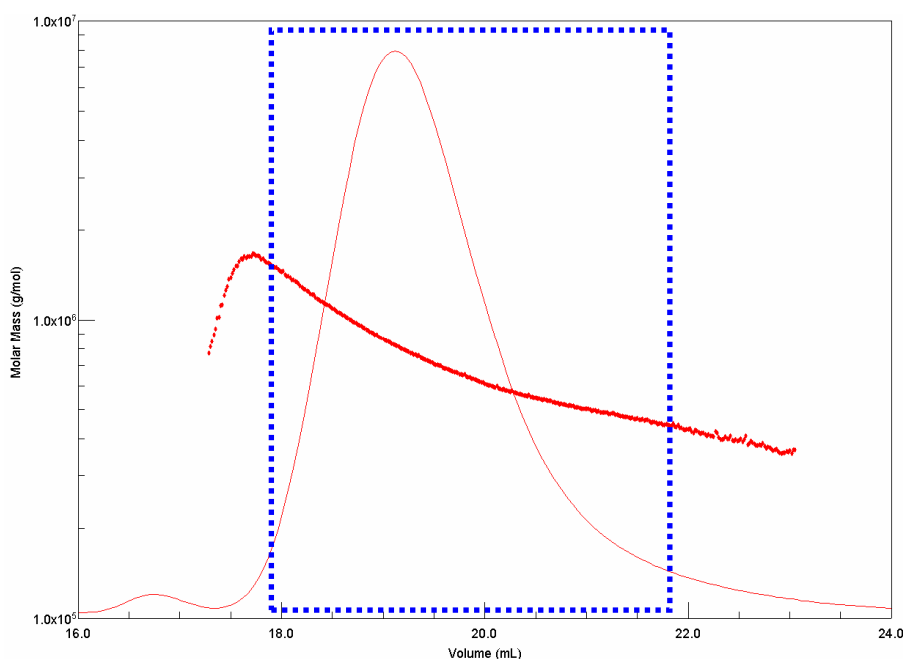


Figure 40: A M_w vs Volume Plot for the Pullulan Standard (800,000 M_w)

Figure 40 shows the M_w vs volume plot for pullulan, this peak should be integrated over this region which is highlighted by the dotted box.

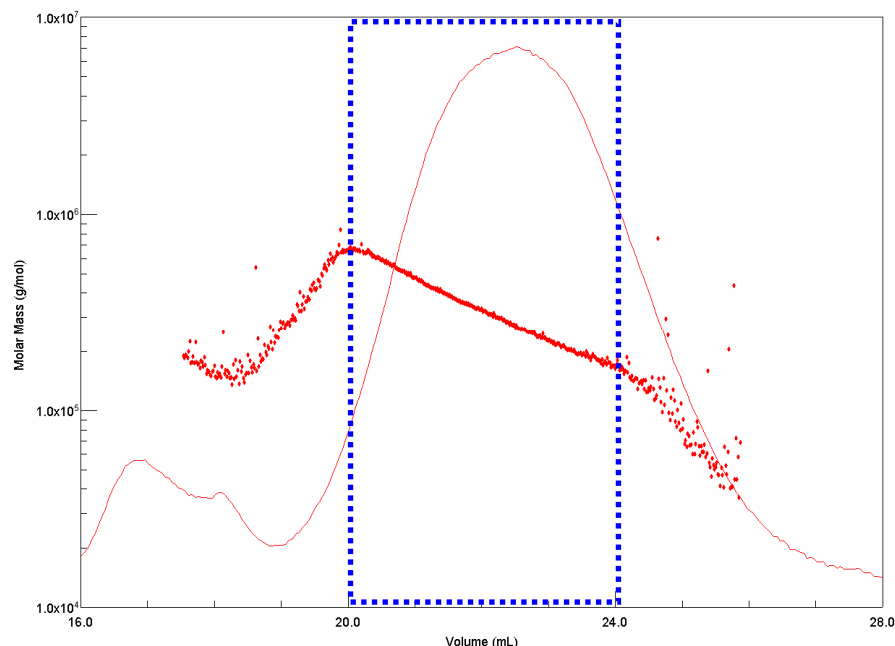


Figure 41: A Molar Mass vs Volume Plot for EPS Produced by *Lb. acidophilus* 5e2

If there are co-eluting or overlapping peaks, integration becomes more problematic. The plot of molar mass vs volume of an EPS sample produced by *Lb. acidophilus* 5e2 is shown in Figure 41, there is a secondary peak on the front shoulder of the principal peak which interfered with an accurate determination of the M_w . The negative slope can be observed across a large section of the peak but not all of the peak. To get an accurate determination of the M_w the integration should be taken over the region with the negative slope. During this region only the principal peak will contribute to the M_w determination. This process has been implemented, when required, for all M_w determinations throughout this work.

Table 22: The M_w Results From EPS Isolated from Other Fermentations

Batch Number	Bacterial Culture	Weight-average Molecular Weight (M_w)	Polydispersity (M_w/M_n)
Xn358 46 hour Fermentation	<i>Lactobacillus acidophilus</i> 5e2	477600	1.218
Xn359 46 hour Fermentation	<i>Lactobacillus helveticus</i> Rosyjski	997300 [#]	1.445 [#]

M_w determination of batches Xn356 and Xn360 are given in sections 3.4.1 and 3.4.2.5 respectively.

[#] dn/dc value for EPS produced by *Lb. acidophilus* 5e2 was used to approximate the M_w , M_w/M_n results.

The M_w determination and polydispersity of batches Xn358 and Xn359 are provided in Table 22. M_w determination of batches Xn356 and Xn360 are given in sections 3.4.1 and 3.4.2.5 respectively.

3.4 Results of the Timed Fermentation Studies of *Lb. acidophilus* 5e2

The production of exopolysaccharide during the fermentation process of LAB is not fully understood. Lin and Chang Chien⁷³ have monitored the yield and molecular weight during the fermentation of two types of *Lactobacillus helveticus* (BCRC14030 and BCRC14076) and a *Streptococcus thermophilus* BCRC14085. They have reported that for *Lactobacillus helveticus* BCRC14030 there was a significant increase in the viable counts, the M_w of EPS and the production of EPS throughout fermentation, which decreased towards the final stages as the culture proceeded through its 'death' phase (defined in section 1.2). An investigation was carried out on *Lactobacillus acidophilus* 5e2, initially to determine if there was a change in the M_w of EPS produced throughout fermentation.

3.4.1 Timed Fermentation of *Lactobacillus acidophilus* 5e2 - Preliminary Study

Firstly, a preliminary study was undertaken to see whether the M_w of the EPS produced by *Lactobacillus acidophilus* 5e2 would change during the fermentation process. The study monitored the fermentation for 72 hours, the majority of samples were taken between 11 – 24 hours, this is where the exponential phase for the growth of *Lactobacillus acidophilus* 5e2 had been reported¹⁸². The samples were collected in sterile glass bottles and the EPS was isolated and the M_w and solid content were determined.

Table 23: Table of Fermentation Results (Batch Xn356)

Time Point (Hours)	Weight-Average Molecular Weight (g mol^{-1})	Solid Content ($\mu\text{g mL}^{-1}$)
0	-	-
11	181300	68.0
12	148500	42.0
13	245300	92.0
14	268000	84.0
15	241600	88.0
16	277500	94.0
17	307000	116.0
18	314100	114.0
19	260600	72.0
20	281300	96.0
21	379800	142.0
22	282700	134.0
23	409900	152.0
24	781100	234.0
38	1219000	226.0
48	1769000	258.0
72	492800	182.0

The results for the determination of the solid content ($\mu\text{g mL}^{-1}$) and also the weight-average molecular weight measurement for each time point are provided in Table 23 and the variation in M_w with time is plotted in Figure 42.

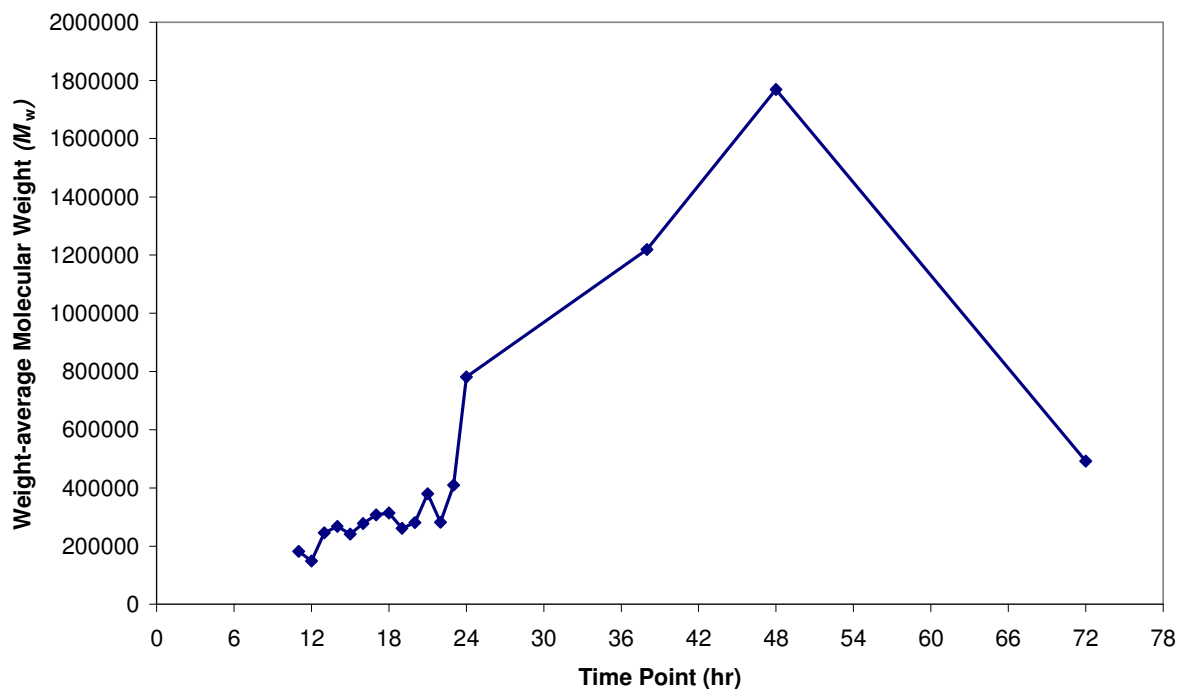


Figure 42: Graph of Molecular Weight against Time for Batch Xn356 during Fermentation

The plot of M_w against time (Figure 42), shows a dramatic change in the M_w of EPS produced throughout the fermentation process. Between 12 – 24 hours there is a gradual increase in M_w , this is followed by a significant increase which continues for the next 24 hours (until 48 hours). During the final 24 hours of fermentation, the M_w decreases to approximately the same size distribution as at 24 hours. Unfortunately, the majority of the sampling was carried out in the early stages.

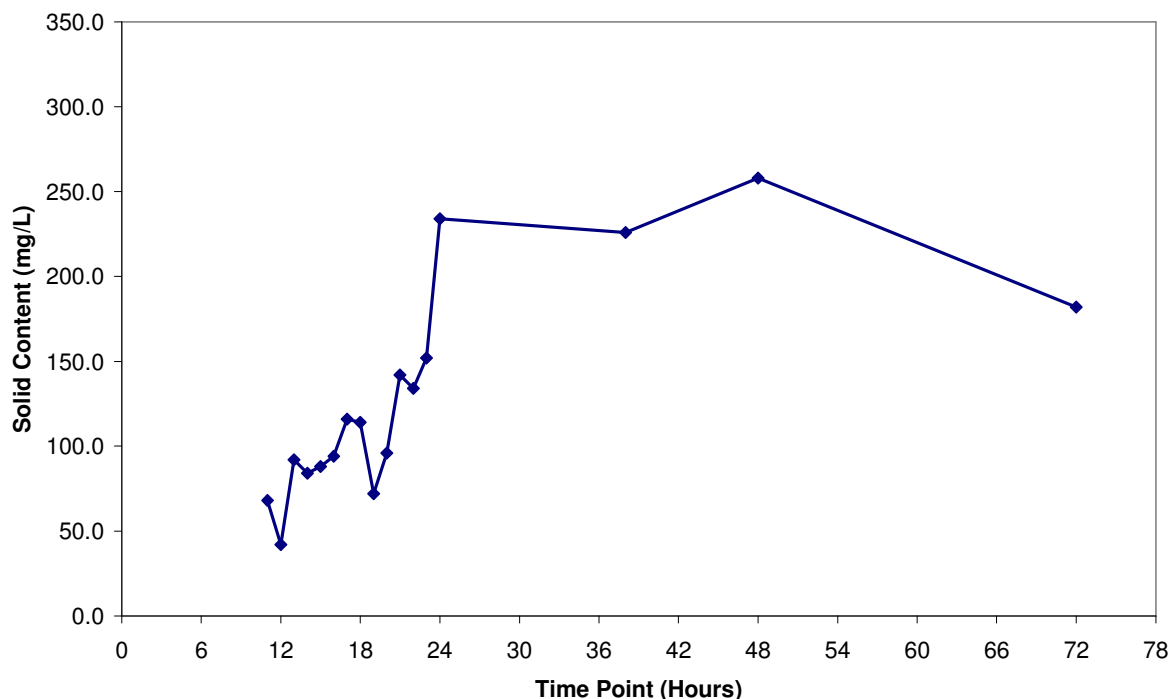


Figure 43: Solid Content Isolated for Each Time Point during the Fermentation Process

The solid content isolated at each time point was plotted (see Figure 43). The solid content of the samples follows the same general trend as the change in M_w of the EPS: there is a distinct increase as the fermentation proceeds, which is followed by a slight decrease towards the end of the fermentation.

3.4.2 Timed Fermentation of *Lactobacillus acidophilus* 5e2 (Batch Xn360)

The results generated from the preliminary study were generally very informative, but more frequent time sampling was needed to verify what was happening during the stationary phase of the fermentation. This would hopefully provide a full explanation of the EPS production during the fermentation of *Lactobacillus acidophilus* 5e2 in skimmed milk.

The fermentation procedure was monitored at more regular intervals throughout the whole 72 hour fermentation: samples (30 mL) were taken every three hours. *Lactobacillus acidophilus* 5e2 was fermented for 72 hours using the conditions described in section 2.2.3.1. This study was primarily carried out to monitor the changes to the M_w and the

amount of EPS produced, but other tests were performed in order to record the growth of *Lactobacillus acidophilus* 5e2, these were done by measuring the viable counts, turbidity and sodium hydroxide consumption during the fermentation. The results for the tests are shown in Table 24.

Table 24: Results of 72 hour Fermentation (Batch Xn360)

Sample Time Point (hr)	Viable Count (cfu mL ⁻¹)	log ₁₀ cfu mL ⁻¹	Turbidity Abs _(650nm)	% of Total NaOH (4M) Consumed	Solid Content (µg mL ⁻¹)	Weight-Average Molecular Weight (g mol ⁻¹)
0	100	2.00	0.0222	0.00	0.0	0
3	316	2.50	0.0251	1.13	13.3	342500
6	776	2.89	0.0394	4.69	31.7	364900
9	8320	3.92	0.0549	12.44	28.3	378200
12	20900	4.32	0.0990	24.54	81.7	530900
15	21400	4.33	0.0938	42.40	85.0	679200
18	20900	4.32	0.0998	64.23	83.3	910300
21	17800	4.25	0.0845	76.36	116.7	926300
24	15800	4.20	0.0872	82.86	123.3	1289000
27	18200	4.26	0.0974	86.23	125.0	1285000
30	28200	4.45	0.1051	88.72	126.7	1209000
33	16200	4.21	0.1045	90.45	116.7	1189000
36	15100	4.18	0.1135	91.86	108.3	1288000
39	17800	4.25	0.0740	92.87	125.0	1212000
42	14800	4.17	0.0739	93.92	118.3	1225000
45	14100	4.15	0.0839	94.77	120.0	1219800
48	13800	4.14	0.0843	95.73	126.7	1328000
51	6160	3.79	0.1317	96.72	136.7	1251000
54	6760	3.83	0.1167	97.64	135.0	1295000
57	6450	3.81	0.1145	98.55	135.0	1023000
60	4570	3.66	0.1105	99.22	143.3	1036000
63	2040	3.31	0.1117	99.81	133.3	1073000
66	1905	3.28	0.1183	100.00	126.7	927400
69	2820	3.45	0.1236	100.00	130.0	929300
72	1620	3.21	0.1241	100.00	138.3	928300

3.4.2.1 Viable Counts Results

Viable count (colony forming units per mL, cfu mL⁻¹) is a quantitative expression for the amount of microorganisms present, in this case the amount of *Lactobacillus acidophilus* 5e2. The viable counts for each time point, throughout the 72 hr fermentation, were determined and these are shown in Table 24. A graph of the log₁₀ of the viable counts (cfu mL⁻¹) was then plotted against fermentation time (Figure 44).

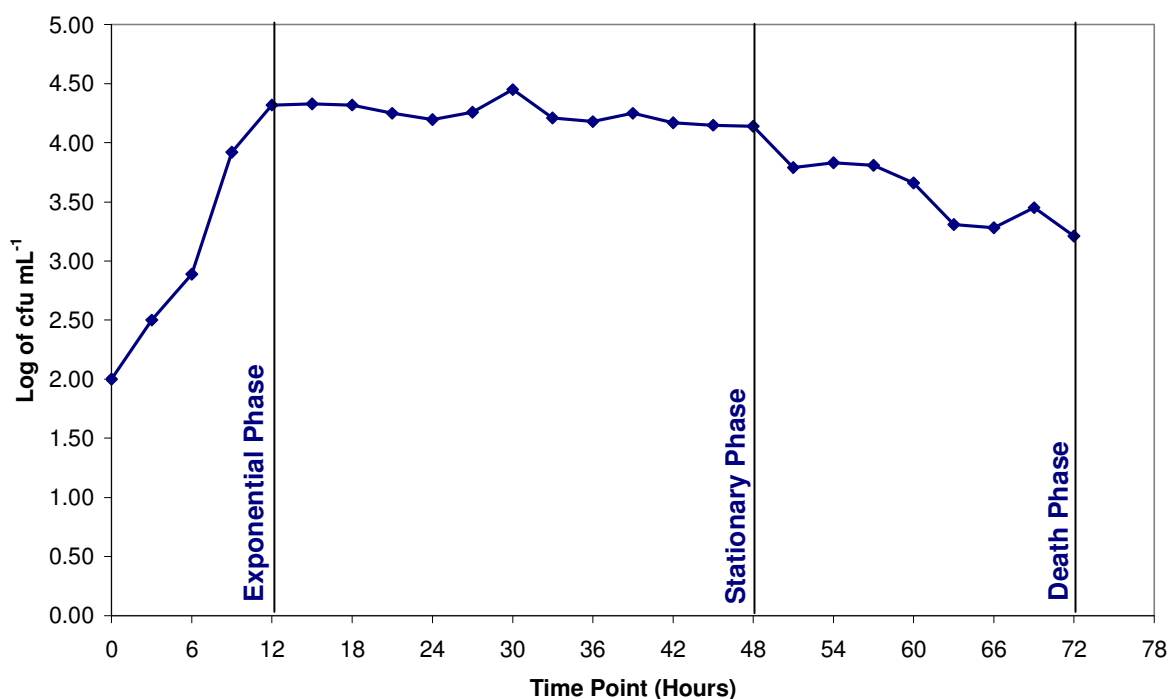


Figure 44: Log of cfu mL⁻¹ for Samples Taken during the 72 hr Fermentation of *Lb. acidophilus*

The viable count results generated show that the growth of *Lb. acidophilus* 5e2 has quickly entered an exponential rate of growth, there is a substantial increase in growth between (0 – 12 hours). After 12 hours, the growth remains approximately stationary until 48 hours, and then slowly decreases towards the end of the fermentation. The reason why the batch entered the exponential phase so rapidly could be explained by the fact that if a bacterial culture in the exponential phase of growth is inoculated into fresh medium, the lag phase is usually bypassed and exponential growth continues¹⁹⁰. Also, previous work carried out at the University of Huddersfield by Elvin⁷², Dunn⁷¹ and Chacon-Romero¹⁸² had optimized the inoculation procedure. Previous work had indicated that EPS was not being produced

during the lag phase, therefore by using a large initial inoculum the lag phase would be reduced. Also, by maintaining the pH at 5.82, this strain of *Lb. acidophilus* has been shown to have optimal conditions for growth. This was studied by Chacon-Romero¹⁸² and it has been reported in section 3.2.1 of this project. An estimate for the magnitude of error associated with these results would be ± 0.2 .

3.4.2.2 Turbidity Results

Turbidity analysis uses spectrophotometry to determine the amount of cells in a culture. This is not a specific test for the amount of *Lb. acidophilus* 5e2 present; all cells in the system will contribute to the reading. This causes the measurements in opaque growth media, such as milk, to be very difficult and accurate readings are often not possible.

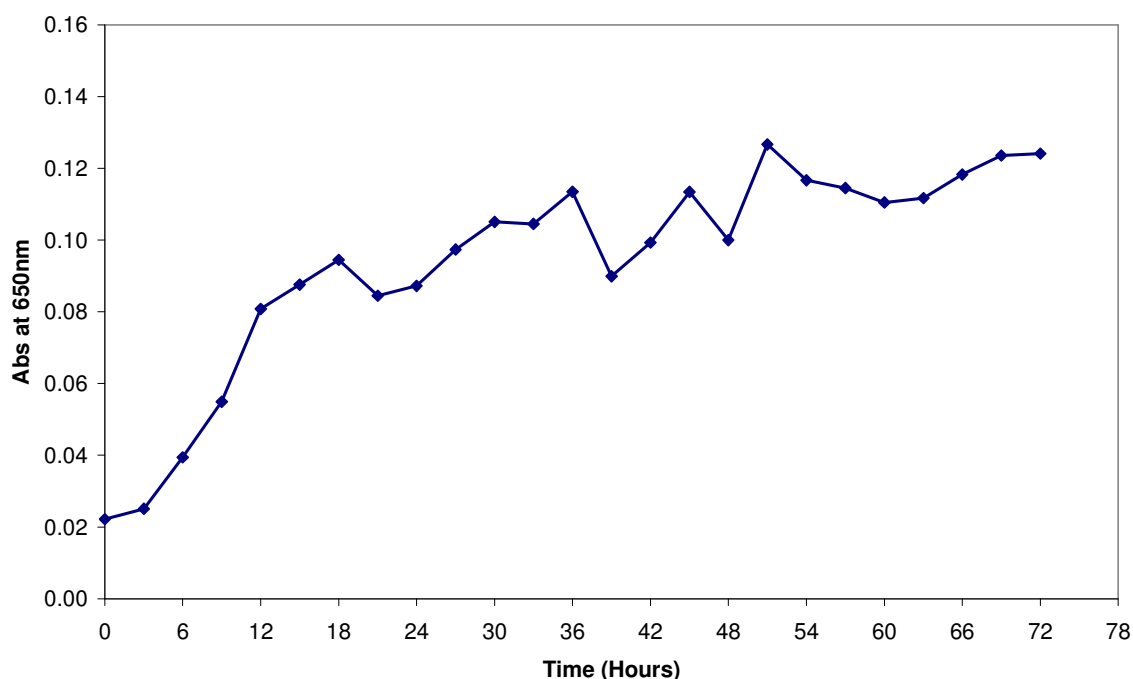


Figure 45: Turbidity of Samples taken during the 72 hr Fermentation of *Lb. acidophilus*

A plot of the turbidity readings for each sample is shown in Figure 45. There appears to be a general trend, that the absorbance_(650 nm) is increasing throughout the fermentation. During the time between 6 – 15 hours the increase in absorbance_(650 nm) is steeper, which coincides with the exponential growth seen in the viable count assay shown in Figure 44. After 15

hours a gradual increase occurs until the end of the fermentation, this is expected because both living and dead cells contribute to the turbidity measurement. There is a drop in turbidity between 39 – 48 hours, but it is not thought to account for anything significant and it can be probably be accredited to the large errors expected from carrying out turbidity analysis on milk samples. An estimate for the magnitude of error would be in the region of ± 0.02 AU.

3.4.2.3 Sodium Hydroxide Consumption

Another method of monitoring cell growth of LAB is by measuring the consumption of sodium hydroxide. For this study the pH of the fermenter is controlled at 5.82 by the addition of sodium hydroxide (4 M). LAB are known to produce lactic acid as the major metabolic end-product of carbohydrate (glucose) fermentation¹³. As bacteria grow and multiply the pH of the medium, in the non-pH controlled fermenter, would decrease. Therefore the amount of sodium hydroxide consumed to regulate pH, in a pH controlled fermenter, would approximately relate to how much LAB is present in the system. Species of *Lactobacillus* produce lactic acid by either homolactic or heterolactic fermentation. Unfortunately, the fermenter (BioFlo 110) was not capable of measuring the amount of ethanol and carbon dioxide produced during fermentation, which may have provided information about which type of fermentation pathway was occurring (homolactic or heterolactic).

The amount of sodium hydroxide (4 M) consumed was recorded as each sample was taken.

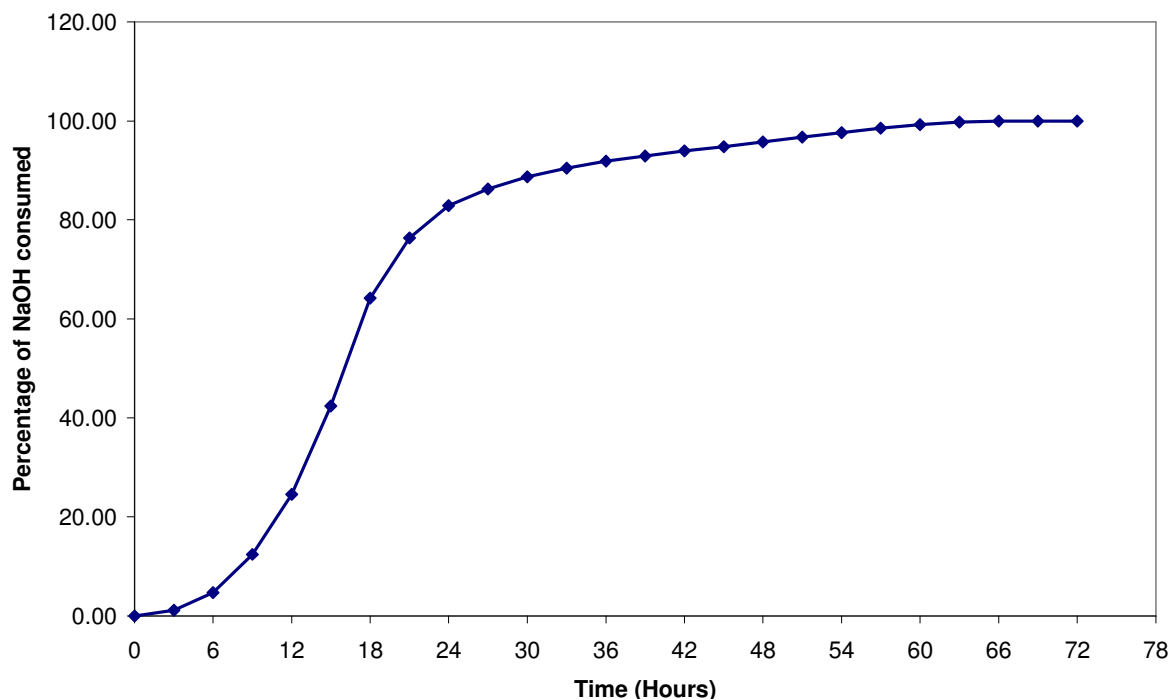


Figure 46: Sodium Hydroxide Consumption during the Fermentation of *Lb. acidophilus* 5e2

A plot of sodium hydroxide consumption during the fermentation is provided in Figure 46. The results are expressed as a percentage of the total amount of sodium hydroxide used throughout the 72 hour fermentation. The graph shows a moderate increase in consumption during the first 9 hours, the increase becomes more significant between 9 and 21 hours and there was a gentle increase up to and including 63 hours. There was only a modest consumption of sodium hydroxide between 63 and 72 hours. The large amounts of sodium hydroxide used in the early stages of the fermentation agree with results for the viable counts and turbidity analysis seen in sections 3.4.2.1 and 3.4.2.2 respectively.

The results from these techniques (viable count, turbidity and NaOH consumption) all indicate that the fermentation conditions used gave adequate growth of *Lactobacillus acidophilus* 5e2. The results provided information of the rate of growth of *Lactobacillus acidophilus* 5e2 which will be discussed in relation to the yield of EPS obtained in section 3.4.2.4.

3.4.2.4 Solid Content of Samples Taken During the 72 hr Fermentation (Dry Weight mg L^{-1})

The solid content of samples taken every 3 hours during the 72 hour fermentation was determined. As shown in section 3.2.2, the percentage of carbohydrate in the solid residue recovered by the isolation procedure (described in section 2.2.5.1) has been shown to be approximately 77.1 %, this must be considered when analysing the solid content results.

The results are provided in Table 24 and are plotted in Figure 47.

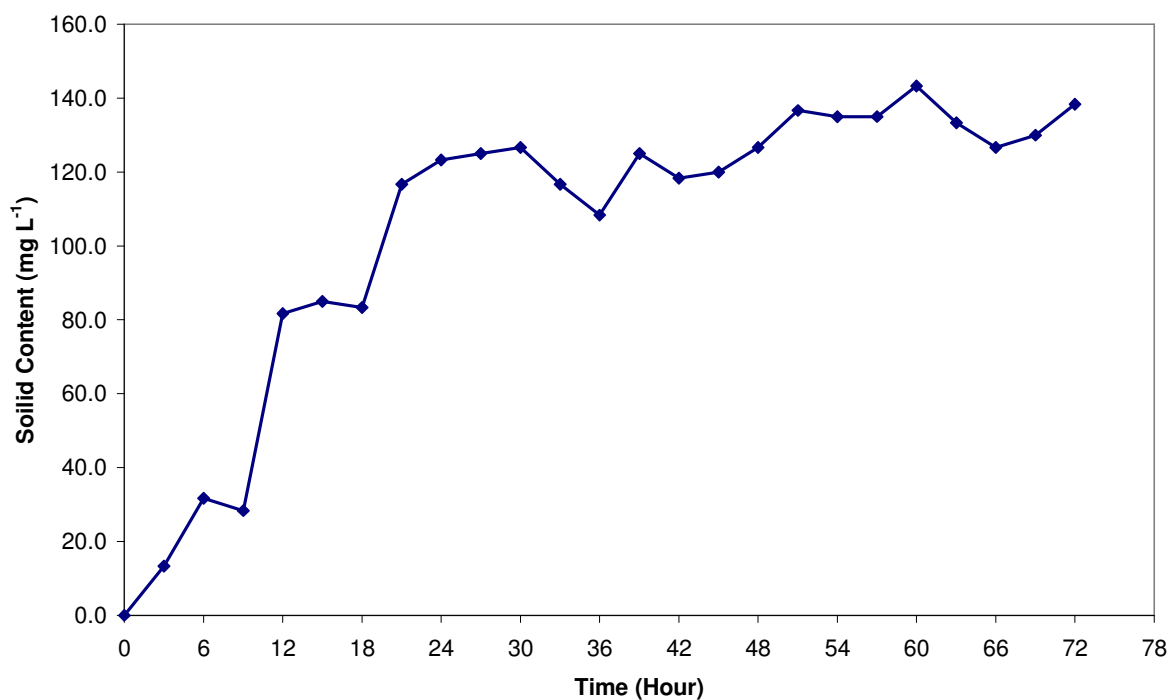


Figure 47: Solid Content Recovered during the 72 hr Fermentation of *Lb. acidophilus* 5e2

As described in section 3.2.1 there are several factors that may contribute to inaccuracies in these results, which must not be overlooked, therefore only general comments can be made about the graph shown in Figure 47. The graph shows an increase in solid content throughout the fermentation, the largest increase occurs between 0 – 24 hours which coincides with increases observed with the viable count, turbidity and sodium hydroxide consumption measurements. The graph shows fluctuations in the correlation between the solid content and fermentation time, which can be attributed to the difficult and lengthy recovery process of the EPS. Therefore an estimate for the magnitude of error for the solid content is $\pm 15\text{mg}$. The results generated, in this study, for the solid content (approximate

EPS yield) are similar to those previously reported by Degeest *et al.*¹⁹¹, and Vaningelgem *et al.*¹⁹² and Knoshaug *et al.*¹⁹³. They all reported that EPS production is related to growth of the LAB cultures. Degeest *et al.*¹⁹¹, described that the EPS concentration increased between 8 – 12 hours, it then reduced slightly and then continued to slowly increase until the end of the fermentation (24 hours). The results reported by Vaningelgem *et al.*¹⁹² showed an increase in EPS yield during the first five hours that continued to rise for the duration of the fermentation (25 hours). In each of these publications the purity of their isolated EPS was not provided, which makes comparisons difficult.

3.4.2.5 Results of Weight-average Molecular Weight Determination

The weight-average molecular weights were determined for EPS samples isolated from each time point, these are provided in Table 24 and are plotted against time in Figure 48.

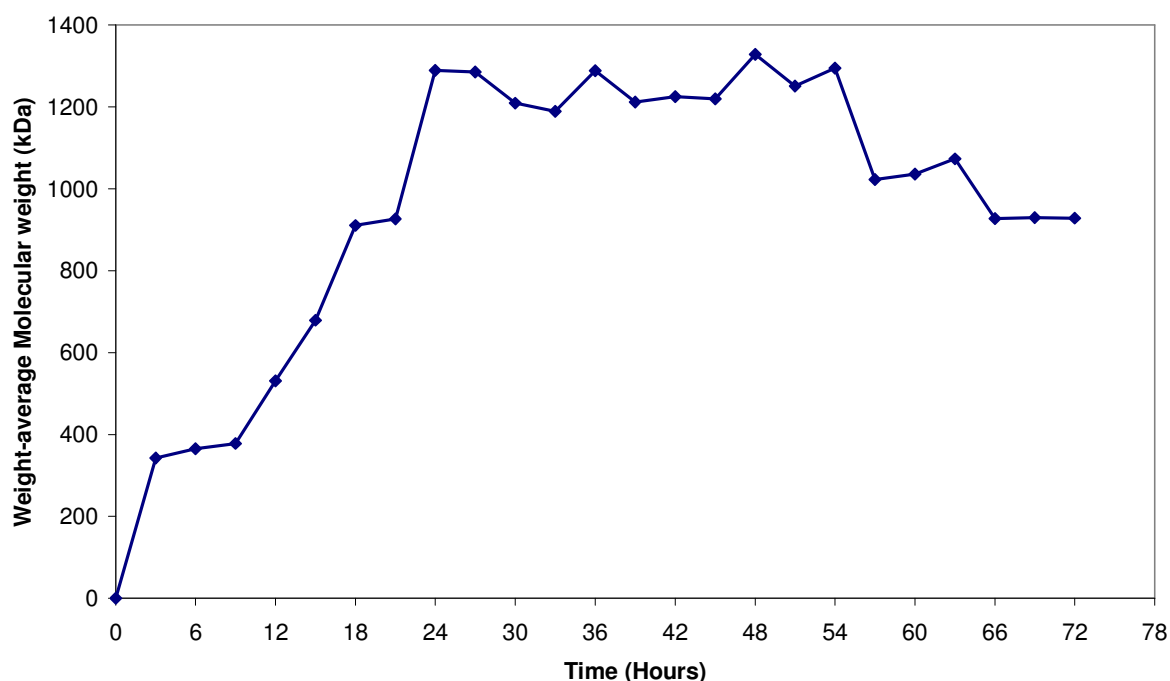


Figure 48: M_w of Samples Taken during The 72 hr Fermentation of *Lb. acidophilus* 5e2

The results shown in Figure 48 show that there was a significant increase in M_w during the first 24 hours of fermentation which was followed by the M_w remaining approximately

constant until 54 hours. The M_w then started to decrease until the fermentation was stopped after 72 hours. The M_w results fluctuates which can be attributed the accuracy of the instrumentation used. An estimate for magnitude of error when determining M_w of EPS by MALLS could be as considerable as $\pm 10\%$. Results reported by Lin and Chien ⁷³ also describe an increase in molecular weight, their results are shown in Table 25.

Table 25: Results Reported by Lin and Chien ⁷³ for the M_w of EPS during Fermentation

Time Point	Highest Weight-average Molecular Weight (kDa)	Fraction (%) of EPS
12	26	100
26	26	68
30	26	77
24	26	100
32	26,500	20
36	26,500	52
48	26,500	19
60	26,500	34
72	2,700	20
84	2,700	23

Lin and Chien ⁷³ reported that the M_w of EPS (isolated from *Lactobacillus helveticus* BCRC14030) remained stationary, at 26 kDa, for the first 24 hours, they then reported a sudden increase to 26,500 kDa after 32 hours which, astonishingly, was an $\sim 100,000\%$ increase in M_w . The M_w remained stationary, at 26,500 kDa, until 60 hours, where it dropped to 2,700 kDa and remained there until the end of the fermentation. The large increase in M_w of EPS they report occurs approximately 12 hours after the end of the exponential phase of growth. This 12 hour delay was also seen in the fermentations discussed in this project (Table 23 and Table 24).

The M_w values that Lin and Chien report are of the highest molecular weight fraction of EPS, this only accounts for as little as 20 % of their total EPS at 32 hours, and also 20 and 23 % for 72 and 84 hours respectively. They do not report the M_w for all the remaining 80 % of their sample fractions.

To date, as far as we are aware, there have not been any previous reports in which the chain length of the exopolysaccharide is related to time. The study reported in this thesis is the most reliable investigation of the EPS production and change in M_w during the fermentation process. The results reported in this section have been published in the International Dairy Journal ¹⁹⁴.

3.4.3 Discussion of Timed Fermentation of *Lactobacillus acidophilus* 5e2

The results given in section 3.4.2 show that the largest changes in EPS yield and M_w are seen at the end of the exponential phases. In the period, between 6 and 15 hours, there was a 25-fold increase in the cell count, which was accompanied by a 3.9-fold increase in yield of EPS and a 3.5-fold increase in the M_w which takes place between 6 and 27 hours. There was a 12 hour delay between the time of the exponential cell growth, to the largest increase in EPS yield and M_w , this was discussed in section 3.4.2.5. Over this region the increase in M_w of EPS closely matches the increase in yield and interestingly, this suggests that the overall number of polysaccharide chains within the system has not significantly changed over this period.

The results suggest that during this period of rapid cell division there was extension of existing EPS chains, which was stimulated by the ready supply of sugar nucleotides that are produced for cell wall and EPS synthesis. The increased rate of polymerisation of the EPS was not matched by a corresponding increase in the rate of cleavage of the polymer from its lipid carrier. Once the fermentation has entered the stationary phase, between 24 and 48 hours, the yield of EPS and the M_w remain constant. On prolonged stirring of the system,

between 48 and 72 hours, the yield remains constant but the M_w slowly falls from 1,300 kDa to 900 kDa. It is not fully understood why this should be the case. One possibility, described by Pham *et al.*⁷⁰, is that cell lysis may release glycosylhydrolases that can digest the EPS, hence reducing exopolysaccharide chain length. However, experiments described in chapter 4 demonstrate that the EPS produced by *Lactobacillus acidophilus* 5e2 is susceptible to hydrodynamic shear and the very large macromolecules may simply be getting fractured by the stirring in the fermentation vessel. Studies, again described in chapter 4, have also shown that an increase in the viscosity of the solvent in which the EPS is dissolved increases the hydrodynamic shear, hence the EPS chain would be more susceptible to fracture. It has been reported by Ruas-Madiedo *et al.*¹²¹, Ayala-Hernandez *et al.*¹¹³ and Yang and Liao¹⁹⁵ that the presence of EPSs significantly increases the viscosity of the fermented milk medium, this would explain the reduction in M_w of EPS during the latter stages of fermentation. Yang and Liao describe that increasing the shear stress by increasing the viscosity or agitation has a detrimental effect on the production of EPS, but this contradicts the increase in the EPS yield observed in this study.

The increase in viable counts between 6 and 15 hours indicates that approximately four new generations of bacteria are produced. However, since the number of new polysaccharide chains has not increased significantly over the same period, it suggests that de-novo EPS synthesis has been switched off. Groot and Kleerebezem⁵⁰ discuss the role of the *epsA*, *epsB* and *epsC* proteins encoded at the 5'-end of the exopolysaccharide gene cluster in the regulation of EPS production in *Lactococcus lactis*. They have found that EPS production is under the control of a phosphor-regulatory system and that if *epsB* is phosphorylated, EPS biosynthesis is terminated. Their results are in agreement with what occurs during the early stages of the fermentation process, the EPS biosynthesis is being switched off by phosphorylation of *epsB*. The results are also in agreement with the fact that they were unable to identify a gene product that controlled exopolysaccharide chain length.

From the result of this study, an explanation is required as to the factors that control chain length. One possibility is that chain length is controlled by a combination of factors including the availability of sugar nucleotides, the length of the fermentation with the subsequent release of glycosylhydrolases and the extent of hydrodynamic shear within the local environment. It is possible that there may not be a need for a specific gene product that directly controls chain length. Until a specific gene is found, the speculation will continue.

4. DEPOLYMERISATION OF EXOPOLYSACCHARIDES

4.1 Introduction

The results from chapter 3 describe how the weight-average molecular weights (M_w) of exopolysaccharides were measured and showed how the M_w changed during the fermentation process. Further analysis of the EPS produced by *Lactobacillus acidophilus* 5e2 was required to explore how the M_w influences the physical properties of their aqueous solutions. This chapter takes a closer look at the weight-average molecular weights of EPSs and shows how depolymerisation techniques can be used to manipulate the physical and chemical properties of aqueous solutions of EPS.

4.2 Depolymerisation of EPS Produced by *Lactobacillus acidophilus* 5e2

To depolymerise exopolysaccharides a chemical or physical process is required, this section investigates three different methods: constant pressure disruption (application of hydrodynamic shear), ultrasonic disruption and acid-catalysed hydrolysis. The results from each technique showed how the polysaccharide backbone was broken and what effect this had on the structure of the repeating oligosaccharide unit. All the depolymerisation studies were performed on EPS produced by *Lactobacillus acidophilus* 5e2. This was due to several reasons, firstly, *Lactobacillus acidophilus* 5e2 provides a good yield of EPS using the fermentation conditions discussed in chapter 3. Secondly, this EPS has been shown to be compatible with the HP-SEC-MALLS, allowing many M_w determinations to be made, without reducing the system's performance. This has not been the case with other EPS cultures studied, which have blocked the HP-SEC-MALLS system, causing lengthy cleaning procedures to be employed.

All the depolymerisation studies were also performed on particular batches of *Lactobacillus acidophilus* 5e2: Xn342, Xn341 and Xn358. These batches gave good yields of EPS and

the isolated EPS gave clean NMR spectra. The HP-SEC-MALLS analysis of EPS isolated from these batches gave a large principal peak with only a relatively small and insignificant secondary peak. A clean HP-SEC-MALLS chromatogram was important because this would allow the changes in weight-average molecular weight of the EPS samples to be measured more precisely.

4.2.1 Depolymerisation of Exopolysaccharides Using a Constant Pressure Disruptor (Application of Hydrodynamic Shear)

The constant pressure disruptor is used in microbiology to open cells so that the DNA, protein, enzyme etc., contained in the cell can be extracted and analysed. The technique uses pressure to force the cells through a narrow orifice. The force acting on the cell, which is responsible for breaking the cell wall, is called hydrodynamic shear. It is this force which was used to break the polymer chains of exopolysaccharides, the constant pressure disruption was used to apply hydrodynamic shear to solutions of EPS.

Constant cell disruption was first carried out using five different pressures (2, 5, 10, 20 and 40 kpsi) the sample was passed through the instrument four times and the weight-average molecular weight, polydispersity and the apparent hydrodynamic radius were all determined by HP-SEC-MALLS after each passage through the instrument.

Table 26: Results for the Constant Pressure Disruption Analysis of EPS Produced by 5e2

Pressure	HP-SEC-MALLS Measurement	Number of cell disruption passes				
		0	1	2	3	4
2 kpsi	Weight-average molecular weight (g mol ⁻¹)	324500	226900	231100	239200	222700
	Percentage of initial M_w (%)	100	69.9	71.2	73.7	68.6
	Polydispersity (M_w/M_n)	1.217	1.212	1.175	1.173	1.155
	Apparent hydrodynamic radius (nm)	17.1	17.0	16.8	16.0	13.3
	% of initial apparent hydrodynamic radius	100	99.4	98.2	93.6	77.8
5 kpsi	Weight-average molecular weight (g mol ⁻¹)	323800	186000	198900	191200	191300
	Percentage of initial M_w (%)	100	57.4	61.4	59.0	59.1
	Polydispersity (M_w/M_n)	1.225	1.163	1.158	1.197	1.192
	Apparent hydrodynamic radius (nm)	18.3	14.7	13.6	14.4	13.8
	% of initial apparent hydrodynamic radius	100	80.3	74.3	78.7	75.4
10 kpsi	Weight-average molecular weight (g mol ⁻¹)	323800	144800	132100	120900	110900
	Percentage of initial M_w (%)	100	44.7	40.8	37.3	34.2
	Polydispersity (M_w/M_n)	1.225	1.198	1.193	1.186	1.161
	Apparent hydrodynamic radius (nm)	18.3	12.6	11.3	11.4	10.8
	% of initial apparent hydrodynamic radius	100	68.9	61.7	62.3	59.0
20 kpsi	Weight-average molecular weight (g mol ⁻¹)	323800	116400	102900	93800	100300
	Percentage of initial M_w (%)	100	35.9	31.8	29.0	31.0
	Polydispersity (M_w/M_n)	1.225	1.184	1.199	1.170	1.208
	Apparent hydrodynamic radius (nm)	18.3	12.7	8.3	7.0	7.2
	% of initial apparent hydrodynamic radius	100	69.4	45.4	38.3	39.3
40 kpsi	Weight-average molecular weight (g mol ⁻¹)	361500	102300	67200	68300	85000
	Percentage of initial M_w (%)	100	28.3	18.6	18.9	23.5
	Polydispersity (M_w/M_n)	1.135	1.222	1.228	1.113	1.208
	Apparent hydrodynamic radius (nm)	18.2	10.5	7.1	8.3	8.9
	% of initial apparent hydrodynamic radius	100	57.7	39	45.6	48.9

A graph was plotted (Figure 49) to show the change in M_w for each pressure after each passage through the constant pressure disruptor.

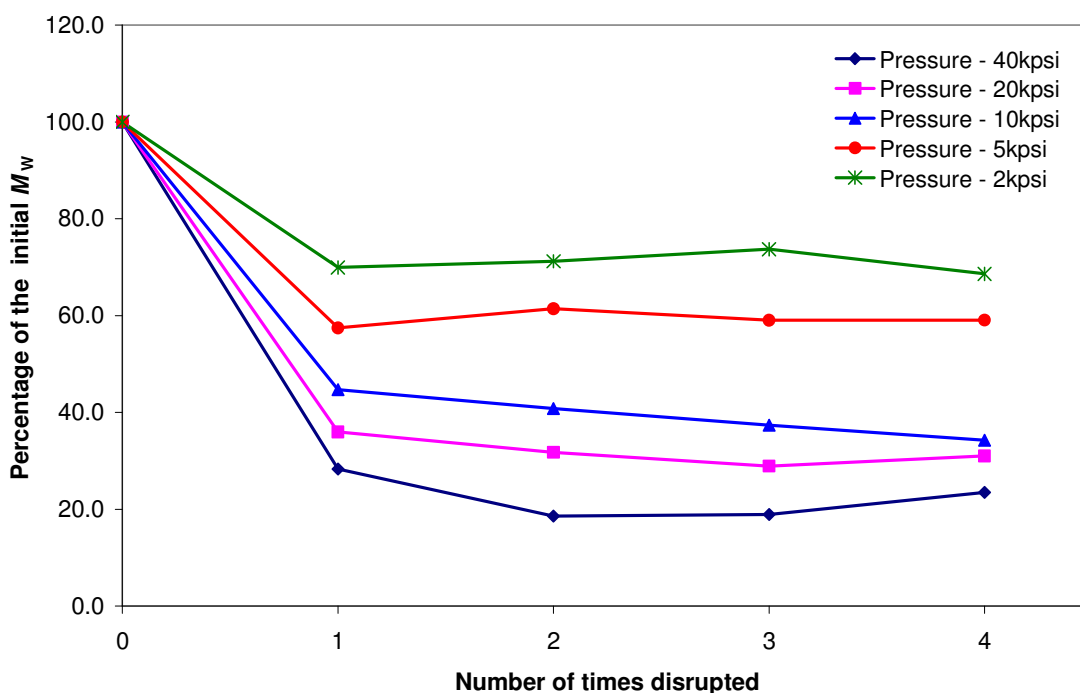


Figure 49: Graph - Constant Pressure Disruption at Different Pressures

The results show that the first passage through the constant pressure disruptor decreases the weight-average molecular weight of the EPS. For each pressure the decrease in M_w is different, the higher the applied pressure the larger the reduction in the length of the polysaccharide chain. At all pressures the largest decrease in molecular weight occurs during the first passage through the constant pressure disruptor, the results seem to plateau for subsequent passes. At each pressure, a limiting M_w was observed, similar findings have been reported for the depolymerisation of polysaccharides using ultrasonic shear (detailed in section 4.2.2). The results for one pass through the cell disruptor at each pressure were studied further and a graph was plotted showing the percentage of initial M_w after passage through the disruptor Vs pressure (see Figure 50).

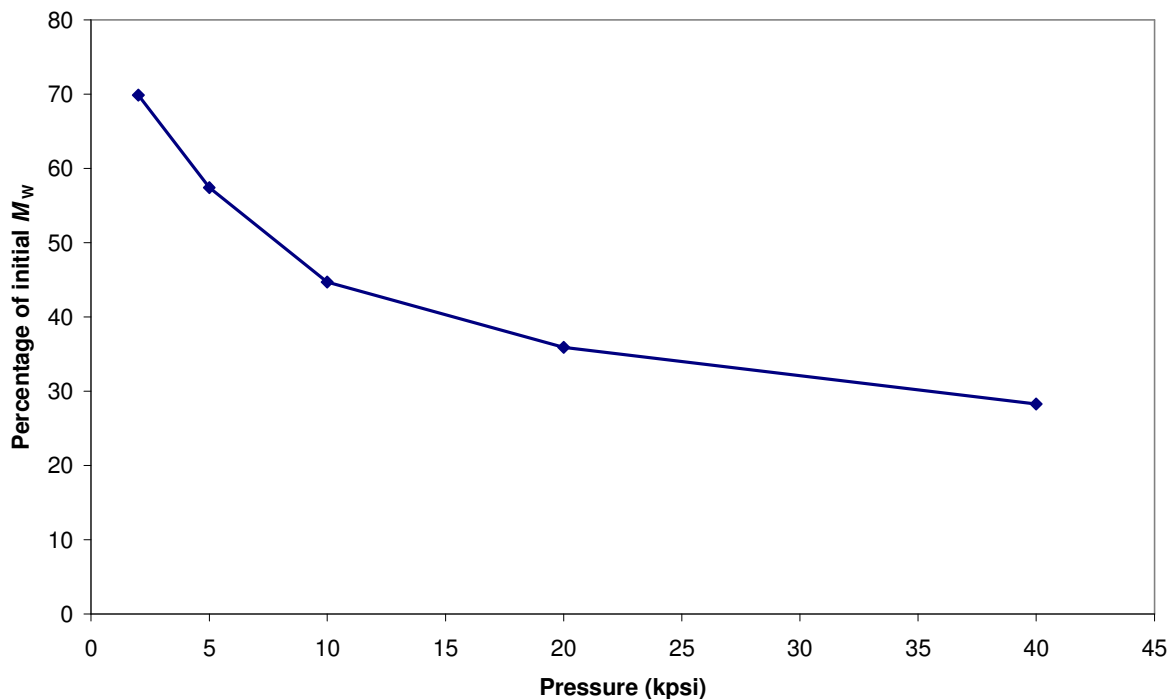


Figure 50: Change in M_w at Different Pressures after One Pass

There is a definite exponential relationship between the pressure used and the change in the weigh-average molecular weight of the EPS, where the reduction in M_w is tending towards a limiting value. The force required to break bonds through the application of shear stress depends on the conformation molecules adopt in solution¹⁹⁶. For a rigid polymer molecule the force necessary for cleavage of the backbone was shown to be inversely proportional to the square of its length¹⁹⁷. The same appears to be true for the results shown in Figure 50, there is a relatively good correlation between the pressure applied to the sample and the inverse square of the percentage mass of the product obtained after passage through the constant pressure disruptor shown in Figure 51.

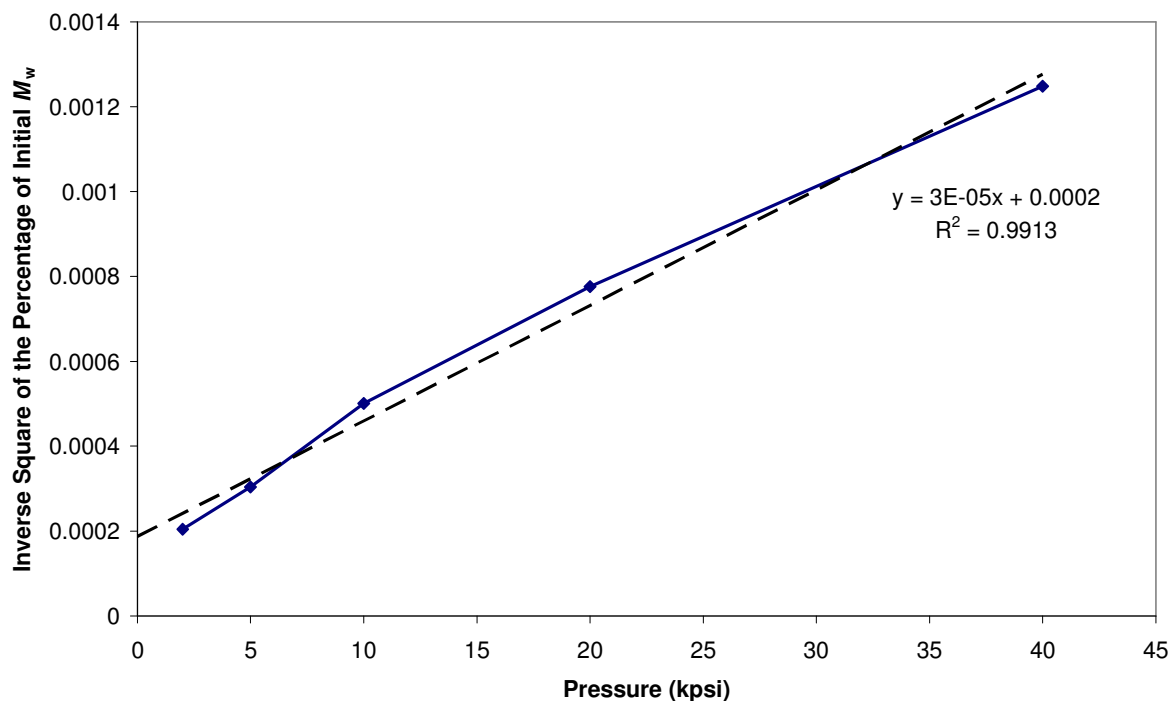


Figure 51: Inverse Square of Percentage M_w Vs Pressure

The correlation of force needed to snap molecules with the inverse square of the mass suggests that it becomes increasingly more difficult to break the molecules as they get smaller; as seen in the experimental results in Figure 49, a limiting mass at which depolymerisation stops is observed for each pressure. Studies of ultrasonic disruption of polysaccharides found similar results with a limiting mass being recorded which could not be reduced, upon continuous irradiation¹⁹⁸.

These results showed that by changing the pressure accordingly, any desired molecular weight could be achieved within an absolute lower limit which is approximately 20 % of the initial M_w . As discussed in the introduction (section 1.4.1) exopolysaccharides play an important role in improving the rheology, texture and mouth feel of fermented products, therefore being able to control the molecular weight of the exopolysaccharides would be of huge benefit for this type of application. It has been reported that an EPS with a larger M_w produces solutions that are more viscous; later in this chapter the relationship between the intrinsic viscosity of EPS (produced by *Lb. acidophilus* 5e2) and M_w will be studied.

The analysis has shown that the M_w of EPS decreases with passage through the constant cell disruptor, the polydispersities of the EPS prepared at different pressures were also measured to see if they altered as the M_w decreased. The polydispersity (M_w/M_n) is a ratio of weight-average molecular weight divided by the number-average molecular weight. A polymer is monodispersed if the M_w/M_n is equal to one, but the term monodispersed is conventionally applied to synthetic polymers which have a ratio less than 1.1¹⁹⁹. The graph in Figure 52 shows the polydispersity measurements from the same set of samples as shown in Figure 49.

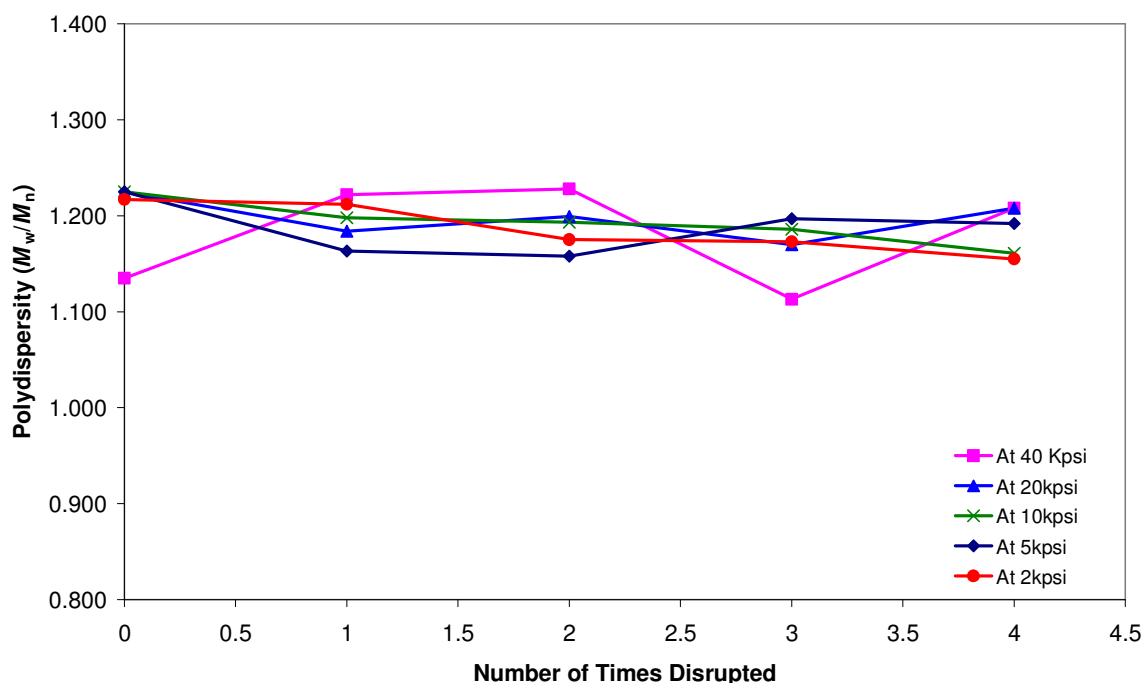


Figure 52: Polydispersity at Different Pressures for Four Passes

The results showed that the polydispersity remained constant at each pressure despite the decrease in M_w , this confirmed that the exopolysaccharide was maintaining the same narrow distribution of M_w after passage through the constant pressure disruptor. To put the polydispersity values into context, a typical synthetic polymer would have a polydispersity value of approximately 4, polyethylene might be more heterogeneous, having a polydispersity of around 30¹⁹⁹. There have been reports using other depolymerisation techniques which have shown the polydispersity to change. Chen *et al.*²⁰⁰ have reported a

decrease in the polydispersity during ultrasonic degradation of chitosan, where the polydispersity decreased from approximately 10 to 2. But the use of enzyme degradation has been shown to increase the polydispersity of cellulose by Pala *et al.*²⁰¹, who report an increase in the polydispersity from approximately 5 to 9, in some cases. The results showing constant polydispersity (Figure 52) suggest that non-random breakages to the polysaccharide chain are occurring. Czechowska-Biskup *et al.*¹²⁶ are another group to have studied ultrasonic disruption of chitosan. They suggest that chain scission proceeds in a non-random manner, where there is a definite minimum chain length which limits the degradation process, and when this is reached no further scission is observed. According to Czechowska-Biskup *et al.*¹²⁶, breakages near the mid-point of the polymer chain are preferred. Therefore, when the exopolysaccharide is subjected to hydrodynamic shear it will be expected to cleave mid chain to generate products with M_w of approximately 50 % of their original values, that maintain a similar polydispersity. This seems to be the case for the results from our experiments (Figure 52).

The apparent hydrodynamic radius of the samples was also determined, where the hydrodynamic radius of a molecule is the size of its radius when in solution, taking into account all the water molecules it carries in its hydration sphere.

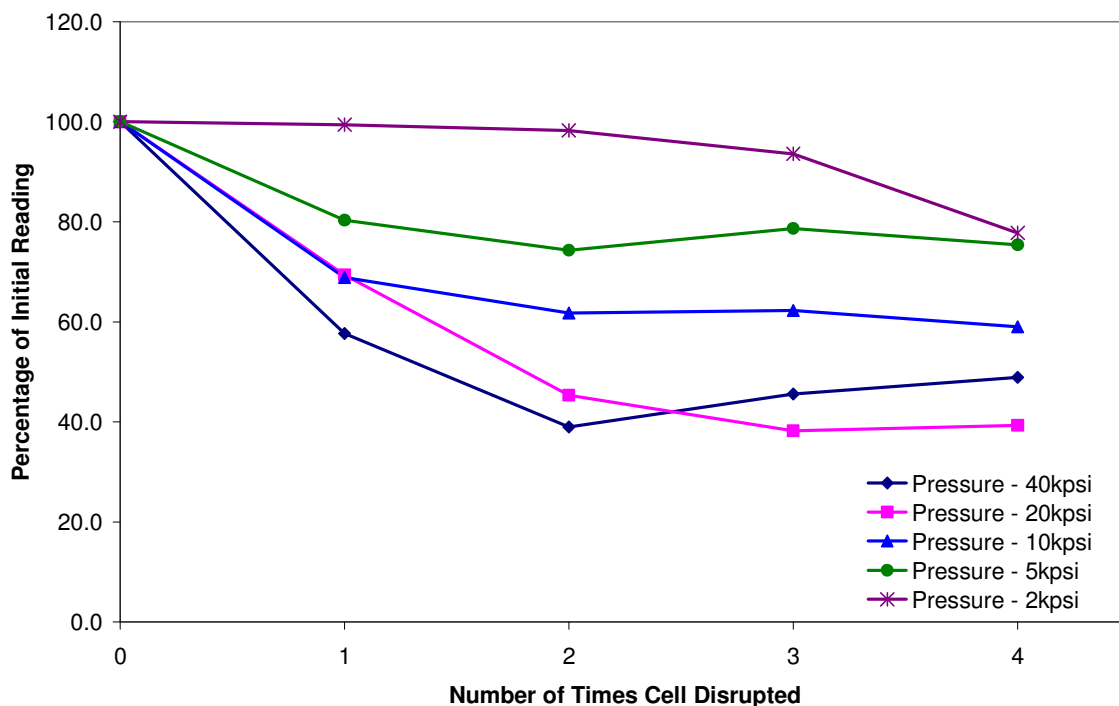


Figure 53: Apparent Hydrodynamic Radius at Different Pressures for Four Passes

A plot of the change in apparent hydrodynamic radius at each pressure for each pass through the constant pressure disruptor is provided in Figure 53. At the higher pressures there is a decrease in the apparent hydrodynamic radius, but the reduction is not as great as seen for the decrease in M_w . When comparing results (using percentage of initial value), after the first pass through the cell disruptor at 40 kpsi, the M_w decreases to 28.3 % of the original value, but the apparent hydrodynamic radius only reduces to 57.7 %. These results suggest that an EPS with a lower molecular weight can hydrate more, relative to its size, than an EPS with a higher molecular weight. To provide an explanation for this, the solution conformation would need to be determined, as the conformation may be different after being subjected to hydrodynamic shear. For example, Tuinier *et al.*¹⁸³ states that, in solution, exopolysaccharides are not rigid rods but behave as random coil polymers. Therefore a change in the conformation of the polysaccharide after constant pressure disruption could cause the coiled exopolysaccharides to straighten, hence, changing the apparent hydrodynamic radius.

The constant pressure disruption work was then repeated using batch Xn341, but this time the pressure was increased after each pass (1st pass at 2 kpsi, 2nd pass at 5 kpsi etc.). Samples were taken after each pass and the molecular weight was determined.

Table 27: Results of the Constant Pressure Disruption of the EPS using Water as Solvent

Solvent Water - Concentration 250 $\mu\text{g mL}^{-1}$			
Passage through cell disruptor	Pressure (kpsi)	Weight-average molecular weight (g mol^{-1})	Percentage of initial average molecular weight
0	0	563900	100.00
1st	2	459000	81.40
2nd	5	304000	53.91
3rd	10	262000	46.46
4th	20	187000	33.16
5th	40	181000	32.10

The change in M_w was plotted against pressure (Figure 54).

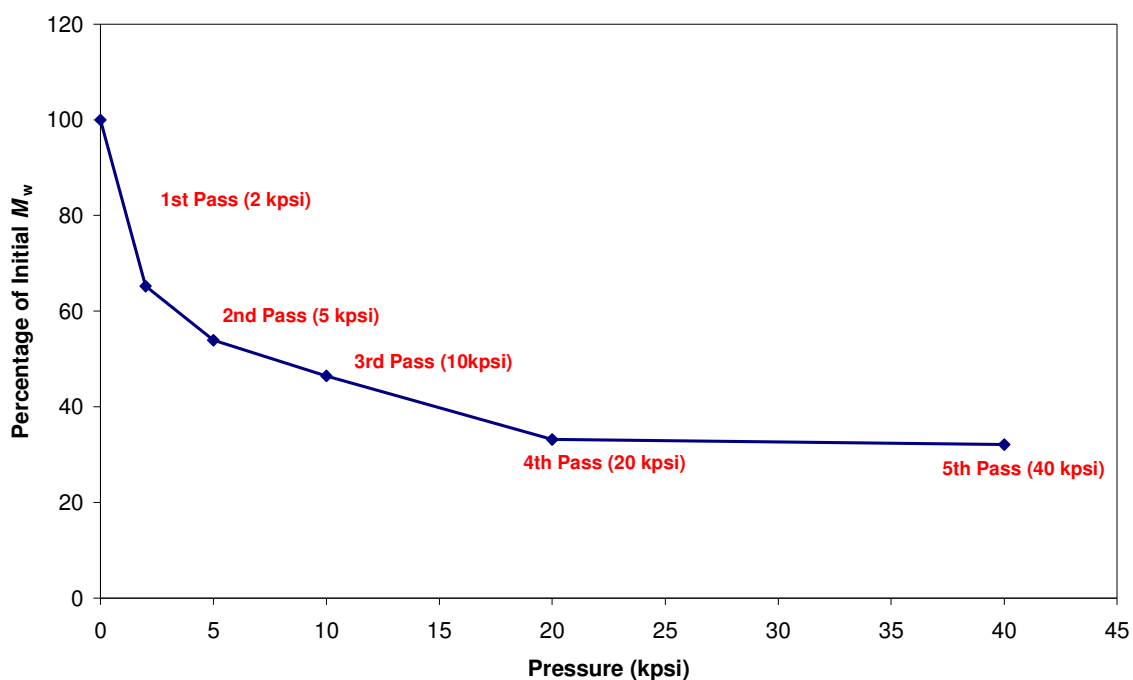


Figure 54: Change in M_w using Different Pressures for Each Pass

The graph in Figure 54 had a similar profile to the graph in Figure 50. Using this procedure the decrease in M_w after the 5th pass (40 kpsi) was the same as the original procedure at 40 kpsi (results in Table 27), when taking the errors of the method into account. This new procedure was developed to allow constant pressure disruption analysis to be carried out on less EPS sample, as only a limited amount of EPS was available.

The viscosity of the solvent has been shown to influence the hydrodynamic shear that is applied on the solute ¹⁹⁹, hence by altering the viscosity of the solvent the degree of depolymerisation using the constant pressure disruptor should change.

The same experimental procedure was then carried out using three different solvents, glycerol, water and a glycerol : water mixture (50:50). These solvents were chosen because they had different kinematic viscosities, as can be seen in Table 28; also the EPS was soluble in each of the solvents.

Table 28: Table of the Viscosities of the Solvents

Solvent	Kinematic Viscosity of Solvent at 20 °C (Shankar and Kumar, 1994) ¹⁷⁸
Water	1.01 cSt
Glycerol: Water	5.26 cSt
Glycerol	1160 cSt

The EPS was dissolved in each solvent and passed through the constant pressure disruptor using the new procedures shown in Table 27. The results that were generated for EPS dissolved in glycerol / water and glycerol are given in Table 29 and the results for EPS dissolved in water were given in Table 27.

Table 29: Results of the Constant Pressure Disruption of the EPS using Two Other Solvents

Solvent Glycerol / Water (50:50) - concentration 250 $\mu\text{g mL}^{-1}$			
Passage through constant pressure disruptor	Pressure (kpsi)	Weight-average molecular weight (g mol^{-1})	Percentage of initial M_w
0	0	549000	100.00
1st	2	292400	53.26
2nd	5	200600	36.54
3rd	10	143600	26.16
4th	20	67130	12.23
5th	40	71230	12.97
Solvent Glycerol - concentration 250 $\mu\text{g mL}^{-1}$			
Passage through constant pressure disruptor	Pressure (kpsi)	Weight-average molecular weight (g mol^{-1})	Percentage of initial M_w
0	0	341500	100.00
1st	2	36070	10.56
2nd	5	33130	9.70
3rd	10	28110	8.23
4th	20	16720	4.90
5th	40	15490	4.54

The results for the percentage of initial M_w for the EPS dissolved in each solvent are plotted in Figure 55.

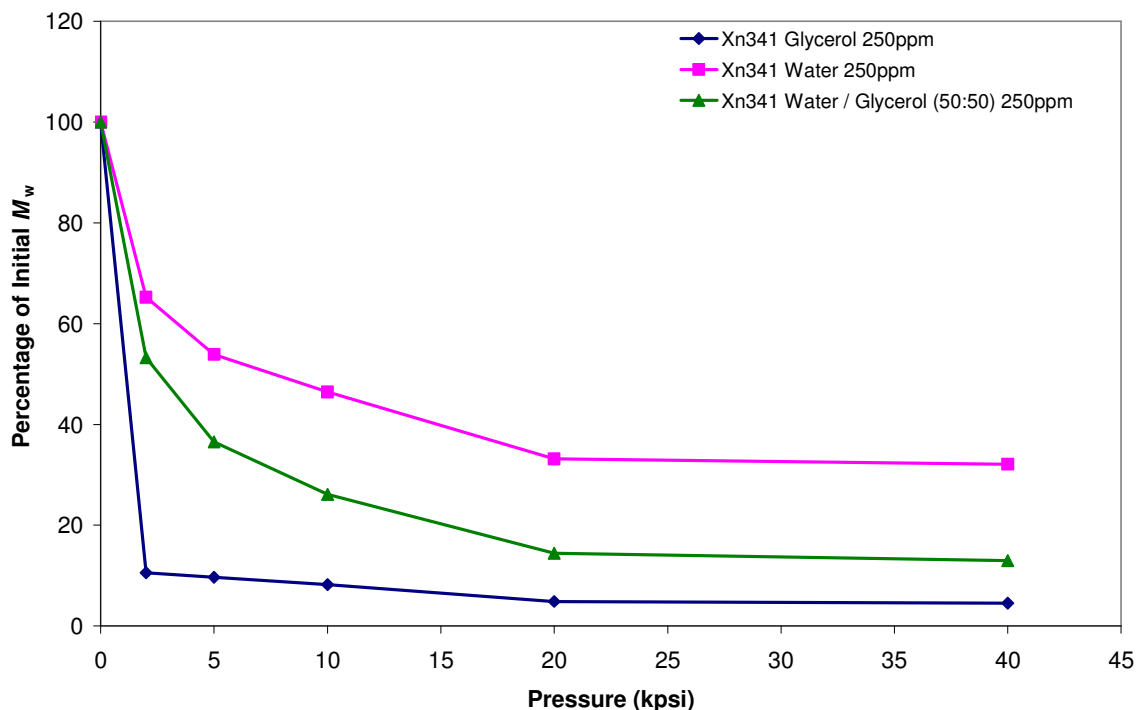


Figure 55: Graph of Constant Pressure Disruption using Different Viscosity Solvents

The graph shows that the M_w of the EPS decreases for each solvent, but more significantly, the degree of depolymerisation for each solvent was different. The results show that the greater the viscosity of the solvent, the greater the degree of depolymerisation of the EPS. Using glycerol as the solvent, the M_w was decreased to $1.5 \times 10^4 \text{ g mol}^{-1}$, i.e. 4.5 % of the initial M_w , compared to a decrease to $1.8 \times 10^4 \text{ g mol}^{-1}$, 32.1 % of the initial M_w , when water was used as the solvent. The results suggest that a more viscous solvent exerts a larger hydrodynamic shear on the EPS. The application of mechanical or shear stress to depolymerise biological macromolecules has a long history, although the majority of studies have concentrated on proteins and nucleic acids¹²⁴⁻¹⁹⁶. Although Harrington and Zimm carried out the majority of their work on DNA, they described the mechanical degradation of polystyrenes in different solvents. They report three techniques of applying hydrodynamic shear by using; a high pressure capillary, a high pressure piston / cylinder and a homogeniser. The high pressure piston / cylinder technique is similar to the constant pressure disruptor, and the results generated for polystyrenes are comparable to the results observed here for EPS (Table 28 and Table 29).

Harrington and Zimm report a decrease to 24 % of the initial M_w after 5 passes through the high pressure piston / cylinder at 3.2 kpsi. There have only been a small number of studies measuring the effect of shear stress on polysaccharides²⁰², other studies have looked at the application of ultrasonic disruption as a technique to depolymerise polysaccharides^{198 203}. Depolymerisation of EPSs using ultrasonic disruption will be discussed in section 4.2.2.

The study discussed in this section, which uses a constant pressure disruptor to apply hydrodynamic shear to exopolysaccharides, appears to be the first of its kind. The controlled manner in which the EPS can be depolymerised should provide the carbohydrate community with a method to explore the rheology of different M_w ranges for a variety of polysaccharides in solution, including EPSs.

Solutions of the EPS were subjected to $^1\text{H-NMR}$ before and after being passed through the pressure disruptor, to determine whether there had been a change to the structure of the repeating oligosaccharide unit. The anomeric region of the $^1\text{H-NMR}$ spectrum was analysed for both samples (Figure 56).

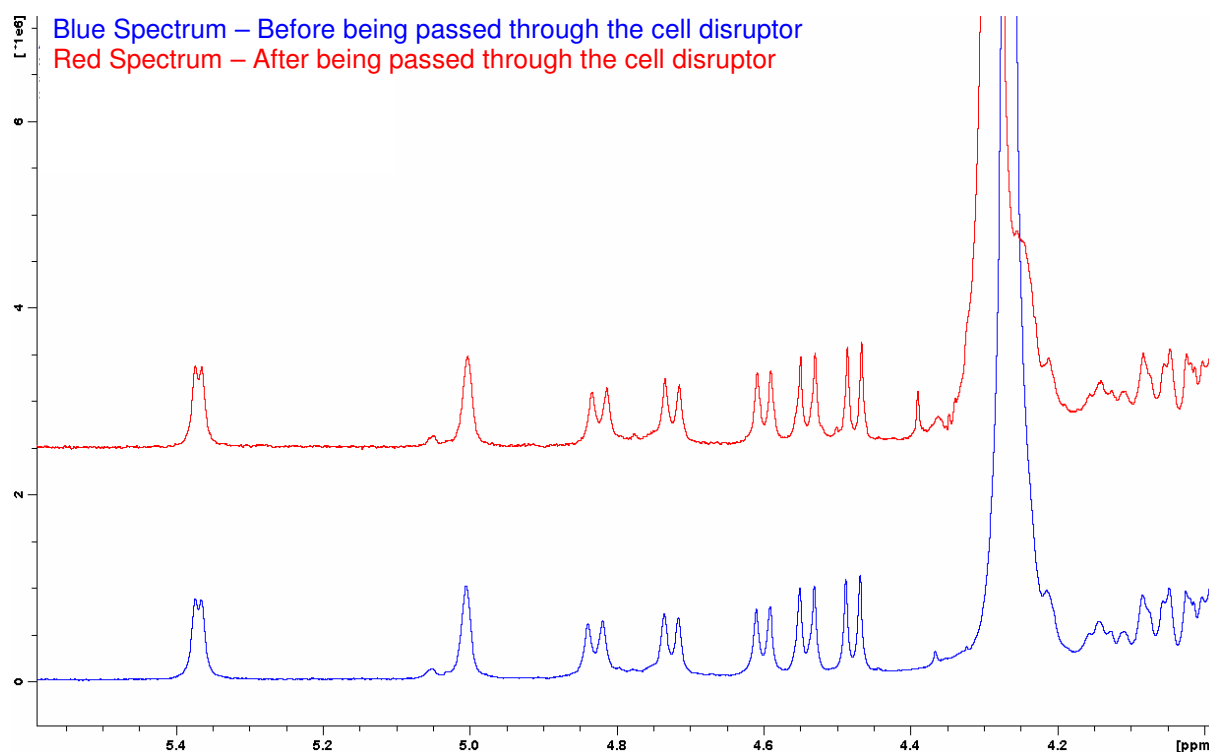


Figure 56: $^1\text{H-NMR}$ Spectrum of the Anomeric Region for EPS Produced by *Lb. acidophilus* 5e2

The $^1\text{H-NMR}$ spectrum, shown in Figure 56, of a constant pressure disrupted sample shows that the anomeric region remains unaltered; this suggests that this depolymerisation technique is not chemically modifying the oligosaccharide repeating unit. The hydrodynamic shear must be creating random glycosidic breakages in the oligosaccharide repeating unit.

4.2.2 Depolymerisation of Exopolysaccharides using Ultrasonic Disruption

The next depolymerisation technique used was ultrasonic disruption; as with the constant pressure disruptor, ultrasonic disruption is used primarily by the Biology Community to extract biological macromolecules from cells. As explained in section 1.7.1.2 ultrasonic disruption works by high frequency electrical energy that is converted to mechanical vibrations, these vibrations create pressure waves which cause the formation of microscopic bubbles or cavities. These expand during negative excursion and implode violently during the positive excursion. This phenomenon is referred to as 'cavitation', which creates millions of shockwaves in the liquid as well as elevating the pressure and temperature. The cumulative effect causes extremely high levels of energy to be released into the liquid. Cavitation generates shear and thermal stresses, whereas constant pressure disruption relies exclusively on hydrodynamic shear.

The force of cavitation causes scission of polysaccharides, which can lead to the production of radicals. Radicals are produced as the glycosidic linkages are broken in a Fenton reaction system²⁰⁴. Radicals are short lived but extremely reactive molecules, capable of degrading all kinds of organic molecules²⁰⁵. Scission of polysaccharides has been successfully measured by Schweikert and co-workers by monitoring the decrease in the viscosity of a polysaccharide solution. Radical scavengers can be added to remove the radicals before they have time to cause unwanted side reactions. Sodium chloride and acetone have been used as radical scavengers in work described by Paradossi *et al.*¹⁷⁹ and other workers have successfully used *n*-butanol²⁰⁶.

In this project acetone (1 %v/v) and sodium chloride (0.1 M) were added to the EPS solutions as radical scavengers. Ultrasonic disruption was carried out on solutions of EPS (1000 $\mu\text{g mL}^{-1}$) using three different amplitudes, 20, 50 and 80 %. The results for the change in M_w and polydispersity during ultrasonic disruption are provided in Table 30.

Table 30: Results - Ultrasonic Disruption of EPS without Temperature Control

Time (Minutes)	Weigh-average Molecular Weight (g mol^{-1})	Percentage of initial M_w	Polydispersity (M_w/M_n)
20 % Amplitude			
0	419000	100.0	1.253
5	49380	11.8	1.130
10	43810	10.5	1.270
15	51270	12.2	1.214
20	35690	8.5	1.402
25	34840	8.3	1.168
30	45120	10.8	1.509
35	28400	6.8	1.667
40	25490	6.1	1.322
45	34530	8.2	1.474
50	16090	3.8	1.835
50 % Amplitude			
0	885300	100.0	1.098
5	139500	15.8	1.435
10	41210	4.7	1.746
15	35370	4.0	1.804
20	26720	3.0	1.555
25	82140	9.3	1.512
30	86490	9.8	1.280
35	26330	3.0	1.942
40	83500	9.4	1.345
45	76320	8.6	1.447
50	44470	5.0	1.572
80 % Amplitude			
0	406300	100.0	1.812
5	55860	13.7	1.777
10	28220	6.9	1.580
15	43660	10.7	1.942
20	32070	7.9	1.663
25	44600	11.0	1.229
30	73320	18.0	1.372
35	60780	15.0	1.797
40	45350	11.2	1.887
45	31960	7.9	1.760
50	46400	11.4	1.218

A plot of the M_w recorded after disruption at each amplitude is given in Figure 57; the ultrasonic disruption was carried out for 50 minutes without temperature control.

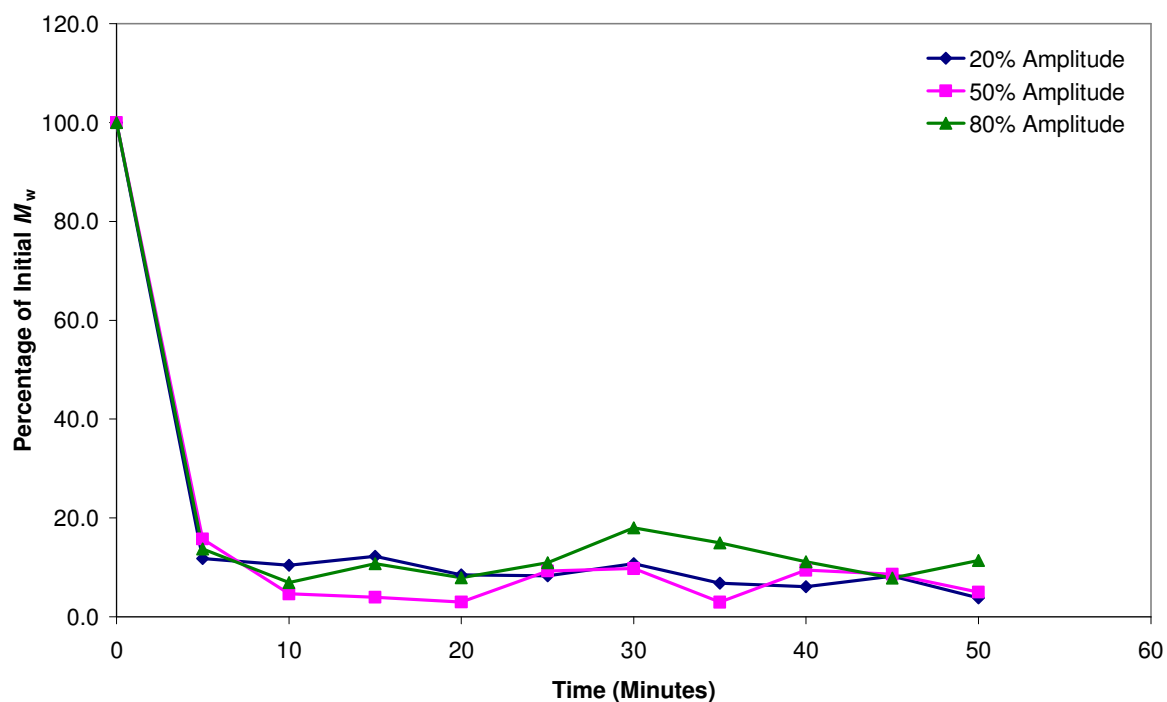


Figure 57: Graph – Ultrasonic Disruption Results of EPS (No Temperature Control)

The results generated show that when ultrasonic disruption is performed without temperature control, the polysaccharide chain is broken quickly. The EPS chain length was reduced to approximately the same M_w for each different amplitude and this occurred exclusively within the first five minutes. Subsequent sonication, for the next 45 minutes, does not alter the EPS chain length. The sudden decrease in the first five minutes was probably due to the heat produced. As discussed earlier in this section, there is significant heat production during the cavitation process, the increase in heat, decreases the activation energy required for the shockwaves to break the EPS chain.

The changes in polydispersity during the ultrasonic disruption are reported in Table 30, when plotted (Figure 58) they show a similar pattern to the polydispersity results seen for the depolymerisation using the constant pressure disruptor.

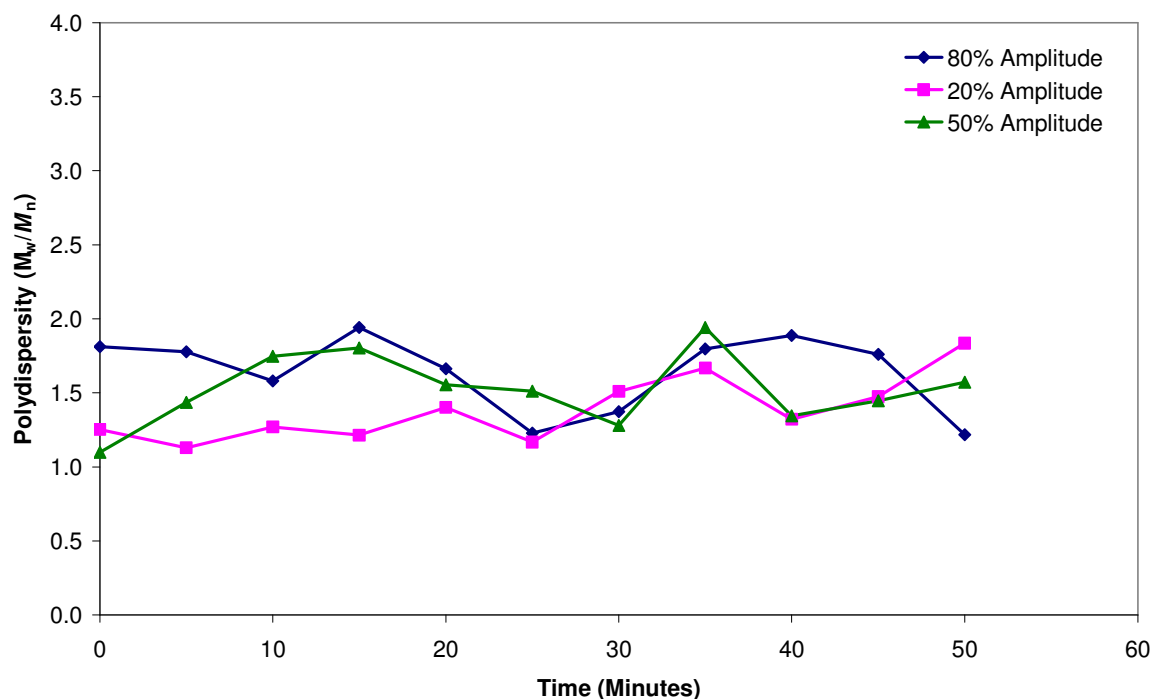


Figure 58: Polydispersity Results for Ultrasonic Disrupted EPS (No Temperature Control)

The polydispersity of the EPS solutions, measured at each amplitude, remains constant throughout the ultrasonic disruption. The T_0 values at each amplitude differ because different batches of EPS were used. These results show similarities to the polydispersity values determined for the EPS solutions that were depolymerised by hydrodynamic shear discussed in section 4.2.1. The results lead to the same conclusion, where non-random scission is evident, and that the breakages are occurring mid-chain. As discussed previously (section 4.2.1), Czechowska-Biskup *et al.*¹²⁶ have reported that mid-chain breaking of polysaccharides is preferred.

The depolymerisation of EPS using ultrasonic disruption was repeated, surrounding the EPS solutions with an ice bath to control the temperature; the results are given in Table 31.

Table 31: Results - Ultrasonic Disruption of EPS Solutions in an Ice-bath

Time (Minutes)	Weigh-average Molecular Weight (g mol ⁻¹)	Percentage of initial M_w
20% Amplitude		
0	425600	100.0
5	382500	89.9
10	350100	82.3
15	294000	69.1
20	205000	48.2
25	175600	41.3
30	182300	42.8
35	166500	39.1
40	194000	45.6
45	181600	42.7
50	170800	40.1
50% Amplitude		
0	425600	100.0
5	266200	62.5
10	205000	48.2
15	136100	32.0
20	87750	20.6
25	100200	23.5
30	71550	16.8
35	86390	20.3
40	76880	18.1
45	87080	20.5
50	74540	17.5
80% Amplitude		
0	425600	100.0
5	151000	35.5
10	102300	24.0
15	64500	15.2
20	65800	15.5
25	42020	9.9
30	36960	8.7
35	45170	10.6
40	33370	7.8
45	46190	10.9
50	47710	11.2

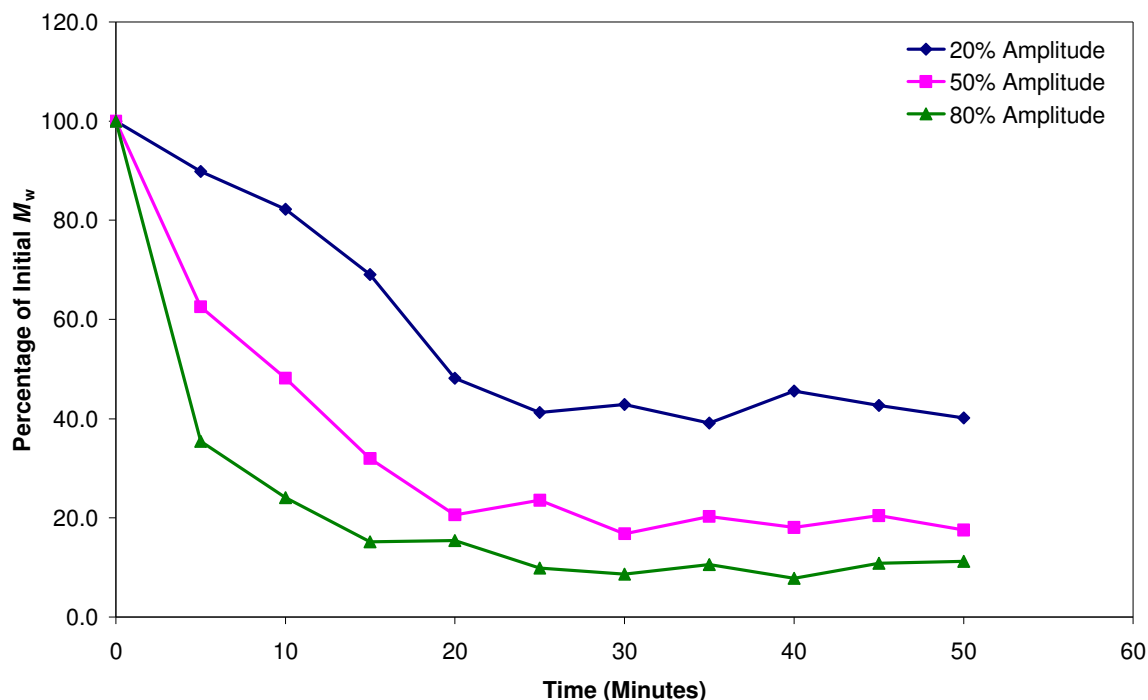


Figure 59: Graph – Ultrasonic Disruption Results of EPS (Using an Ice-bath)

The results presented in the graph (Figure 59) show that, in ice, the EPS depolymerises at a slower, more controlled rate. Clear differences can be seen between the three amplitudes: using greater amplitude increases the degree of depolymerisation. The results generated show that after 50 minutes of ultrasonic disruption, the M_w using 20 % amplitude is 40.1 % of the initial M_w , compared to a decrease to 17.5 % at 50 % amplitude and 11.2 % at 80 % amplitude. From observation of the results, the depolymerisation of the EPS can only be reduced to a limiting value for each amplitude, where no further chain scission is possible. Similar limiting values and have been reported by Basedow and Ebert²⁰⁷, Henglein and Gutierrez²⁰⁸, Malhorta²⁰⁹ and Price *et al.*²¹⁰ who all used ultrasonic disruption to degrade polymers in aqueous solutions. Limiting values for depolymerisation have also been discussed in this report when using the constant pressure disruptor.

The overall depolymerisation, using ultrasonic disruption, is not as controlled as using cell disruption, but the technique can accommodate a much larger sample volume, making this technique more attractive for conducting an experiment to determine the relationship between EPSs M_w and viscosity. An investigation to monitor the relationship between

molecular weight and viscosity of this bacterial polysaccharide is described in section 4.2.3. Work published by other groups, Camino *et al.*¹²⁷ for example, have reported the ultrasonic disruption of hydroxypropylmethylcellulose. They refer to their depolymerisation technique as the application of high-intensity ultrasound, but in their experiment they describe using an identical ultrasonic processor as was used in this thesis. The results they report for the reduction in M_w are comparable to those produced here and shown in Figure 59.

The polydispersity results, for the sample surrounded by ice, showed the same trend as previous results that were ultrasonicated without temperature control.

Solutions of EPS were subjected to $^1\text{H-NMR}$ before and after being exposed to ultrasonic disruption, to determine whether there had been a change to the structure of the repeating oligosaccharide unit. The anomeric region of the $^1\text{H-NMR}$ spectrum was analysed for both samples (Figure 60).

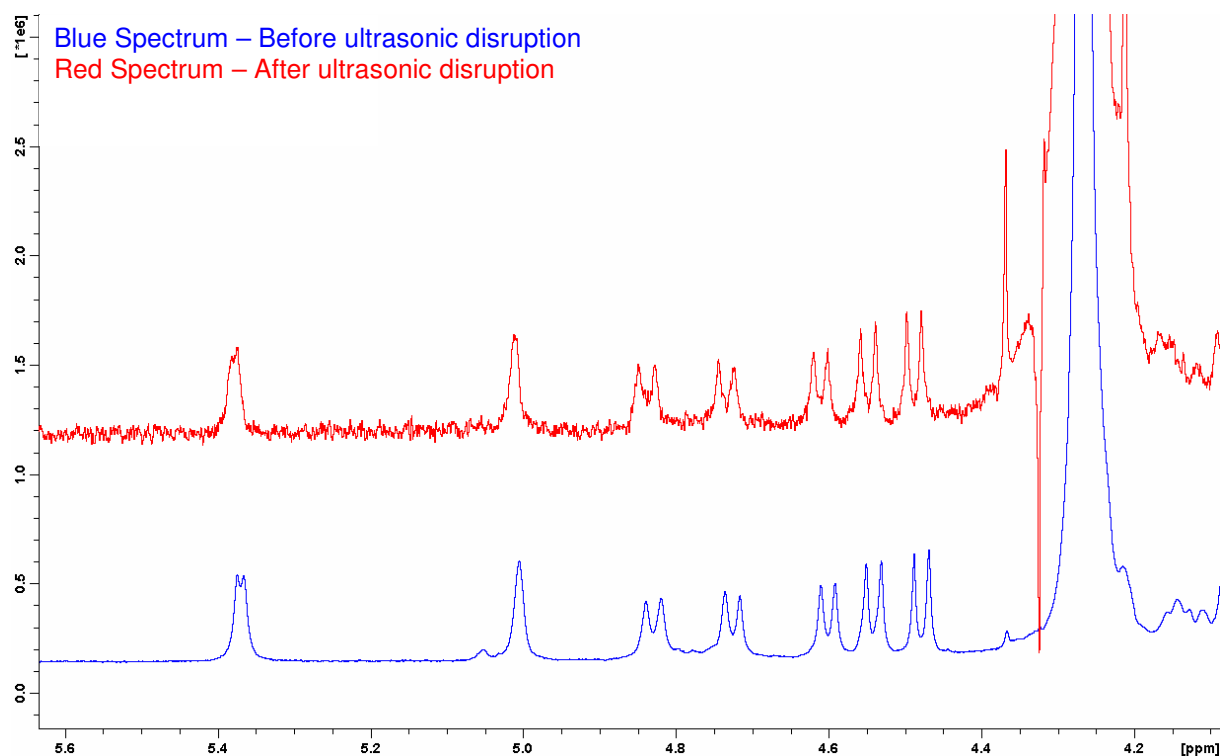


Figure 60: $^1\text{H-NMR}$ Spectrum of the Anomeric Region for EPS Produced by *Lb. acidophilus* 5e2

The ^1H -NMR spectra of an ultrasonicated sample shows that the anomeric region remains unaltered; this suggests that this depolymerisation technique produces no modifications to the polysaccharide backbone structure. The spectra of the EPS sample before (blue spectrum) and after (red spectrum) ultrasonic disruption are shown in Figure 60. The signal to noise ratio of EPS after ultrasonic disruption is much lower because of the presence of sodium chloride, which was added during the sample preparation. The solution contained five times more NaCl than EPS. It is well documented that salts reduce the signal strength of both ^1H and ^{13}C -NMR analysis²¹¹. The EPS solution could have been dialysed to remove the salt, but it was not expected to be of any benefit, as the peaks in the NMR could still be interpreted.

The ^1H -NMR for ultrasonicated EPS gives a similar spectrum to constant pressure disrupted EPS, confirming that by using these two physical depolymerisation techniques, random breakages in the oligosaccharide repeating unit are occurring.

4.2.3 Intrinsic Viscosity Measurements of EPS Solutions

There have been several publications which report that the viscosity of a polysaccharide solution can be reduced by depolymerisation, as previously discussed. Iida *et al.*²⁰³, have used ultrasonic disruption to effectively decrease the viscosity of gelatinous starch. In this section the intrinsic viscosity measurement of the EPS produced by *Lactobacillus acidophilus* 5e2, at different M_w distributions, is reported and discussed.

The approximate intrinsic viscosities for a series of EPS solutions which have different weight-average molecular weights were determined using an Ostwald glass capillary viscometer. All measurements were recorded at 20 ± 1 °C, using the average of three concordant determinations. The intrinsic viscosities could only be calculated approximately because of the insufficient temperature control of the water bath. Temperature significantly affects viscosity measurements; therefore only instrumentation capable of controlling the

temperature by at least ± 0.2 °C should be used to measure viscosity. The results generated from this study were used mainly for the purpose of assessing changes in intrinsic viscosity, not calculating accurate values. Ultrasonic disruption was used to create EPS solutions of different weight-average molecular weights as described in section 4.2.2. A sample of EPS ($1000 \mu\text{g mL}^{-1}$) produced by *Lactobacillus acidophilus* 5e2 was split into four equal portions. Each sample was sonicated for different lengths of time to change the molecular weight distribution (see Table 32). The density and drain times were determined for three concentrations of each sonicated sample solution (A – D) and the η/η^* was calculated using Equation 1, where t is the drain time of the sample, and t^* the drain time of the sample diluent, and ρ is the density of the sample and ρ^* the density of the sample diluent.

$$\eta / \eta^* = (t / t^*) * (\rho / \rho^*)$$

Equation 1¹⁹⁹

Table 32: Viscosity Results and Determination of Approximate Intrinsic Viscosity

Batch: Xn358		Concentration (g dL ⁻¹)	Sample A No Sonication	Sample B 10 min Sonication	Sample C 20 min Sonication	Sample D 40 min Sonication
Measurements	Density at 20 °C (g cm ⁻³)	0.1	1.0151	1.0151	1.0151	1.0151
		0.05	1.0091	1.0091	1.0091	1.0091
		0.025	1.0055	1.0055	1.0055	1.0055
		Sample Diluent	0.9982	0.9982	0.9982	0.9982
	Average Drain Time [#] at 20 °C (sec)	0.1	430.01	387.59	380.05	362.02
		0.05	372.54	355.75	349.23	343.51
		0.025	350.07	342.13	339.86	337.08
		Sample Diluent	333.32	333.32	333.32	333.32
Calculated Values	η/η^*	0.1	1.312	1.183	1.160	1.105
		0.05	1.130	1.079	1.059	1.042
		0.025	1.058	1.034	1.028	1.019
		Sample Diluent	1.000	1.000	1.000	1.000
	$(\eta/\eta^*-1)/C_p$	0.1	3.119	1.825	1.595	1.045
		0.05	2.598	1.578	1.184	0.836
		0.025	2.320	1.360	1.108	0.748
		Sample Diluent	-	-	-	-

The densities of each set of concentrations (Samples A – D) were assumed to be the same before and after ultrasonic disruption. C_p = concentration in g dL⁻¹. [#] Average of three repeats

The $(\eta/\eta^*-1)/C_p$ value was then calculated for each concentration of the sonicated sample solutions (A – D) and then plotted against the concentration. The approximate intrinsic viscosity was determined for each sample solution by calculating the intercept of the trendline, shown in Figure 61 and these are presented in tabular form in Table 33.

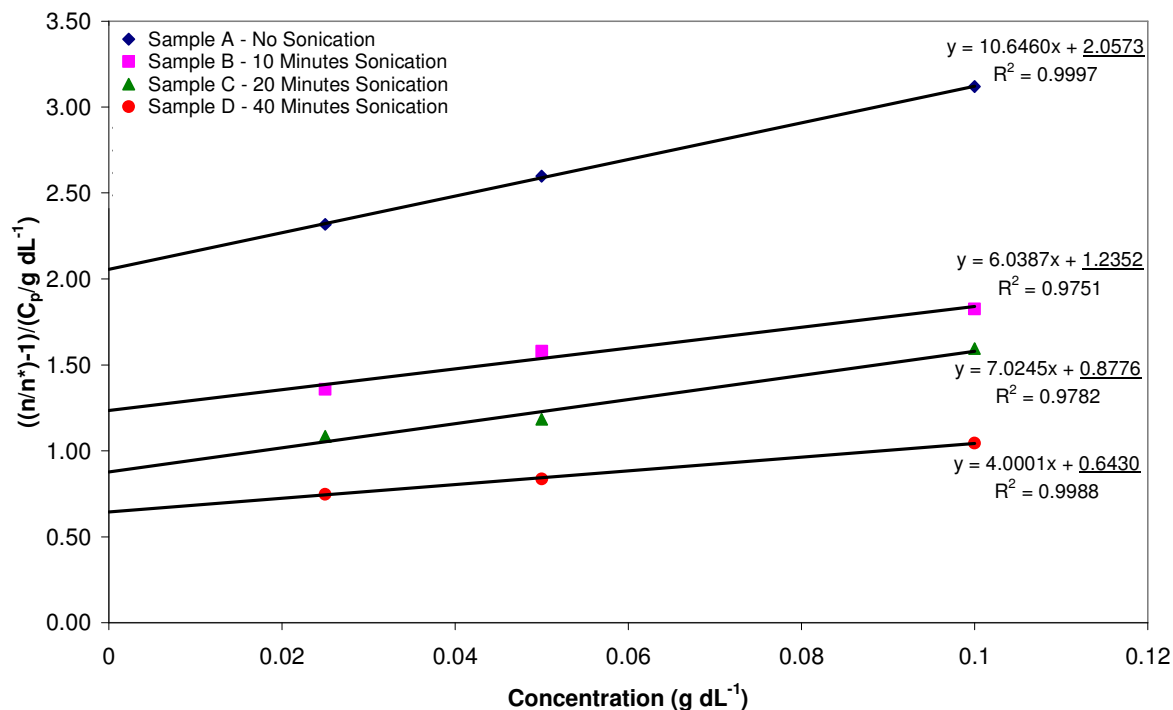


Figure 61: Determination of the Intrinsic Viscosities at Each Molecular Weight Distribution

For each set of samples an increase in concentration gave a longer drain time. Also, as expected, the calculated intrinsic viscosities decreased for the sample solutions with lower weight-average molecular weights. The drain time for Sample C ($1000 \mu\text{g mL}^{-1}$) was slightly longer when compared to times for the other solutions, this caused the gradient of the slope to be steeper than expected. This can probably be attributed to some solid particles affecting the drain time through the glass capillary viscometer or fluctuation in the temperature of the water bath.

Table 33: Results - Intrinsic Viscosity and Weight-average Molecular Weights for Each Sample

Batch: Xn358	Sample A No Sonication	Sample B 10 min Sonication	Sample C 20 min Sonication	Sample D 40 min Sonication
Approximate Intrinsic Viscosity $[\eta]$ (dL g^{-1})	2.057	1.235	0.878	0.643
Gradient	10.646	6.039	7.025	4.000
M_w (g mol^{-1})	477600	304500	213900	159000
Percentage of initial M_w	100.0%	63.8%	44.8%	33.3%

The intrinsic viscosity is the contribution of the solute to the viscosity of a solution. A plot of approximate intrinsic viscosity against the weight-average molecular weight of the EPS is given in Figure 62. The graph shows that the relationship between the two variables is not directly proportional.

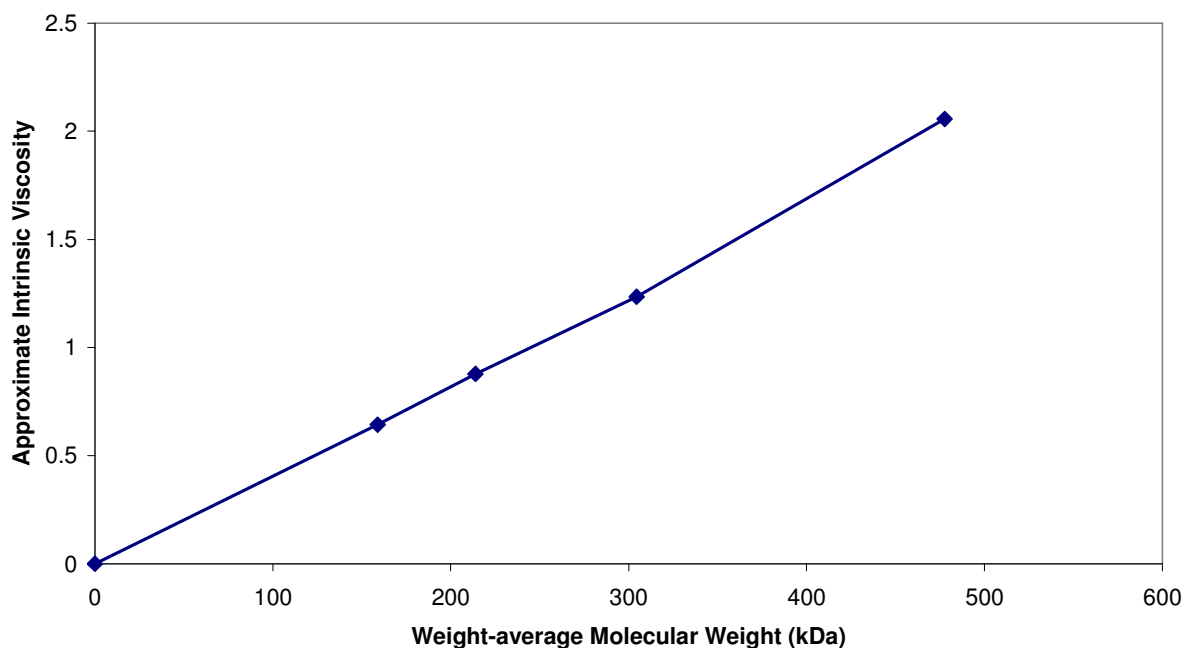


Figure 62: Approximate Intrinsic Viscosity against Weight-average Molecular Weight

Further information can be determined by applying the Mark–Houwink–Kuhn–Sakurada equation which gives the relationship between intrinsic viscosity and molecular weight.

$$[\eta] = K * M_w^a$$

Equation 2: Mark–Houwink–Kuhn–Sakurada Equation¹⁹⁸

Using this equation it is possible to determine the stiffness of the polymer chain. Exponent a can reflect the chain geometry such as branched, sphere, rod or coil. The slope (term a) can be calculated from a plot of $\log [\eta]$ against $\log M_w$.

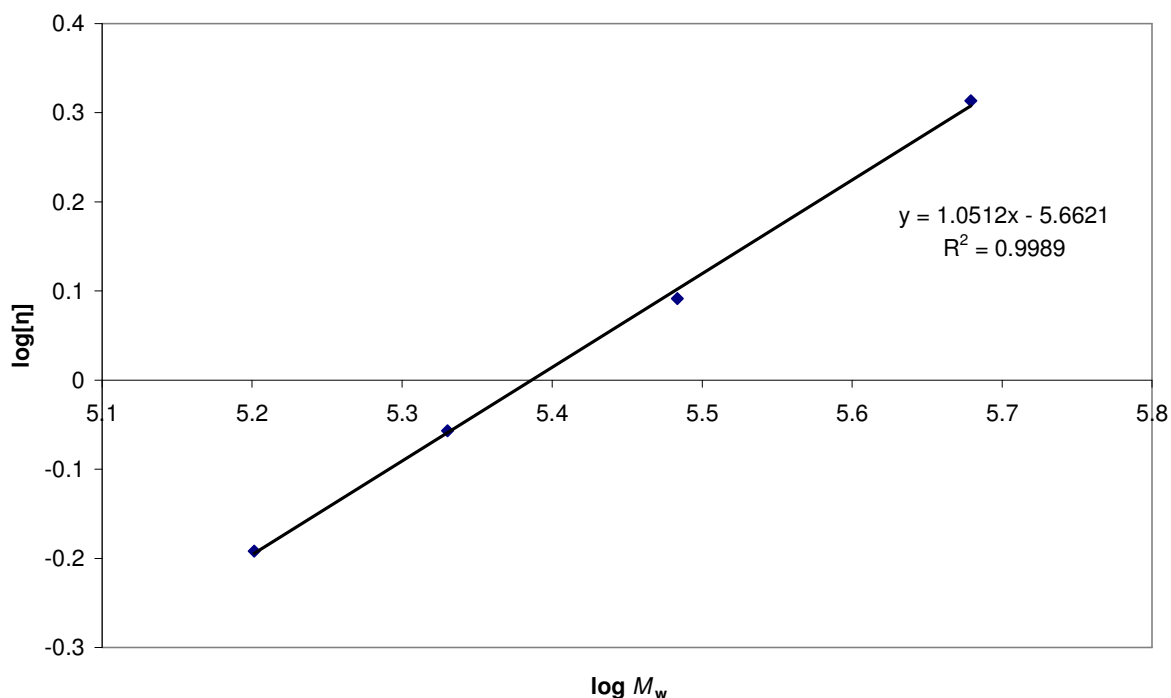


Figure 63: Mark–Houwink–Kuhn–Sakurada Plot of the EPS produced by *Lb. acidophilus* 5e2

A plot of $\log [\eta]$ against $\log M_w$ for the results generated from the EPS produced by *Lb. acidophilus* 5e2 can be seen in Figure 63, which gives a value for a of approximately 1.0. If in solution, term a relates to the following chain geometry: if the polymer molecules are rigid rods, then $a = 2$. On the other extreme, if the polymers are hard sphere, $a = 0$. If $a = 1$, the polymers are semi-coils²¹². The result of 1.0 suggests that the chain geometry for the EPS produced by *Lb. acidophilus* 5e2 is semi-coil, but it must be taken into account that this value has been calculated from approximate intrinsic viscosity values.

The intrinsic viscosity results for the EPS produced by *Lb. acidophilus* 5e2 were compared to other polysaccharides that have been reported. Direct comparisons of the intrinsic viscosities of polysaccharides are often misleading, due the dependence on molecular weight. The EPS produced by *Lb. acidophilus* 5e2 had an intrinsic viscosity of approximately 0.6 – 2.0 dL g⁻¹ over the M_w range of 1.59x10⁵ – 4.78x10⁵ g mol⁻¹, which compares to guar (10 – 11 dL g⁻¹, between 50 – 90 °C)²¹³; pectin (3 – 6 dL g⁻¹, for M_w 145000 – 180000 g mol⁻¹)²¹⁴ and an EPS from *Cyanospira capsulata* (~22 dL g⁻¹, in 0.1 M

NaCl, M_w not provided) ²¹⁵. Another EPS, *Lactococcus lactis* subsp. *Cremoris* ARH53, has also been reported to have an M_w of 1.47×10^6 g mol⁻¹ and an intrinsic viscosity of approximately 20 dL g⁻¹ ¹⁶⁸. When compared to these values, the intrinsic viscosity of the EPS produced by *Lb. acidophilus* 5e2 is not very viscous, this suggests that without chemical modifications this particular EPS could not be used as a thickening, stabilizing or gelling agent in foods or pharmaceuticals. Groot *et al.* ⁵⁰ state that an intrinsic viscosity as high as 20 dL g⁻¹, normally corresponds to weight-averaged molar weights of the order of 10^6 g mol⁻¹. The EPS produced by 5e2 has a M_w of 4.78×10^5 g mol⁻¹, but only an intrinsic viscosity of 2.0 dL g⁻¹, showing that the intrinsic viscosity is low.

Polysaccharides with high intrinsic viscosities normally contain charged groups and branches, such as xanthan for example, which contains (1→4) β-D-glucose units along its backbone, and a substituted trisaccharide at the carbon C3 position on every other D-glucose residue. The trisaccharide consists of a D-glucuronic acid unit between two D-mannose units, approximately half of the terminal D-mannose units contain a pyruvic acid residue linked via keto groups to the 4 and 6 positions, with an unknown distribution. The D-mannose linked to the main chain contains an acetyl group at position O-6 ²¹⁶.

Other polysaccharides, biosynthesised from plants, such as pectins and alginates are used for their gelling properties. These sugars are not neutral and contain monosaccharides that bear carboxylic acids or sulphated groups. The charged nature of these sugars provides them with solubility in water, even when of high molecular weight.

One reason why the intrinsic viscosity of the EPS produced by *Lb. acidophilus* 5e2 was low could have been because the intrinsic viscosity of the EPS was measured using solutions that contained sodium chloride (100mM). There has been work published by Khourvieh *et al.* ²¹⁷, reporting that the intrinsic viscosity of xanthan decreases to less than 50 % when the intrinsic viscosity of the polysaccharide is measured in sodium chloride (40 mM) as opposed

to water containing no sodium chloride. It is believed that the sodium chloride influences the structure of xanthan, making it become more ordered in conformation. This is due to the ionic strength of the sodium chloride. This same effect could be the reason why a low viscosity has been observed for the EPS produced by *Lactobacillus acidophilus* 5e2: the sodium chloride concentration in the solution was 100mM, more than double that used in the xanthan study. The sodium chloride was present to provide chloride ions to scavenge for any radicals produced by the ultrasonic disruption process. In hindsight, the solutions should have been dialysed after sonication to remove the sodium chloride, this would be a recommendation for any future intrinsic viscosity work on EPSs that uses ultrasonic disruption. If there is a difference in the viscosity of an EPS in the absence and presence of salt, then the EPS is showing polyelectrolyte behaviour.

The application of physical methods, hydrodynamic shear and ultrasonic disruption to depolymerisation of exopolysaccharides has been shown to be restricted by the limiting values, where the no further scission of the chain is possible. The techniques have been able to provide a method to determine the intrinsic viscosity of the EPS, but they have not been able to reduce the polymer chains down to oligosaccharide units, which would be useful for intact structural analysis by LC-MS to be discussed in chapter 5.

4.2.4 Depolymerisation Using Mild Acid-catalysed Hydrolysis

The constant pressure and ultrasonic disruption depolymerisation techniques use the application of physical forces to break polysaccharide chains. Using ultrasonic disruption and hydrodynamic shear (applied using a constant pressure disruptor) the M_w of EPSs can be reduced in a controlled manner but to a limiting value. It is also possible to depolymerise using mild acid-catalysed hydrolysis as a depolymerisation technique. This process uses the application of a chemical reaction to break the polysaccharide chain; because of this, it was expected that this technique would potentially modify the structure of the EPS as discussed in section 1.7.1.4.

Acid-catalysed hydrolysis was carried out on a solution of EPS ($1000 \mu\text{g mL}^{-1}$) using mild conditions (trifluoroacetic acid (0.2 M) at $30 \text{ }^\circ\text{C}$). Samples were removed from the reaction mixture periodically, neutralised and the M_w of the EPS was determined. The results for the M_w and polydispersity of the EPS are given in Table 34.

Table 34: Results – Mild Acid-catalysed Hydrolysis of EPS Produced by *Lb. acidophilus* 5e2

Time (Minutes)	M_w of Major Peak (g mol^{-1})	Percentage of Initial M_w
0	489100	100.00
30	399200	81.62
60	353000	72.17
90	314700	64.34
120	298800	61.09
150	247700	50.64
180	200500	40.99
210	199000	40.69
240	195500	39.97
270	199700	40.83
300	171800	35.13
330	150700	30.81
360	158600	32.43
390	160600	32.84
420	116400	23.80
450	130100	26.60
1260	59930	12.25
1500	53710	10.98

A plot of the results for the percentage of initial M_w of the EPS against time are provided in Figure 64.

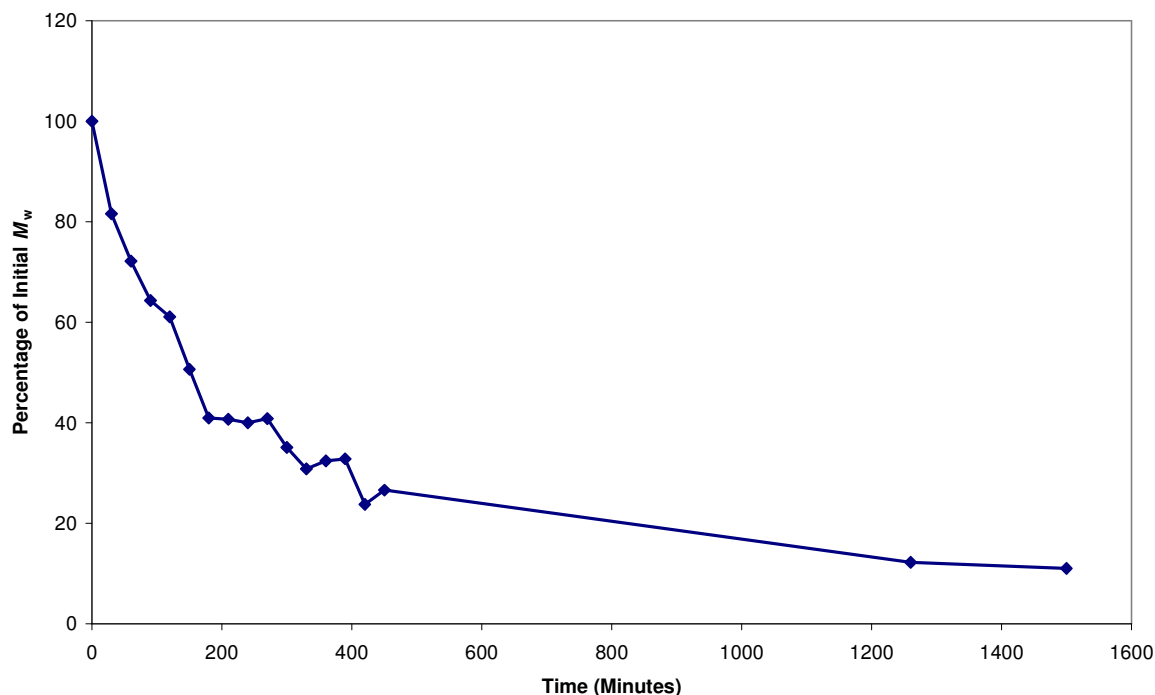


Figure 64: Graph – Percentage of Initial M_w against Time for the Hydrolysis of the EPS

The M_w of the EPS decreases during mild acid-catalysed hydrolysis, on completion of the reaction, after 1500 minutes, the M_w of the EPS produced by *Lb. acidophilus* 5e2 had decreased to approximately 11 % of the initial M_w . The hydrolysis reaction has the profile of a first order reaction.

The decrease in M_w of EPS would decrease much more rapidly if a stronger acid was used e.g. sulphuric acid, and also if a higher temperature was employed. Complete acid hydrolysis is a fundamental part of monosaccharide analysis of polysaccharides, which has been discussed in section 1.6.1.1. Using stronger acid and higher temperature would reduce exopolysaccharides all the way to monosaccharides, by using conditions such as TFA (2 M) at 120 °C for 3 hours. Complete acid hydrolysis to monosaccharides will be discussed in chapter 5.

It is known that acid-catalysed hydrolysis would remove the *N*-acetyl-groups on the *N*-acetylglucosamine residue, modifying it to a glucosamine⁸³. It is clear from the ¹H-NMR spectra that there is substantial modification of the EPS (Figure 65).

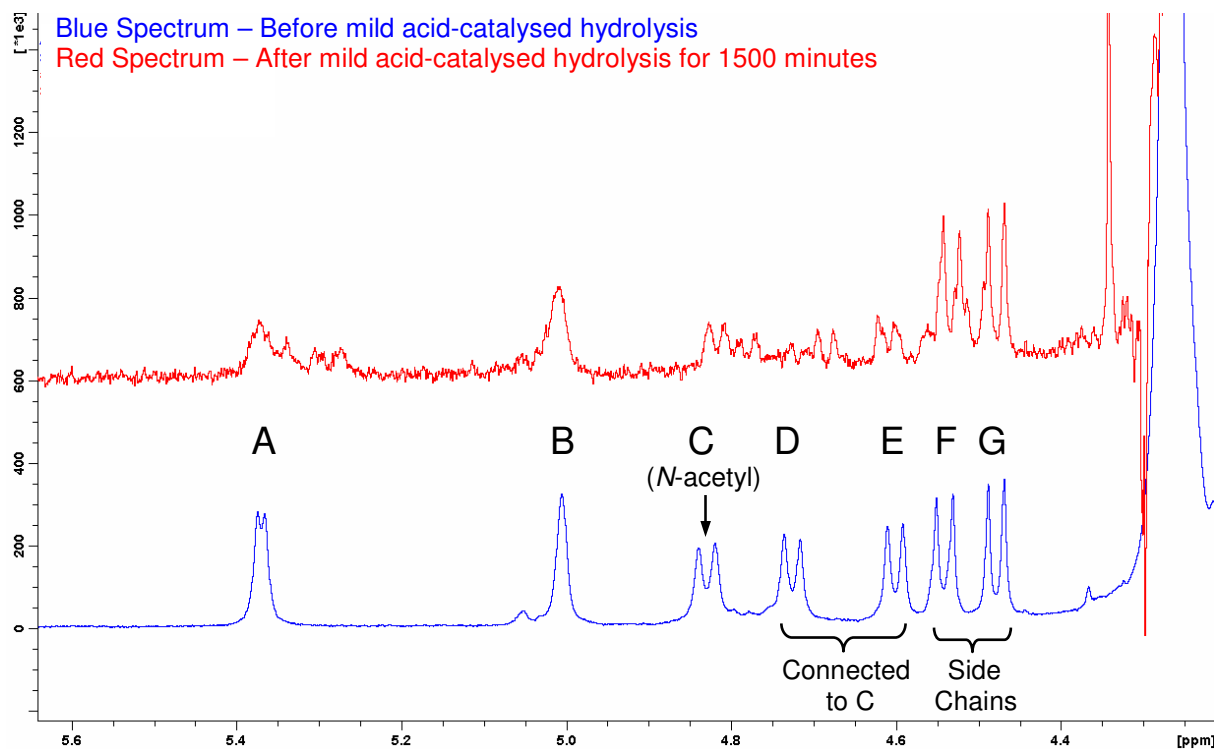


Figure 65: ¹H-NMR of EPS Produced by 5e2 after Acid Hydrolysis (1500 minutes)

There are extra signals seen in the ¹H-NMR spectrum for the EPS sample after hydrolysis (Red Spectrum), these clearly suggesting that there has been some modification to the oligosaccharide repeating unit. The ¹H-NMR signals for the hydrolysed EPS sample are not very intense, this is thought to be due to the chemical degradation of the EPS, and to the presence of salts, from the neutralisation of trifluoroacetic acid. Sodium carbonate was used to quench the hydrolysis reaction. The problem with this technique, when comparing it to the physical methods, is that chemical modifications occur to the structure, which may reduce the application of this technique to be used for controlled depolymerisation.

5. NEW METHODS FOR ANALYSIS OF EXOPOLYSACCHARIDES

5.1 Introduction

In this chapter, novel methods for the structural analysis of exopolysaccharides are described. Firstly a novel method for the analysis of monosaccharide composition will be discussed. Secondly, a novel LC-MS method for the analysis of intact oligosaccharides will be explored. Finally, linkage analysis of exopolysaccharides using a novel LC-MS-MS approach will be considered.

5.2 Reductive Amination of Carbohydrates

The most common sugar residues found in the exopolysaccharides secreted from LAB are D-glucose, D-galactose, L-rhamnose and *N*-acetyl-aminosugars⁵. A procedure for labelling the carbohydrates using reductive amination, providing monosaccharides with both a UV chromophore and charge, is discussed in this section.

The process of reductive amination is explained in section 1.7.2.1, where an amine reacts with a carbonyl group to form an aminol species, which subsequently loses one molecule of water in a reversible reaction to form an imine. The imine is then reduced to a secondary amine. Successful reductive amination has been carried out by reaction of benzylamine¹³⁶, 2-aminobenzoic acid¹³⁷ and 2-aminobenzamide¹³⁷, with reducible carbohydrates.

In this study the derivatisation procedure described by Suzuki *et al.*¹³⁸, provided the best results: the derivatisation procedure was fast and the amine used was readily available and relatively inexpensive. The reaction used a 50 times molar excess of amine (*p*-aminobenzonitrile) and a small amount of acid to catalyse formation of the imine. The imine was then reduced using a relatively mild reducing agent, sodium cyanoborohydride, to form a

secondary amine, as shown in Figure 66. The majority of excess reagents were removed by liquid / liquid extraction using ethyl acetate.

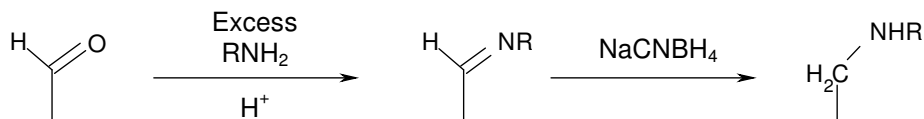


Figure 66: Reductive Amination Reaction

The first carbohydrate examined was D-glucose; this monosaccharide was known to be one of the two most common components of EPSs secreted by LAB ⁵. To determine if the derivatisation of D-glucose was successful, the purified reaction product was subjected to analysis by mass spectrometry and NMR. For NMR analysis to be carried out, a large amount of pure pABN-labelled D-glucose was required. The reductive amination was first carried out on a larger scale, where D-glucose (1.0 g) was derivatised. Preparative HPLC was then used to isolate the pure pABN-glucose from the other reagents and the sample was then subjected to LC-MS and 1D- and 2D-NMR analysis. .

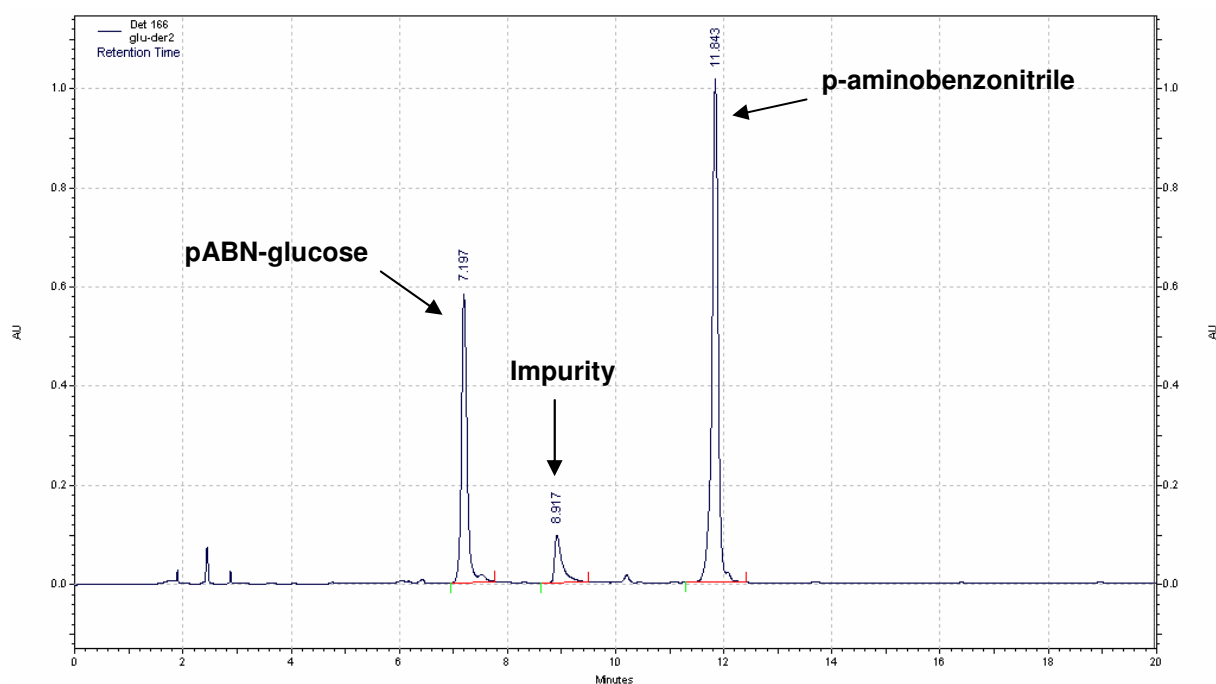


Figure 67: Preparative HPLC Chromatogram of pABN-glucose using UV Detection at 280 nm

An example of the gradient chromatography of the crude reaction mixture is shown in Figure 67 (10 % - 90 % acetonitrile gradient and a UV wavelength of 280 nm). This large excess of pABN obtained after the ethyl acetate extraction can be seen in the chromatogram in Figure 67. The moderately water soluble nature of pABN made it difficult to extract completely using ethyl acetate. There is also a small amount of an imine impurity present, at approximately 8.92 minutes.

Using preparative chromatographic conditions the pABN-glucose peak was collected. Samples were collected from ten separate chromatographic runs, the combined fractions were lyophilized (freeze dried) overnight to produce a pure sample of pABN-glucose (1.1 g).

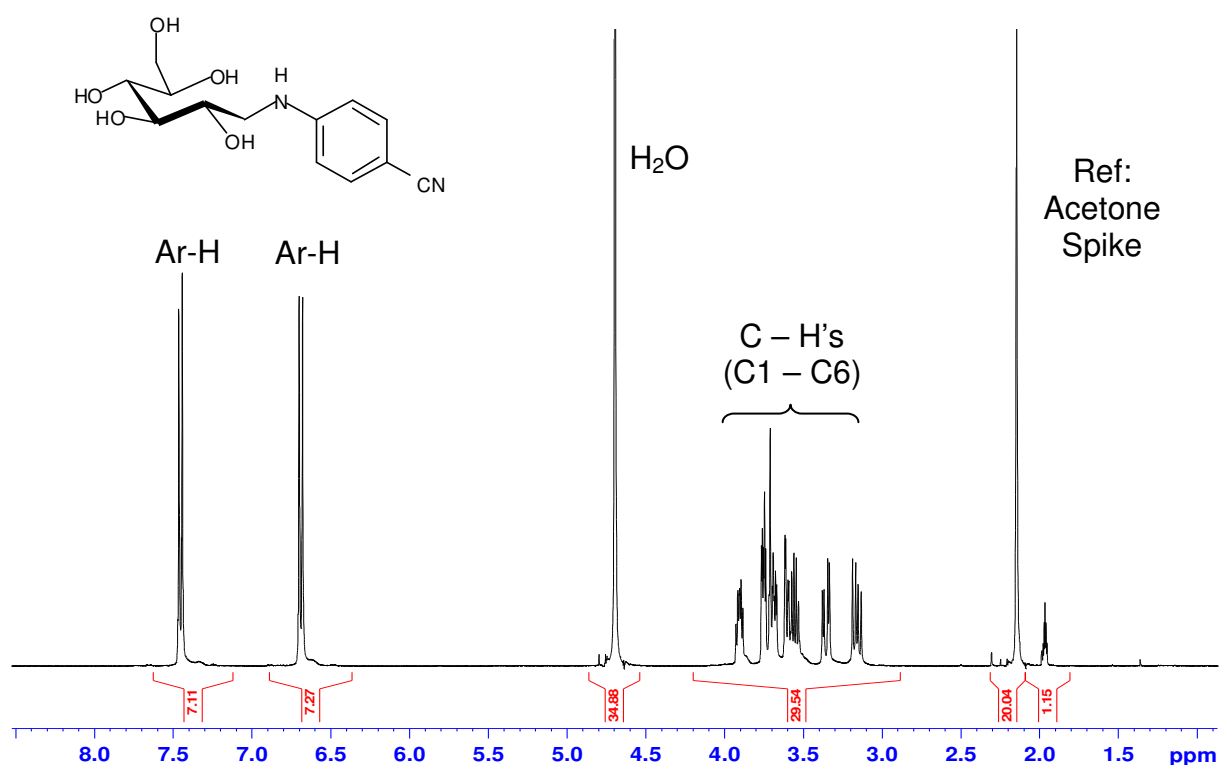


Figure 68: ¹H-NMR Spectrum of pABN-glucose in D₂O

The ¹H-NMR spectrum, shown in Figure 68, confirms the presence of the aromatic ring at 6.7 and 7.5 ppm. The large singlets at 2.3 and 4.7 ppm were due to reference acetone spike and water respectively. The -CHs on the ring opened monosaccharide chain are between

3.2 and 4.0 ppm. The –CHs were then assigned using an expanded ^1H - ^1H -COSY NMR spectrum.

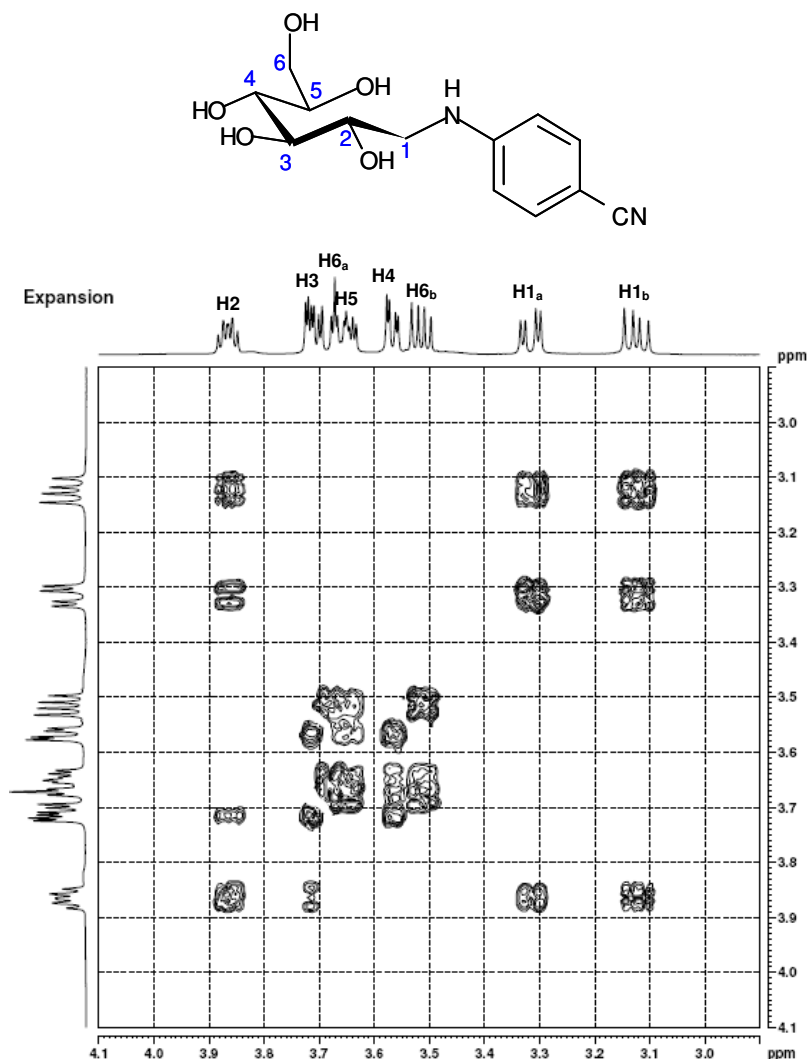


Figure 69: Expanded ^1H - ^1H -COSY Spectrum of pABN-glucose in D_2O

The peaks for the –CHs are all visible, with the two H1 sets of ABX (H1_a and H1_b) visible at approximately 3.13 and 3.32 ppm. The other –CH signals are labelled in Figure 69. The ^1H -NMR and ^1H - ^1H -COSY NMR spectra confirmed the structure of pABN-glucose.

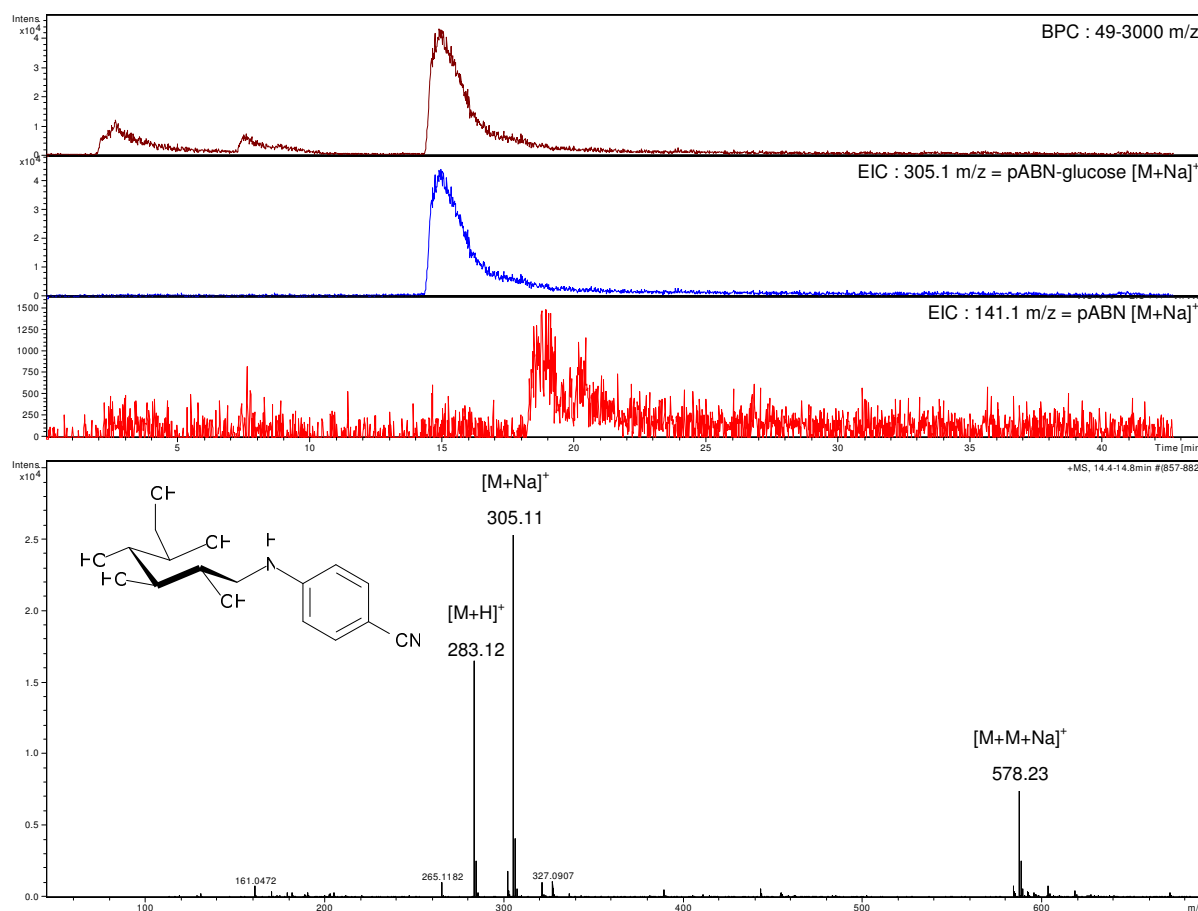


Figure 70: Base Peak Chromatogram of pABN-glucose with Mass Spectrum of Principal Peak

The Base peak chromatogram (BPC) (Figure 70) shows a large principal peak. Extracted ion chromatograms were used to highlight the pABN-glucose (305.1 m/z) and the excess pABN reagent (141.1 m/z). A mass spectrum of the principal peak clearly shows the presence of the sodiated and protonated molecular ions of pABN-glucose. Even after extraction with ethyl acetate, a small amount of pABN remains due to the slightly water soluble nature of the reagent.

Electrospray ionisation was used which is regarded as a relatively soft ionisation technique, meaning that the molecular ion is often the most abundant ion, as it is for pABN-glucose. The abundance of the protonated adducts can be increased by the addition of acid to the mobile phase (e.g. formic acid). The nature of the soft ionisation means that structural information is not normally available. Using cone-voltage fragmentation can provide structural information, but this is not always easily interpreted, therefore the use of MS/MS is

often the only way of providing the necessary fragmentation required for structural evaluation.

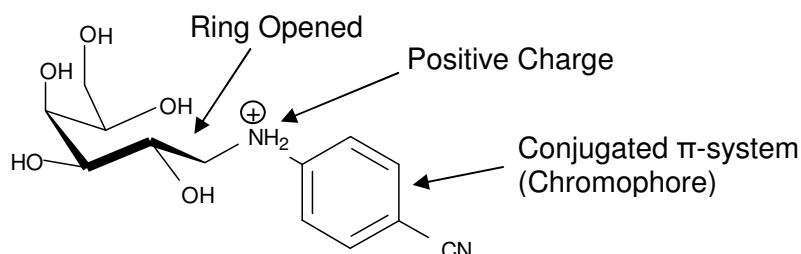


Figure 71: Structure of pABN-Labelled D-glucose

The reductive amination using p-aminobenzonitrile provides a ring opened D-glucose derivative which possesses a chromophore and, under acidic conditions, the structure has a formal positive charge, making the analysis by UV and mass spectrometry detection possible. The fragmentation patterns produced in the MS/MS of the derivatised monosaccharide generate a series of ions due to fragmentation within the backbone.

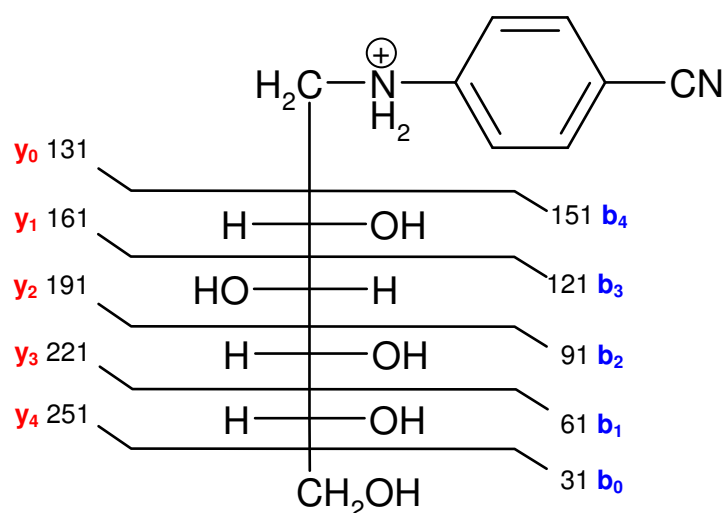


Figure 72: b- and y-ion Series for the Fragmentation of pABN-glucose

This method of labelling of such fragmentation patterns was introduced by Domon and Costello²¹⁸, see Figure 72.

The y -ion series is more likely to be seen, as each y -ion will carry a formal positive charge on the nitrogen. This method of labelling has been implemented throughout this chapter for monosaccharide and linkage analysis.

5.2.1 Reductive Amination of Standard Monosaccharides

The reductive amination was carried out on a series of standard monosaccharides that are found in exopolysaccharides produced by LAB. D-Galactose, D-mannose, D-N-acetylglucosamine and D-glucosamine were all subjected to reductive amination with *p*-aminobenzonitrile and then the derivatives were examined using mass spectrometry to confirm their structures. These reactions were carried out on a smaller scale than for D-glucose, where only 18mg of each monosaccharide was used. The mass spectra of these structures are given in the appendix section 5.7.1.

Each monosaccharide was successfully derivatised by reductive amination, the $[M+Na]^+$ ion was the most abundant ion in all cases.

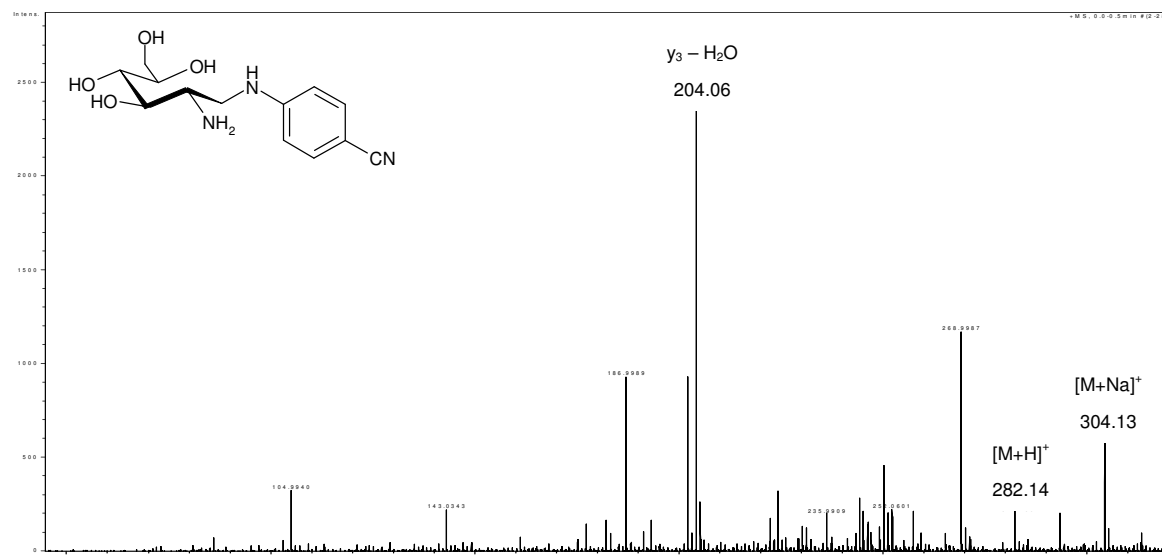


Figure 73: pABN-glucosamine

There appears to be a large amount of fragmentation in the pABN-glucosamine sample, it is unclear why this would be the case. The base peak at 204.1 m/z, is probably due to the $y_3 - H_2O$ ion, which has also been seen in the pABN-glucose mass spectrum.

This series of pABN-labelled monosaccharides was used as standards for the capillary zone electrophoresis analysis of unknown monosaccharides. The capillary zone electrophoresis analysis is discussed in section 5.4.1.

5.2.2 Reductive Amination of Oligosaccharides

There have been a number of publications that have used the derivatisation of oligosaccharides to characterise them by LC-MS. After the success of the reductive amination of monosaccharides using pABN, described above, the Suzuki method was also carried out on an oligosaccharide, which contained a reducing end. Maltohexanose, an oligosaccharide with six continuous D-glucose units linked together via α -1,4-glycosidic linkages, was ideally suited to optimize the method. To ensure that the oligosaccharide would derivatise, the initial reductive amination conditions were applied, which used a 50 times molar excess of pABN. Maltohexanose was reacted with pABN and was infused into the mass spectrometer.

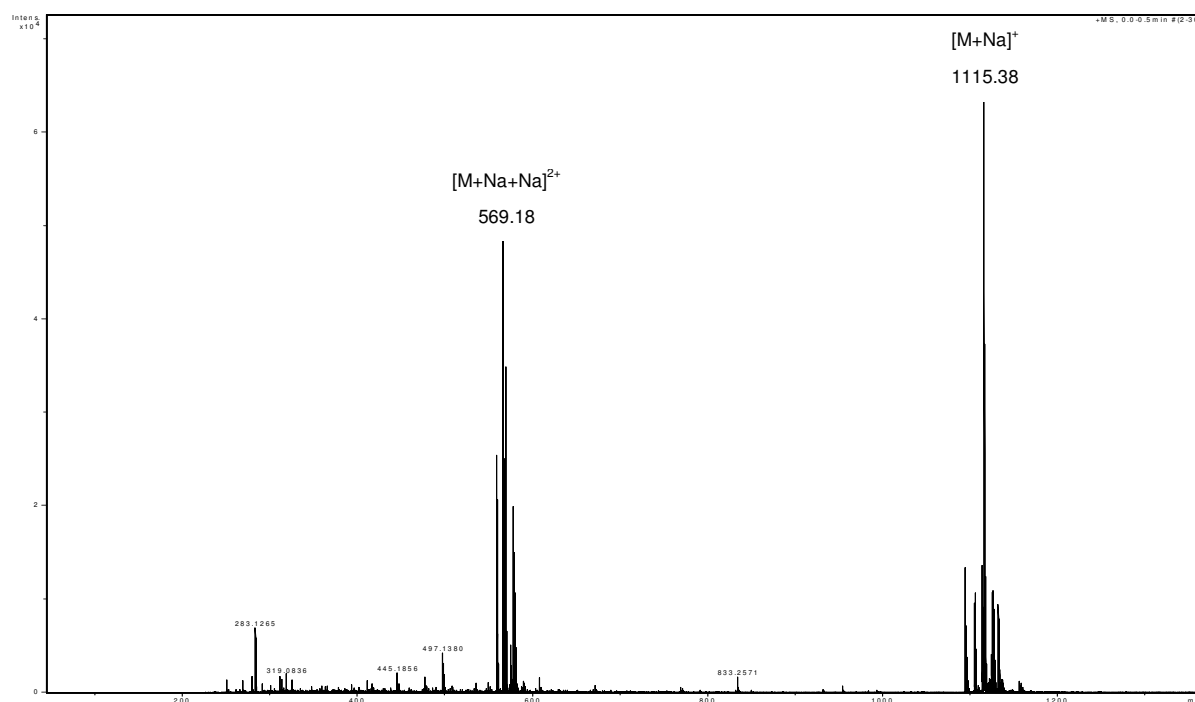


Figure 74: Mass Spectrum of pABN-maltohexanose

The mass spectrum of pABN-maltohexanose confirms the successful labelling, showing both the $[M+Na]^+ = 1115.38$ m/z and the $[M+Na+Na]^{2+} = 569.18$ m/z. The purity of the derivatised pABN-maltohexanose was determined by HPLC using a UV detector (280 nm).

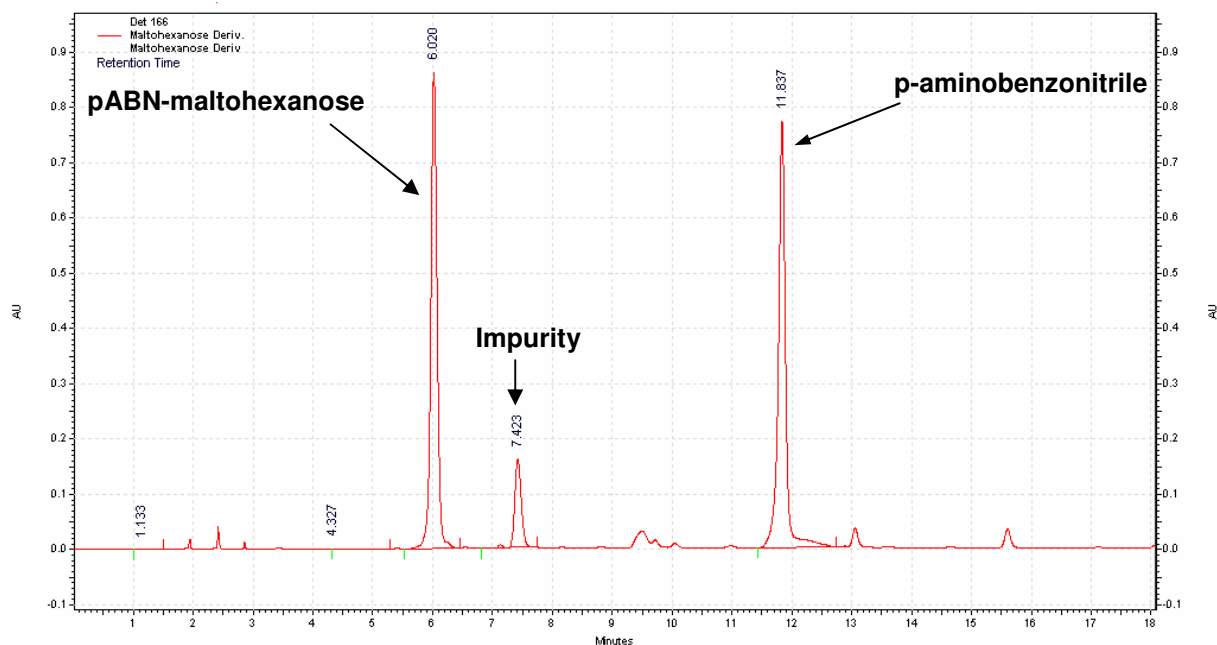


Figure 75: HPLC Chromatogram of pABN-maltohexanose

The derivatised pABN-maltohexanose was analysed using HPLC with gradient elution (10 % - 90 % acetonitrile gradient). The chromatogram shows that some p-aminobenzonitrile remains after the extraction with ethyl acetate, probably because this reaction was carried out using a 50 times molar excess of pABN. The order in which the peaks eluted is as expected, the polar nature of the oligosaccharide causes it to elute before the pABN, and there is also an impurity present, which is due to the formation of the imine which has not been reduced by the sodium cyanoborohydride.

To confirm the identity of the pABN-maltohexanose the sample was analysed by LC-MS and the expected masses (pABN-maltohexanose, $[M+Na]^+ = 1115$ m/z and pABN, $[M+Na]^+ = 141$ m/z) were further examined using extracted ion chromatograms.

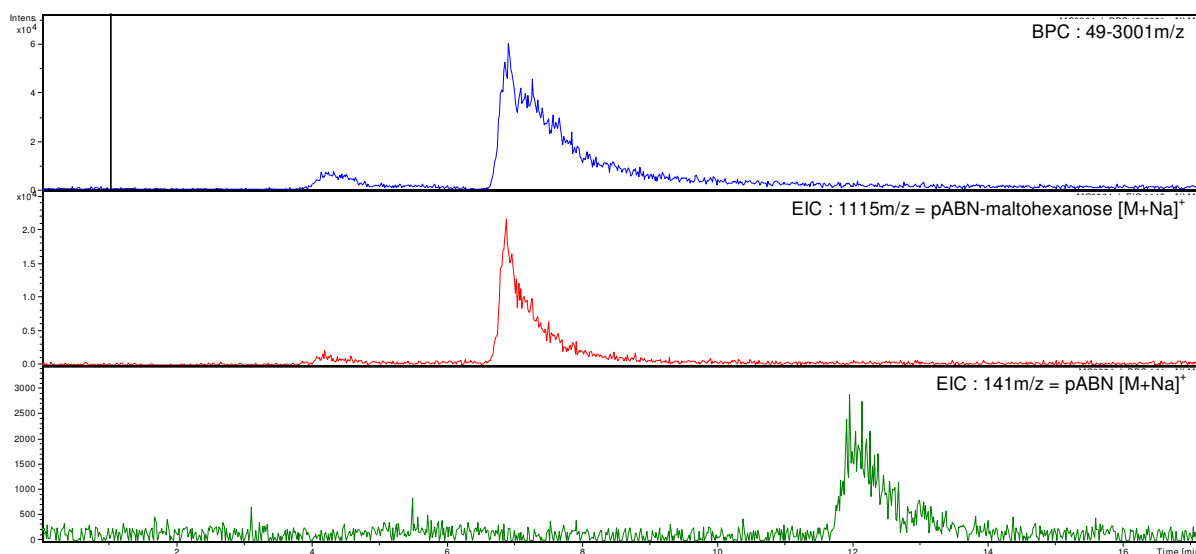


Figure 76: LC-MS Chromatogram of pABN-maltohexanose

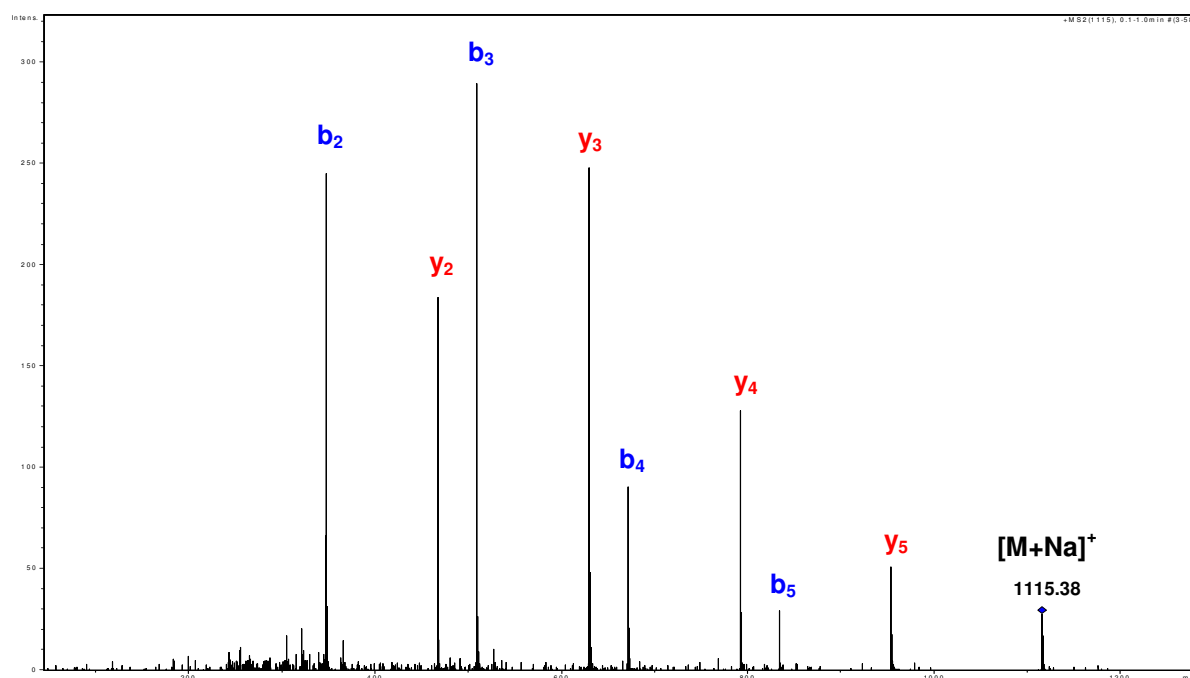
The chromatogram clearly shows the peaks are separated and have the correct mass to charge ratios. The response for pABN is lower than that observed when analysing the monosaccharides and this is due to the instrumental conditions used, these were optimized for the detection of the larger compounds, such as pABN-maltohexanose. Under these conditions, masses lower than 500 m/z appeared with low intensity and the presence of a large excess of pABN is not as problematic as is the case with the monosaccharide analysis. One of the main objectives for derivatising maltohexanose was to determine whether MS/MS could be used to gain structural information about oligosaccharides. There have been several publications reporting the analysis of intact oligosaccharides, Broberg¹³⁶, Cheng²¹⁹. However, their procedures do not involve any pre-treatment to generate the oligosaccharides, which will be necessary for the analysis of EPSs.

MS/MS conditions were optimized by altering the collision energy, collision RF, transfer time and pre-pulse storage. The spectrum could be further enhanced by changing the isolation width and MS/MS collision energy. The following conditions were used (Table 35).

Table 35: Optimized Mass Spectrometer Conditions for pABN-maltohexanose

MS conditions	
Collision Energy	10.0 eV z ⁻¹
Collision RF	500.0 Vpp
Transfer time	100.0 μs
Pre Pulse Storage	10.0 μs
MS/MS conditions	
Selected m/z	1115.38
Isolation width	1.0 m/z
Collision Energy	80.0 eV

Using these conditions, pABN-maltohexanose gave the following MS/MS spectrum shown in Figure 77. Previous reports by Reinhold and co-workers^{220 221}, who pioneered LC-MS analysis of carbohydrates, indicated that relatively low-energy collision conditions should lead to extensive fragmentation of the glycosidic bonds between the monosaccharides.

**Figure 77: MS/MS Spectrum of the [M+Na]⁺ Peak of pABN-maltohexanose**

A series of b- and y-ions produced from the parent ion (1115 m/z, $[M+Na]^+$) are visible in Figure 77. This spectrum contains masses corresponding to cleavages across the glycosidic bonds between the monosaccharide units, as shown in Figure 78.

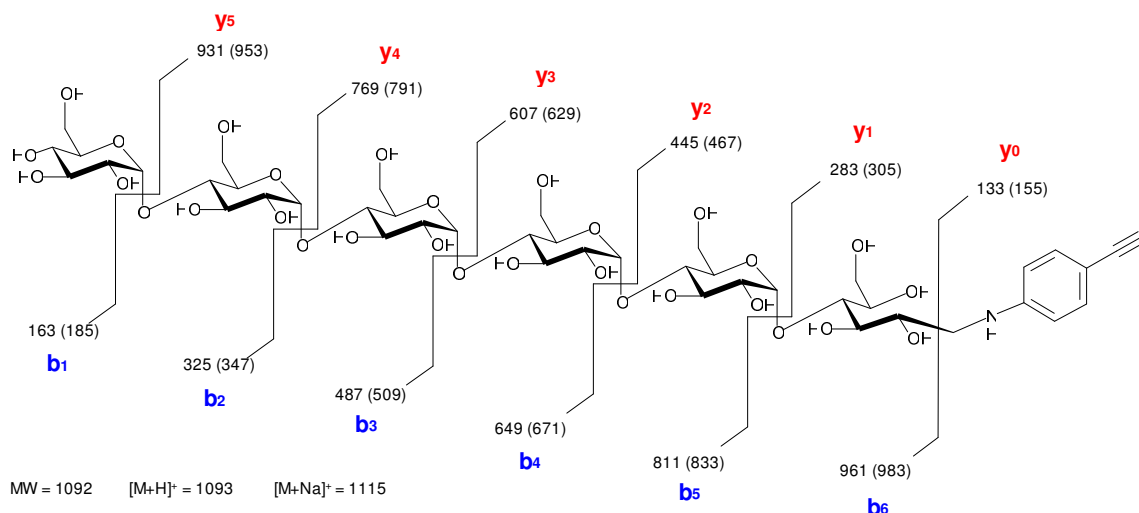


Figure 78: Structure and Predicted Masses of pABN-maltohexanose

This was a very encouraging result; both the b- and y-ion series are clearly visible. Using this technique it could be possible to determine the structure of the repeating unit of exopolysaccharides, providing information about branching and the backbone sequence. To get details of branch points it will be necessary to get fragmentation within each ring. Using the nomenclature reported by Domon and Costello²¹⁸, these intra ring cleavages are identified as x- and a-ions, as shown in Figure 79. The x- and a-ions are required to discriminate between different linkage positions around the ring.

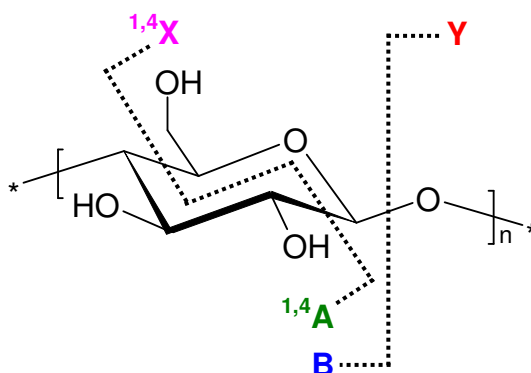


Figure 79: Diagram showing the ^{1,4}x- and ^{1,4}a-ion Cleavage of a Monosaccharide Unit

Although the b- and y-ions were observed, there is little evidence in Figure 78 for cleavages within the ring. Broberg ¹³⁶ has observed ^{1,4}x-ion cleavages, but only when using high fragmentation amplitudes (1.5 V) on an ion trap mass spectrometer. Other cleavages are possible: Maslen *et al.* ¹³⁷ have reported that by using a MALDI-CID mass spectrometer, the ^{0,2}x-, ^{1,5}x- and ^{0,2}a- and ^{3,5}a-ion can also be produced.

Further experiments using the Bruker MicrOTOF-q mass spectrometer, which used larger collision energies, were unable to produce cleavages within the monosaccharide rings. Future work would have to use different types of mass spectrometer such as ion trap or MALDI-CID as used by Broberg ¹³⁶ and Maslen *et al.* ¹³⁷ described above.

5.3 Acid-Catalysed Hydrolysis of Carbohydrates

As mentioned earlier, existing derivatisation reactions are used for the analysis of oligosaccharides. For the analysis of exopolysaccharides it will be necessary to depolymerise the polymer before the derivatisation process can be applied. An established method to depolymerise di-, oligo- and polysaccharides into monosaccharide units is to use acid-catalysed hydrolysis. This process hydrolyses the glycosidic bond between two monosaccharides, the mechanism for this reaction is given in section 1.7.1.3. To hydrolyse sugars, different acids and conditions can be used but during the work described here trifluoroacetic acid was used exclusively.

5.4 Capillary Zone Electrophoresis of Monosaccharides

As described earlier, capillary zone electrophoresis is capable of resolving isomeric monosaccharides using borate buffering systems. Recent work published by Xia ⁹⁰ has reported that capillary zone electrophoresis was able to separate a range of derivatised isomeric monosaccharides using a borate eluent system. His methodology used 1-naphthyl-

3-methyl-5-pyrazolone (NMP) to derivatise the monosaccharides, then used CZE to separate complexes formed between the derivatised monosaccharides and borate. The theory behind this is discussed in detail in section 1.6.1.1, where the borate forms complexes of different strengths with the available hydroxyl groups of the monosaccharides. It was envisaged that this type of separation could be used to determine the monosaccharide composition of EPSs produced by LAB. The proposed method was to hydrolyse the EPS into monosaccharides, label them with pABN and then to separate and quantify the pABN-labelled monosaccharides as complexes with borate using CZE. To identify the monosaccharides, their migration time would be compared to the migration times of a series of standard pABN-labelled monosaccharides.

5.4.1 Determination of pABN-Labelled Monosaccharide Standards by CZE

Five pABN-labelled monosaccharides were analysed by CZE to determine their migration times. Each standard was prepared at a concentration of 100 $\mu\text{g mL}^{-1}$. Relative migration times were used to compensate for the slight fluctuations of migration times. The migration times of each of the five pABN-labelled monosaccharide standards were divided by the corresponding electroosmotic flow to give the relative retention times in Table 36. The chromatograms for the pABN-labelled monosaccharides are provided in the appendix section 5.7.2.

Table 36: Retention Times of pABN-labelled Monosaccharides (100 µg mL⁻¹)

pABN-Labelled Monosaccharide	Approximate Migration Time (Minutes)	Relative Migration Time	Signal to Noise Ratio	Quantification Limit (µg mL ⁻¹)
D-glucose	7.9	1.61 ± 0.01	164	6.1
D-galactose	9.0	1.89 ± 0.02	154	6.5
D-mannose	7.5	1.55 ± 0.01	162	6.2
D-N-acetyl-glucosamine	7.6	1.56 ± 0.01	138	7.2
D-glucosamine	6.3	1.27 ± 0.01	80	12.5

Migration time divided by the time of the electroosmotic flow. The typical electroosmotic flow was approximately 4.85 minutes. Errors calculated from five repeat injections.

These migration times were compared to peaks obtained from EPS samples that had been hydrolysed to monosaccharides and derivatised to determine their monosaccharide composition; the relative ratios of the peak areas in each EPS sample were used to calculate the ratio of the monosaccharides.

The results in Table 36 clearly show that CZE is able to successfully resolve a series of pABN-labelled monosaccharides common to EPSs produced by LAB. Each standard was analysed by CZE at a concentration of 100 µg mL⁻¹. The signal to noise ratios were calculated using the equation:

$$\text{Signal to Noise Ratio} = \frac{2H}{h}$$

Where, H = Peak height at the maxima, h = Average height of background noise.

Equation 3: Signal to Noise Ratio²²²

The peak heights and background noise from each sample chromatogram are provided on the relevant chromatograms in the appendix section 5.7.2. The quantification limit (QL) can

be defined as the concentration where the signal to noise ratio is equal to 10:1 ²²³. Using the signal to noise ratio the QL was approximated and the values are shown in Table 36. The QL values range between 6.1 $\mu\text{g mL}^{-1}$ – 12.5 $\mu\text{g mL}^{-1}$, which is not as sensitive when compared to the HP-AEC-PAD analysis which will be discussed later.

5.4.2 Monosaccharide Composition of EPSs Produced by Lactic Acid Bacteria

A novel approach, using CZE to determine the monosaccharide composition of exopolysaccharides was carried out on two previously characterised EPS samples; the EPS produced by *Lactobacillus delbrueckii* subsp. *bulgaricus* NCFB2074 ⁷⁸ and the EPS produced by *Lactobacillus acidophilus* 5e2 ¹⁷⁷. The EPS samples were first hydrolysed to monosaccharides and then the monosaccharides were labelled using pABN. As with the standard monosaccharides, CZE, using a borate buffering system, was then used to separate the labelled monosaccharides, and the migration times were compared to the migration times given in Table 36. This procedure was faster than the current gas chromatography method reported by Gerwig *et al.* ⁸¹, which is the current method for analysing monosaccharides.

The EPS produced by *Lactobacillus delbrueckii* subsp. *bulgaricus* NCFB2074 was analysed first, this EPS was known to contain three D-glucose and four D-galactose units in the repeating oligosaccharide.

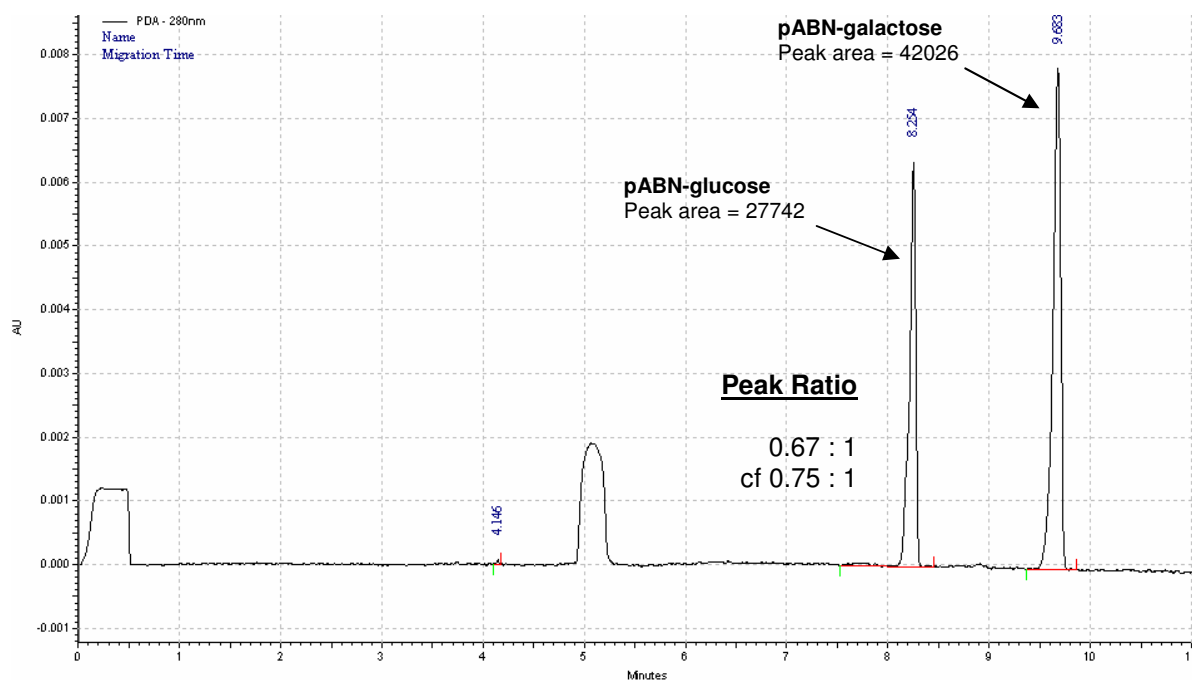


Figure 80: Example of a CZE Chromatogram of the EPS Produced by NCFB2074

The CZE chromatogram (Figure 80) shows two peaks that correspond to pABN-glucose and pABN-galactose, the peak areas show a ratio of 0.67:1 (D-glucose : D-galactose). Although the monosaccharide composition of this particular EPS was relatively simple, the result was very encouraging. Next the EPS produced by *Lactobacillus acidophilus* 5e2 was analysed by CZE. The repeating unit of this EPS was known to contain three D-glucose units, three D-galactose units and one *N*-acetyl-glucosamine unit. The *N*-acetyl-glucosamine would appear as a chemically modified glucosamine, having lost the *N*-acetyl during the acid-catalysed hydrolysis step of the sample preparation.

Using the same chromatographic conditions as for the EPS produced by NCFB2074, the EPS was analysed to give the chromatogram shown in Figure 81.

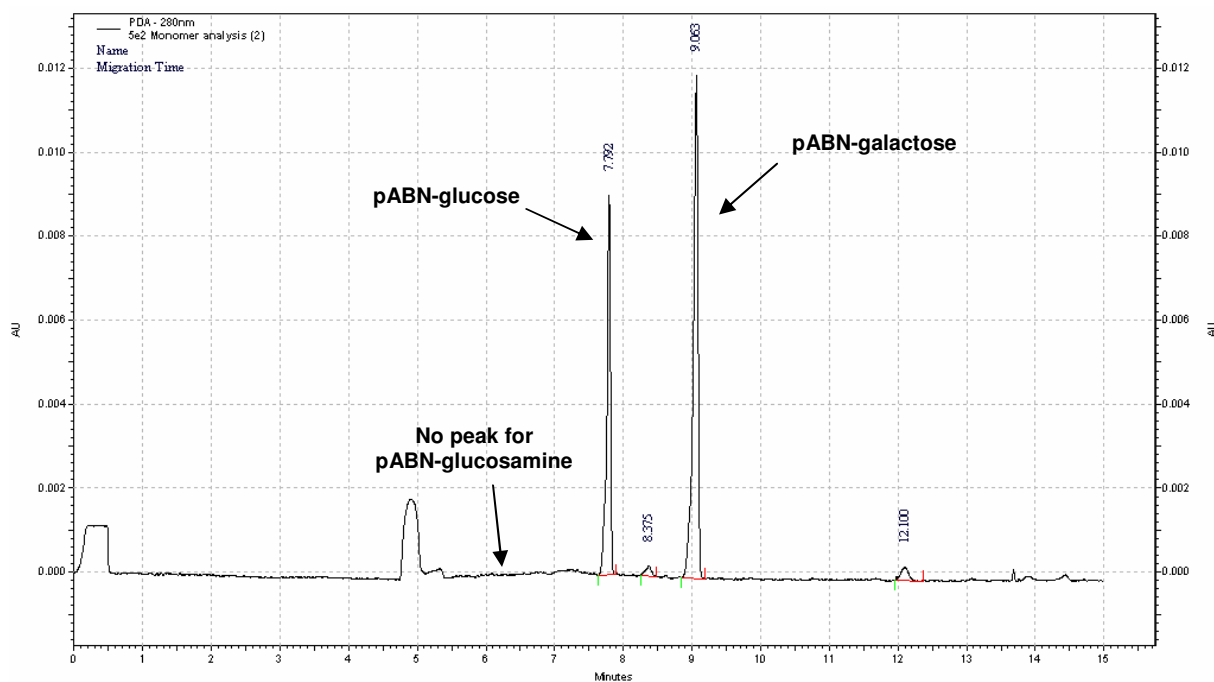


Figure 81: CZE Chromatogram of the EPS Produced by *Lb. acidophilus* 5e2

The results were not as expected, as can be seen in Figure 81, peaks for pABN-glucose and pABN-galactose are observed but no peak for *N*-acetyl-glucosamine could be detected. As explained above, the acid-catalysed hydrolysis procedure would remove the *N*-acetyl group leaving glucosamine⁸³. Therefore a peak corresponding to pABN-glucosamine, at approximately 6.3 minutes, should have been observed.

To determine why the *N*-acetyl-glucosamine peak was not present in the EPS sample, the hydrolysis and pABN-labelling was carried out on the monomer *N*-acetyl-glucosamine.

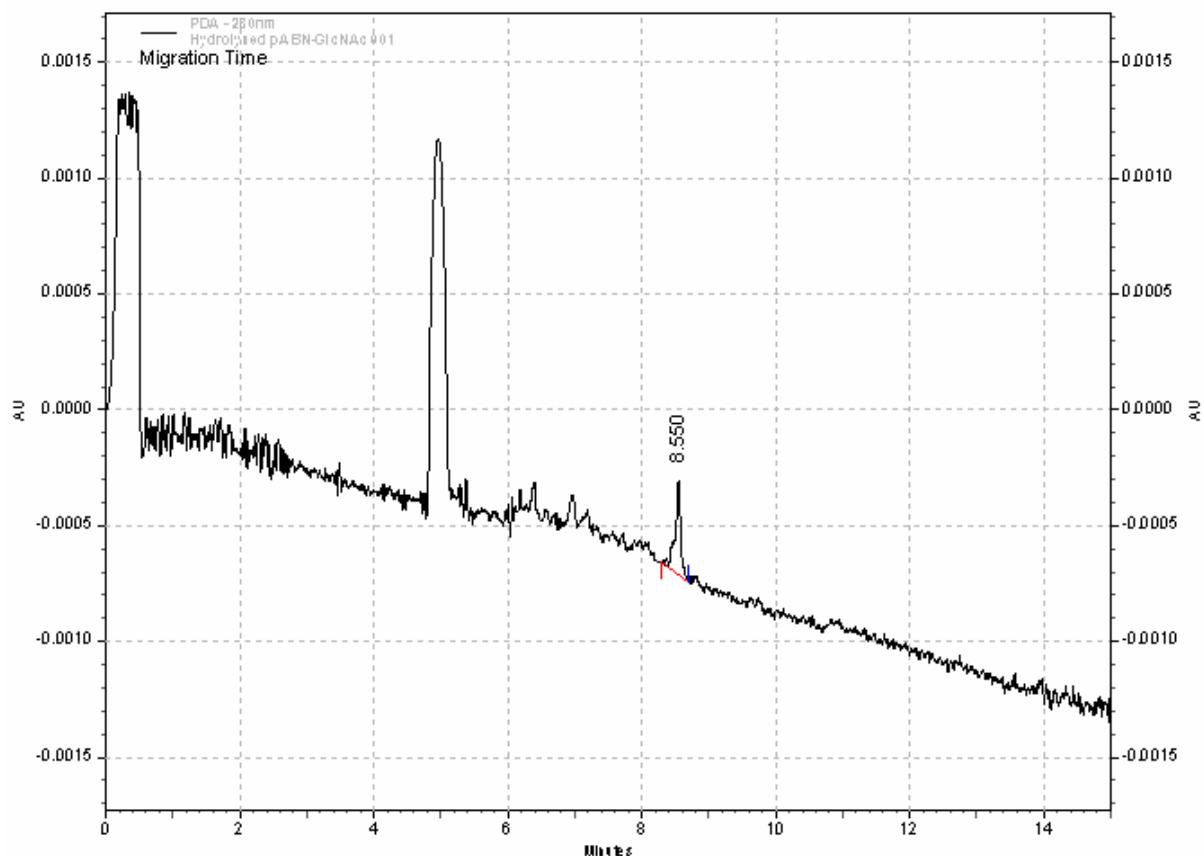


Figure 82: CZE Chromatogram of Hydrolysed and pABN-labelled *N*-acetyl-glucosamine

A peak for pABN-glucosamine should have been seen, but no peak of any significance was observed in the CZE chromatogram (Figure 82), there was a small peak at 8.6 minutes but this was seen as background in all of the samples. To determine why D-glucosamine was not being observed further analysis would be required, which is suggested in the chapter 6.

This method was able to determine the D-glucose and D-galactose composition of EPS in approximately 1 day, which was significantly faster than the current GC method, which takes approximately 3 days to complete. In our research group, HP-AEC-PAD has also been used to determine the monosaccharide composition of EPSs. The technique has been shown to be much more sensitive than CZE, reporting quantification limits of $0.1 \mu\text{g mL}^{-1}$, approximately 100 times smaller than reported for this method. Furthermore, when using HP-AEC-PAD the sugar residues do not require labelling with pABN to improve their detection. The only problem encountered with HP-AEC-PAD is that the peak shape can be

poor and the retention times can often fluctuate. These problems do not occur in CZE analysis, therefore monosaccharide composition by CZE is worthy of further development but only if the problems of detecting *N*-acetyl-amino sugars can be resolved.

5.5 Methylation of Carbohydrates

Failure to produce cross ring cleavage of intact oligosaccharides in LC-MS-MS experiments required an alternative strategy for identifying the positions of linkages. Therefore it was decided to try and identify linkage positions by methylating the free hydroxyls. Out of the various methylation reactions reviewed in section 1.6.2 the two most applicable were evaluated for the analysis of EPS samples using LC-MS.

5.5.1 Methylation – ‘Hakomori Procedure’

The first methylation procedure used was based on that described by Hakomori⁹², where the dimethylsulfinyl anion acts as a base and removes the free hydroxyl protons on the monosaccharide and then methyl iodide is added to form methoxy- groups. This methylation procedure was applied to the linkage analysis of sugars by Stellner *et al.*⁹¹ and ever since has been the major method used for the linkage analysis of carbohydrates. In this section of the study the Hakomori methylation was carried out on both free monosaccharides and pABN-derivatised carbohydrates depending on the application. The methylation of pABN-glucose, pABN-maltohexanose and exopolysaccharides are all described.

5.5.1.1 Methylation of pABN-glucose

The pABN-glucose, isolated by preparative HPLC in section 5.2, was methylated using the Hakomori procedure. The methylated pABN-glucose was dried under nitrogen at 40 °C and dissolved in acetonitrile before being infused into the mass spectrometer. For all reactions

that involved pABN-labelling of methylated carbohydrate, the procedure for reductive amination was modified slightly, where a 1:1 molar equivalent of pABN to carbohydrate was used in the reaction. This was because the product was now methylated and the ethyl acetate extraction could not be used to remove the excess pABN, as it would also remove the methylated product. The change to the protocol had no significant effect on the quality and yield of the product produced.

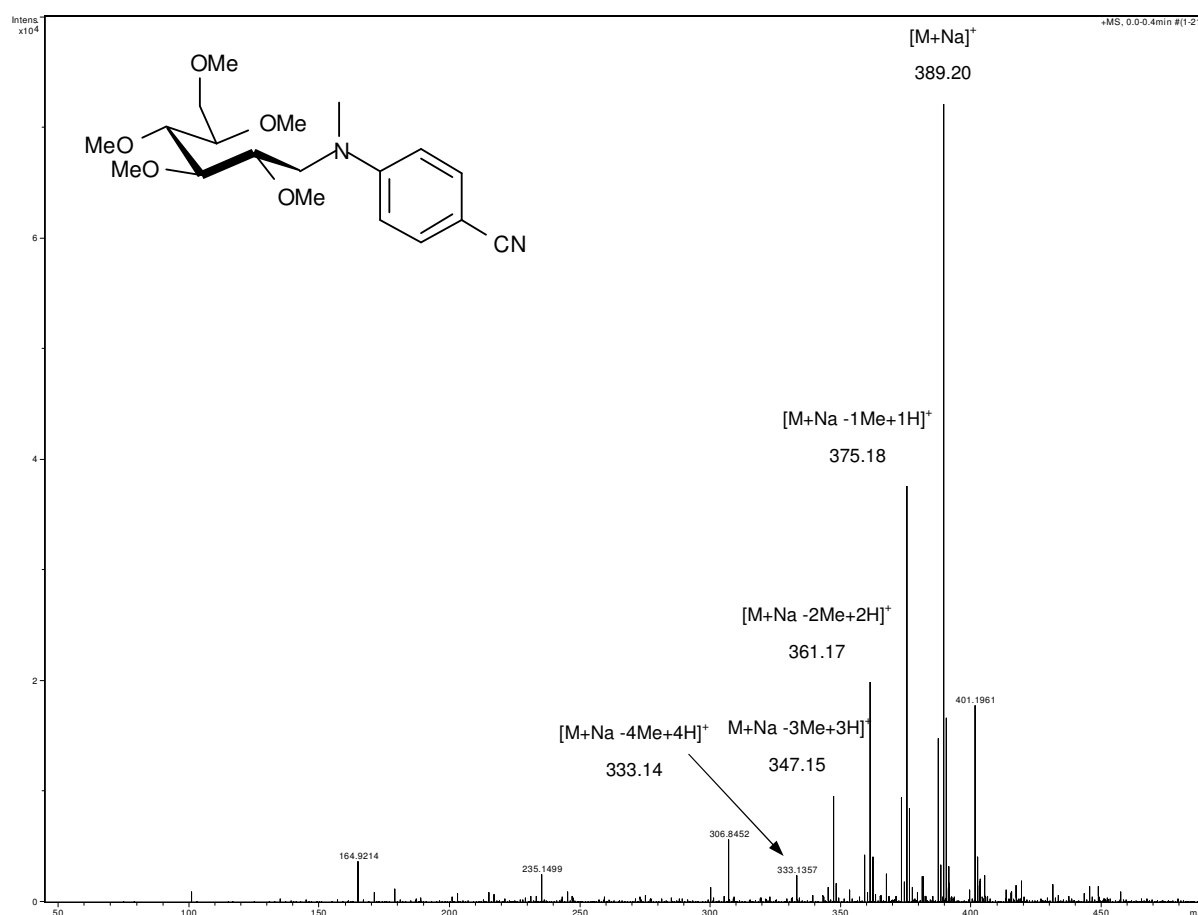


Figure 83: Mass Spectrum of Methylated pABN-glucose

The mass spectrum (Figure 83) shows that full methylation had been achieved ($[M+Na]^+ = 389.2$ m/z) but several partially methylated species were present. Ions for species corresponding to those having between one to four methyl groups missing were all seen ($[M+Na]^+ = 333.14, 347.15, 361.17$ and 375.18 m/z). These ions were observed in the mass spectrum with masses that correspond to protonated hydroxyl groups, *i.e.* these ions are likely to arise from partial methylation of the sugar rather than fragmentation of the

methylated species. The sample was subjected to LC-MS to see if the partially methylated species could be separated, hence, confirming whether or not they were generated in the MS by fragmentation.

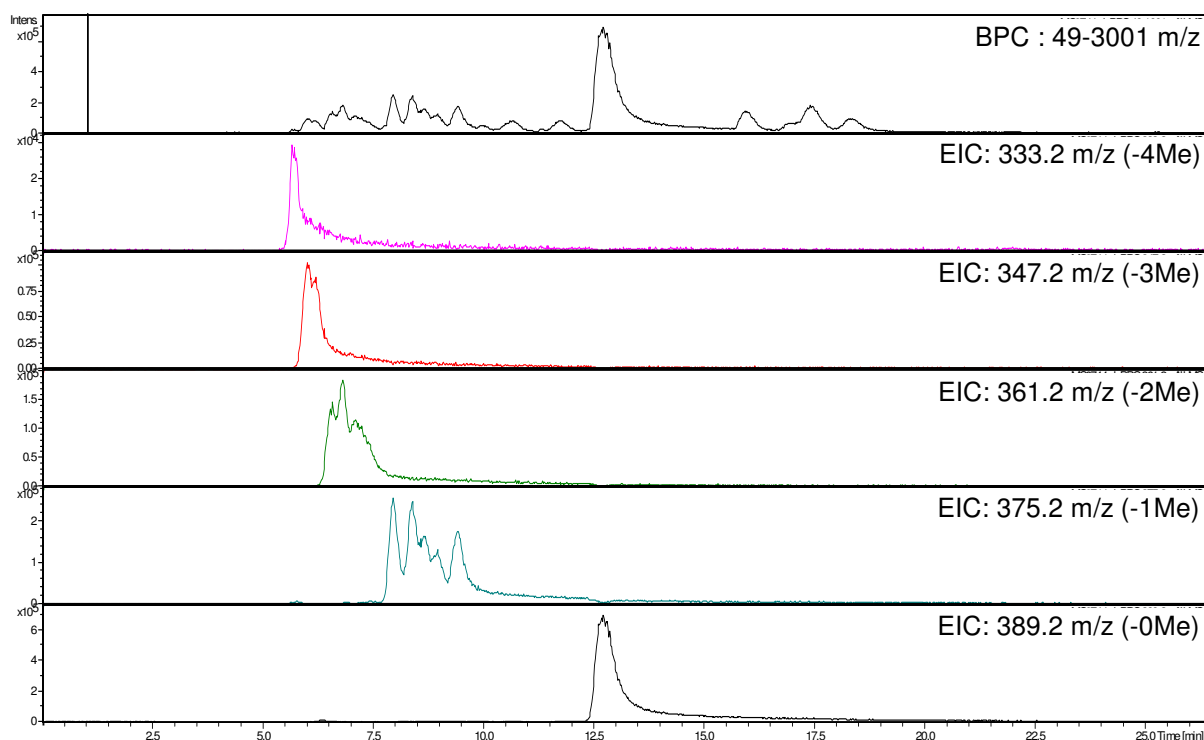


Figure 84: LC-MS Chromatogram of Methylated pABN-glucose

The chromatogram in Figure 84 shows peaks due to partially methylated pABN-glucose, confirming that the ions observed in Figure 83 are not just due to fragmentation of the fully methylated species. Ciucanu and Kerek⁹³ reviewed the Hakomori methylation procedure, stating that per-*O*-methylation is unlikely, and *N*-methylation is even more unlikely. Their studies have shown low yields (0.3 mol of per-*O*-methylated derivative per mol of sugar), despite these findings, the Hakomori method is extensively used for the structural analysis of carbohydrates.

The reason partial methylation occurred could be simply due to the time the dimsyl ions (or dimethylsulfinyl carbanion) had to react with hydroxyl groups on the monosaccharide.

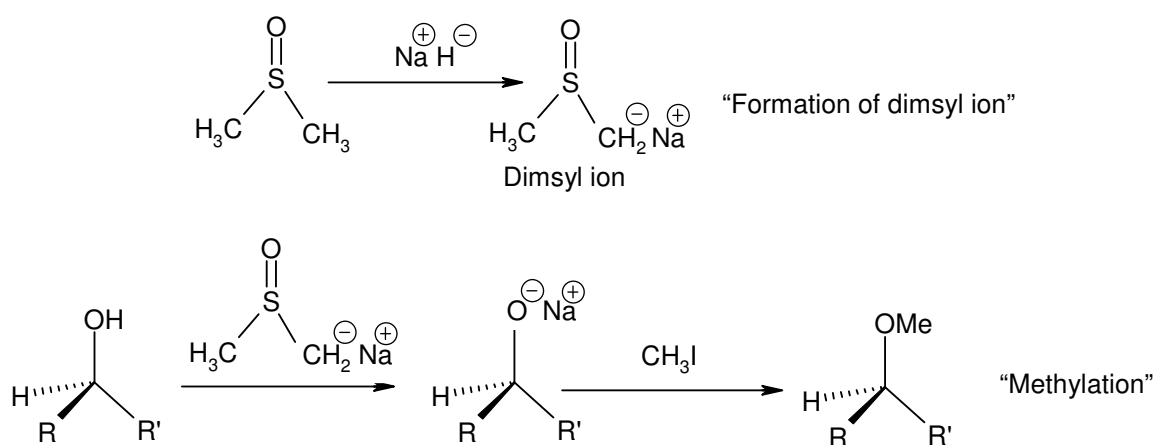


Figure 85: Formation of Dimsyl Ion and Methylation Reaction

In the reaction procedure, initially, the dimsyl ion is produced and this then reacts with the hydroxyl group leaving an alkoxy oxygen, which is then methylated using methyl iodide. There is a distinctive colour change during this reaction, where the reaction mixture changes from a yellow / straw colour to a deep brown. The brown colour is either due to the formation of the dimsyl ion or the production of the I_3^- ion as the methyl is removed. Further investigation of this reaction was required.

5.5.1.2 Deuterated Methylated pABN-glucose

To confirm that the peaks seen in Figure 83 are due to partially methylated pABN-glucose, a simple experiment was set up to measure the number of remaining hydroxyl groups present. Using deuterated solvents (acetonitrile and deuterium oxide), the remaining exchangeable protons on the hydroxyls were deuterated; hence the mass to charge ratio of each peak would increase by one mass unit for every hydroxyl group present.

To deuterate the sample, the methylated pABN-glucose was freeze dried and re-dissolved in a solvent composed of deuterated acetonitrile and deuterium dioxide (50:50). The sample was then infused into the mass spectrometer.

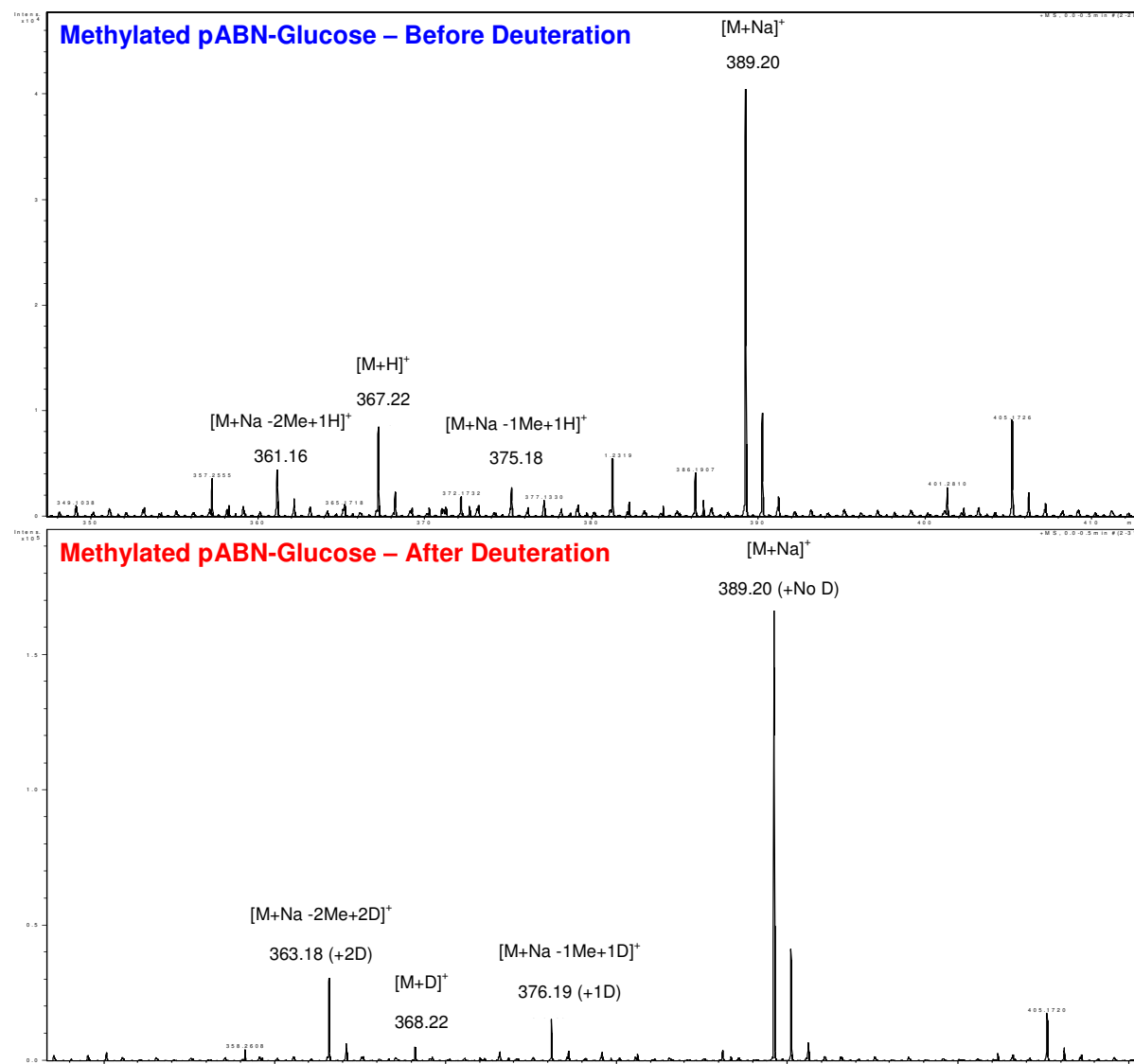


Figure 86: Mass Spectrum of pABN-glucose Before and After Deuteriation

The mass spectra from before and after deuteriation can be seen in Figure 86. As expected the peak due to fully methylated pABN-glucose does not increase in mass. The partially methylated species, -1Me, -2Me and -3Me, all increase by one mass unit for each missing methyl group. This confirms that the peaks in Figure 83 are in fact due to partially methylated monomers.

5.5.1.3 Timed Methylation

An experiment was set up to monitor the progress of the methylation reaction. A portion of the reaction mixture was removed every 30 minutes and the extent of methylation was

expressed as a ratio between the peak area of the fully methylated species, $[M+Na]^+ = 389.2$ m/z, and the partially methylated species with two methyl groups missing, $[M+Na]^+ = 361.2$ m/z, which was the next most abundant species. The samples were analysed by LC with UV detection at 280 nm. The peak areas of the fully methylated species and the partially methylated species (two missing methyl groups) were compared to determine the extent of methylation throughout the reaction. The chromatograms are given in the appendix section 5.7.3.

Table 37: Time Methylation Reaction Results

Reaction Time (Minutes)	HPLC Peaks Area at 280 nm		
	Partially Methylated pABN-glc (AU)	Fully Methylated pABN-glc (AU)	Ratio
30	31.3	90.2	2.88
60	37.8	94.3	2.49
90	54.5	135.1	2.48
120	41.5	111.9	2.70
150	37.8	96.5	2.55
180	48.7	135.2	2.78
210	66.1	189.9	2.87

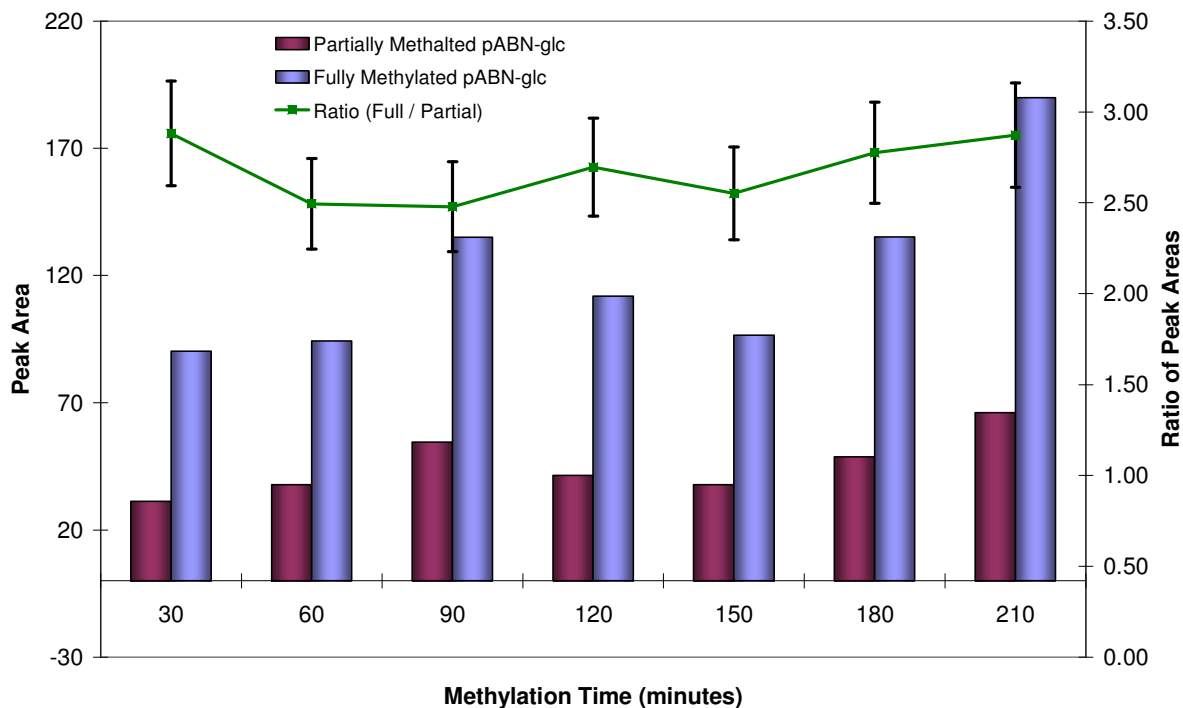


Figure 87: Graph – Timed Methylation Reaction

The results generated showed that the yield of the fully methylated pABN-glucose increased, but so did that of the partially methylated compound. The green line, which represents a ratio of the peak areas of the two species, does not increase, only fluctuates throughout the 3.5 hour reaction. The results are in agreement with Ciucanu and Kerek⁹³, confirming poor yield of per-*O*-methylation. From the results generated, it is evident that a longer reaction time increases the yield of the methylated products.

Further investigation of the Hakomori methylation procedure was carried out on a pABN-labelled oligosaccharide, this study was carried out to provide additional information about why partial methylation was occurring.

5.5.1.4 Methylation of pABN-oligosaccharides

Despite the Hakomori procedure producing partial methylation for pABN-glucose, this method was used to methylate a pABN-labelled oligosaccharide. It was envisaged that the

analysis of this pABN-labelled oligosaccharide would provide more information about which hydroxyl positions are not being methylated, when partial methylation occurred.

Methylated pABN-maltohexanose showed a large distribution of products, as can be seen in Figure 88. The peaks observed ranged from the fully methylated product (1409.69 m/z), to a partially methylated species that had eleven missing methyl groups (1255.53 m/z).

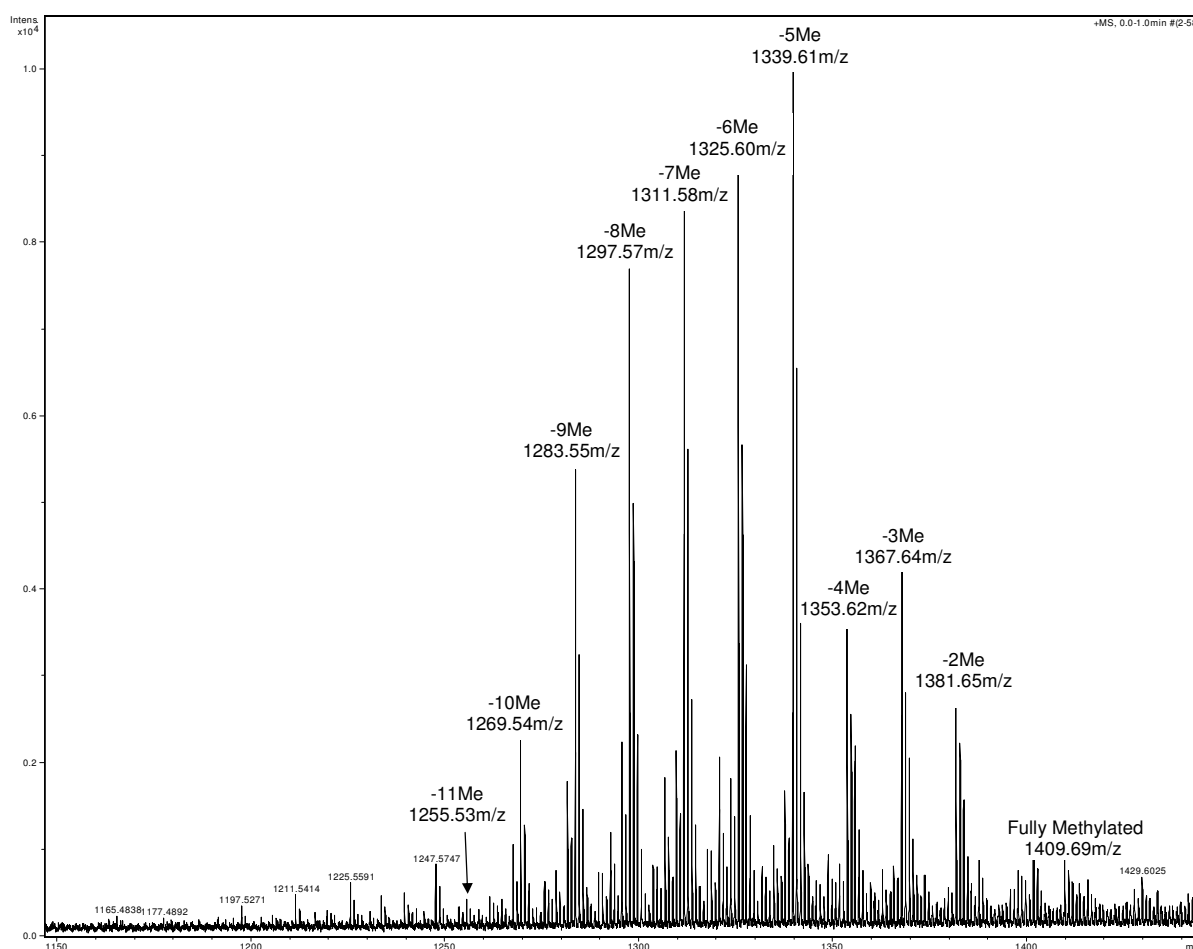


Figure 88: Mass Spectrum of Methylated pABN-maltohexanose

The distribution of products was interesting, the partially methylated pABN-maltohexanose with 1 missing methyl group was not observed, only the mass to charge ratios of 1409.7 m/z (fully methylated) and 1381.6 m/z (two missing methyl groups) were present. This was similar to the methylated pABN-glucose system, where the peak area for the UV absorbance for two missing methyl groups was always greater than that for one missing methyl group.

The, overall distribution had similarities to a Gaussian distribution where the three most intense ions occurred in the middle, which were partially methylated pABN-maltohexanose with 5, 6 and 7 missing methyl groups. The $[M+Na]^+$ series of ions had the greatest intensity but the $[M+H]^+$ ions were also visible, and had the same overall distribution.

5.5.1.5 Deuteration of Methylated pABN-maltohexanose

Again, to confirm that partial methylation was occurring, deuteration of the methylated pABN-maltohexanose was carried out to measure the number of remaining hydroxyl groups present. The proton on each remaining hydroxyl was exchanged for deuterium, hence the masses of each peak would increase by one mass unit for every hydroxyl group present. The methylated pABN-maltohexanose was freeze dried and re-dissolved in a mixture of deuterated acetonitrile and deuterium oxide. The sample was then infused into the mass spectrometer.

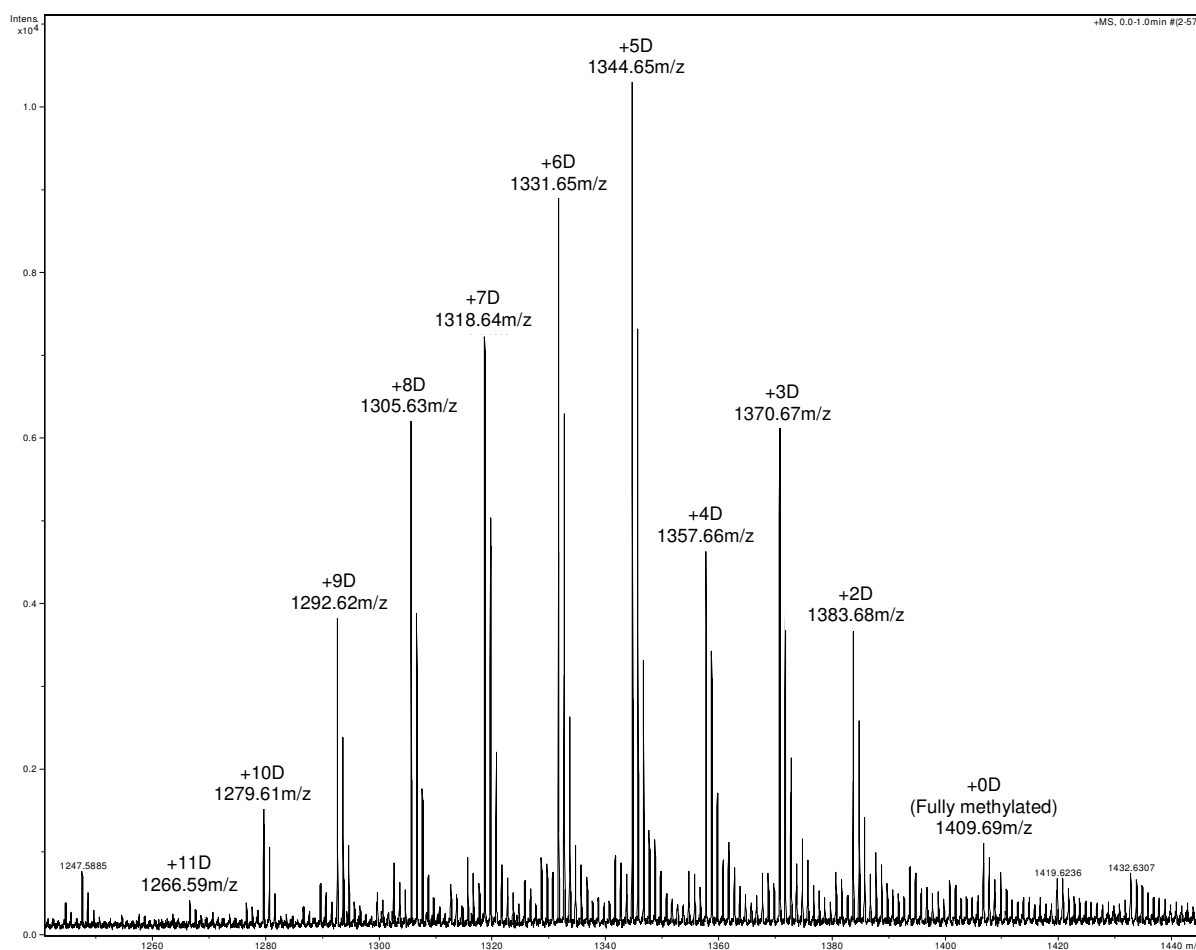


Figure 89: Deuterated Methylated pABN-maltohexanose

The masses observed, in Figure 89, confirm that the methylated pABN-maltohexanose was only partially methylated. The fully methylated peak (1409.69 m/z) did not increase in mass because there were no hydroxyl (-OH) groups to deuterate. The other peaks all increased by one m/z unit per missing methyl group. The distribution of the deuterated species was similar to the distribution of the protonated system seen in Figure 88, with products ranging from the fully methylated oligosaccharides to those with eleven missing methyl groups.

5.5.1.6 LC-MS Analysis of Methylated pABN-maltohexanose

To confirm that these partially methylated peaks were not due to fragmentation of the fully methylated ion, the sample was subjected LC-MS. The LC-MS chromatogram was recorded and extracted ion chromatograms (EIC) were taken for each expected mass to charge ratio.

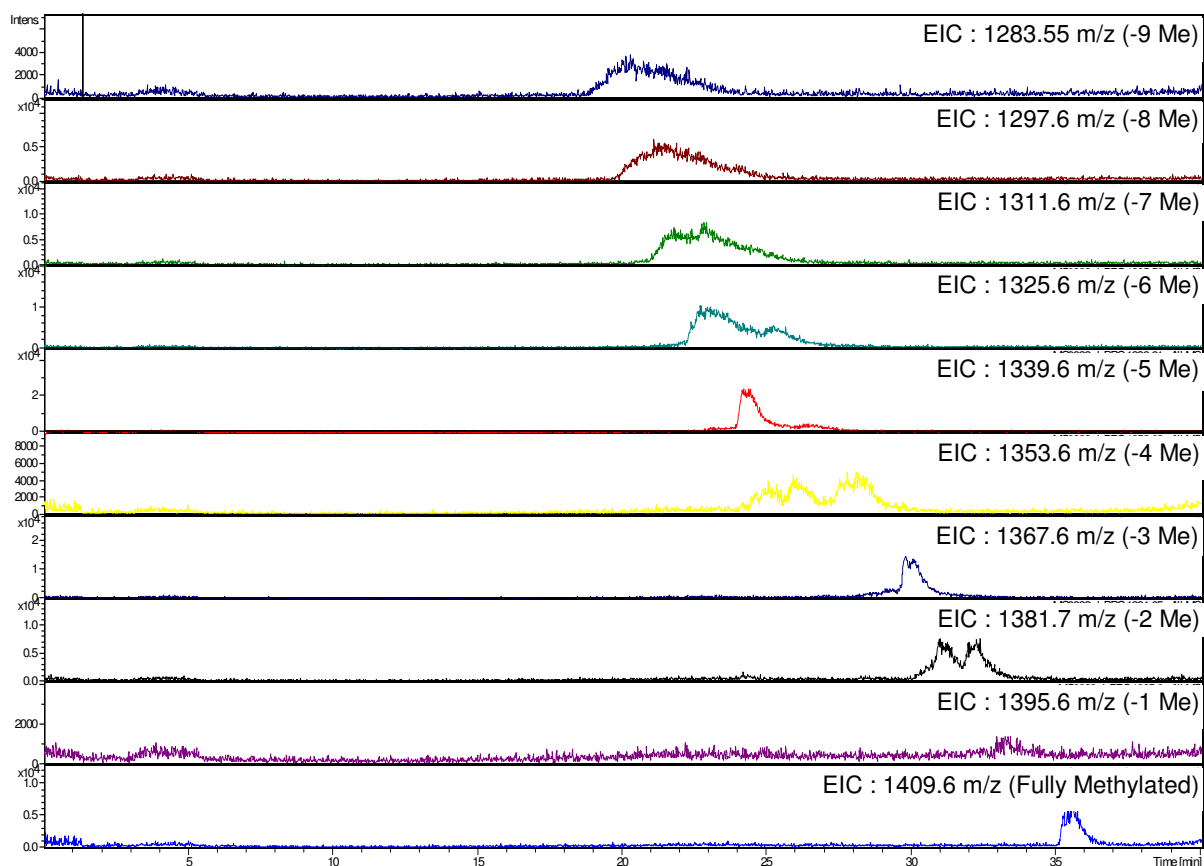
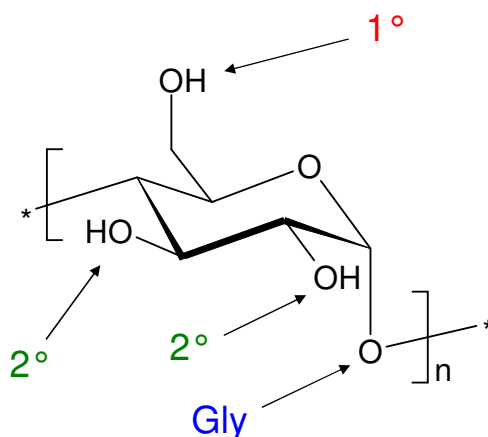


Figure 90: EIC of Partially Methylated pABN-maltohexanose

The EIC for expected mass to charge ratio for each partially methylated product is observed in the LC-MS chromatogram shown in Figure 90. Although the peak shape is broad, each partially methylated species was present, and under the chromatographic conditions employed there, were partially separated. The relative intensities of these peaks correlate to the intensities of the peaks observed in Figure 88, hence confirming that the peaks in the infused mass spectrum (Figure 88) exist as partially methylated species and are not just due to fragmentation of the fully methylated pABN-maltohexanose.

On closer inspection of the extracted ion chromatogram of the LC-MS chromatogram shown in Figure 90, the spectrum for 1381.6 m/z (-2Me groups missing), it is clear that there are two distinctive peaks present which suggests that two main isomers exist.



Glycosidic (Gly) > Primary (1°) > Secondary (2°)

Figure 91: Positions of Methylation

According to Ciucanu and Kerek⁹³ the order of reactivity of each hydroxyl group dictates the ease with which they are methylated. Therefore, methylation should occur in the following sequence, glycosidic > primary > secondary (Figure 91). pABN-maltohexanose does not have any hydroxyl on the glycosidic positions, therefore the primary hydroxyl attached to the carbon C6 position will be methylated first. The next site of methylation would be the secondary hydroxyls, at the carbon C2 and C3 positions. Due to the α -(1→4)-linkages of maltohexanose, methylation would be most likely to occur at the carbon C3 positions in preference to the carbon C2 position, because of reduced steric hindrance, this theory is supported by Adden and Mischnick⁹⁷, where they react amylose α (1→4), and cellulose β (1→4), with deuterated methyl iodide (MeI- d_3). Adden and Mischnick⁹⁷ reported preferential methylation at the carbon C2 for cellulose, and at the carbon C3 for amylose.

It must also be noted that Ciucanu⁹⁸ suggests that for complex carbohydrates the order of methylation can be modified due to the presence of intramolecular hydrogen bond interactions and steric effects. In the maltohexanose, if random methylation was occurring, one missing methyl group could potentially produce 19 different isomeric species, further investigation was required.

Further work into methylation was carried out using an alternative methylation procedure which has been employed by Mischnick's group^{96 97 224 225}, using a sodium hydroxide – methyl iodide system, that was first developed by Ciucanu and Kerek⁹³. As mentioned earlier, Ciucanu⁹⁸, reports that his methylation procedure is superior to the Hakomori dimethyl anion – methyl iodide approach, although others, such as Price²²⁶ disagree.

5.5.2 Methylation – ‘Ciucanu Procedure’

The second methylation procedure investigated was based on that described by Ciucanu and Kerek⁹³ but was later developed for neutral polysaccharides in aqueous samples by Ciucanu and Caprita⁹⁴. This method uses an excess of powdered sodium hydroxide to scavenge any water present in the sample, the absence of water increases the degree of per-*O*-methylation. As with the Hakomori methylation procedure, this method of methylation was first carried out on pABN-glucose, and then applied to pABN-maltohexanose.

5.5.2.1 Methylated of pABN-glucose

The Ciucanu methylation procedure was carried out on pABN-glucose and the sample was subjected to LC-MS analysis.

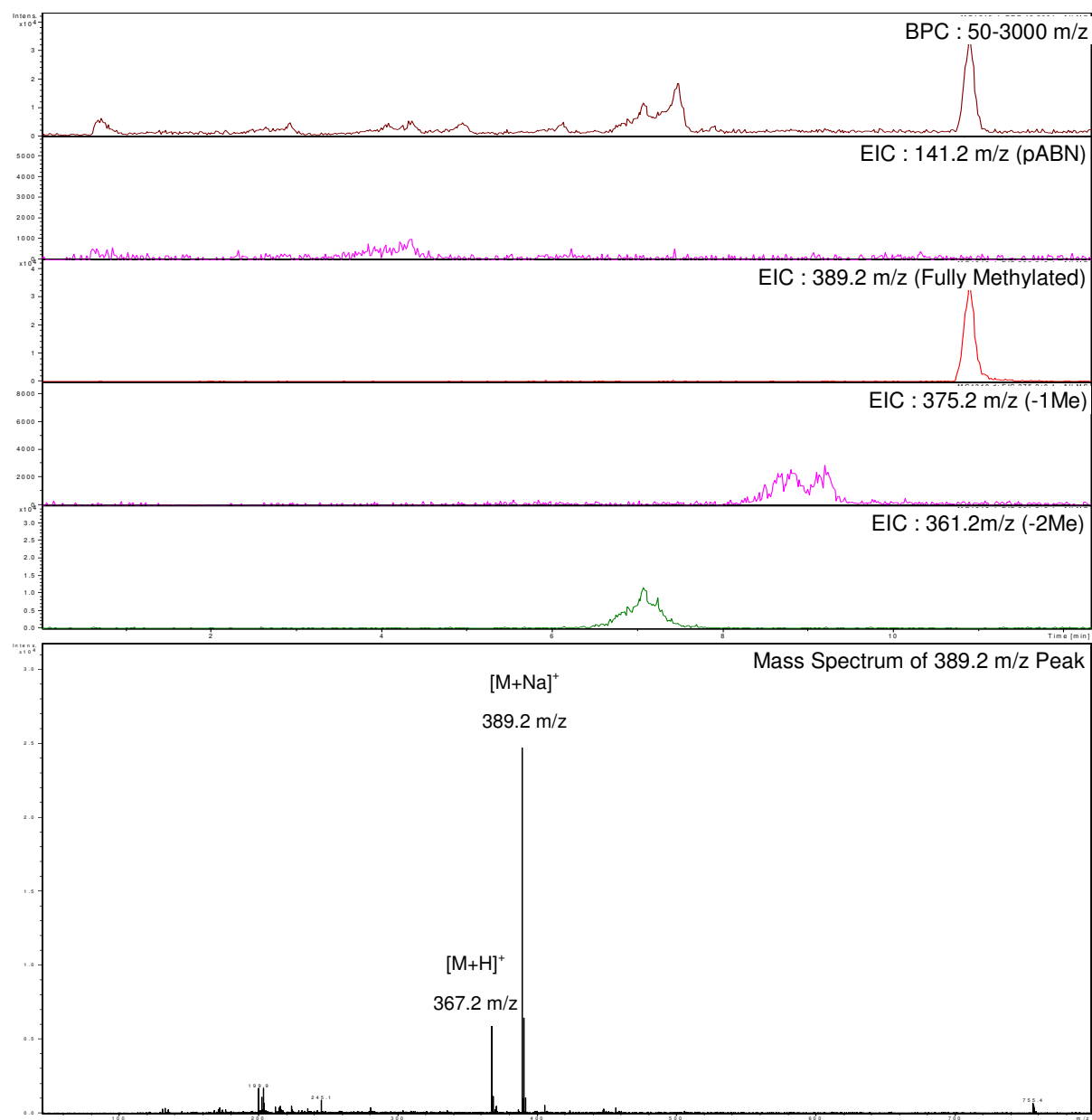


Figure 92: LC-MS Chromatogram of Methylated pABN-glucose (BPC)

This methylation procedure produced a large peak for the fully methylated species, with a retention time of 10.8 minutes. In comparison to the Hakomori methylation procedure, this method provides a much larger amount of the per-*O*-methylated derivative. There were several other peaks present, which were attributed to partially methylated pABN-glucose. These are labelled in Figure 92.

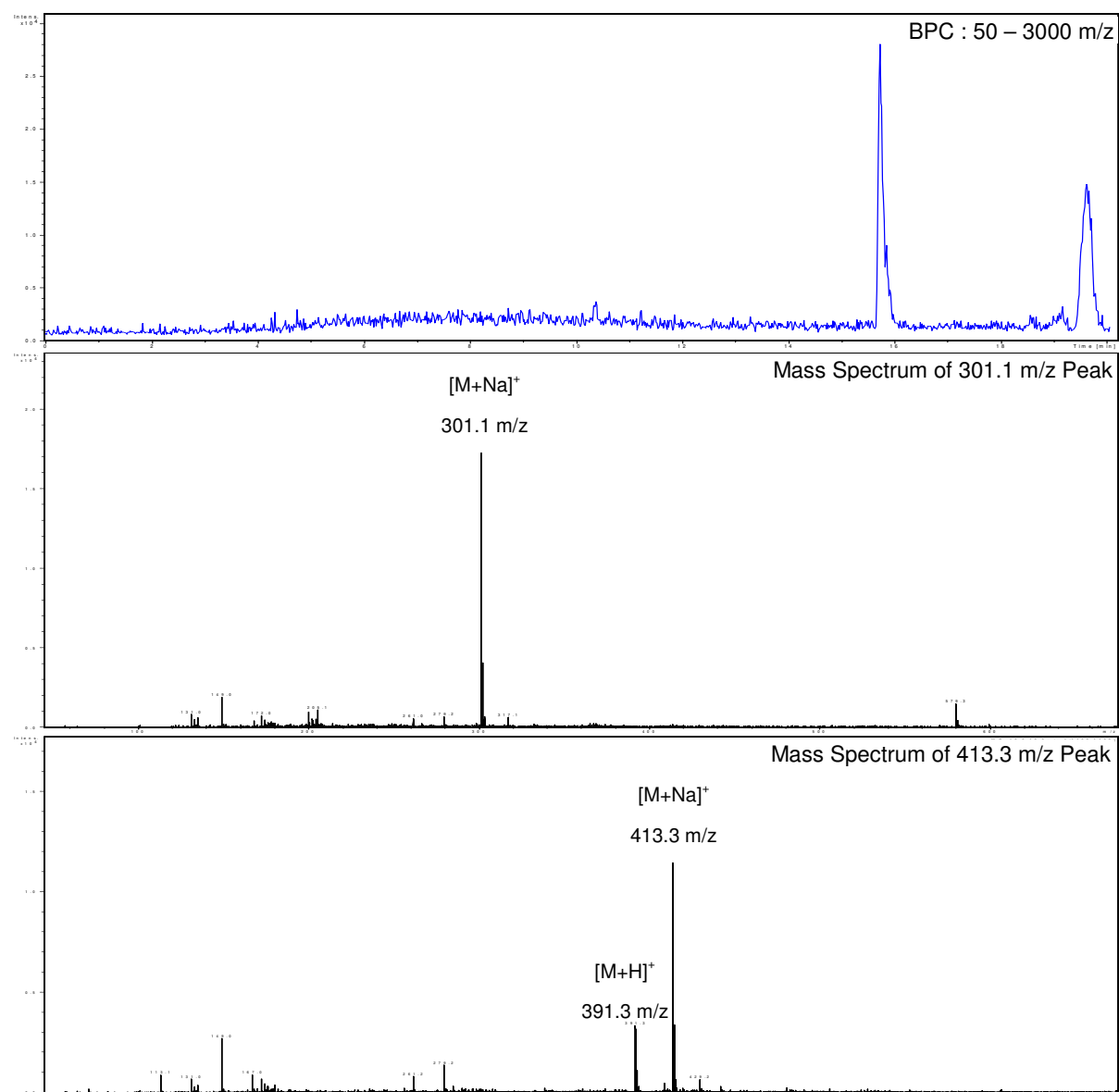


Figure 93: LC-MS Chromatogram of Acetonitrile / Water Blank (BPC)

Throughout this work, extra peaks were observed towards the end of the gradient elution. An acetonitrile / water blank was run to try to determine the origin of the peaks. The LC-MS chromatogram in Figure 93 shows two peaks present in an acetonitrile / water blank. This suggests that they were coming from the system and not the samples. After MS analysis the peaks were thought to be from plasticizer contamination. The plasticizers were identified from the list of ESI background ions and contaminants encountered in modern mass spectrometers, published by Keller *et al.*²²⁷. The plasticizer peaks were thought to be caused by the plastic tubing in the LC or the septum from the vials. They always eluted at the end of the gradient run, when the mobile phase composition exceeded 80 % acetonitrile.

These plasticizers, diisooctyl phthalate ($[M+Na]^+ = 413$ m/z) and dibutyl phthalate ($[M+Na]^+ = 301$ m/z), contain large alkyl groups which are relatively non-polar, therefore would require a high concentration of organic solvent to elute them in a reverse phase system. Using the 10 – 90 % acetonitrile gradient, the plasticizers did not interfere with the analysis of the derivatised carbohydrates, therefore no further development of the method was required to remove them from the system.

5.5.2.2 Methylation of pABN-maltohexanose

To compare the degree of methylation using the Ciucanu procedure to the Hakomori procedure, pABN-maltohexanose was methylated. The reaction time and quantity of methyl iodide required was varied to optimize the method. pABN-maltohexanose was methylated under the different reaction conditions, which are provided in Table 38. The degree of methylation and the percentage relative abundance of the per-*O*-methylated product was measured and compared for each of the different samples. The percentage relative abundance was calculated by dividing the abundance of the fully methylated peak by the total abundance of all of the peaks due to partially and fully methylated pABN-maltohexanose. The mass spectra for each sample are given in the appendix section 5.7.4.

Table 38: Results – To Optimize Ciucanu Methylation Procedure

Sample No.	Reaction Time (Minutes)	Amount of Methyl iodide used (μl)	Visible Degrees of Methylation	Percentage Relative Abundance of per-O-methylation
1	10	60	Full to 7 missing methyls	6.10%
2	20	60	Full to 6 missing methyls	31.25%
3	60	60	Full to 6 missing methyls	31.43%
4	60	300	Full to 6 missing methyls	36.08%
5	60	1500	Full to 8 missing methyls	22.51%

The investigation to optimise this methylation procedure, showed that using methyl iodide (300 μl), and a reaction time of 60 minutes gave the greatest relative abundance of the per-O-methylated product. It also provided the narrowest degree of methylated species. These reaction conditions were used in subsequent studies when the 'Ciucanu methylation procedure' was used.

5.5.2.3 Deuteration of Methylated pABN-maltohexanose

As with the Hakomori procedure (section 5.5.1.5), a methylated pABN-maltohexanose (using the 'Ciucanu methylation procedure') was deuterated to confirm that partial methylation was occurring. A methylated pABN-maltohexanose sample (Sample 4, Table 38) was freeze dried and re-dissolved in a solvent composed of equal portions of deuterated acetonitrile and deuterium oxide. The sample was then infused into the mass spectrometer.

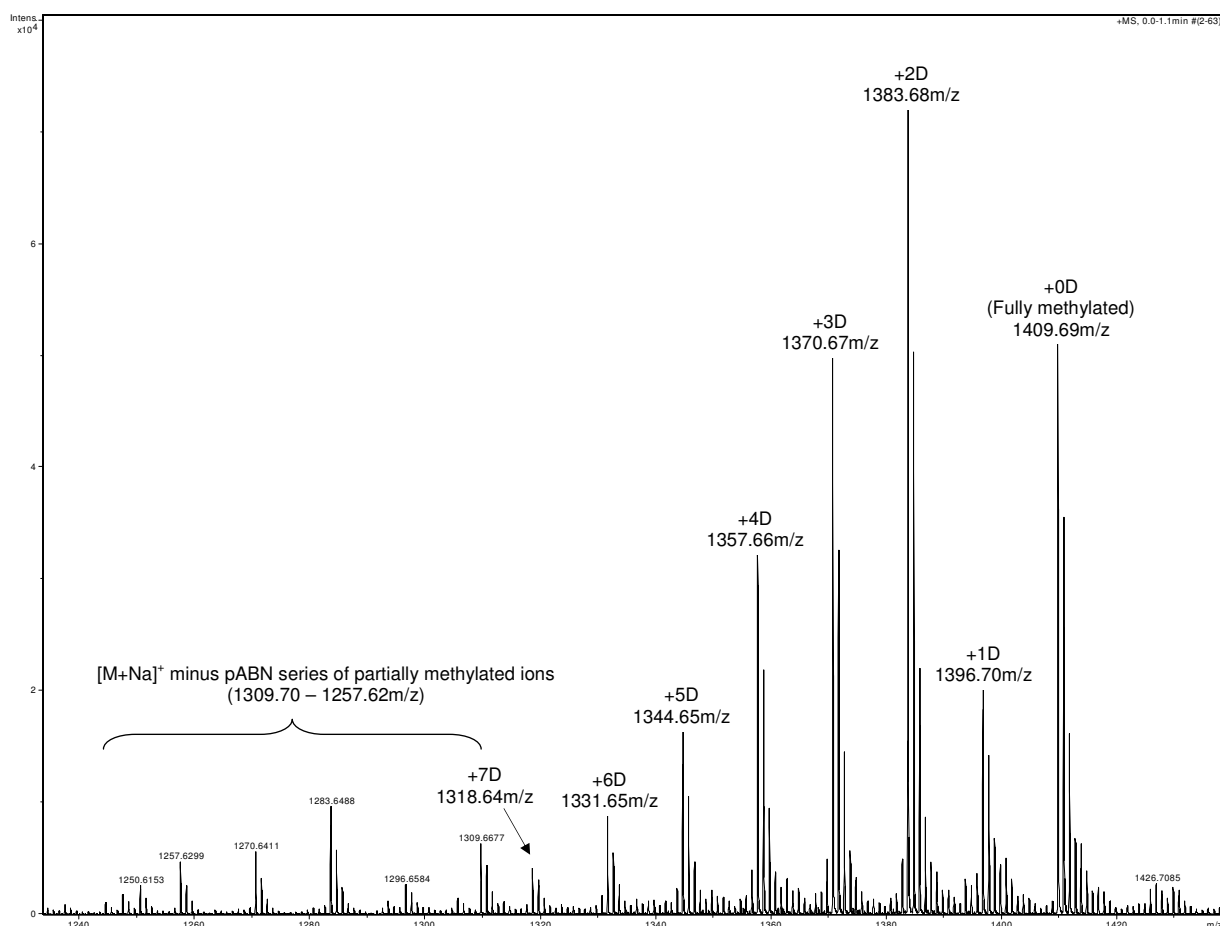


Figure 94: Deuterated Methylated pABN-maltohexanose

The increases by one m/z unit for each hydroxyl group present in the partially methylated species confirmed the partial methylation. As expected, the fully methylated ion did not increase in m/z , but its abundance was reduced in comparison to the spectrum for the non-deuterated sample. This was thought to be due to the fully methylated product not being as soluble in D_2O as the other partially methylated species. A distribution of ions was observed that corresponded to methylated maltohexanose that was not pABN labelled.

Further analysis using LC-MS-MS was used to determine where the missing hydroxyl groups were located along each partially methylated pABN-maltohexanose.

5.5.2.4 LC-MS-MS Analysis of Methylated pABN-maltohexanose

To try to establish which hydroxyl positions were not being methylated LC-MS-MS analysis was carried out on $[M+Na]^+$ ions of each partially methylated pABN-maltohexanose. It was envisaged fragmentation of an isolated $[M+Na]^+$ would break the glycosidic linkages and analysis of the B- and Y-series of ions would show where the missing methyl groups were situated. This would establish whether partial methylation was occurring randomly or whether methylation was being restricted to certain sites. A methylated pABN-maltohexanose sample (Sample 4, Table 38) was first subjected to LC-MS analysis.

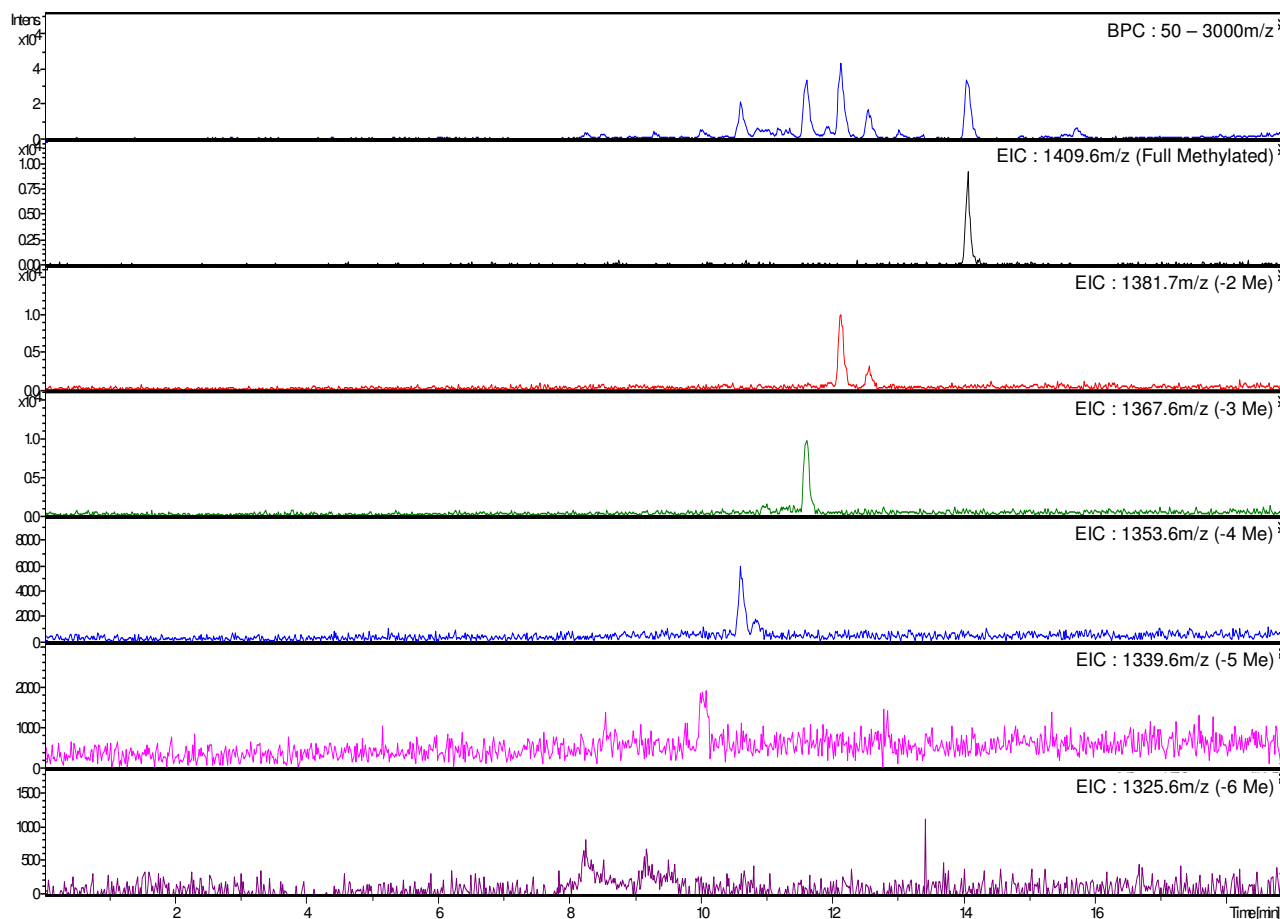


Figure 95: LC-MS of Methylated pABN-maltohexanose

The base peak chromatogram detected several peaks, these were individually identified as samples with two, three, four, five or six missing methyl groups using EICs (Figure 95). The MS/MS analysis was carried out on ions of m/z given in Table 39.

Table 39: Methylated pABN-maltohexanose Ions Analysed by LC-MS-MS

Isolated MS/MS ions	Number of missing methyl groups
1409.6 m/z	0 (Fully Methylated)
1381.6 m/z	Loss of 2
1367.6 m/z	Loss of 3
1353.6 m/z	Loss of 4

The MS/MS spectra for each isolated ion of methylated pABN-maltohexanose can be seen in appendix section 5.7.5.

The fragmentation patterns for each isolated ion listed in Table 39 showed distinct peaks for both the b- and y-ion series. Further analysis of the MS/MS spectra confirms that the free hydroxyl positions are distributed randomly along the six member oligosaccharide chain. The sets of fragmentation patterns for the Y-ion series of each isolated MS/MS ion (Table 39) suggest that the free hydroxyl positions occur mainly on the two monosaccharide units closest to the pABN end of the structure. Unfortunately, the fragmentation patterns of the B-ions contradict the results from the y-ions, which show that the mass spectrometer is detecting more than one single structure for the isolated ion. The mass spectrometer is detecting many isomeric products that differ by the position of the free hydroxyl.

This work carried out on the methylation of pABN-maltohexanose has significantly increased the yield of per-*O*-methylation, but the problem of random, partial methylation still exists.

5.5.3 Comparison of the Methylation Procedures Used

Price (2008) ²²⁶ states that the Hakomori methylation procedure is better than the Ciucanu methylation procedure. Conclusions drawn from the results of the two methylation procedures generated in this work disagree with the report by Price. Both procedures have

similar extraction methods, which potentially remove any partially methylated pABN-labelled sugars and therefore the only difference is in the methylation reactions themselves.

From a practical perspective, the Ciucanu methylation procedure is much easier to carry out: the removal of excess reagents is simpler, and the reaction reaches the same degree of completion much faster, without the need to heat the sample.

5.6 Novel Linkage Analysis of Carbohydrates using LC-MS-MS

The derivatisation procedures described in the previous sections (pABN-labelling and methylation) were used to develop a novel technique to characterise the linkage patterns of EPSs.

5.6.1 *Disaccharide Standards*

The method was first attempted on disaccharides, where the position of the glycosidic linkage was known. A series of disaccharides, each with different glycosidic linkages (1,1-, 1,2-, 1,3-, 1,4- and 1,6-linked) were used. The structures of all these disaccharide standards are given in

Table 9. Each disaccharide was first methylated, then hydrolysed and then pABN-labelled. Finally the standards were subjected to LC-MS-MS analysis to separate the derivatives and to generate fragmentation patterns. The fundamentals are similar to those used in the current GC-MS methodology⁹¹, but this novel procedure is faster and potentially more sensitive. Each disaccharide was first methylated and hydrolysed into two sugar residues,

after labelling with pABN, one derivatised sugar residue corresponded to the terminal ($[M+H]^+ = 347.1$ m/z) and one derivatised sugar residue corresponded to a linked sugar, containing one free hydroxyl group located where the glycosidic linkage was originally located ($[M+H]^+ = 325.1$ m/z).

A schematic of the reaction is given in Figure 96, which highlights the differences between the structures of the two derivatised sugar residues.

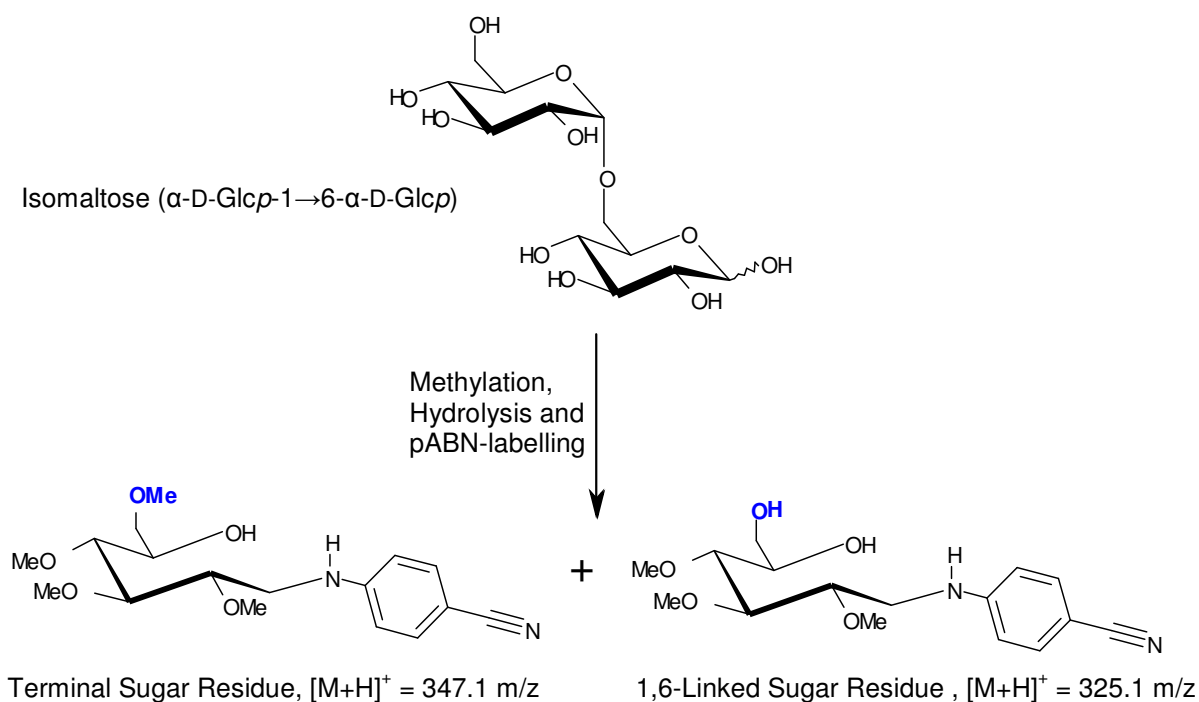


Figure 96: An Overview of the Proposed Linkage Analysis Reaction

The position of the extra hydroxyl group will change depending on the position of the glycosidic linkage between the disaccharides. It was envisaged that this change in position could be identified through inspection of the MS/MS fragmentation patterns. The greatest amount of linkage information was generated when using the protonated ions ($[M+H]^+$), for MS/MS analysis of the sugar residues.

The mass spectrometry conditions were optimized for the MS/MS analysis of these sugar residues, see Table 40. These conditions provided fragmentation patterns for use in

evaluating the linkages (80 – 350 m/z). All samples subjected to LC-MS and LC-MS-MS were prepared at a concentration of 250 $\mu\text{g mL}^{-1}$.

Table 40: Optimized MS and MS/MS Conditions for the Linkage Analysis

MS conditions	
Collision Energy	4.0 eV z ⁻¹
Collision RF	200.0 Vpp
Transfer time	148.0 μs
Pre Pulse Storage	6.0 μs
MS/MS conditions	
Selected m/z [M+H] ⁺	325.1 & 347.1 m/z
Isolation width	1.0 m/z
Collision Energy	15.0 eV

The MS/MS spectra of each disaccharide standard are provided in appendix section 5.7.6.

Even when using optimized conditions, the b- and y-ion series were not clearly observed; ions due to further fragmentation, such as losses of MeOH and H₂O were evident, and in the greatest abundance. This made the assignment of the b- or y-ion series extremely difficult, losses of 18 m/z (H₂O), 32 m/z (MeOH), 36 m/z (2H₂O) and 50 m/z (MeOH & H₂O) all had to be considered. A table which lists the masses of the b- and y-ion series with the further fragmentation is given in appendix section 5.7.7. The loss of several MeOH / H₂O gave peaks that were identical for both y_n and y_{n-1} and also the further fragmentation caused some of of the b- and y- ions to have equal m/z, making assignment of these ions difficult: mass to charge ratios of 131.1 m/z, 143.1 m/z and 175.1 m/z were possible from further fragmentation of both b- and y-ion series.

5.6.1.1 Deuterated System

To help to deduce the origin of each ion, the series of disaccharide standards were subjected to deuterium exchange and then analysed by LC-MS-MS. To ensure the samples remained deuterated, deuterium oxide replaced water in the mobile phase. The spectra for each sample are given in appendix section 5.7.8.

An increase of one m/z was seen for each exchangeable proton that was located on the hydroxyl groups and nitrogen, this gave an increase from $[M+H]^+ = 325.1 m/z$ to $[M+D]^+ = 329.1 m/z$ for sugar residues that previously had a glycosidic linkage in either the 2-, 3-, 4- or 6- position and an increase from $[M+H]^+ = 339.1 m/z$ to $[M+D]^+ = 342.1 m/z$ for terminal sugar residues. An example of exchange with deuterium oxide of an exchangeable proton in the 6-position is shown in Figure 97.

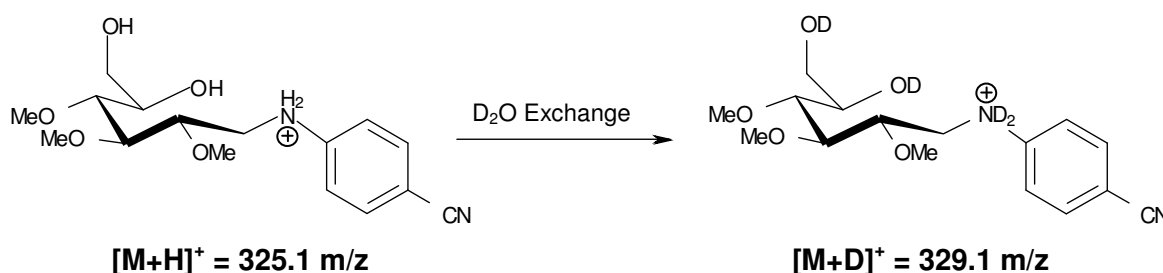


Figure 97: Deuterium Oxide Exchange of 1,6-linked Sugar Residue

Each deuterated disaccharide fragment was subjected to LC-MS-MS, using slightly altered chromatographic conditions to compensate for the increase in back pressure caused by using deuterium oxide in the mobile phase.

The linkage analysis of the deuterated disaccharide standards provided information about how the sugar residues were fragmenting using MS/MS. The molecular ion was visible for all of the standards, where losses of MeOD (-33 m/z) and D₂O (-20 m/z) were observed. As with the protonated disaccharide standards, neither the Y- nor B- ion series were seen again, further losses of MeOH (-32 m/z), HDO (-19 m/z) and 2HDO (-38 m/z) were observed.

There is evidence of rearrangements occurring, as losses were observed that were not possible by simple elimination of neutral molecules e.g. loss of $2\text{H}_2\text{O}$.

Deuterating the disaccharide standards did not help deduce where each ion originated; because of further fragmentation, there were still mass to charge ratios that could be attributed to y_n or y_{n-1} and also b- or y-ions.

Using the protonated or deuterated systems, significant differences between the disaccharide standards could not be established. Even when examining the spectra for masses that were unique for a particular linkage position, the further fragmentation or rearrangements prevented unequivocal assignment of the linkage position.

5.6.1.2 Linkage Analysis using Sodium Cyanoborodeuteride

A different approach was used to try to distinguish between ions from the B- and Y- series. This involved increasing each ion in the y-series by one m/z unit. Sodium cyanoborodeuteride was used during the reductive amination, instead of sodium cyanoborohydride.

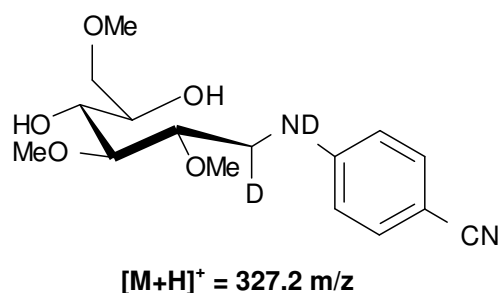


Figure 98: Product from the Reductive Amination using Sodium Cyanoborodeuteride

The product that is formed, when sodium cyanoborodeuteride is used to reduce the imine is shown in Figure 98. Two deuteriums are attached, but the exchangeable deuterium is lost when the product comes into contact with a source of protium (e.g. water). Due to limited amounts of each disaccharide standard, this reaction was only performed on cellobiose

where the monosaccharides are linked through an α -1,4-glycosidic bond. The MS spectrum can be seen in appendix section 5.7.9.

The spectrum shows that all of the fragment ions which are due to the y-ion series increase by one m/z unit, changing them to even numbers. The particular m/z of interest (131.1 m/z, 143.1 m/z and 175.1 m/z), showed a one unit increase, but also the original ion remained. This shows that these fragmentation ions are due to both the y- and b-ion series. The ratios differ slightly, the ratio between peaks 131.1 m/z to 132.1 m/z is approximately 1:2.5, for 143.1 m/z to 144.1 m/z is approximately 1:1.2 and for 175.1 m/z to 176.1 m/z is approximately 1:1.6. This shows that these masses were due to both the b- and y-ion series. Due to the position of the formal charge, it is expected that the majority of ions produced from MS/MS analysis of these derivatised ring-opened sugars would be due to the y-series. This is certainly the case, with all but two distinct ions from the y-series. The b-ions present were also subject to further losses of MeOH (-32 m/z) and H₂O (-18 m/z). The only ions that were observed without these further losses were the y₀ and y₁.

The conclusions drawn from this work are that the optimised MS/MS conditions were able to generate fragmentation spectra, but the procedure suffered from further losses of MeOH and H₂O. This meant that significant differences between the different disaccharide standards could not be found. Ideally, for this method to be successful, the MS/MS fragmentation would need to break the carbon-carbon backbone, without removing the -OMe and -OH groups, hence providing clean y- and b-ions. For this method to succeed, future work would need to concentrate on altering the fragmentation conditions or using different chemistry to replace the methylation procedure, to provide substituents which are not as prone to fragmentation. This may prove difficult as methyl groups are regarded as the most difficult to remove, once attached.

5.6.2 Linkage Analysis of Oligosaccharides

Despite the proposed linkage analysis method being unable to completely distinguish between the disaccharide standards, an attempt was made to use this procedure to determine the linkage patterns of an oligosaccharide. Maltohexanose was used, with a structure consisting of six monosaccharides that are each linked through an α -1,4-glycosidic bond. The reaction procedure, shown in Figure 96, was applied and the expected residues produced were one terminal residue and five identical 1,4-linked residues. The product from the reaction was subjected to LC-MS analysis. The peak retention times and peak areas of these two residues were compared to see if the method was capable of resolving the peaks and then quantifying the peaks.

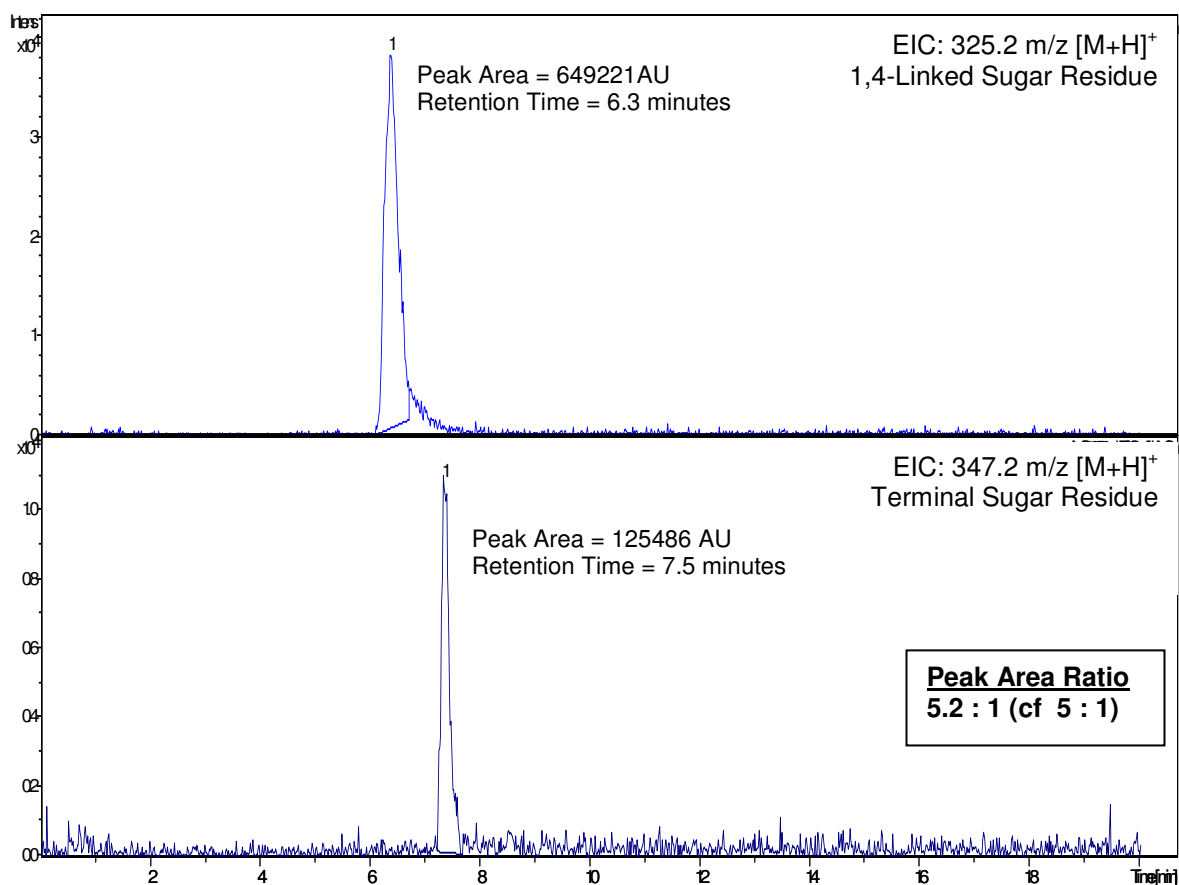


Figure 99: LC-MS Chromatogram of the Linkage Analysis of Maltohexanose

The LC-MS method was capable of separating the 1,4-linked (6.3 minutes) and terminal (7.5 minutes) sugar residues. The order in which the peaks eluted was as expected, where the

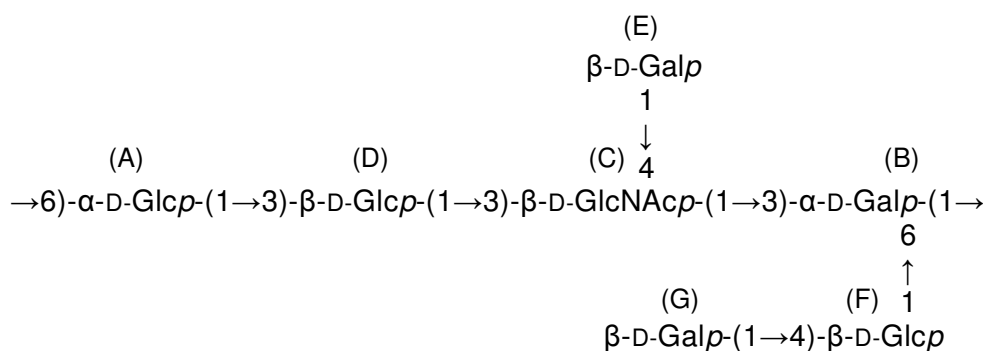
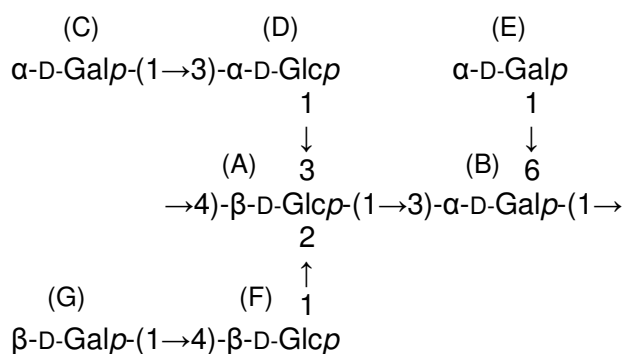
extra hydroxyl group on the 1,4-linked residue made the compound slightly more polar, hence, elute earlier. The extracted ion chromatograms were used to calculate the peak areas for the two different sugar residues (Figure 99); the peak areas were expressed as a peak area ratio. The results show a 5.2:1 ratio for the residues of the 1,4-linked sugars to the terminal sugar, which is close to the theoretical ratio of 5:1. The problems of partial methylation, previously discussed, could be contributing to the differences between the calculated and theoretical values. To calculate the ratio more accurately, the peak area of each sugar residue should be calculated from a calibration curve, which has been generated from standards of known concentration.

Although the results were not conclusive, this exercise demonstrated the potential application of this approach to linkage analysis to quantify different sugar residues in a simple homopolysaccharide.

5.6.3 Linkage Analysis of Exopolysaccharides

The linkage analysis of complex oligosaccharides has been routinely determined by GC-MS for many years, this type of analysis is time consuming and not very sensitive. A novel, faster and more sensitive technique would be to use LC-MS to determine the linkage pattern of exopolysaccharides. The proposed linkage analysis procedure was used to examine two previously characterised EPS samples; the EPS produced by *Lactobacillus delbrueckii subsp. bulgaricus* NCFB2074⁷⁸ and the EPS produced by *Lactobacillus acidophilus* 5e2¹⁷⁷. The structures of the two exopolysaccharides are given in Figure 100. Both are complex heteropolysaccharides, consisting of seven monosaccharides in their repeating unit.

The procedure first methylates all the available hydroxyl groups on the exopolysaccharides, then uses acid-catalysed hydrolysis to break the polymer chain into monosaccharide units. These partially methylated monosaccharides were then pABN-labelled and subjected to LC-MS analysis.

EPS Produced by *Lactobacillus acidophilus* 5e2 (Laws *et al.*, 2008) ¹⁷⁷EPS Produced by *Lb. delbrueckii* subsp. *bulgaricus* NCFB2074 (Harding *et al.*, 2005) ⁷⁸**Figure 100: Structures of the Exopolysaccharides used for the Linkage Analysis**

The following derivatised monomers were expected for the EPS produced by *Lactobacillus acidophilus* 5e2 (Table 41) and the EPS produced by *Lactobacillus delbrueckii* subsp. *bulgaricus* NCFB2074 (Table 42).

Table 41: Table of Expected Structures for the Repeating Unit of the EPS Produced by 5e2

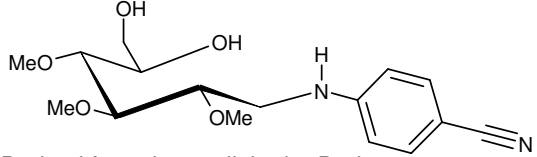
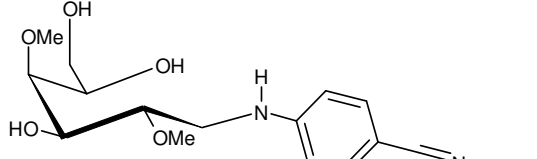
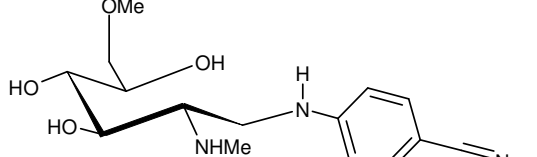
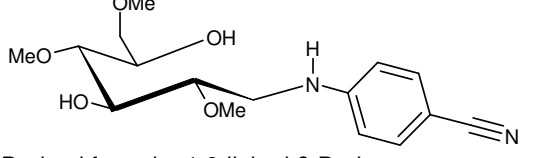
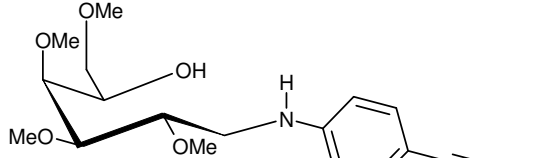
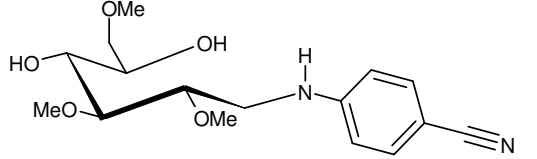
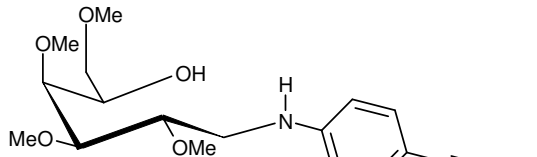
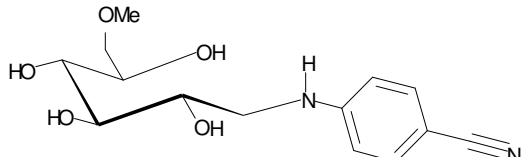
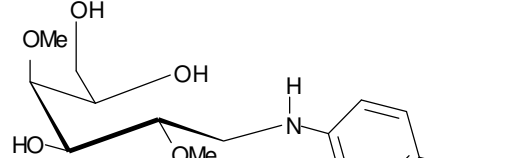
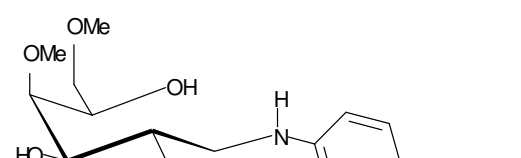
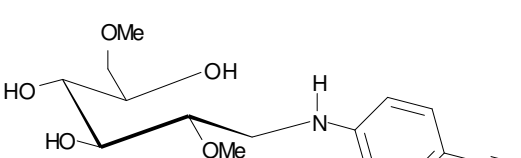
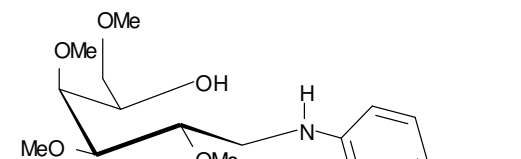
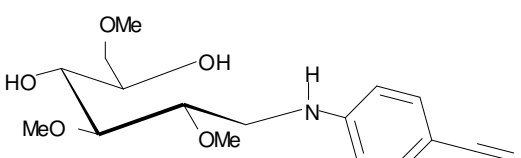
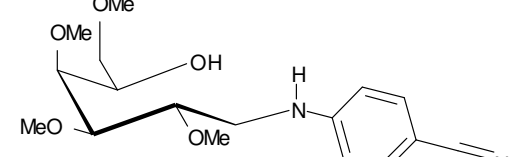
Structure	Unit	Expected Masses (m/z)	
		[M+H] ⁺	[M+Na] ⁺
 <p>Derived from the 1,6-linked α-D-glucose</p>	A	325.1	347.1
 <p>Derived from the 1,3,6-linked α-D-galactose</p>	B	311.1	333.1
 <p>Derived from the 1,3,4-linked β-D-N-acetyl glucosamine</p>	C	310.1	332.1
 <p>Derived from the 1,3-linked β-D-glucose</p>	D	325.1	347.1
 <p>Derived from the first terminal β-D-galactose</p>	E	339.1	361.1
 <p>Derived from the 1,4-linked β-D-glucose</p>	F	325.1	347.1
 <p>Derived from the second terminal β-D-galactose</p>	G	339.1	361.1

Table 42: Table of Expected Structures for the Repeating Unit of the EPS from NCFB2074

Structure	Unit	Expected Masses (m/z)	
		[M+H] ⁺	[M+Na] ⁺
 <p>Derived from the 1,2,3,4-linked α-D-glucose</p>	A	297.1	319.1
 <p>Derived from the 1,3,6-linked α-D-galactose</p>	B	311.1	333.1
 <p>Derived from the first terminal β-D-galactose</p>	C	339.1	361.1
 <p>Derived from the 1,3-linked β-D-glucose</p>	D	325.1	347.1
 <p>Derived from the terminal β-D-glucose</p>	E	339.1	361.1
 <p>Derived from the 1,4-linked β-D-glucose</p>	F	325.1	347.1
 <p>Derived from the second terminal β-D-galactose</p>	G	339.1	361.1

The expected structures and masses of the derivatized monosaccharides from the EPS produced by *Lactobacillus acidophilus* 5e2 (shown in Table 41), highlighted potential problems which the chromatography must overcome. As can be seen, residues (B) and (C) have unique masses, but residues (E) and (G) are identical in both mass and structure. The expected masses for residues (A), (D) and (F) are the same but the structures are isomers of each other. The method had to be capable of resolving different isomers in order to determine the glycosidic linkage positions.

For the EPS produced by *Lactobacillus delbrueckii* subsp. *bulgaricus* NCFB2074 the structures for residues (A) and (B) have unique masses, whereas residues (D) and (F) are isomeric, as are (E), (C) and (G). This time the terminal D-galactoses, residues (C) and (G), are identical with each other in mass and structure.

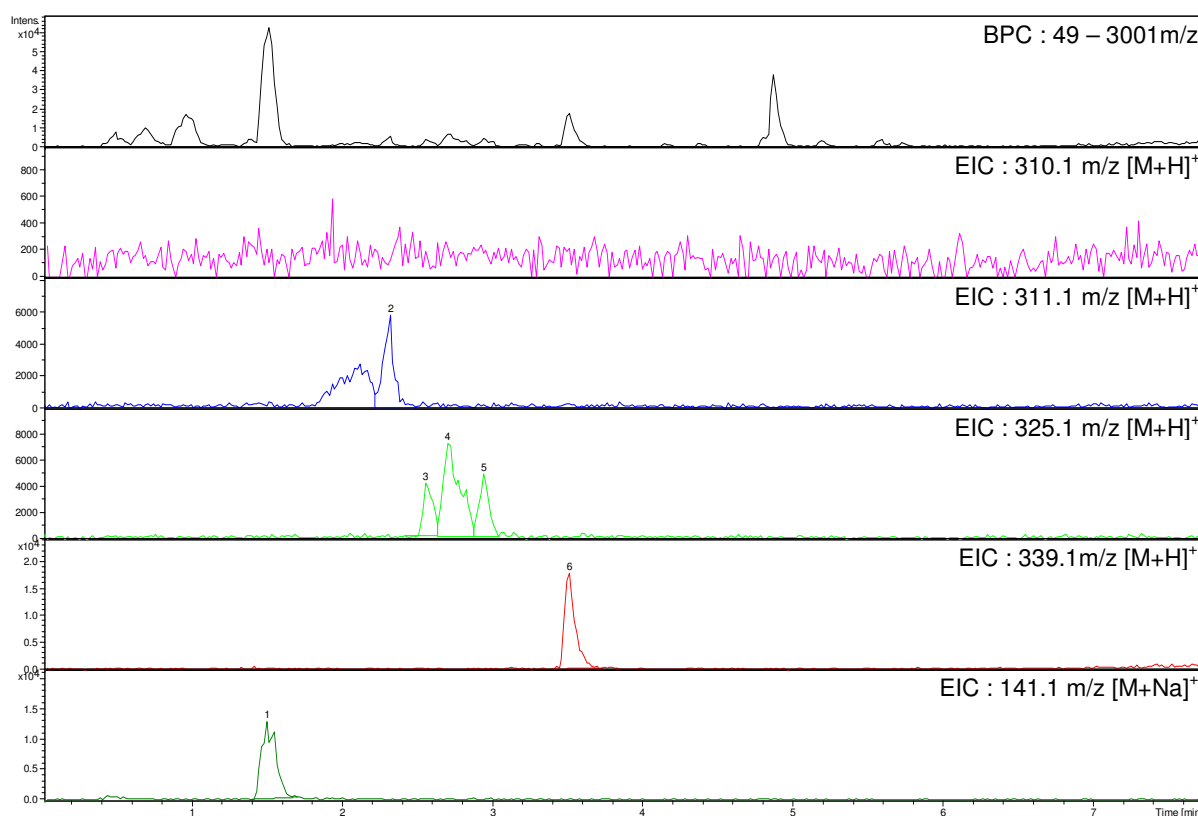


Figure 101: LC-MS Chromatogram of the Linkage Analysis of the EPS produced by 5e2

Table 43: LC-MS Peak Area Results for the Linkage Analysis of the EPS produced by 5e2

Peak No.	Retention Time	Monosaccharide Residue	Peak Area	Ratio	c.f. Ratio
1	1.5	Excess pABN (141.1 m/z)	82136	-	-
2	2.3	(C)	29440	1.0 [#]	1
3	2.6	(A) or (D) or (F)	22738	0.8	1
4	2.7	(A) or (D) or (F)	34439	1.2	1
5	2.9	(A) or (D) or (F)	25369	0.9	1
6	3.5	(E) and (G)	60966	2.1	2

[#]Ratios relative to monosaccharide residue (C), monosacchride residue (B) was not observed.

The derivatised monomers generated by treatment of the EPS produced by 5e2 were resolved by HPLC (Figure 101). From the table of expected masses (Table 41), there should be three peaks for the isomers with mass 325.1 m/z, which are all visible. One peak at mass 339.1 m/z, which is visible at a retention time of approximately 3.5 minutes, corresponds to the two identical terminal β -D-galactose residues. This peak is present at approximately twice the intensity as that of the earlier eluting peaks (1 : 2.1, c.f. 1 : 2), which is as expected. There should only be one peak for 311 m/z, derived from the 1,3,6-linked α -D-galactose, but a second peak, at a lower retention time was also visible. This may be due to monosaccharide residue (C) which has a mass of 310 m/z, and has been incorporated into the extracted ion chromatogram due to the isolation width being set to one. This has not been proven, and as with the CZE analysis of the EPS produced by 5e2, discussed in section 5.4.2, the *N*-acetyl-glucosamine residue is not visible at the expected mass (310.1 m/z) using EIC, hence further investigation is required. Even though the experiment used a 1:1 ratio of pABN to analyte, the peak due to pABN ($[M+Na]^+ = 141$ m/z) was still present but it is significantly reduced in size and is clearly resolved from the peaks of interest.

The second EPS sample was then analysed by the same method. This EPS does not contain an *N*-acetyl-amino sugar, therefore all residues were expected to be visible.

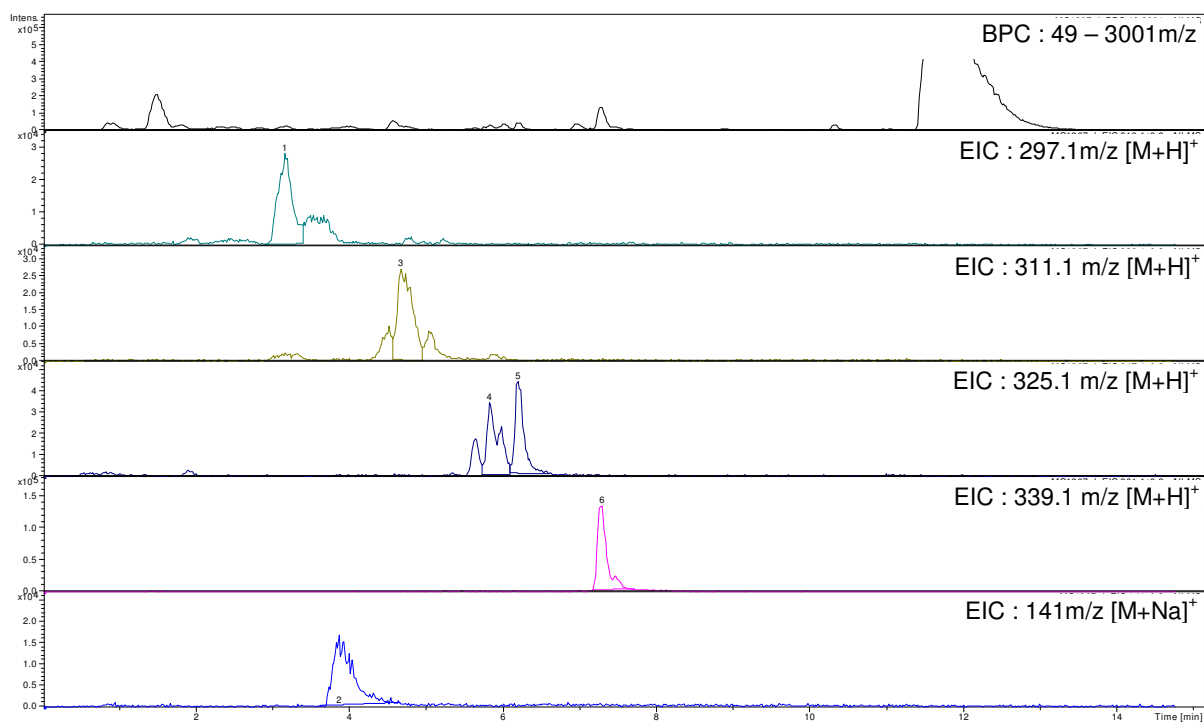


Figure 102: LC-MS Chromatogram of the Linkage Analysis of the EPS produced by NCFB2074

Table 44: LC-MS Peak Areas for the Linkage Analysis of the EPS produced by NCFB2074

Peak No.	Retention Time	Monosaccharide Residue	Peak Area	Ratio	c.f. Ratio
1	1.5	(A)	35580	1.0 [#]	1
2	2.3	Excess pABN (141.1 m/z)	27408	-	-
3	2.6	(B)	36561	1.0	1
4	2.7	(D) or (F)	37124	1.0	1
5	2.9	(D) or (F)	34998	1.0	1
6	3.5	(C), (E) and (G)	113043	3.2	3

[#] Ratios relative to monosaccharide residue (A).

As with the previous analysis of the EPS produced by 5e2, the BPC and EIC for the expected masses are shown in Figure 102. Again there is one large peak correlating to mass 399.1 m/z. This peak contains three terminal D-galactose residues, and is approximately three times more intense than the single peak for mass 311.1 m/z (1:3.2, c.f.

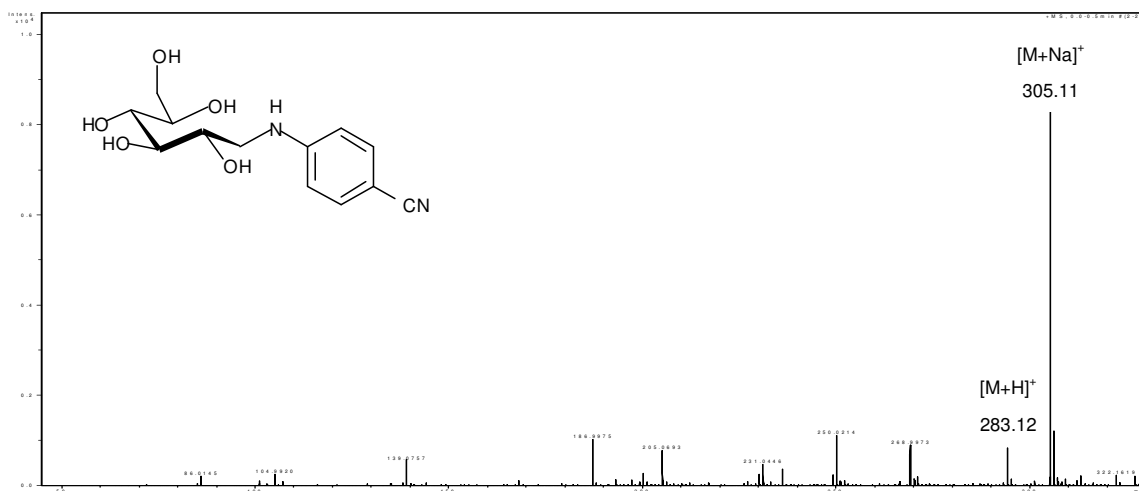
1:3). The EIC for mass 325.1 m/z contains two main peaks, but two smaller peaks are also visible and are partially resolved. One reason for these extra peaks could be that a small proportion of the terminal sugars is maybe partially methylated, producing a peak with an m/z 14 less than expected. The same explanation could be applied to explain the extra peaks in the extracted ion chromatograph for 311.1 m/z, one at each side of the principal peak. The EIC for mass 297.1 m/z contains one peak of approximately the correct size relative to the other peaks (Table 44), and also several other peaks which elute later, and can not be explained without further investigation.

These results are encouraging and with further method development this aspects of this methodology could eventually be used to confirm the linkage analysis of carbohydrates. Basic comparisons between the current GC-MS method and the proposed LC-MS method show that there are improvements in both sensitivity and analysis time. But until the method is capable of providing unequivocal linkage analysis, a quantitative comparison between the methods will not be possible.

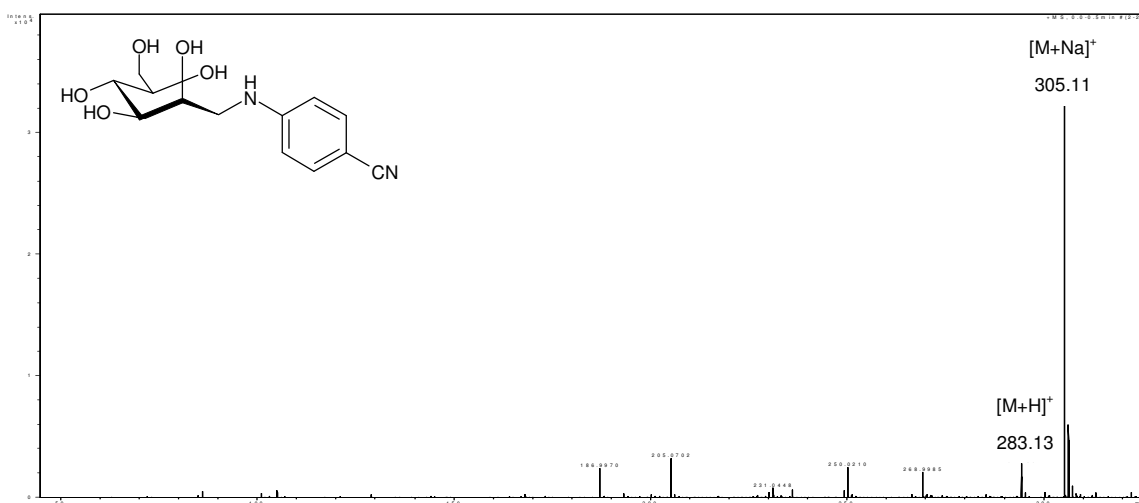
5.7 Appendices

5.7.1 Mass Spectra of pABN-labelled Monosaccharides

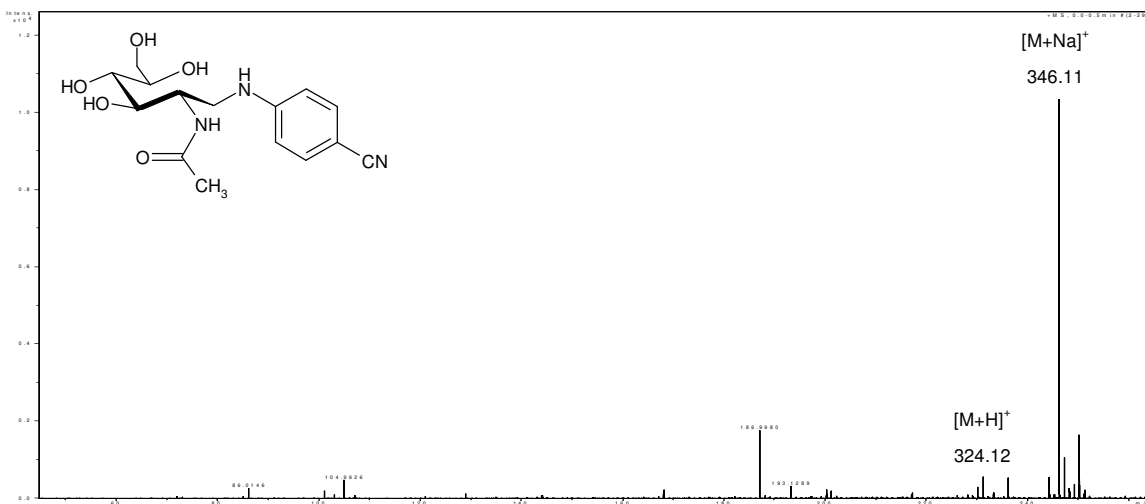
5.7.1.1 Mass Spectrum of pABN-galactose



5.7.1.2 Mass Spectrum of pABN-mannose

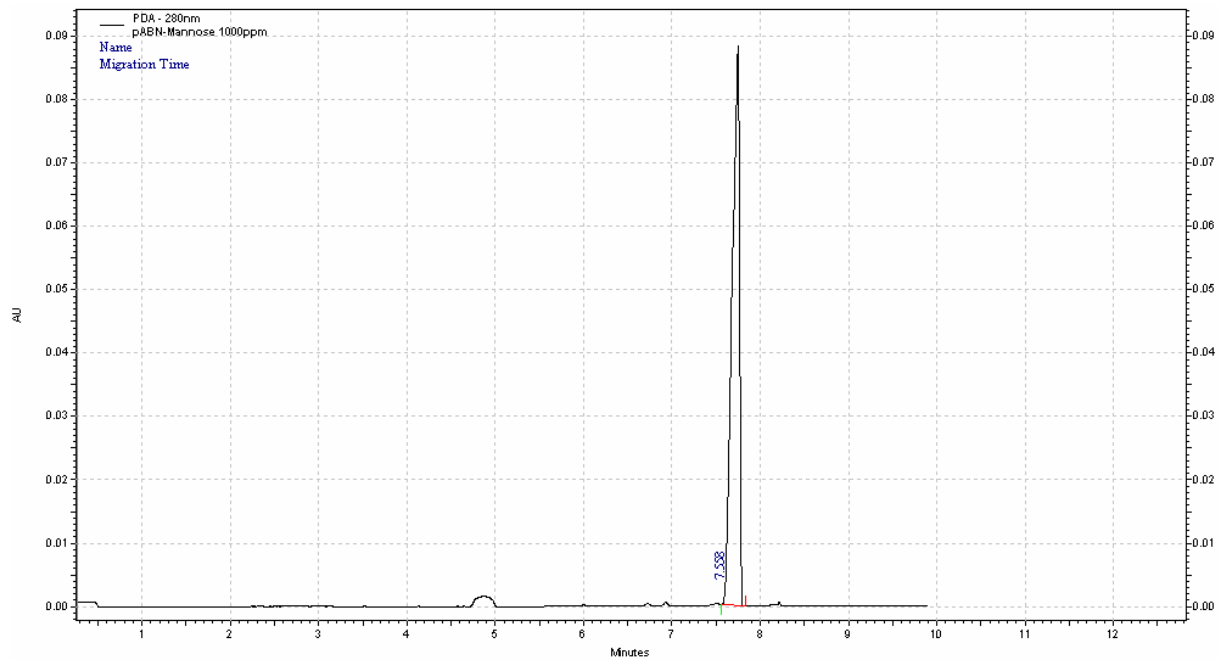


5.7.1.3 Mass Spectrum of pABN-N-acetyl-glucosamine

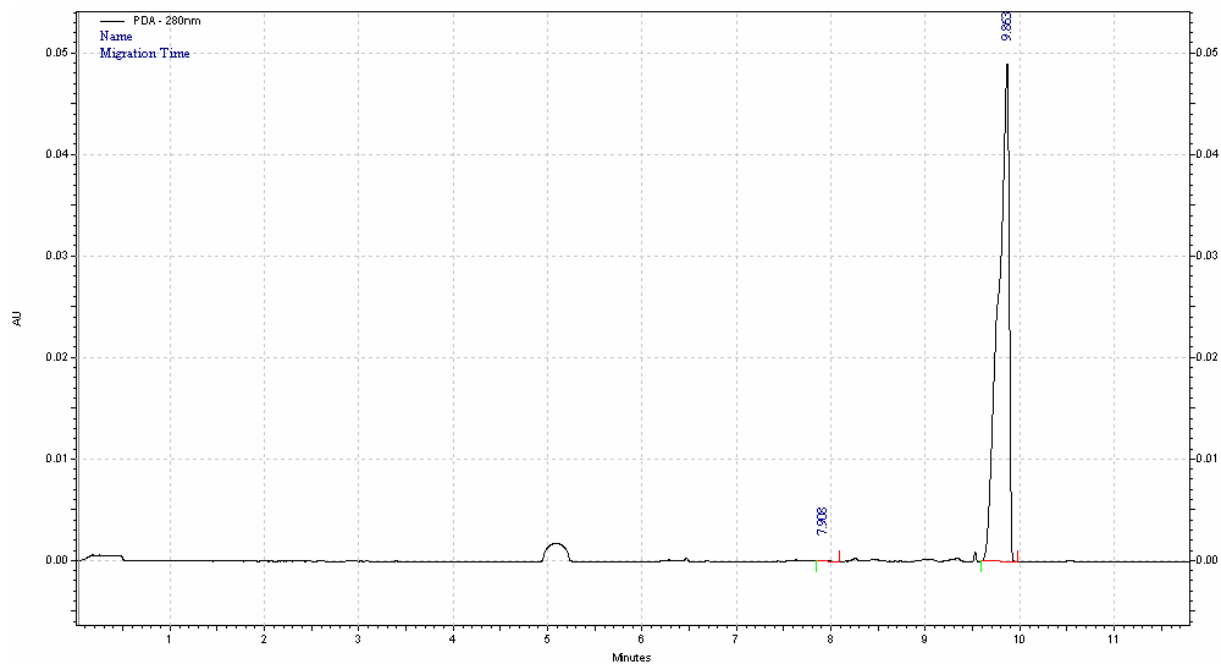


5.7.2 Examples of the CZE Chromatograms for the pABN-labelled Monosaccharides

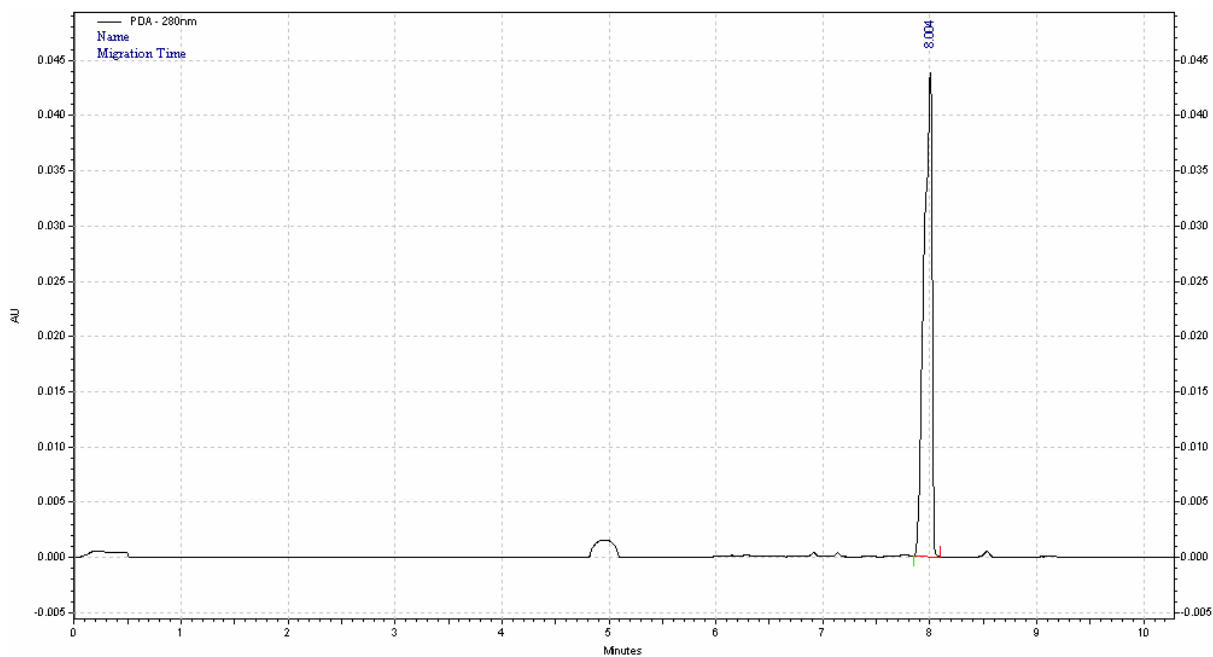
5.7.2.1 pABN-mannose



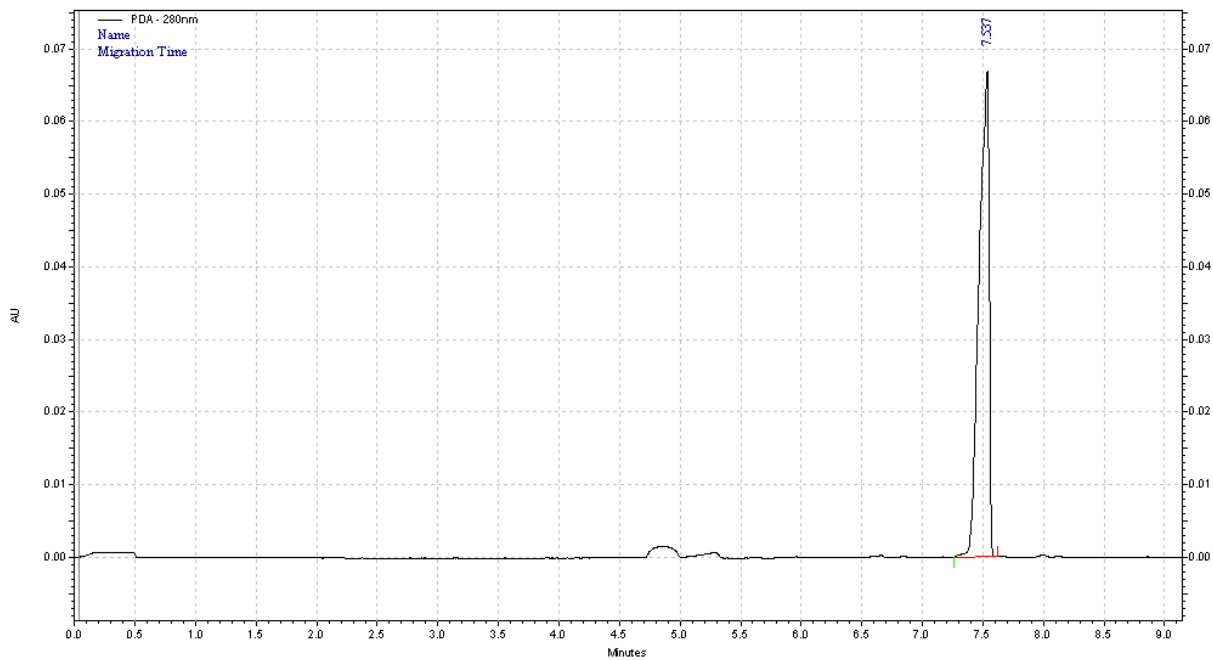
5.7.2.2 pABN-galactose

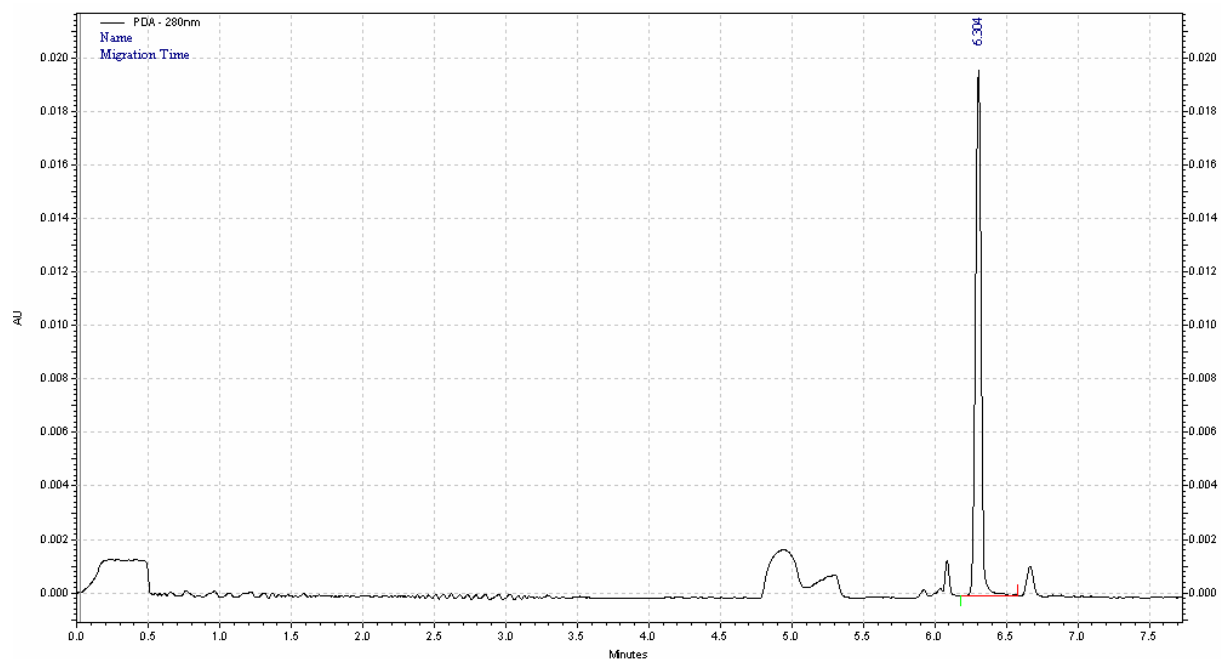


5.7.2.3 *pABN-glucose*



5.7.2.4 *pABN-N-acetyl-glucosamine*

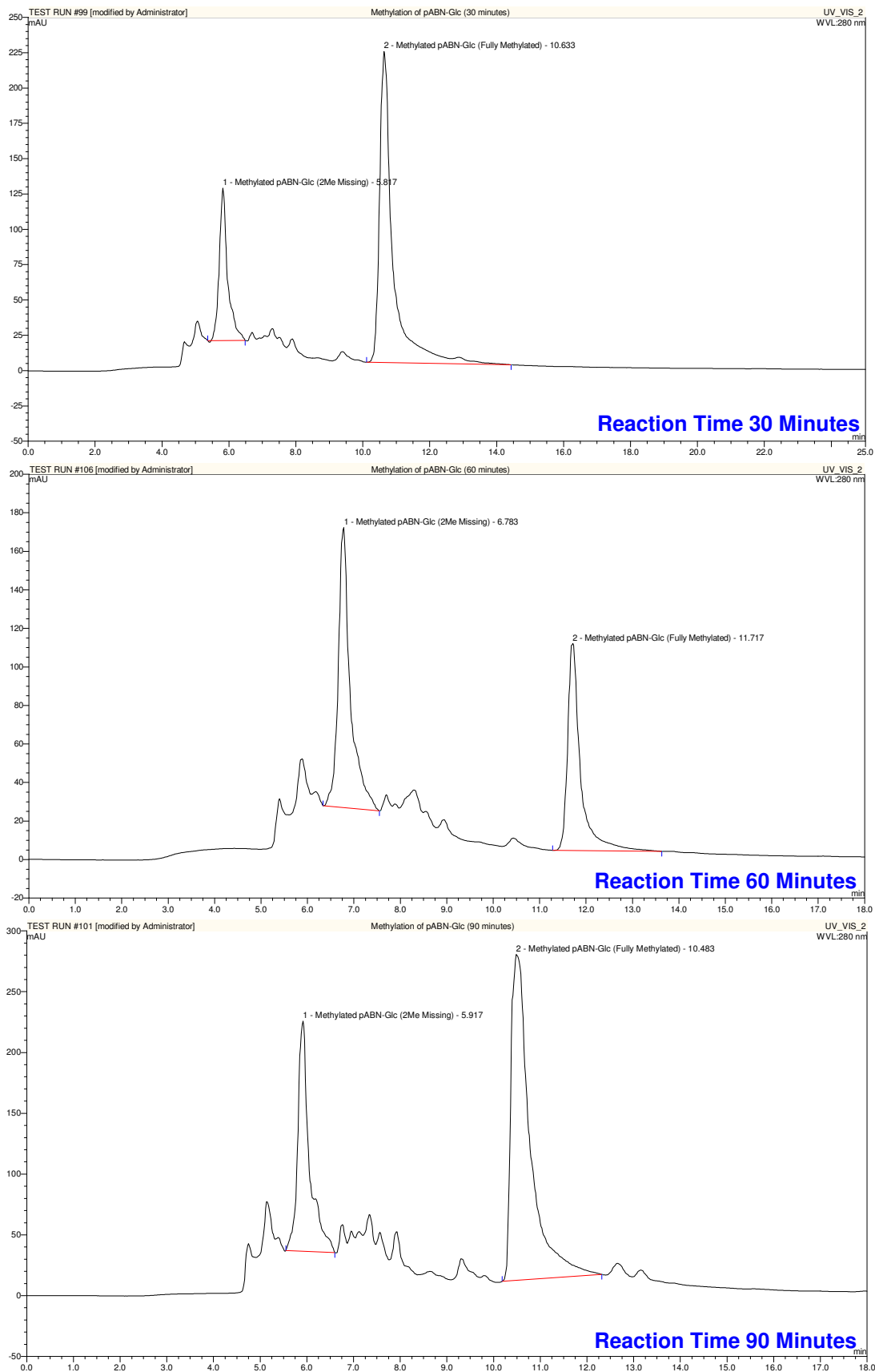


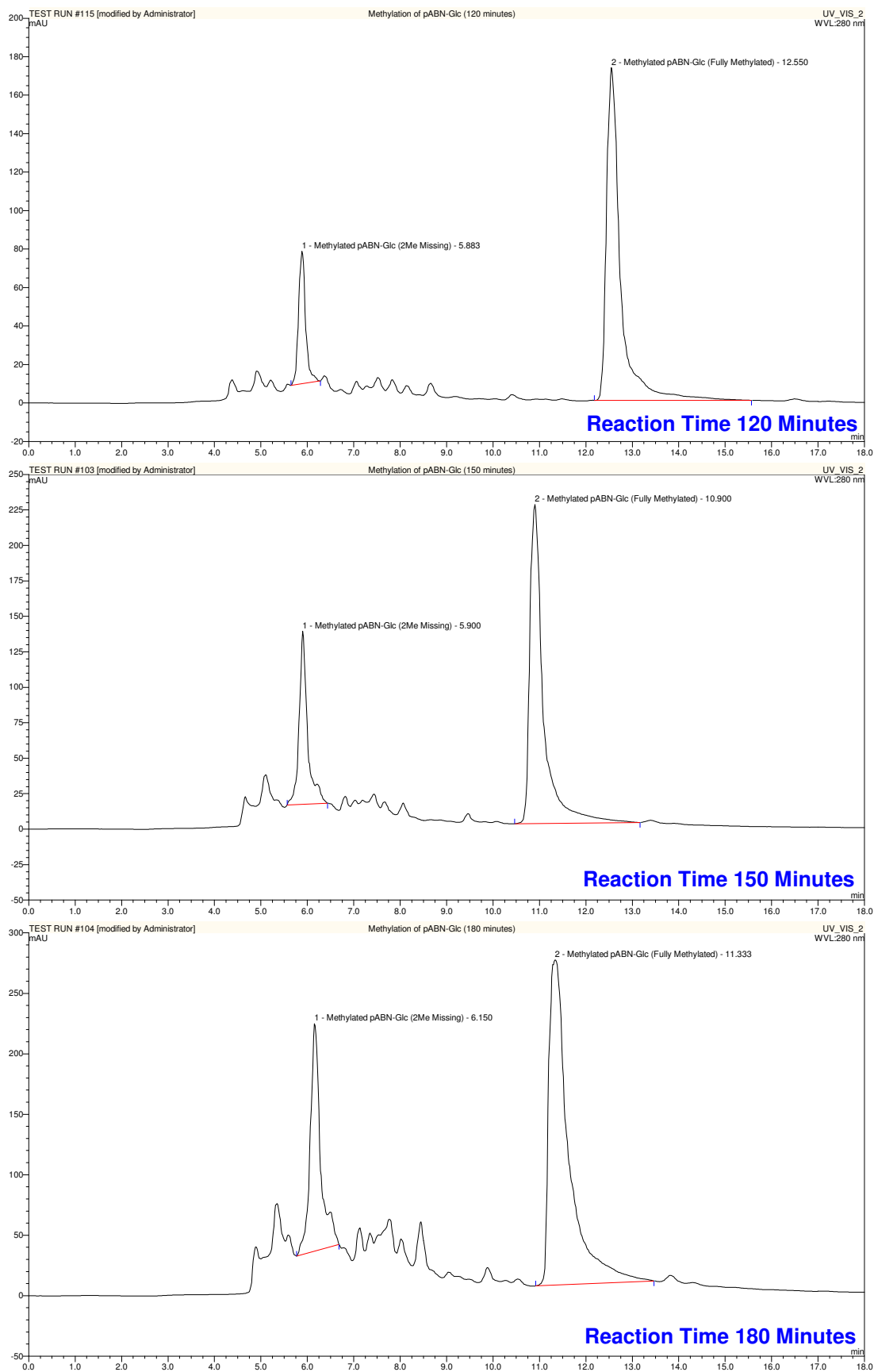
5.7.2.5 *p*ABN-glucosamine5.7.2.6 Peak Heights and Noise for CZE Analysis of *p*ABN-labelled Monosaccharides

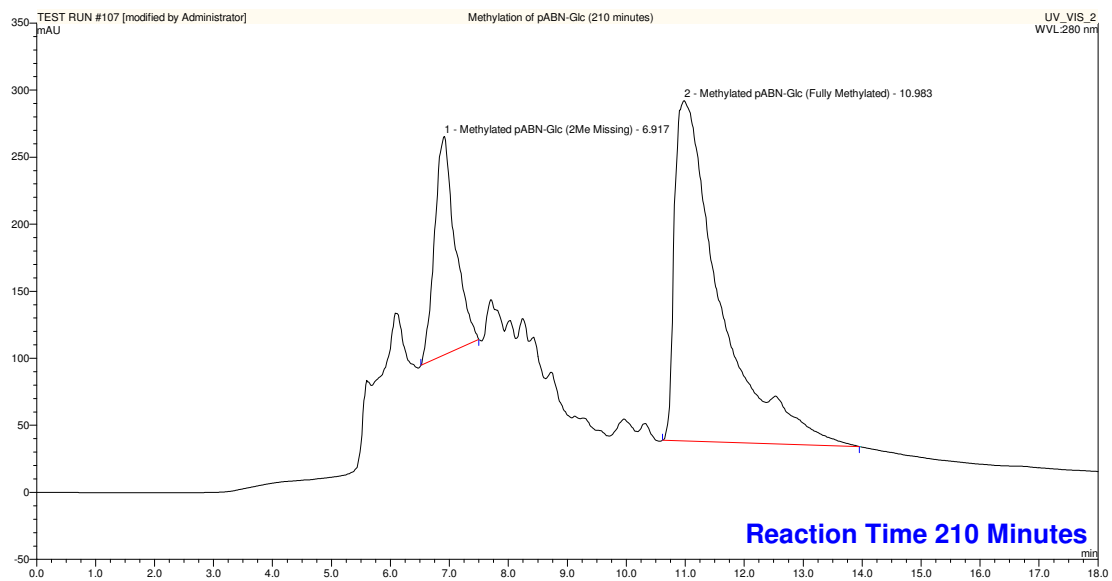
pABN-labelled Monosaccharide (100 $\mu\text{g mL}^{-1}$)	Peak Height (<i>H</i>)	Background noise (<i>h</i>)	Signal to Noise Ratio
D-glucose	3362	41	164
D-galactose	4312	56	154
D-mannose	3888	48	162
D- <i>N</i> -acetyl-glucosamine	4002	58	138
D-glucosamine	2920	73	80

Average Results from the replicate injections

5.7.3 UV Chromatograms For Timed Methylation Reaction

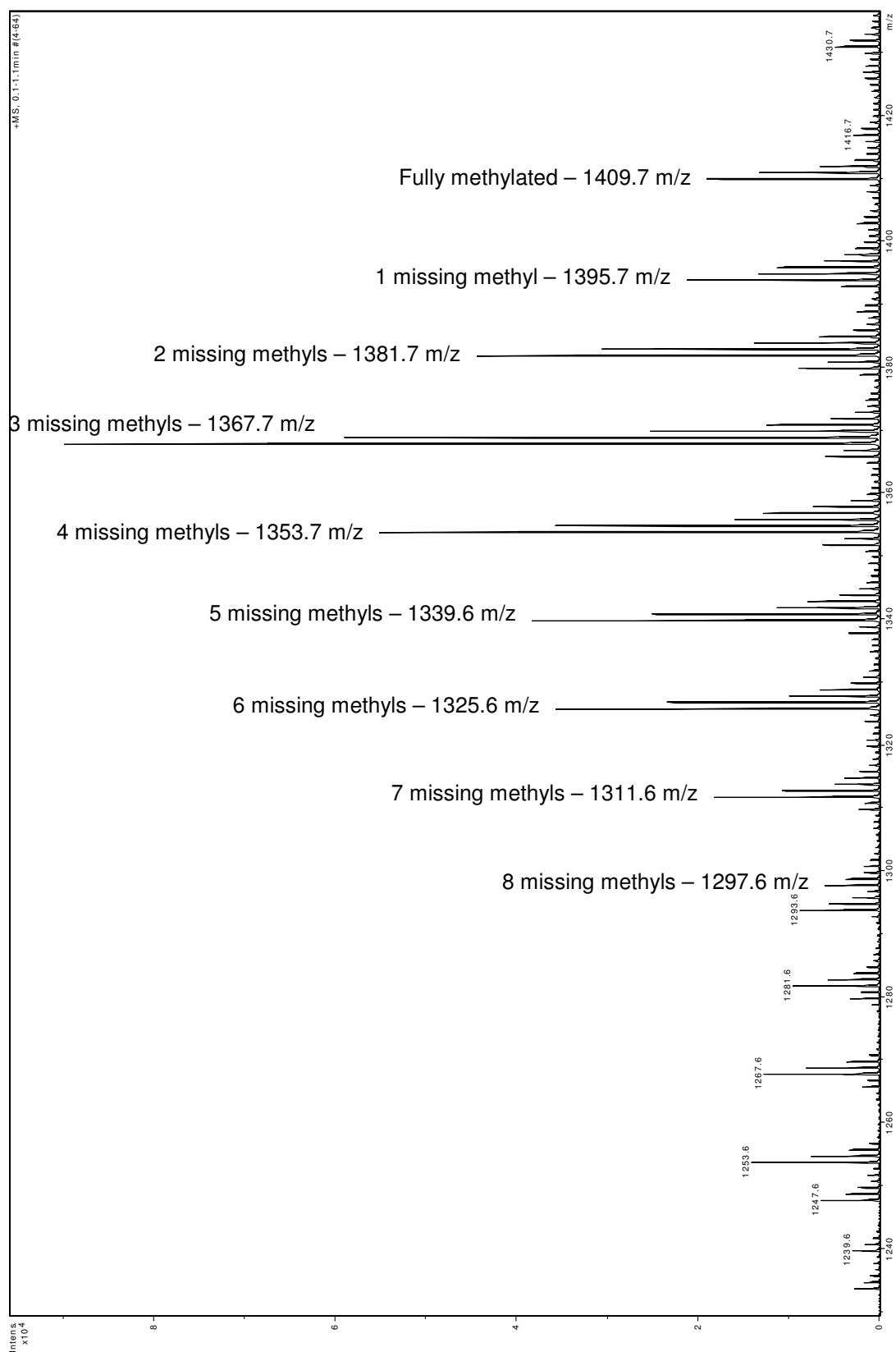


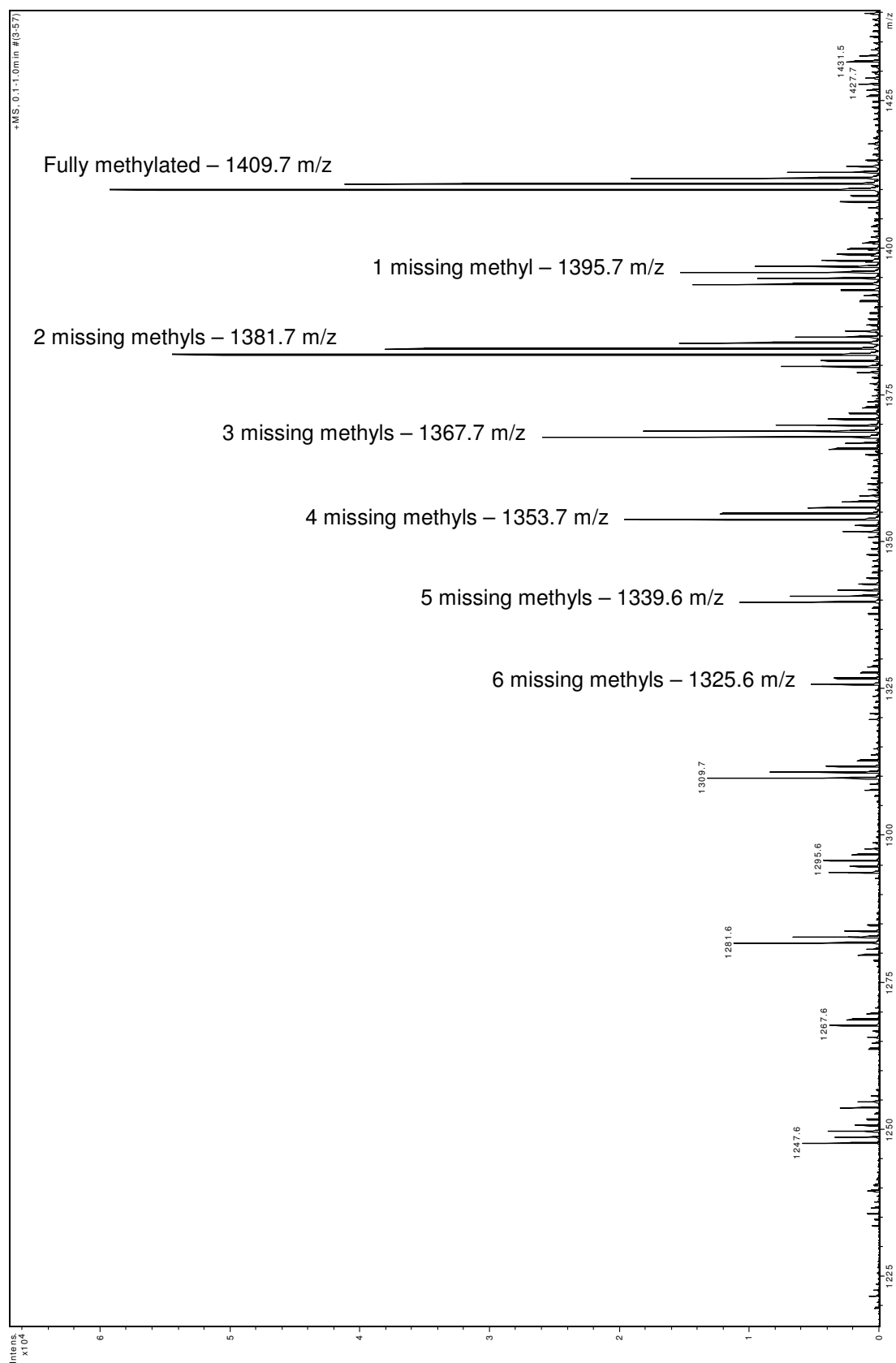


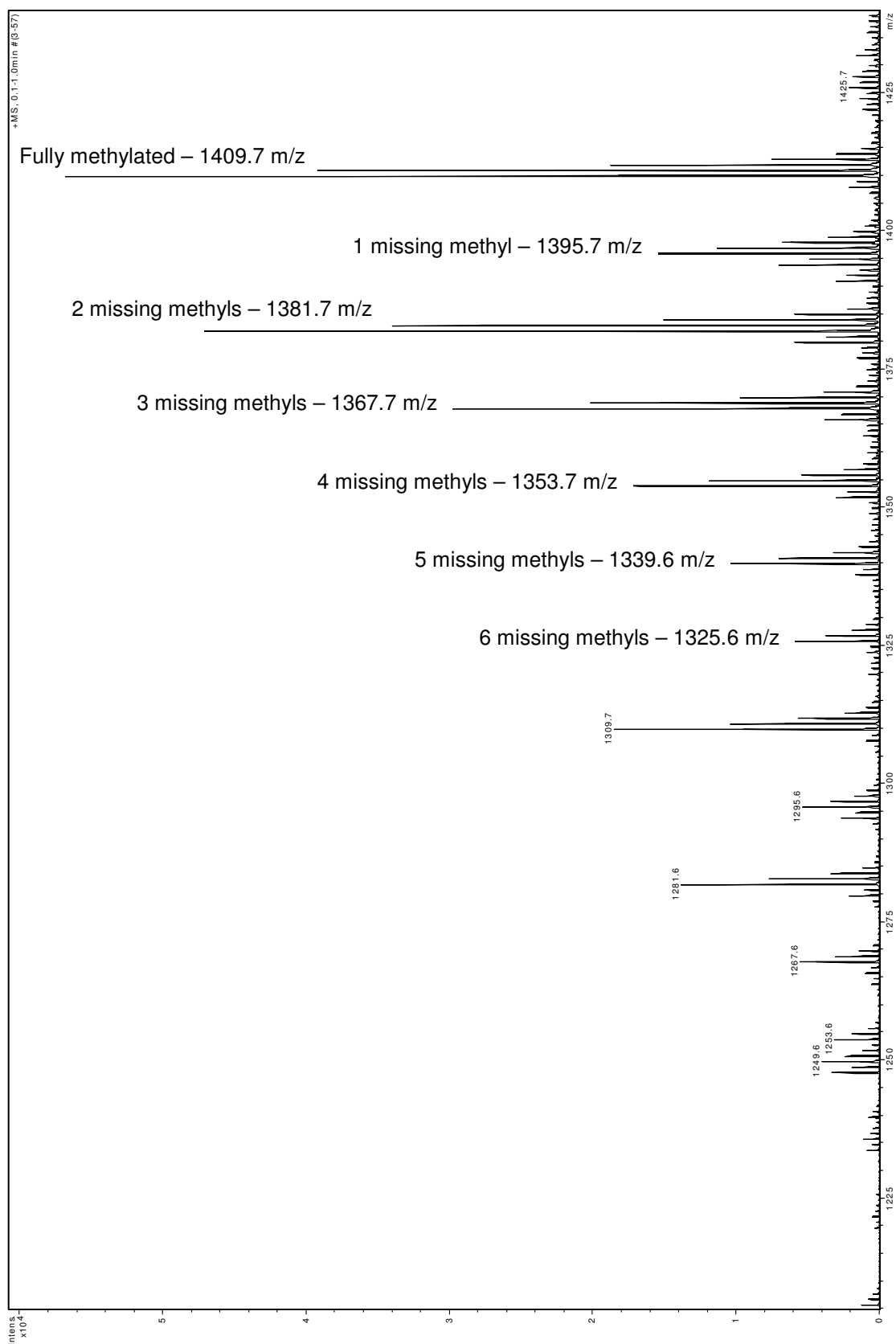


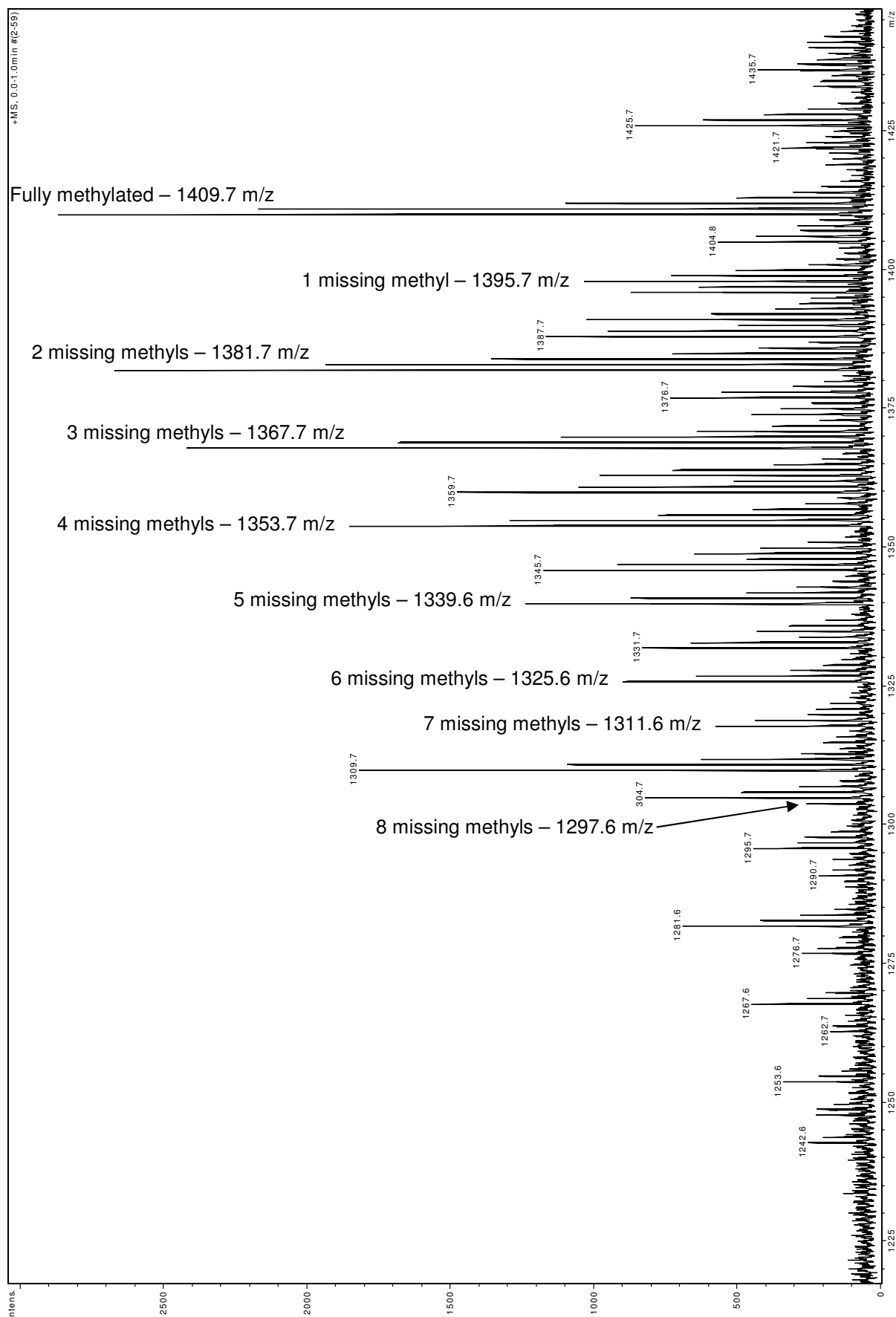
5.7.4 MS/MS Spectra – Optimising the Methylation of pABN-maltohexanose

5.7.4.1 Methylation using Methyl Iodide (60 μ l), Reaction Time 10 minutes



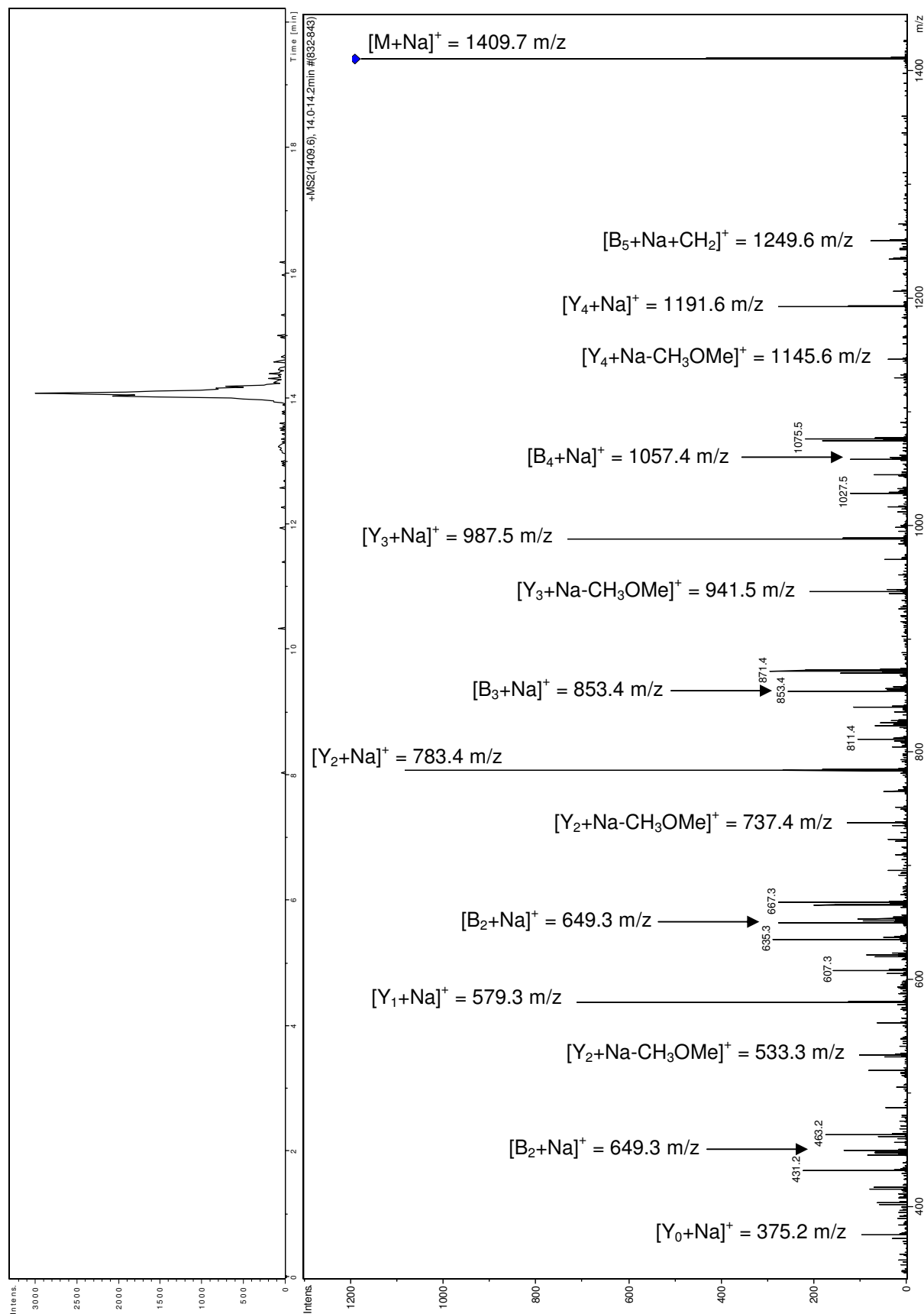
5.7.4.2 Methylation using Methyl Iodide (300 μ l), Reaction Time 20 minutes

5.7.4.3 Methylation using Methyl Iodide (300 μ l), Reaction Time 60 minutes

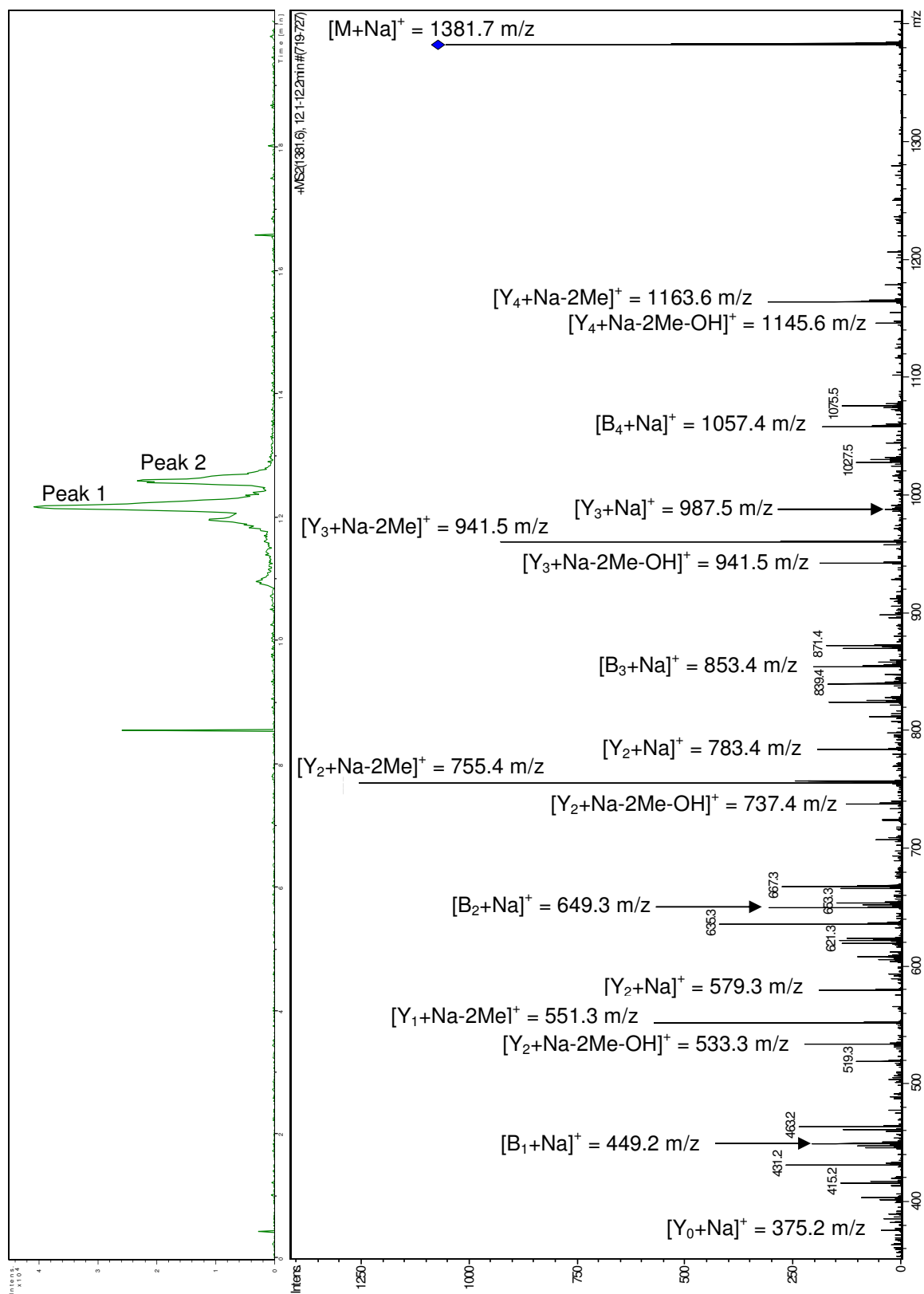
5.7.4.4 Methylation using Methyl Iodide (1000 μ l), Reaction Time 60 minutes

5.7.5 MS/MS Spectra – Analysis of Partially Methylated pABN-maltohexanose

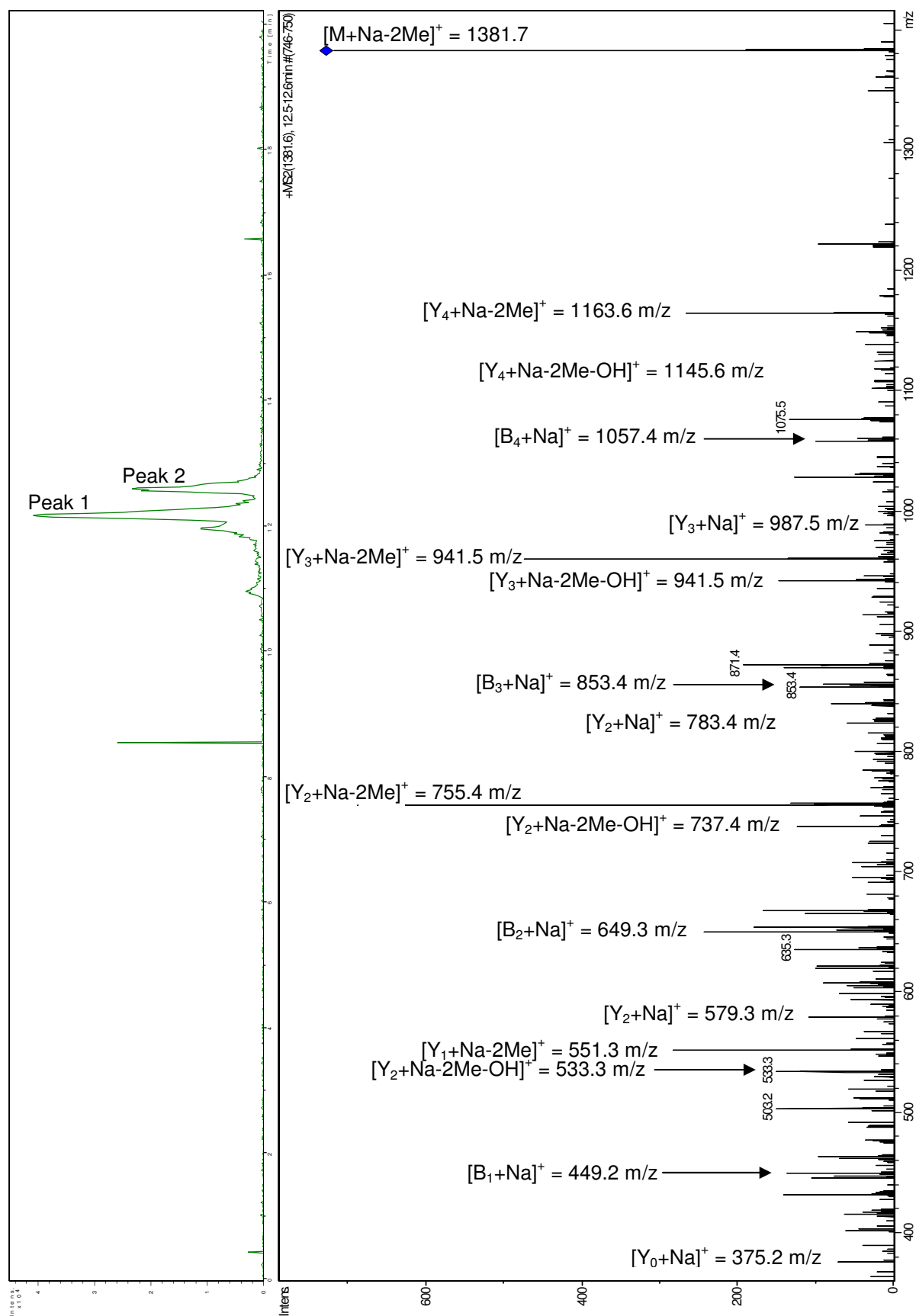
5.7.5.1 Fully Methylated pABN-maltohexanose – 1409.6 m/z



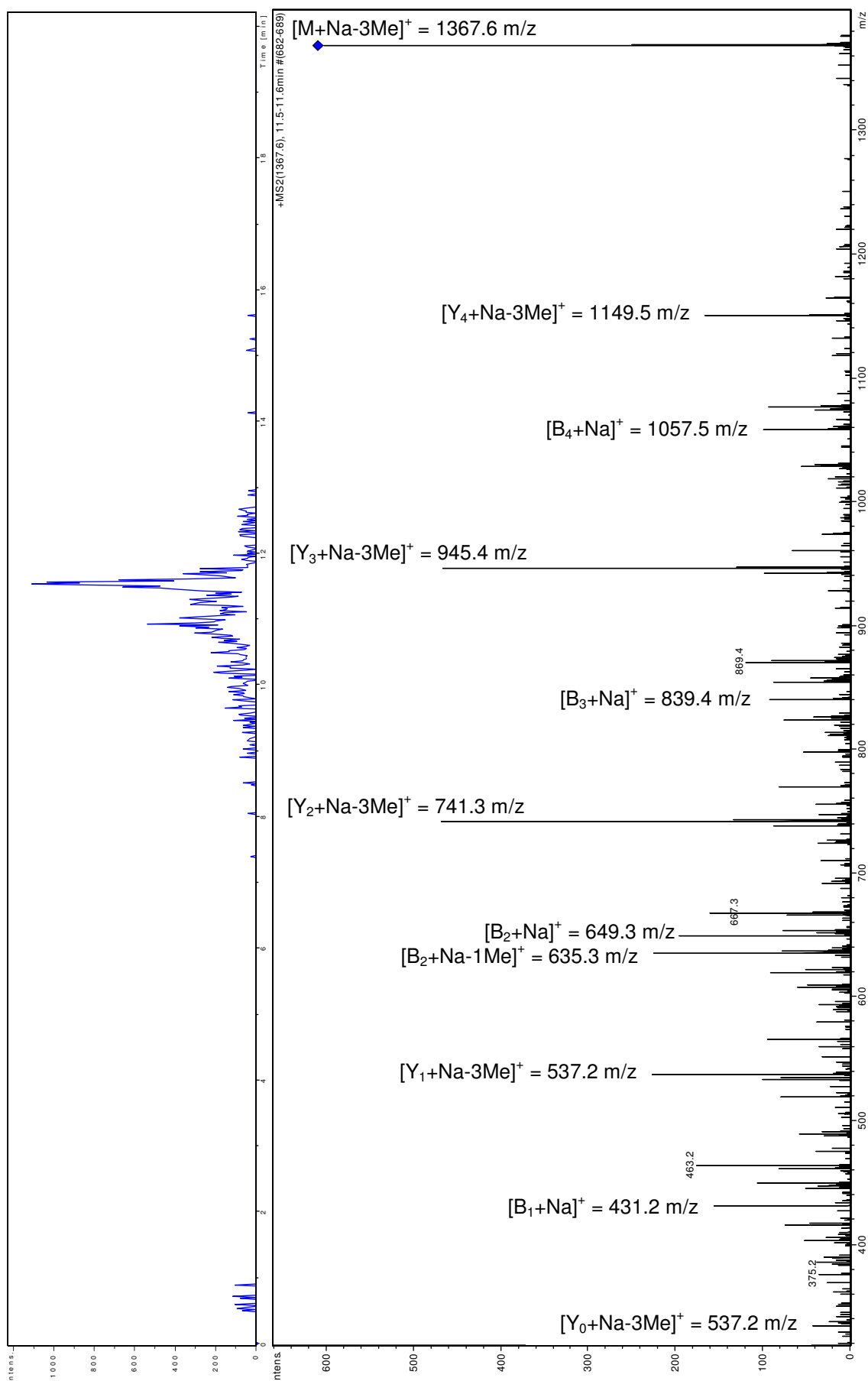
5.7.5.2 Partially Methylated pABN-maltohexanose – 1381.6 m/z (Peak 1)



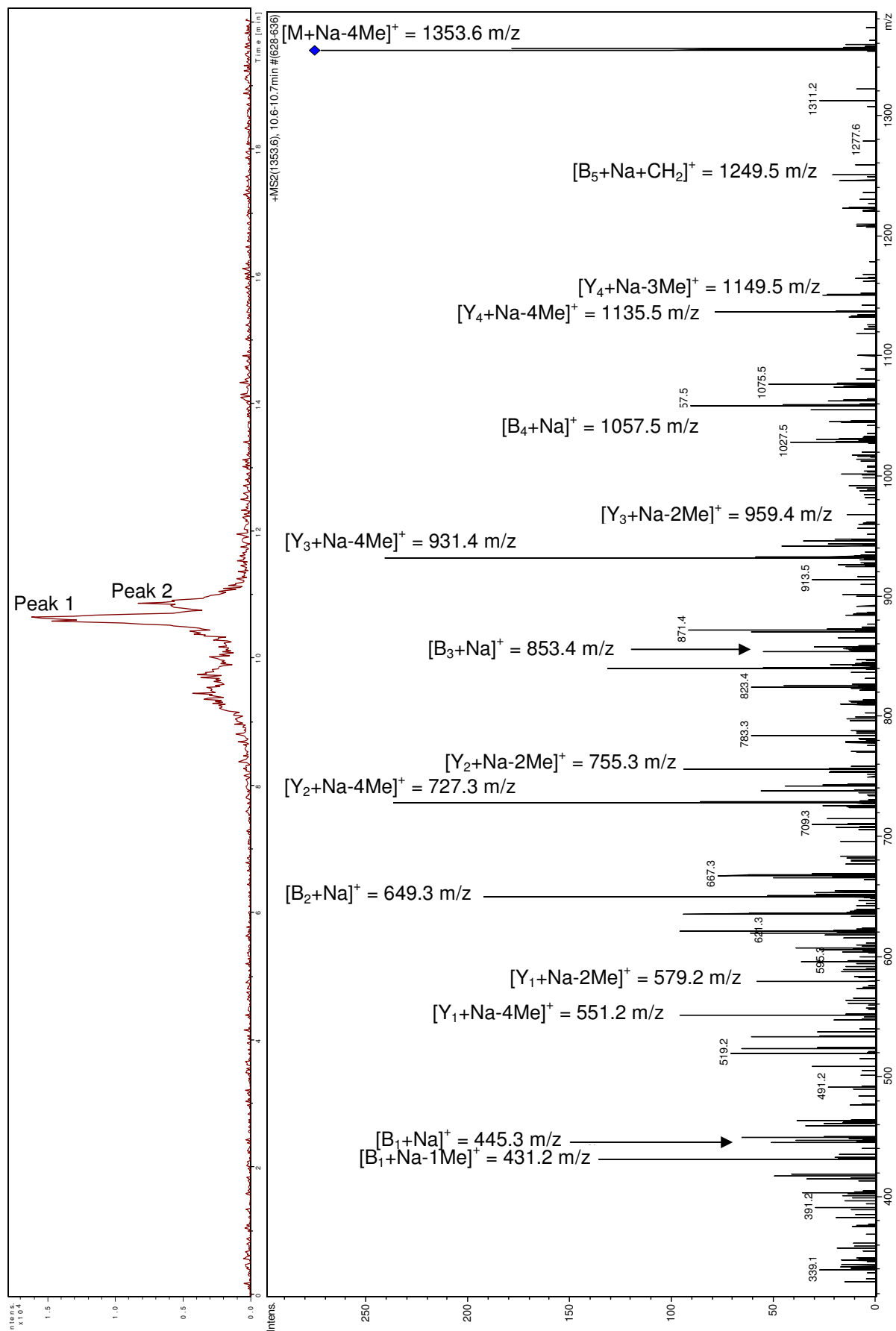
5.7.5.3 Partially Methylated pABN-maltohexanose – 1381.6 m/z (Peak 2)



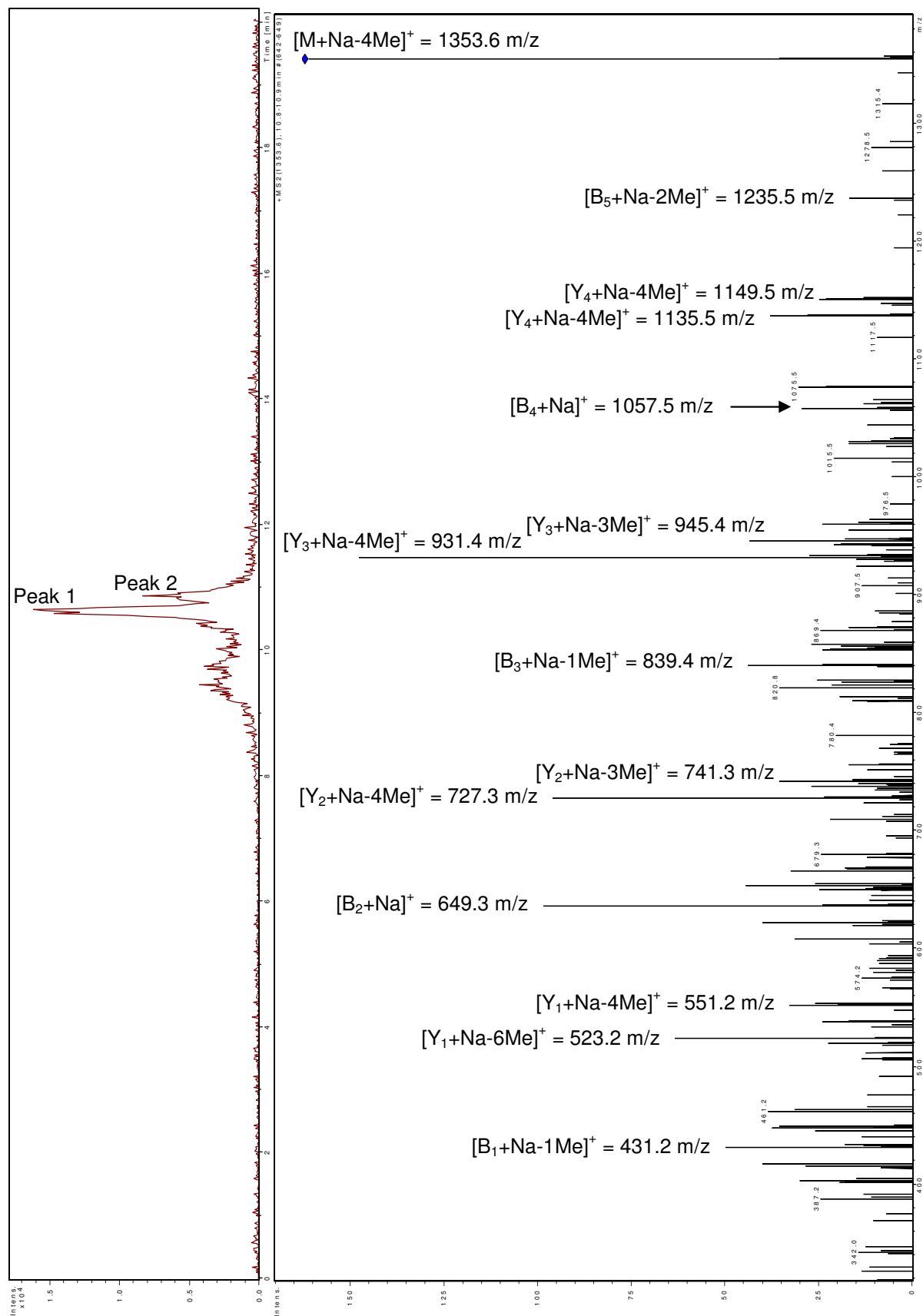
5.7.5.4 Partially Methylated pABN-maltohexanose – 1367.6 m/z



5.7.5.5 Partially Methylated pABN-maltohexanose – 1353.6 m/z (Peak 1)

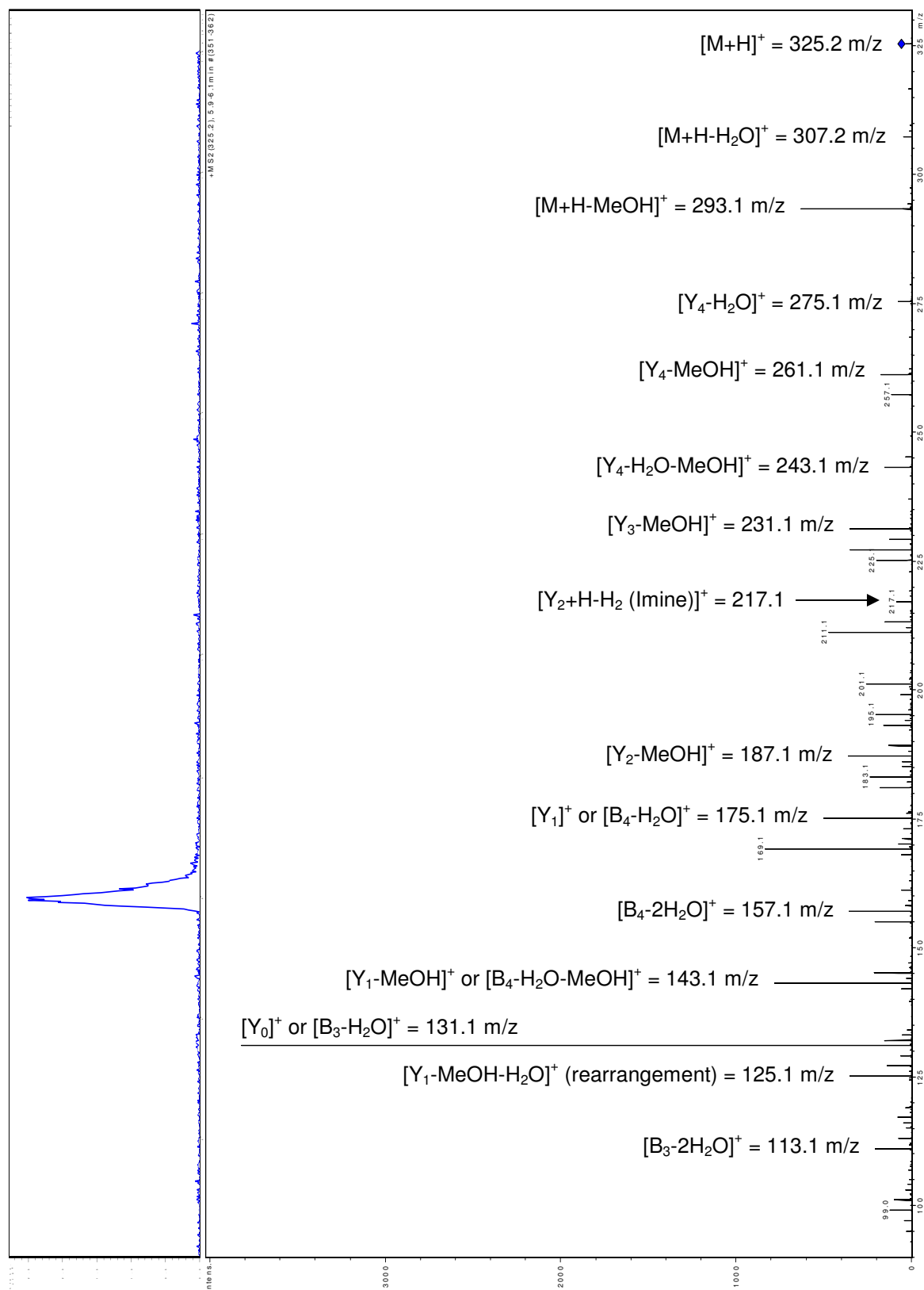


5.7.5.6 Partially Methylated pABN-maltohexanose – 1353.6 m/z (Peak 2)

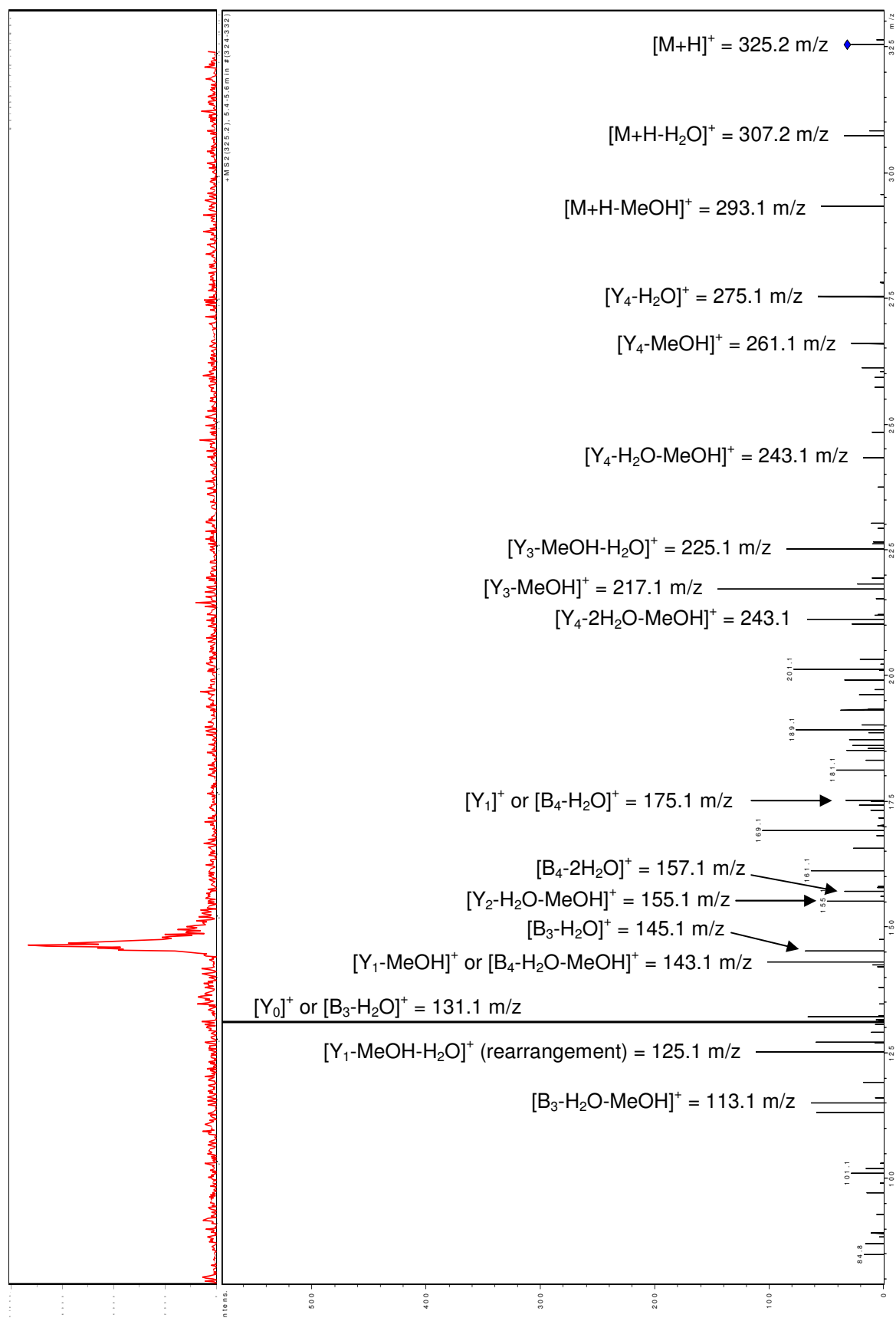


5.7.6 MS/MS Spectra – Linkage Analysis of Disaccharide Standards

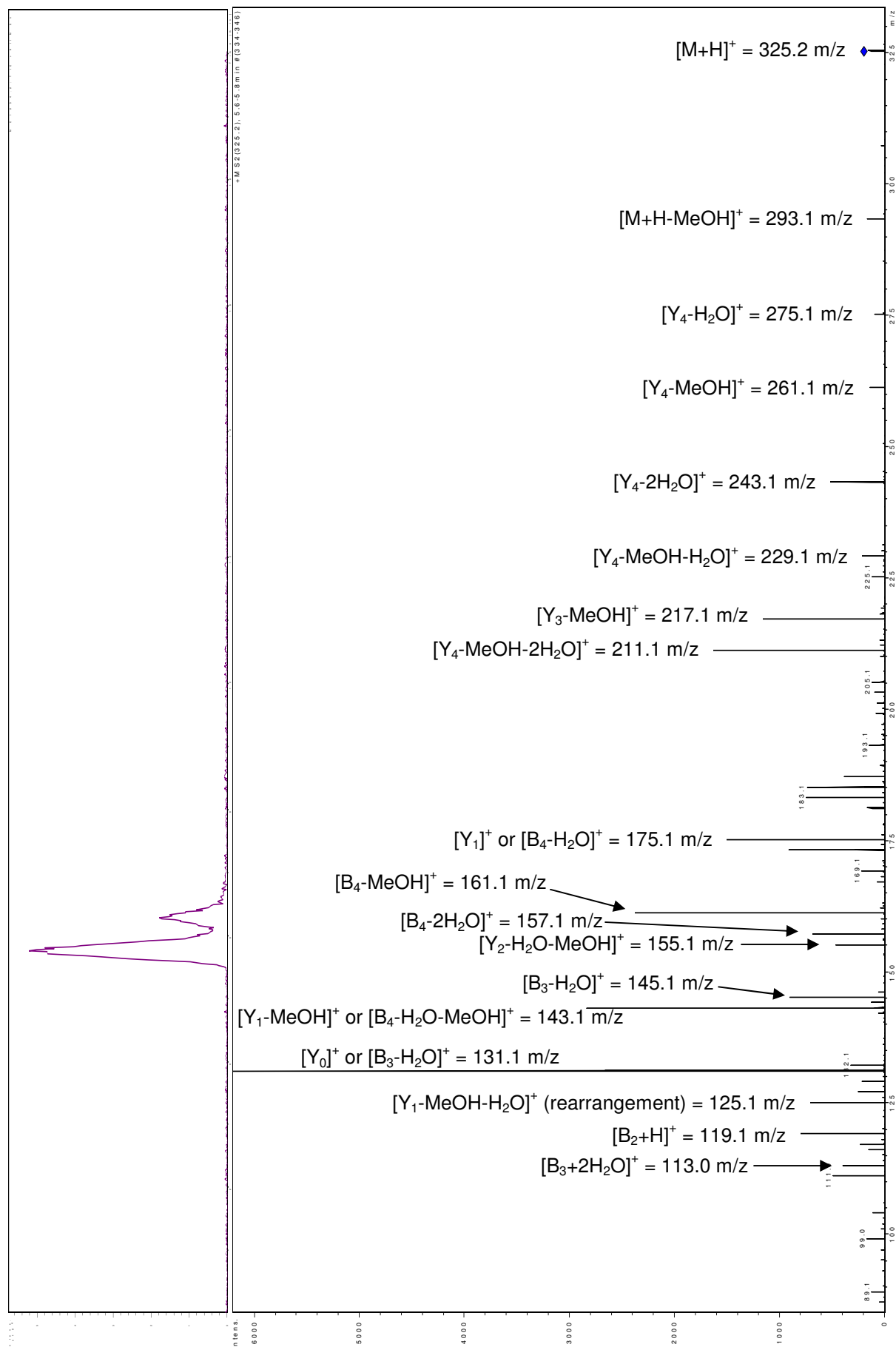
5.7.6.1 Gentibiose (1,6-linked)



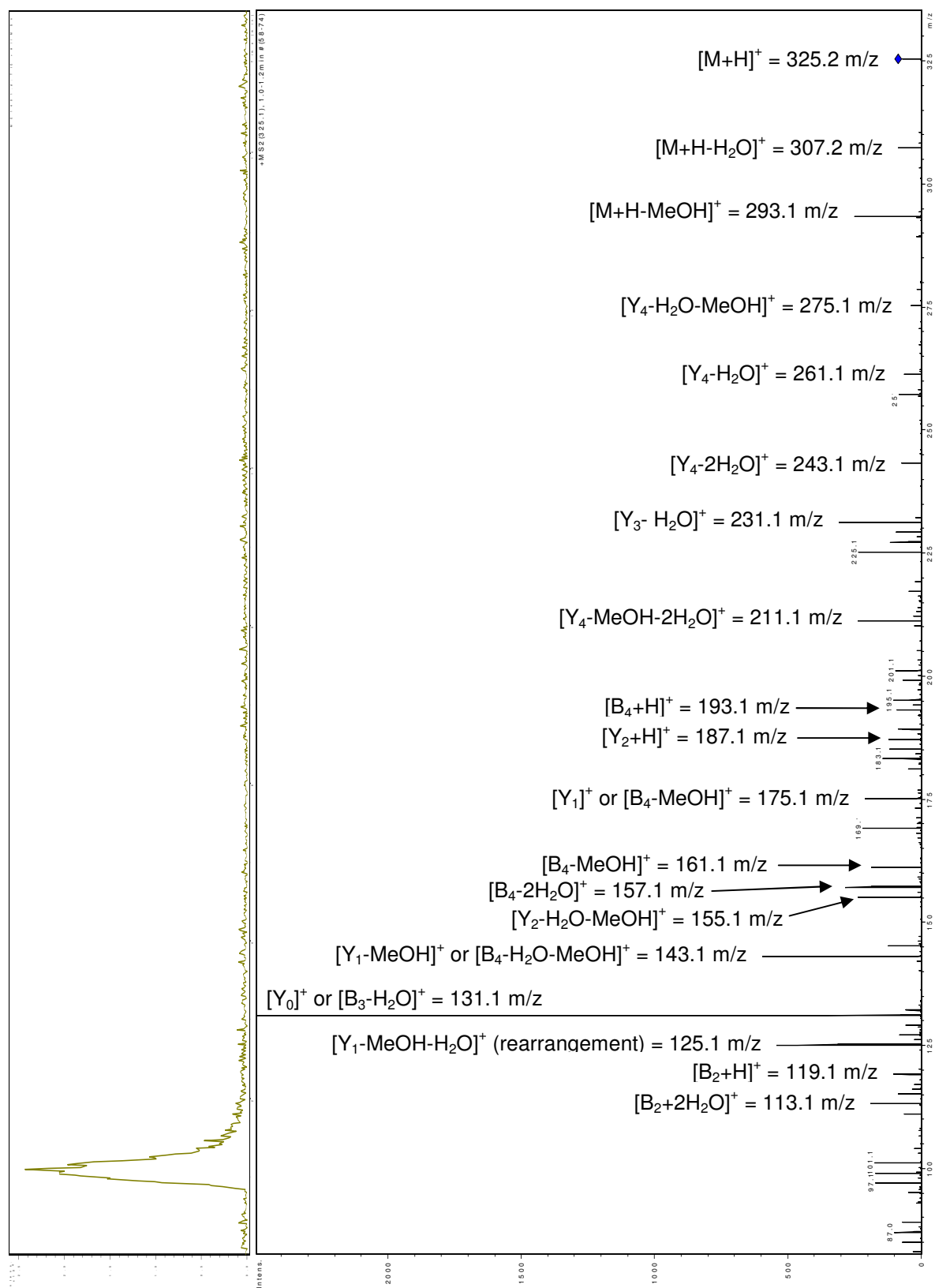
5.7.6.2 2-Mannobiose (1,2-Linked)



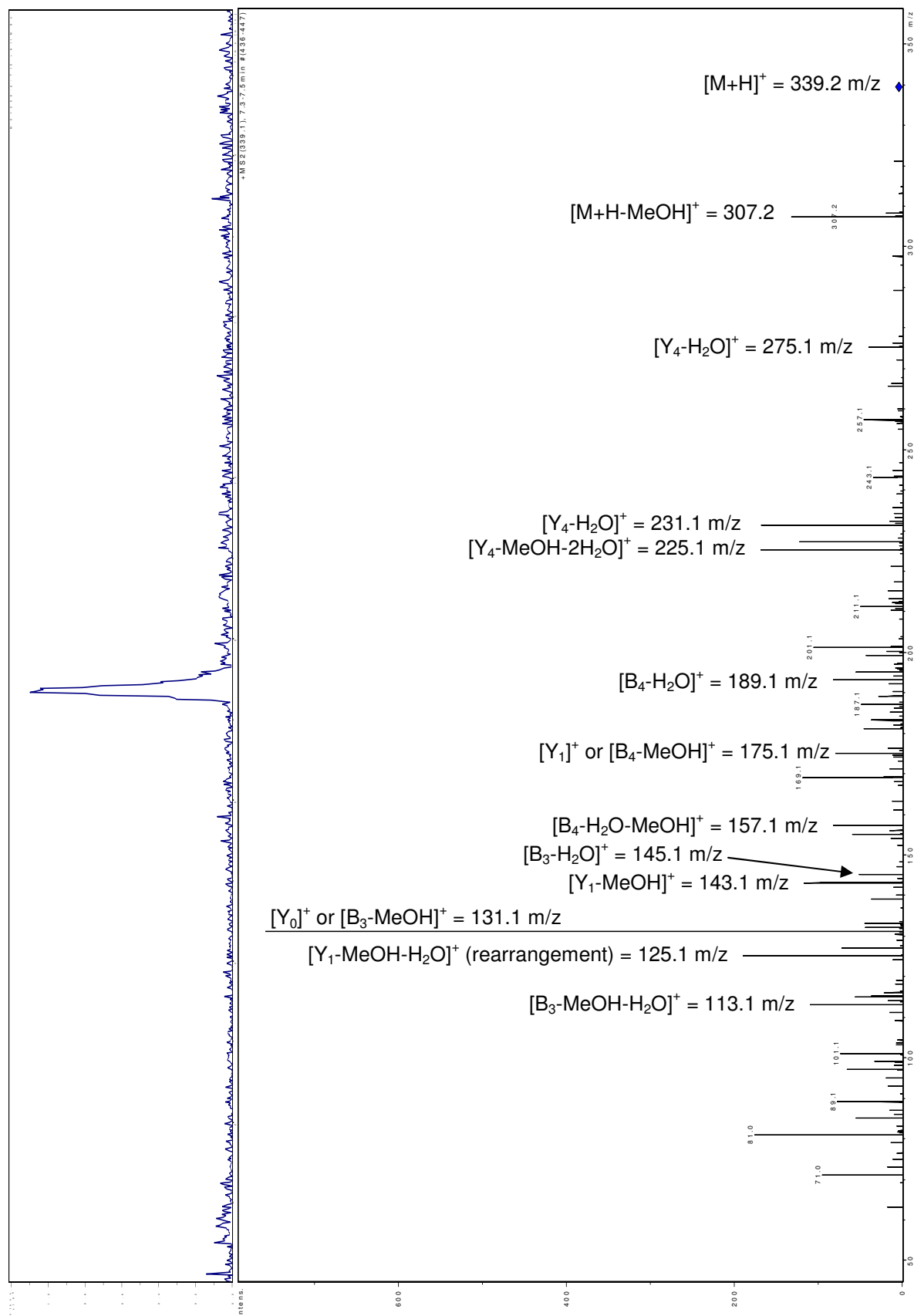
5.7.6.3 3-Galactobiose (1,3-Linked)



5.7.6.4 Cellobiose (1,4-Linked)



5.7.6.5 Trehalose (1,1-Linked)



5.7.7 Fragmentation Masses for *y*- and *b*- Series

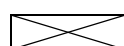
Terminal	$[M+H]^+$	Y_4	Y_3	Y_2	Y_1	Y_0	B_0	B_1	B_2	B_3	B_4
		339	293	263	219	175	131	45	75	119	163
-H ₂ O	321	275	245	201	157	113	27	57	101	145	189
-MeOH	307	261	231	187	143	99	13	43	87	131	175
-H ₂ O+MeOH	289	243	213	169	125	81	5	25	69	113	157
-2H ₂ O	303	257	227	183	139	95	9	39	83	127	171

1,2 - Linked	$[M+H]^+$	Y_4	Y_3	Y_2	Y_1	Y_0	B_0	B_1	B_2	B_3	B_4
		325	279	249	205	161	131	45	75	119	163
-H ₂ O	307	261	231	187	143	113	27	57	101	145	175
-MeOH	293	247	217	173	129	99	13	43	87	131	161
-H ₂ O+MeOH	275	229	199	155	111	81	5	25	69	113	143
-2H ₂ O	289	243	213	169	125	95	9	39	83	127	157

1,3 - Linked	$[M+H]^+$	Y_4	Y_3	Y_2	Y_1	Y_0	B_0	B_1	B_2	B_3	B_4
		325	279	249	205	175	131	45	75	119	149
-H ₂ O	307	261	231	187	157	113	27	57	101	131	175
-MeOH	293	247	217	173	143	99	13	43	87	117	161
-H ₂ O+MeOH	275	229	199	155	125	81	5	25	69	99	143
-2H ₂ O	289	243	213	169	139	95	9	39	83	113	157

1,4 - Linked	$[M+H]^+$	Y_4	Y_3	Y_2	Y_1	Y_0	B_0	B_1	B_2	B_3	B_4
		325	279	249	219	175	131	45	75	105	149
-H ₂ O	307	261	231	201	157	113	27	57	87	131	175
-MeOH	293	247	217	187	143	99	13	43	73	117	161
-H ₂ O+MeOH	275	229	199	169	125	81	5	25	55	99	143
-2H ₂ O	289	243	213	183	139	95	9	39	69	113	157

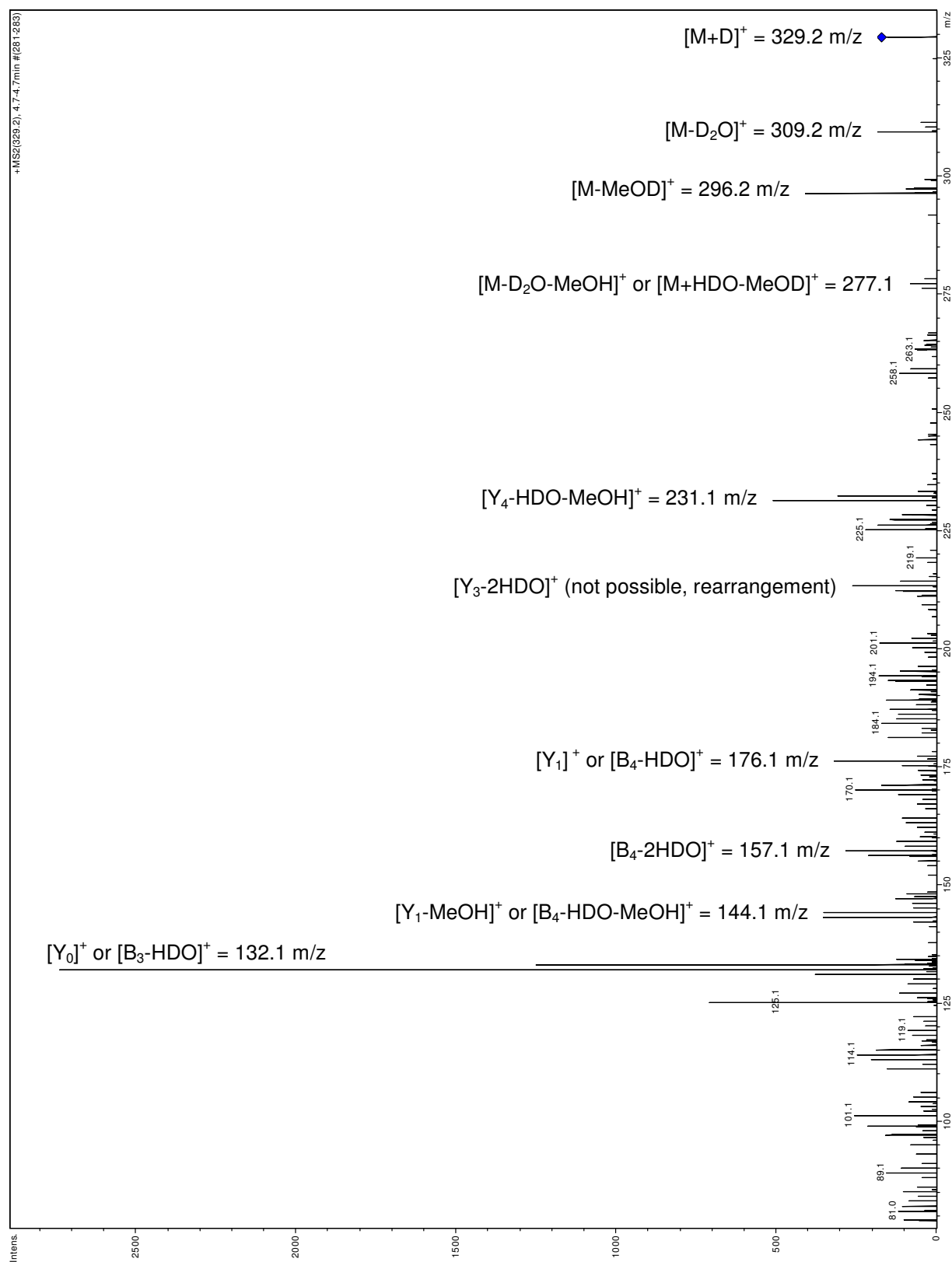
1,6 - Linked	$[M+H]^+$	Y_4	Y_3	Y_2	Y_1	Y_0	B_0	B_1	B_2	B_3	B_4
		325	293	263	219	175	131	31	61	105	149
-H ₂ O	307	275	245	201	157	113	13	43	87	131	175
-MeOH	293	261	231	187	143	99	1	29	73	117	161
-H ₂ O+MeOH	275	243	213	169	125	81	19	11	55	99	143
-2H ₂ O	289	257	227	183	139	95	5	25	69	113	157



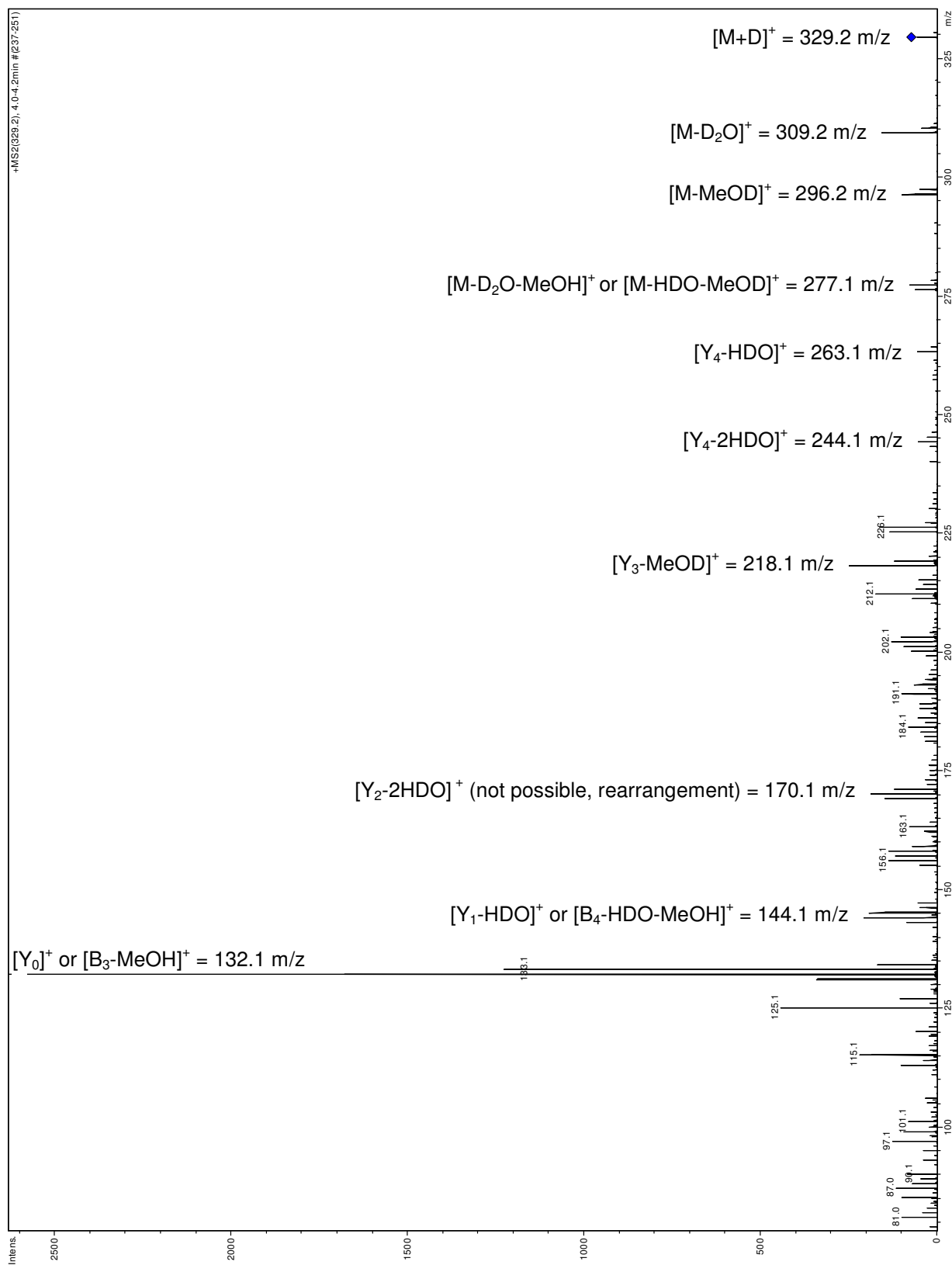
Fragment ion not possible

5.7.8 MS/MS Spectra – Linkage Analysis of Deuterated Disaccharide Standards

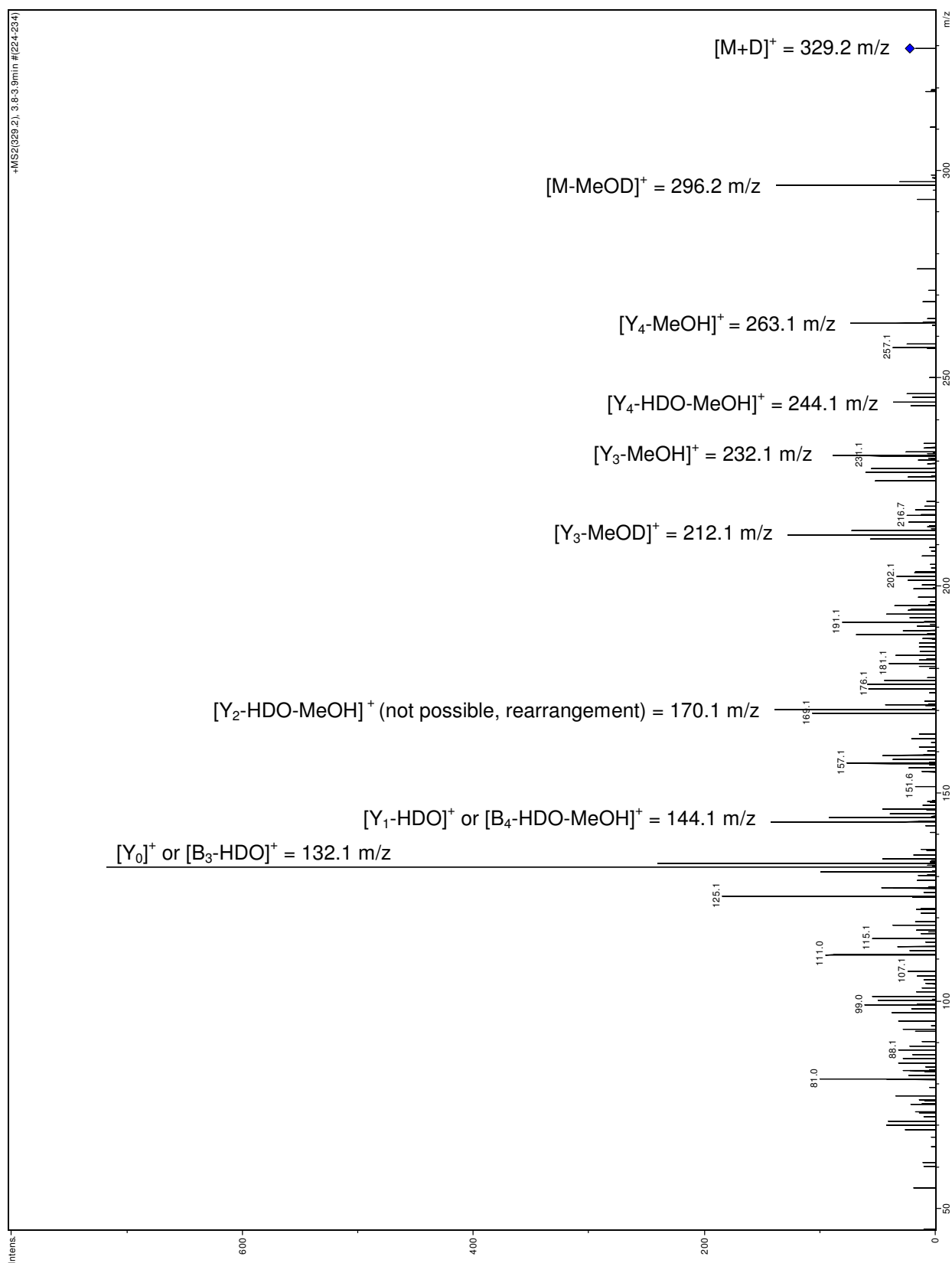
5.7.8.1 Deuterated Cellobiose (1,4-Linked)



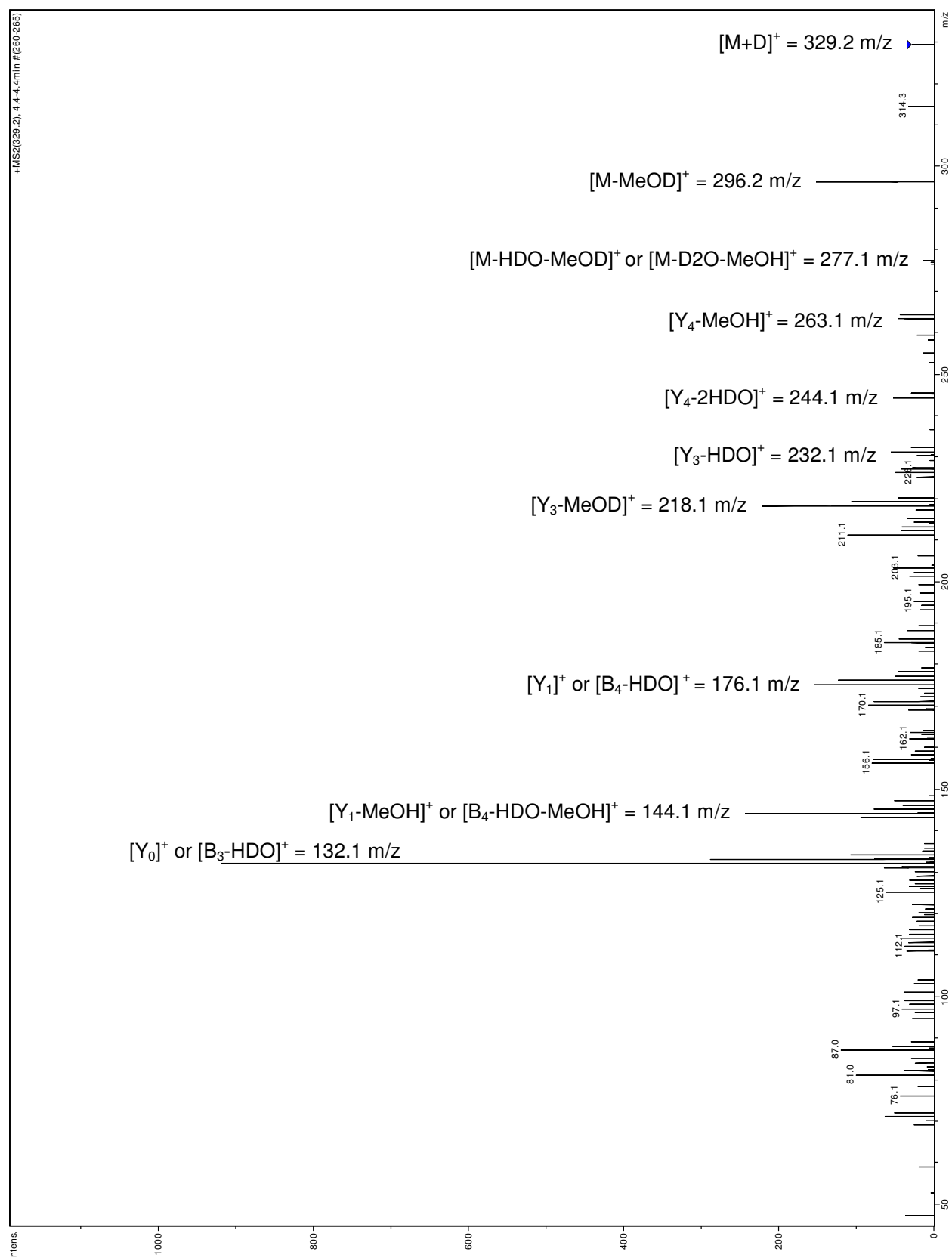
5.7.8.2 Deuterated 2-mannobiose (1,2-Linked)



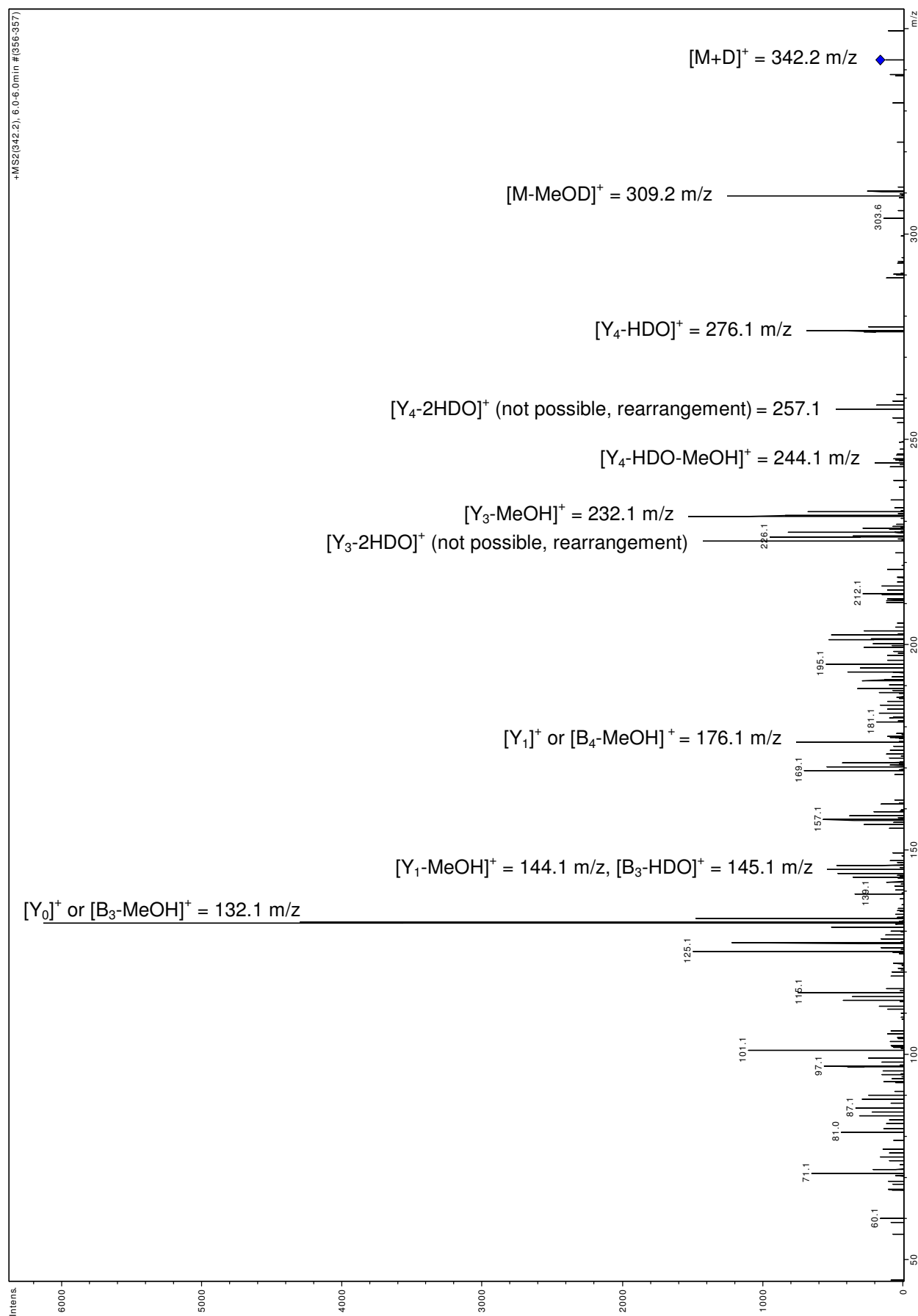
5.7.8.3 Deuterated Gentibiose (1,6-Linked)

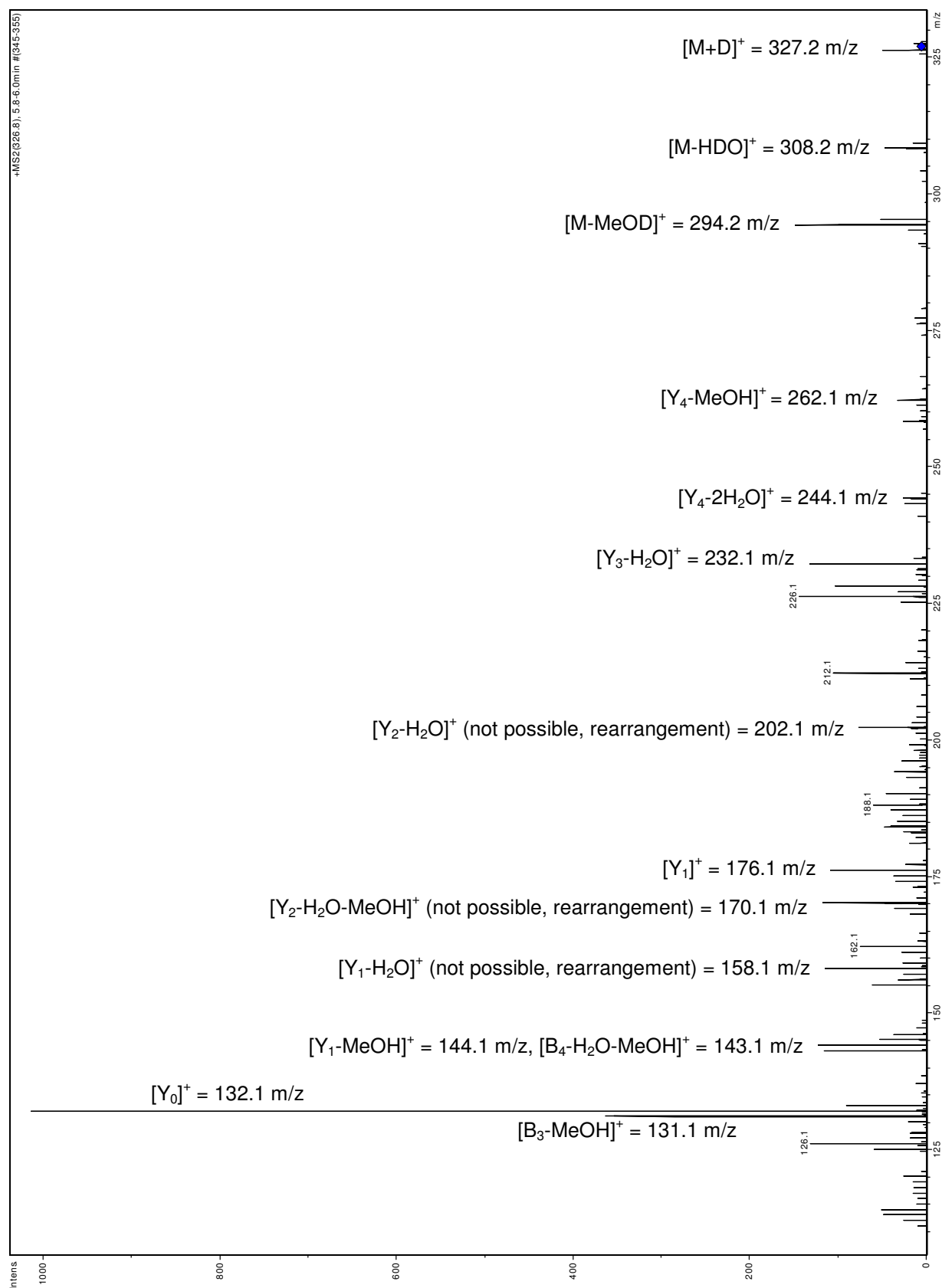


5.7.8.4 Deuterated 3-Galactobiose (1,3-Linked)



5.7.8.5 Deuterated Trehalose (1,1-Linked Terminal)



5.7.9 MS/MS Spectrum of Cellobiose (1,4-Linked) using Sodium Cyanoborodeuteride

6. CONCLUSIONS

6.1 Production and Characterisation of Exopolysaccharides

Two LAB cultures, *Lactobacillus acidophilus* 5e2 and *Lactobacillus helveticus* Rosyjski were inoculated to milk and grown as the milk was fermented. The EPS produced by the cultures was isolated and purified using a technique developed at the University of Huddersfield to provide a solid white residue which was soft in texture. The solids content from the batches of *Lactobacillus acidophilus* 5e2 fermented for 24 – 27 hours at 37 °C was between 124 – 133 mg L⁻¹, increasing to 281 mg L⁻¹ when fermented for 46 hours at 42 °C. Only one batch of *Lactobacillus helveticus* Rosyjski was grown providing a solid content of 237 mg L⁻¹ after 46 hours fermentation. The composition of the solid residue recovered differed slightly from batch to batch but contained approximately 80 % carbohydrate, <2 % protein and <0.8 % DNA. The remaining portion was not identified but was assumed to consist of moisture and inorganic material. Using an adapted ultra-filtration method, the critical solubility of the crude EPS produced by *Lactobacillus acidophilus* 5e2 was shown to be 1800 µg mL⁻¹ for batch Xn358.

The structure of a novel exopolysaccharide produced by *Lactobacillus acidophilus* 5e2 has been fully characterised and published in Carbohydrate Research (Laws *et al.*, 2008)¹⁷⁷. The monosaccharide analysis showed that the repeating oligosaccharide structure consisted of three D-glucose units, three D-galactose units and one D-N-acetylglucosamine units, which were confirmed by inspection of the anomeric region of the ¹H-NMR. Linkage analysis by GC-MS showed that there were two terminal, four di-linked and two tri-linked monosaccharides, confirming that the repeating oligosaccharide contains a monosaccharide branch and a disaccharide branch. Data from the 2D-NMR experiments confirmed these linkages and showed which monosaccharides were linked to each other in the repeating unit of the EPS. Further 2D-NMR experiments are required to determine the structure for the

EPS produced by *Lactobacillus helveticus* Rosyjski. The structural evaluation of this EPS is expected to be completed in the near future.

The M_w of the EPS produced by *Lactobacillus acidophilus* 5e2 was determined using HP-SEC-MALLS. To provide a more accurate determination of M_w a specific refractive index increment (dn/dc) value was required for the EPS. A value of 0.198 mL g^{-1} was determined and used in all subsequent calculation of the M_w for the EPS.

The HP-SEC-MALLS system was evaluated using a pullulan standard (800,000 M_w) of known M_w and polydispersity. The system gave the correct M_w , with a RSD of 0.2 %. The M_w results for the EPS produced by *Lactobacillus acidophilus* 5e2 were batch dependent, differing due to the fermentation conditions used. Longer fermentation produced EPS with larger M_w , this was studied further using prolonged fermentations, where samples were removed periodically throughout the milk fermentation. The EPS was isolated from each time point and the yield and M_w determined. The timed fermentation results, interestingly, showed a significant increase in M_w during the first 24 hours of fermentation, which was followed by the M_w remaining approximately constant until 54 hours. The M_w then started to decrease until the fermentation was stopped after 72 hours. Until the M_w began to decrease the increase in M_w of EPS closely matched the increase in EPS yield, this suggests that the overall number of polysaccharide chains within the system has not significantly changed over this period. The increased rate of polymerisation of the EPS was not matched by a corresponding increase in the rate of cleavage of the polymer from its lipid carrier. Prolonged stirring of the system resulted in a slow fall in the average molecular weight, and the reason for this is not fully understood. Cell lysis may release glycosylhydrolases able to digest the EPS or the EPS could be susceptible to hydrodynamic shear from stirring in the vessel. The increase in viable counts between 6 and 15 hours indicates that approximately four new generations of bacteria are produced. However, since the number of new

polysaccharide chains has not increased significantly over the same period, this suggests that de-novo EPS synthesis has been switched off.

6.1.1 Future Work

Further work related to these studies could include completing the structural determination of the EPS produced by *Lactobacillus helveticus* Rosyjski. Further 2D-NMR experiments are required to deduce the structure.

A measurement of the viscosity of the growth media throughout the fermentation process would prove very informative. There have been many publications supporting the notion that EPS production increases the viscosity of the fermented milk. For a future study, the viscosity measurement could be taken of the milk media at each time point. The viscosity of the media and the M_w measurements of the EPS could then be related to viscosity data generated for EPS of different M_w reported in this thesis. This type of viscosity analysis could be added to the testing regime for all future fermentations.

Other timed fermentations designed to indicate the measurement of M_w as a function of time could be carried out on different LAB cultures, e.g. *Lactobacillus helveticus* Rosyjski. However this could be problematic for this particular culture, because the EPS has poor solubility which was observed when attempting the NMR and HP-SEC-MALLS analysis.

6.2 Depolymerisation of Exopolysaccharides

Further analysis of the EPS produced by *Lactobacillus acidophilus* 5e2 was required to understand how the M_w of EPS influences the physical properties when in aqueous solutions. Physical and chemical depolymerisation techniques were used to reduce the chain length of the EPS produced by *Lactobacillus acidophilus* 5e2. Two physical techniques: constant pressure disruption (application of hydrodynamic shear) and ultrasonic disruption were used, along with a chemical technique, acid-catalysed hydrolysis.

Constant pressure disruption is a technique which uses pressure to force an aqueous sample through a narrow orifice, exerting hydrodynamic shear on the sample. The results using constant pressure disruption showed that this technique could reduce the molecular weight of EPSs in a controlled manner by altering the pressure applied. There was an exponential relationship between the pressure and the decrease in M_w of the EPS. As the M_w of the EPS decreased, the polydispersity remained constant, maintaining a narrow distribution of molecular weight, implying that the polysaccharide chain was breaking in a non-random manner. Further experiments using solvents with different viscosities to dissolve the EPS were carried out. The results suggested that solvents with greater viscosity exert a larger hydrodynamic shear on the EPS, hence breaking it faster and to a greater extent. Due to the physical nature of this depolymerisation technique, a limiting value was found at which point no further depolymerisation was possible. This value was approximately 15000 g mol^{-1} , for the EPS produced by *Lactobacillus acidophilus* 5e2.

Ultrasonic disruption was the next technique used to depolymerise the EPS produced by *Lactobacillus acidophilus* 5e2. This technique features a phenomenon referred to as 'cavitation', which creates millions of shockwaves in the liquid, the cumulative effect of which causes extremely high levels of energy to be released into the liquid, generating shear and thermal stresses. The results of this technique also showed that the EPS was being broken down over time in a controlled manner. Larger amplitudes provided greater depolymerisation. As with constant cell disruption, the polydispersity of the EPS showed no significant changes throughout the ultrasonic process, again suggesting that the polysaccharide chain was being cleaved in a controlled manner. This depolymerisation technique also had a limiting value, which was found to be approximately 16000 g mol^{-1} .

A study of the variation of the viscosity of aqueous solution of the EPS produced by *Lactobacillus acidophilus* 5e2 was undertaken to measure the approximate intrinsic viscosity relative to the M_w of the EPS. Solutions of EPS were sonicated for different times to

produce different M_w . The approximate intrinsic viscosities were determined using an Ostwald glass capillary viscometer at 20 ± 1 °C. The EPS produced by *Lb. acidophilus* 5e2 had an intrinsic viscosity of approximately $0.6 - 2.0$ dL g⁻¹ over the M_w range of $1.59 \times 10^5 - 4.78 \times 10^5$ g mol⁻¹, which was relatively low when compared to that of other polysaccharides that had been reported, such as xanthan or pectin. Application of the Mark–Houwink–Kuhn–Sakurada equation suggested that the chain geometry for the EPS produced by *Lb. acidophilus* 5e2 is semi-coil, but it must be taken into account that this value has been calculated from approximate intrinsic viscosity values.

It is also possible to use mild acid-catalysed hydrolysis as a depolymerisation technique. This process uses the application of a chemical reaction to break glycosidic linkages between monosaccharides on the polysaccharide chain. Using mild conditions, TFA (0.2 M) at 30 °C, the EPS produced by *Lactobacillus acidophilus* 5e2 was depolymerised. The results showed controlled depolymerisation of the EPS, the concentration vs time profile for the hydrolysis reaction was first order. The ¹H-NMR results of the acid hydrolysed EPS sample showed that the chemical reaction was changing the structure of the repeating oligosaccharide unit, probably by removing the *N*-acetyl group from *N*-acetyl glucosamine. Also, certain glycosidic linkages may have been preferentially hydrolysed compared to others. Both of these events would cause a shift in the signals that were seen in the anomeric region of the ¹H-NMR spectrum.

The depolymerisation techniques explored have been shown to be beneficial in terms of polysaccharide analysis. The controlled manner in which the EPS was depolymerised makes the techniques suited to a wide range of applications. The drawbacks of these methods are that limiting values of depolymerisation were found using the physical techniques and chemical modifications were observed when using acid-catalysed hydrolysis.

6.2.1 Future Work

Further work could investigate the use of mild acid-catalysed hydrolysis to depolymerise the exopolysaccharides to oligosaccharides and then, using LC-MS-MS, the structures could be determined to see if specific glycosidic linkages are breaking, or if the structure for the repeating unit can be obtained. In this report, a novel approach to oligosaccharide analysis is described which uses LC-MS-MS. With further development, this technique could eventually be used to determine the structure of intact repeating oligosaccharides of exopolysaccharides, making the analysis faster and more sensitive than methods currently available.

Further work could be carried out on the EPS produced by *Lactobacillus acidophilus* 5e2 using other depolymerisation techniques, such as enzymic and microwave assisted depolymerisation. It would have been interesting to compare results for these differing depolymerisation techniques, and suggest how they would suit different applications.

6.3 Novel Methods of Analysis

The final chapter of this work looked at novel methods for the analysis of EPS. EPSs have been structurally characterised in a similar fashion for many years, but these techniques are time consuming and lack sensitivity. The Carbohydrate community would benefit from novel approaches which implement more modern analytical techniques.

Carbohydrates, in particular neutral carbohydrates, are difficult to detect at low levels due to their lack of a chromophore and formal charge. A derivatisation technique was applied to rectify this problem and improve their detection. This was achieved by labelling the reducing end of a carbohydrate with p-aminobenzonitrile, using a reductive amination reaction. The derivatisation procedure was first trialled on simple monosaccharides. LC-MS and NMR were used to evaluate the completion of the reaction. The results showed that pABN was successfully used to derivatise a range of neutral monosaccharides. The mass spectrometer

conditions were optimised for the analysis of mono-, di- and oligosaccharides. The LC-MS-MS analysis of maltohexanose, a six unit oligosaccharide, showed that the B- and Y-ion series were observed, but the X- and A-ion series were not visible. Further work could be done on the ion-trap or MALDI-CID mass spectrometer, in particular increasing the fragmentation amplitude to cause the production of X- and A-ions to aid with the structural evaluation.

A method was developed utilising capillary zone electrophoresis to separate a range of monosaccharides common to EPSs produced by LAB. The monosaccharides were pABN-labelled and the separation was aided using a borate buffer system. The intended application of the method was in determining the monosaccharide composition of EPS samples. Initial results were encouraging; the composition of a published EPS produced by *Lactobacillus delbrueckii* subsp. *bulgaricus* NCFB2074 was confirmed by this method. A problem was encountered when analysing the EPS produced by *Lactobacillus acidophilus* 5e2, where the *N*-acetyl-glucosamine could not be detected. It was expected that the *N*-acetyl group would be removed by acid hydrolysis, which should have left a glucosamine residue. Neither the *N*-acetyl-glucosamine nor the glucosamine were detected. This problem could not be explained, despite further investigation. However this method has shown that the rapid analysis of EPSs is possible, cutting analysis time down from three days to one day.

Two methylation procedures were used in an attempt to achieve per-*O*-methylation of an EPS sample. Methods documented by Hakomori (1964) and Ciucanu and Kerek (1984) were used to methylate the hydroxyl groups on mono-, di- and oligosaccharides. The Hakomori procedure uses dimethylsulfinyl anion as a base, the free hydroxyl protons on the monosaccharide are removed and then methyl iodide is added to form methoxy- groups. Initial work, methylating pABN-glucose, showed that per-*O*-methylation was not occurring, providing a range of partially methylated species. This was confirmed by LC-MS and

analysis of deuterated products. An investigation into the methylation reaction of pABN-glucose showed that the ratio of fully methylated product to partially methylated product does not significantly improve over time. The yield of fully methylated product increased throughout, but so did that of the partially methylated species. Analysis of methylated pABN-maltohexanose also showed partial methylation, where the overall distribution had similarities to a Gaussian distribution, where the most intense ions occurred in the middle, which had 5, 6 and 7 missing methyl groups. LC-MS confirmed that the partial methylation was not caused by fragmentation of the per-O-methylated product. This method was not robust enough to be used for the analysis of EPS, therefore the Ciucanu and Kerek methylation procedure, which uses sodium hydroxide as the basic agent, was investigated.

The Ciucanu and Kerek method was shown to be superior, producing more per-O-methylated product. The procedure was optimised by altering the amounts of reagents and reaction time, but still incomplete methylation was observed. A study using LC-MS-MS attempted to locate the positions of the missing methyl groups. From the results generated, the free hydroxyls appeared to be distributed randomly.

Using the derivatisation processes described, a novel method for the linkage analysis of exopolysaccharides was developed. The method was trialled using a series of disaccharides, each with different glycosidic linkages (1,1-, 1,2-, 1,3-, 1,4- and 1,6-linked). Each disaccharide was first methylated and hydrolysed into two sugar residues, after labelling with pABN, one derivatised sugar residue corresponded to the terminal sugar and one derivatised sugar residue corresponded to a linked sugar and contained one extra hydroxyl group located at the linkage position. LC-MS-MS analysis was used to separate the sugar derivative, and to generate fragmentation patterns. Optimised MS conditions provided detailed fragmentation patterns, but the b- and y- ion series were not clearly observed, ions due to further reaction, such as losses of MeOH and H₂O were evident, and in great abundance. The loss of several MeOH / H₂O gave peaks that were identical for y_n and y_{n-1}

and further fragmentation reaction generated the b- and y- ions with equal m/z, making assignment of these ions difficult.

Deuterating the samples to aid identification of the b- and y- ions proved unsuccessful, and did not help deduce where each ion had originated. The use of sodium cyanoborodeuteride in the reductive amination reaction to increase the entire y- ion series by one m/z helped and showed that the majority of ions observed were due to the y- ion series, but could not prevent further fragmentation from occurring, which prevented the different linkage positions from being identified. Despite the proposed linkage analysis method proving unable to completely distinguish between the disaccharide standards, this procedure was used to probe the linkage patterns of maltohexanose. The fragmentation data was not examined, instead this investigation concentrated on peak retention times and peak areas.

The LC-MS method was capable of separating the 1,4-linked and terminal sugar residues, with peak area ratio of 5.2 : 1 (1,4-linked : terminal), which is close to the theoretical ratio of 5 : 1. From these encouraging results, the EPSs produced by both *Lactobacillus delbrueckii* subsp. *bulgaricus* NCFB2074 and *Lactobacillus acidophilus* 5e2 were examined using this methodology. The results were positive; peaks were detected for each differently linked sugar residue. The relative peak areas of each sugar residue were close to those expected for both EPS samples. Unfortunately, the *N*-acetyl-glucosamine monosaccharide residue was not observed either as *N*-acetyl-glucosamine or glucosamine. This was probably due to the similar problems that were encountered using the CZE method, where it was suspected that *N*-acetyl-glucosamine was destroyed during acid hydrolysis. Basic comparisons between the current GC-MS method and the proposed LC-MS method show that there are improvements in both sensitivity and analysis times when using the LC-MS method. However, as the method was not capable of providing unequivocal linkage analysis, a quantitative comparison between the methods was not possible.

6.3.1 Future Work

Further work is required to resolve the problem of detecting *N*-acetyl amino sugars by CZE for monosaccharide composition analysis. A similar problem was encountered for the linkage analysis by LC-MS, the peak for the *N*-acetyl amino sugars was not visible. It is likely that similar factors are preventing the detection of this peak in both methods, where the *N*-acetyl amino sugar is being broken down during the acid hydrolysis stage of the reaction. Further work could involve the analysis of *N*-acetyl-D-lactosamine, which comprises of a β -D-galactose-(1 \rightarrow 4)-*N*-acetyl-D-glucosamine. This simple disaccharide could be analysed by both procedures, to evaluate their feasibility and possibly determine which steps of the procedures are problematic. Work has been started, but so far has proved inconclusive.

Other future developments for linkage analysis by LC-MS should concentrate on preventing elimination reactions. This is essential if this method is to be used as the preferred technique for the linkage analysis of polysaccharides. One approach might be to use a different functional group to substitute the available hydroxyl hydrogens i.e. instead of using methyl groups. Benzoylation, ethylation, or acetylation, for example, could be used. Although, it is likely that similar, unwanted fragmentation of these groups would be seen. Methylation was used in this study because methyl groups are thought to be stable. Any derivatisation method chosen must be able to derivatise all available hydroxyl groups. Partial derivatisation only leads to complications when interpreting peaks in the LC-MS chromatograms.

Another approach could be to use a different type of mass spectrometer. There is a requirement for a mass spectrometer to provide conditions that can break the carbon-carbon backbone bonds, but leave the derivatised side groups unaltered. This may prove difficult based on their relative strengths. There is little difference between the bond energies of carbon-carbon bonds (348 kJ mol^{-1}) in comparison to the carbon-oxygen bonds (360 kJ mol^{-1}).

Although problems were encountered with these analytical approaches to the linkage analysis of polysaccharides, further work using the suggestions above, could provide the Carbohydrate Community with new, faster and more sensitive methods for the analysis of complex polysaccharides.

7. REFERENCES

1. Collins, P.; Ferrier, R. *John Wiley and Sons Ltd* **1995**.
2. Stick, R. V.; Williams, S. J., Eds. *Carbohydrates: The Essential Molecules of Life*, 2nd ed.; Elsevier Science, **2009**; Vol. Chapter 11 - Glycoproteins and Proteoglycans
3. Bhagavan, N. V., Ed. *Medical Biochemistry*, 4th ed.; Academic Press, **2002**; Vol. Chapter 10 - Heteropolysaccharides I: Glycoproteins and Glycolipids
4. Furukawa, K.; Tsuchida, A.; Furukawa, K., Eds. *Comprehensive Glycoscience*; Elsevier Science, **2007**; Vol. 3 - Biosynthesis of Glycolipids.
5. De Vuyst, L.; Degeest, B. *Fems Microbiology Reviews* **1999**, *23*, 153-177.
6. Fredrickson, J. K.; Zachara, J. M.; Balkwill, D. L.; Kennedy, D.; Li, S. M. W.; Kostandarites, H. M.; Daly, M. J.; Romine, M. F.; Brockman, F. J. *Applied and Environmental Microbiology* **2004**, *70*, 4230-4241.
7. Whitman, W. B.; Coleman, D. C.; Wiebe, W. J. *Proceedings of the National Academy of Sciences of the United States of America* **1998**, *95*, 6578-6583.
8. Ishige, T.; Honda, K.; Shimizu, S. *Current Opinion in Chemical Biology* **2005**, *9*, 174-180.
9. www.cehs.siu.edu/fix/medmicro/pix/walls.gif. **2009**
10. Gram, S. *Fortschritte der Medicin*. **1984**, *2*, 185-189.
11. Sears, C. L. *Anaerobe* **2005**, *11*, 247-251.
12. Fuller, R. *Journal of Applied Bacteriology* **1989**, *66*, 365-378.
13. Liu, S. Q. *International Journal of Food Microbiology* **2003**, *83*, 115-131.
14. Chandan, R. C., Ed. *Manufacturing Yogurt and Fermented Milks*, 1st ed.; Blackwell Publishing Ltd: Oxford, **2006**
15. Ludbrook, K. A.; Russell, C. M.; Greig, R. I. *Journal of Food Science* **1997**, *62*, 597-&.
16. Stephen, A. M., Ed. *Food Polysaccharides and their Application* 1st ed.; Marcel Dekker Inc.: New York, **1995**
17. Kim, H. S.; Gilliland, S. E. *Journal of Dairy Science* **1983**, *66*, 959-966.
18. Garcia-Ruiz, A.; Bartolome, B.; Martinez-Rodriguez, A. J.; Pueyo, E.; Martin-Alvarez, P. J.; Moreno-Arribas, M. V. *Food Control* **2008**, *19*, 835-841.
19. du Toit, M.; Franz, C.; Dicks, L. M. T.; Schillinger, U.; Haberer, P.; Warlies, B.; Ahrens, F.; Holzapfel, W. H. *International Journal of Food Microbiology* **1998**, *40*, 93-104.
20. Commane, D.; Hughes, R.; Shortt, C.; Rowland, I. *Mutation Research-Fundamental and Molecular Mechanisms of Mutagenesis* **2005**, *591*, 276-289.
21. Hosono, A.; Lee, J. W.; Ametani, A.; Natsume, M.; Hirayama, M.; Adachi, T.; Kaminogawa, S. *Bioscience Biotechnology and Biochemistry* **1997**, *61*, 312-316.
22. Kailasapathy, K.; Chin, J. *Immunology and Cell Biology* **2000**, *78*, 80-88.
23. Maeno, M.; Yamamoto, N.; Takano, T. *Journal of Dairy Science* **1996**, *79*, 1316-1321.
24. Cross, M. L.; Stevenson, L. M.; Gill, H. S. *International Immunopharmacology* **2001**, *1*, 891-901.
25. Merk, K.; Borelli, C.; Korting, H. C. *International Journal of Medical Microbiology* **2005**, *295*, 9-18.

26. Solga, S. F. *Medical Hypotheses* **2003**, *61*, 307-313.
27. Characklis, W. G.; Cooksey, K. E. *Advances in Applied Microbiology* **1983**, *29*, 93-138.
28. Sutherland, I. W. *Comprehensive Glycoscience* **2007**, *2*, 521-558.
29. Ruas-Madiedo, P.; Hugenholtz, J.; Zoon, P. *International Dairy Journal* **2002**, *12*, 163-171.
30. Tombs, M.; Harding, S. E., Eds. *An Introduction to Polysaccharide Biotechnology* 1st ed.; CRC Press Inc: UK, **1997**
31. Sandford, P. A.; Baird, J. *Academic Press, New York* **1983**, *2*, 411-490.
32. Sutherland, I. W. *Microbiological Sciences* **1986**, *3*, 5-9.
33. Rosalam, S.; England, R. *Enzyme and Microbial Technology* **2006**, *39*, 197-207.
34. Folkenberg, D. M.; Dejmek, P.; Skriver, A.; Ipsen, R. *Journal of Texture Studies* **2005**, *36*, 174-189.
35. Denadra, M. C. M.; Desaad, A. M. S. *International Journal of Food Microbiology* **1995**, *27*, 101-106.
36. Schiffrin, E. J.; Rochat, F.; Linkamster, H.; Aeschlimann, J. M.; Donnethughes, A. *Journal of Dairy Science* **1995**, *78*, 491-497.
37. Duenas, M.; Irastorza, A.; Fernandez, K.; Bilbao, A. *Journal of Food Protection* **1995**, *58*, 76-80.
38. Loesche, W. J. *Microbiological Reviews* **1986**, *50*, 353-380.
39. Rozen, R.; Bachrach, G.; Bronshteyn, M.; Gedalia, I.; Steinberg, D. *Fems Microbiology Letters* **2001**, *195*, 205-210.
40. Oliveira, D. R., Ed. *Biofilms - Science and Technology* 1st ed.; Kluwer Academic Publishers: Dordrecht, **1992**
41. Poulsen, L. V. *Food Science and Technology-Lebensmittel-Wissenschaft & Technologie* **1999**, *32*, 321-326.
42. Azeredo, J.; Oliveira, R. *Biofouling* **2000**, *16*, 17-27.
43. Laws, A.; Gu, Y.; Marshall, V. *Biotechnology Advances* **2001**, *19*, 597-625.
44. Kleerebezem, M.; van Kranenburg, R.; Tuinier, R.; Boels, I. C.; Zoon, P.; Looijesteijn, E.; Hugenholtz, J.; de Vos, W. M. *Antonie Van Leeuwenhoek International Journal of General and Molecular Microbiology* **1999**, *76*, 357-365.
45. Simoni, R. D.; Roseman, S. *Journal of Biological Chemistry* **1973**, *248*, 966-976.
46. Thompson, J.; Thomas, T. D. *Journal of Bacteriology* **1977**, *130*, 583-595.
47. Oba, T.; Doesburg, K. K.; Iwasaki, T.; Sikkema, J. *Archives of Microbiology* **1999**, *171*, 343-349.
48. Qian, N.; Stanley, G. A.; Bunte, A.; Radstrom, P. *Microbiology-Uk* **1997**, *143*, 855-865.
49. Welman, A. D.; Maddox, I. S. *Trends in Biotechnology* **2003**, *21*, 269-274.
50. Groot, M. N. N.; Kleerebezem, M. *Journal of Applied Microbiology* **2007**, *103*, 2645-2656.
51. Jolly, L.; Stingele, F. *International Dairy Journal* **2001**, *11*, 733-745.
52. De Vuyst, L.; De Vin, F.; Vaningelgem, F.; Degeest, B. *International Dairy Journal* **2001**, *11*, 687-707.
53. Mcgrath, B. C.; Osborn, M. J. *Journal of Bacteriology* **1991**, *173*, 3134-3137.
54. Liu, D.; Cole, R. A.; Reeves, P. R. *Journal of Bacteriology* **1996**, *178*, 2102-2107.

55. Sutherland, I. W. *International Dairy Journal* **2001**, *11*, 663-674.
56. Cerning, J.; Bouillanne, C.; Landon, M.; Desmazeaud, M. *Journal of Dairy Science* **1992**, *75*, 692-699.
57. Grobben, G. J.; Sikkema, J.; Smith, M. R.; Debont, J. A. M. *Journal of Applied Bacteriology* **1995**, *79*, 103-107.
58. Grobben, G. J.; vanCasteren, W. H. M.; Schols, H. A.; Oosterveld, A.; Sala, G.; Smith, M. R.; Sikkema, J.; deBont, J. A. M. *Applied Microbiology and Biotechnology* **1997**, *48*, 516-521.
59. Marshall, V. M.; Cowie, E. N.; Moreton, R. S. *Journal of Dairy Research* **1995**, *62*, 621-628.
60. Degeest, B.; de Vuyst, L. *Applied and Environmental Microbiology* **1999**, *65*, 2863-2870.
61. Low, D.; Ahlgren, J. A.; Horne, D.; McMahon, D. J.; Oberg, C. J.; Broadbent, J. R. *Applied and Environmental Microbiology* **1998**, *64*, 2147-2151.
62. Ai, L. Z.; Zhang, H.; Guo, B. H.; Chen, W.; Wu, Z. J.; Wu, Y. *Carbohydrate Polymers* **2008**, *74*, 353-357.
63. Looijesteijn, P. J.; Hugenholtz, J. *Journal of Bioscience and Bioengineering* **1999**, *88*, 178-182.
64. De Vuyst, L.; Vanderveken, F.; Van de Ven, S.; Degeest, B. *Journal of Applied Microbiology* **1998**, *84*, 1059-1068.
65. Kimmel, S. A.; Roberts, R. F.; Ziegler, G. R. *Applied and Environmental Microbiology* **1998**, *64*, 659-664.
66. Gamar-Nourani, L.; Blondeau, K.; Simonet, J. W. *Journal of Applied Microbiology* **1998**, *85*, 664-672.
67. Dupont, I.; Roy, D.; Lapointe, G. *Journal of Industrial Microbiology & Biotechnology* **2000**, *24*, 251-255.
68. Gasse, M. A.; Sims, K. A.; Frank, J. F. *Food Science and Technology-Lebensmittel-Wissenschaft & Technologie* **1997**, *30*, 273-278.
69. Petry, S.; Furlan, S.; Crepeau, M. J.; Cerning, J.; Desmazeaud, M. *Applied and Environmental Microbiology* **2000**, *66*, 3427-3431.
70. Pham, P. L.; Dupont, I.; Roy, D.; Lapointe, G.; Cerning, J. *Applied and Environmental Microbiology* **2000**, *66*, 2302-2310.
71. Dunn, H., University of Huddersfield, **2002**
72. Elvin, M., University of Huddersfield, **2001**
73. Lin, T. Y.; Chang Chien, M. F. *Food Chemistry* **2007**, *100*, 1419-1423.
74. Vincent, S. J. F.; Faber, E. J.; Neeser, J. R.; Stingle, F.; Kamerling, J. P. *Glycobiology* **2001**, *11*, 131-139.
75. Lemoine, J.; Chirat, F.; Wieruszkeski, J. M.; Strecker, G.; Favre, N.; Neeser, J. R. *Applied and Environmental Microbiology* **1997**, *63*, 3512-3518.
76. Gruter, M.; Leeflang, B. R.; Kuiper, J.; Kamerling, J. P.; Vliegthart, J. F. G. *Carbohydrate Research* **1993**, *239*, 209-226.
77. Shihata, A.; Shah, N. P. *International Dairy Journal* **2002**, *12*, 765-772.
78. Harding, L. P.; Marshall, V. M.; Hernandez, Y.; Gu, Y. C.; Maqsood, M.; McLay, N.; Laws, A. P. *Carbohydrate Research* **2005**, *340*, 1107-1111.

79. Rodriguez-Carvajal, M. A.; Sanchez, J. I.; Campelo, A. B.; Martinez, B.; Rodriguez, A.; Gil-Serrano, A. M. *Carbohydrate Research* **2008**, *343*, 3066-3070.
80. Doco, T.; Wieruszkeski, J. M.; Fournet, B.; Carcano, D.; Ramos, P.; Loones, A. *Carbohydrate Research* **1990**, *198*, 313-321.
81. Gerwig, G. J.; Kamerling, J. P.; Vliegenthart, J. F. G. *Carbohydrate Research* **1978**, *62*, 349-357.
82. Fox, A.; Morgan, S. L.; Hudson, J. R.; Zhu, Z. T.; Lau, P. Y. *Journal of Chromatography* **1983**, *256*, 429-438.
83. Biermann, C. J.; McGinnis, G. D., Eds. *Analysis of Carbohydrates by GLC and MS*, 1st ed.; CRC Press Inc., **1989**
84. Cataldi, T. R. I.; Campa, C.; Angelotti, M.; Bufo, S. A. *Journal of Chromatography A* **1999**, *855*, 539-550.
85. Panagiotopoulos, C.; Sempere, R.; Lafont, R.; Kerherve, P. *Journal of Chromatography A* **2001**, *920*, 13-22.
86. Paulus, A.; Klockow, A. *Journal of Chromatography A* **1996**, *720*, 353-376.
87. S. Hofstetter-Kuhn, S.; A. Paulus, A.; Gassmann, E.; Widmer, H. M. *Anal. Chem.* **1991**, *63*, 1541-1547.
88. Dawber, J. G.; Hardy, G. E. *Journal of the Chemical Society-Faraday Transactions I* **1984**, *80*, 2467-2478.
89. Boseken, J. *Advance Carbohydrate Chemistry* **1949**, *4*, 189-210.
90. Xiao, S.; Chen-Xu, D.; Ling-Jun, L.; You-Ruia, S.; Zhi-Weib, S.; Jin-Mao, Y. *Chinese Journal of Analytical Chemistry* **2008**, *36*, 280-284
91. Stellner, K.; Saito, H.; Hakomori, S. I. *Archives of Biochemistry and Biophysics* **1973**, *155*, 464-472.
92. Hakomori, S. *J. Biochem (Tokyo)* **1964**, *55*, 205-208.
93. Ciucanu, I.; Kerek, F. *Carbohydrate Research* **1984**, *131*, 209-217.
94. Ciucanu, I.; Caprita, R. *Analytica Chimica Acta* **2007**, *585*, 81-85.
95. Kohno, M.; Suzuki, S.; Kanaya, T.; Yoshino, T.; Matsuura, Y.; Asada, M.; Kitamura, S. *Carbohydrate Polymers* **2009**, *77*, 351-357.
96. Tuting, W.; Adden, R.; Mischnick, P. *International Journal of Mass Spectrometry* **2004**, *232*, 107-115.
97. Adden, R.; Mischnick, P. *International Journal of Mass Spectrometry* **2005**, *242*, 63-73.
98. Ciucanu, I. *Analytica Chimica Acta* **2006**, *576*, 147-155.
99. Purdie, T.; Irvine, J. C. *J. Chem. Soc* **1903**, *83*, 1021-1037.
100. Purdie, T.; Irvine, J. C. *J. Chem. Soc* **1904**, *83*, 1049-1070.
101. R. Kuhn, R.; Trischmann, H. *Chem. Ber.* **1963**, *96*, 284-287.
102. Denham, W. S.; Woodhouse, H. *J. Chem. Soc* **1913**, *103*, 1735-1741.
103. Leeflang, B. R.; Faber, E. J.; Erbel, P.; Vliegenthart, J. F. G. *Journal of Biotechnology* **2000**, *77*, 115-122.
104. Harding, L. P.; Marshall, V. M.; Elvin, M.; Gu, Y. C.; Laws, A. P. *Carbohydrate Research* **2003**, *338*, 61-67.

105. Maina, N. H.; Tenkanen, M.; Maaheimo, H.; Juvonen, R.; Virkki, L. *Carbohydrate Research* **2008**, *343*, 1446-1455.
106. Tafazzoli, M.; Grhiasi, M. *Carbohydrate Research* **2007**, *342*, 2086-2096.
107. Bubb, W. A. *Nippon Nogeikagaku Kaishi-Journal of the Japan Society for Bioscience Biotechnology and Agrochemistry* **1998**, *72*, 549-554.
108. Ricker, R. D.; Sandoval, L. A. *Journal of Chromatography A* **1996**, *743*, 43-50.
109. Barth, H. G.; Boyes, B. E.; Jackson, C. *Analytical Chemistry* **1994**, *66*, R595-R620.
110. Wyatt, P. J. *Analytica Chimica Acta* **1993**, *272*, 1-40.
111. Fishman, M. L.; Cescutti, P.; Fett, W. F.; Osman, S. F.; Hoagland, P. D.; Chau, H. K. *Carbohydrate Polymers* **1997**, *32*, 213-221.
112. Hwang, H. J.; Kim, S. W.; Xu, C. P.; Choi, J. W.; Yun, J. W. *Journal of Applied Microbiology* **2003**, *94*, 708-719.
113. Ayala-Hernandez, I.; Goff, H. D.; Corredig, M. *Journal of Dairy Science* **2008**, *91*, 2583-2590.
114. Harding, S. E. *Carbohydrate Research* **2005**, *340*, 811-826.
115. Theisen, C.; Johann, C.; Deacon, M. P.; Harding, S. E., Eds. *Refractive Increment Data Book for Polymer and Biomolecular Scientists*, 1st ed.; Nottingham University Press, **2000**
116. Andersson, M.; Wittgren, B.; Wahlund, K. G. *Analytical Chemistry* **2003**, *75*, 4279-4291.
117. Svedberg, T.; Nichols, J. B. *J. Am. Chem. Soc.* **1923**, *45*, 943-954.
118. Harding, S. E. *Carbohydrate Polymers* **1995**, *28*, 227-237.
119. Marshall, V. M.; Rawson, H. L. *International Journal of Food Science and Technology* **1999**, *34*, 137-143.
120. Tuinier, R.; van Casteren, W. H. M.; Looijesteijn, P. J.; Schols, H. A.; Voragen, A. G. J.; Zoon, P. *Biopolymers* **2001**, *59*, 160-166.
121. Ruas-Madiedo, P.; Tuinier, R.; Kanning, M.; Zoon, P. *International Dairy Journal* **2002**, *12*, 689-695.
122. Sutherland, I. W. *Microbiology-Uk* **2001**, *147*, 3-9.
123. Petry, S.; Furlan, S.; Waghorne, E.; Saulnier, L.; Cerning, J.; Maguin, E. *Fems Microbiology Letters* **2003**, *221*, 285-291.
124. Lovitt, R. W.; Jones, M.; Collins, S. E.; Coss, G. M.; Yau, C. P.; Attouch, C. *Process Biochemistry* **2000**, *36*, 415-421.
125. Middelberg, A. P. J. *Biotechnology Advances* **1995**, *13*, 491-551.
126. Czechowska-Biskup, R.; Rokita, B.; Lotfy, S.; Ulanski, P.; Rosiak, J. M. *Carbohydrate Polymers* **2005**, *60*, 175-184.
127. Camino, N. A.; Perez, O. E.; Pilosof, A. M. R. *Food Colloids 2008 Conference* **2008**, *23*, 1089-1095.
128. Drimalova, E.; Velebny, V.; Sasinkova, V.; Hromadkova, Z.; Ebringerova, A. *Carbohydrate Polymers* **2005**, *61*, 420-426.
129. Bezakova, Z.; Hermannova, M.; Drimalova, E.; Malovikova, A.; Ebringerova, A.; Velebny, V. *Carbohydrate Polymers* **2008**, *73*, 640-646.
130. Rinaudo, M.; Milas, M. *International Journal of Biological Macromolecules* **1980**, *2*, 45-48.
131. Sutherland, I. W. *Carbohydrate Research* **1984**, *131*, 93-104.

132. van Casteren, W. H. M.; de Waard, P.; Dijkema, C.; Schols, H. A.; Voragen, A. G. J. *Carbohydrate Research* **2000**, *327*, 411-422.
133. Nankai, H.; Hashimoto, W.; Miki, H.; Kawai, S.; Murata, K. *Applied and Environmental Microbiology* **1999**, *65*, 2520-2526.
134. Jansson, P. E.; Lindberg, J.; Wimalasiri, K. M. S.; Dankert, M. A. *Carbohydrate Research* **1993**, *245*, 303-310.
135. Sato, S.; Sakamoto, T.; Miyazawa, E.; Kikugawa, Y. *Tetrahedron* **2004**, *60*, 7899-7906.
136. Broberg, A. *Carbohydrate Research* **2007**, *342*, 1462-1469.
137. Maslen, S. L.; Goubet, F.; Adam, A.; Dupree, P.; Stephens, E. *Carbohydrate Research* **2007**, *342*, 724-735.
138. Suzuki, S.; Fujimori, T.; Yodoshi, M. *Analytical Biochemistry* **2006**, *354*, 94-103.
139. Hoffstetterkuhn, S.; Paulus, A.; Gassmann, E.; Widmer, H. M. *Analytical Chemistry* **1991**, *63*, 1541-1547.
140. Oshea, T. J.; Lunte, S. M.; Lacourse, W. R. *Analytical Chemistry* **1993**, *65*, 948-951.
141. Bruno, A. E.; Krattiger, B.; Maystre, F.; Widmer, H. M. *Analytical Chemistry* **1991**, *63*, 2689-2697.
142. Schwaiger, H.; Oefner, P. J.; Huber, C.; Grill, E.; Bonn, G. K. *Electrophoresis* **1994**, *15*, 941-952.
143. Park, Y. M.; Lebrilla, C. B. *Mass Spectrometry Reviews* **2005**, *24*, 232-264.
144. Anumula, K. R.; Dhume, S. T. *Glycobiology* **1998**, *8*, 685-694.
145. Broberg, A. *Carbohydrate Research* **2007**, *342*, 1462-1469.
146. Stinglele, F.; Neeser, J. R.; Mollet, B. *Journal of Bacteriology* **1996**, *178*, 1680-1690.
147. Navarini, L.; Abatangelo, A.; Bertocchi, C.; Conti, E.; Bosco, M.; Picotti, F. *International Journal of Biological Macromolecules* **2001**, *28*, 219-226.
148. Faber, E. J.; van den Haak, M. J.; Kamerling, J. P.; Vliegthart, J. F. G. *Carbohydrate Research* **2001**, *331*, 173-182.
149. Bubb, W. A.; Urashima, T.; Fujiwara, R.; Shinnai, T.; Ariga, H. *Carbohydrate Research* **1997**, *301*, 41-50.
150. Faber, E. J.; Zoon, P.; Kamerling, J. P.; Vliegthart, J. F. G. *Carbohydrate Research* **1998**, *310*, 269-276.
151. Marshall, V. M.; Dunn, H.; Elvin, M.; McLay, N.; Gu, Y.; Laws, A. P. *Carbohydrate Research* **2001**, *331*, 413-422.
152. Robijn, G. W.; Gallego, R. G.; vandenBerg, D. J. C.; Haas, H.; Kamerling, J. P.; Vliegthart, J. F. G. *Carbohydrate Research* **1996**, *288*, 203-218.
153. Robijn, G. W.; Wienk, H. L. J.; vandenBerg, D. J. C.; Haas, H.; Kamerling, J. P.; Vliegthart, J. F. G. *Carbohydrate Research* **1996**, *285*, 129-139.
154. Van Calsteren, M. R., Ed. *Book of Abstracts: First International Symposium on Lactic Acid Bacteria*, 1st ed.: Brussels, **2001**
155. Faber, E. J.; Kamerling, J. P.; Vliegthart, J. F. G. *Carbohydrate Research* **2001**, *331*, 183-194.

156. Robijn, G. W.; Vandenberg, D. J. C.; Haas, H.; Kamerling, J. P.; Vliegthart, J. F. G. *Carbohydrate Research* **1995**, *276*, 117-136.
157. Vanhaverbeke, C.; Bosso, C.; Colin-Morel, P.; Gey, C.; Gamar-Nourani, L.; Blondeau, K.; Simonet, J. M.; Heyraud, A. *Carbohydrate Research* **1998**, *314*, 211-220.
158. Landersjo, C.; Yang, Z.; Huttunen, E.; Widmalm, G., Eds. *Book of Abstracts: First International Symposium on Lactic Acid Bacteria*: Brussels, **2001**
159. Yamamoto, Y.; Nunome, T.; Yamauchi, R.; Kato, K.; Sone, Y. *Carbohydrate Research* **1995**, *275*, 319-332.
160. Stingle, F.; Lemoine, J.; Neeser, J. R. *Carbohydrate Research* **1997**, *302*, 197-202.
161. Yamamoto, Y.; Murosaki, S.; Yamauchi, R.; Kato, K.; Sone, Y. *Carbohydrate Research* **1994**, *261*, 67-78.
162. Staaf, M.; Widmalm, G.; Yang, Z.; Huttunen, E. *Carbohydr Res* **1996**, *291*, 155-64.
163. Staaf, M.; Yang, Z. N.; Huttunen, E.; Widmalm, G. *Carbohydrate Research* **2000**, *326*, 113-119.
164. Robijn, G. W.; Thomas, J. R.; Haas, H.; Vandenberg, D. J. C.; Kamerling, J. P.; Vliegthart, J. F. G. *Carbohydrate Research* **1995**, *276*, 137-154.
165. Yang, Z. N.; Staaf, M.; Huttunen, E.; Widmalm, G. *Carbohydrate Research* **2000**, *329*, 465-469.
166. Nakajima, H.; Hirota, T.; Toba, T.; Itoh, T.; Adachi, S. *Carbohydrate Research* **1992**, *224*, 245-253.
167. van Casteren, W. H. M.; Dijkema, C.; Schols, H. A.; Beldman, G.; Voragen, A. G. J. *Carbohydrate Polymers* **1998**, *37*, 123-130.
168. Yang, Z. N.; Huttunen, E.; Staaf, M.; Widmalm, G.; Tenhu, H. *International Dairy Journal* **1999**, *9*, 631-638.
169. Gruter, M.; Leeflang, B. R.; Kuiper, J.; Kamerling, J. P.; Vliegthart, J. F. G. *Carbohydrate Research* **1992**, *231*, 273-291.
170. van Casteren, W. H. M.; Dijkema, C.; Schols, H. A.; Beldman, G.; Voragen, A. G. J. *Carbohydrate Research* **2000**, *324*, 170-181.
171. Jones, D.; Pell, P. A.; Sneath, P. H. A. *London Academic Press Inc* **1984**, 35-40.
172. de Man, J. *Antonie Van Leeuwenhoek* **1960**, *26*, 77-80.
173. Messer, J. W.; Rice, E. W.; Johnson, C. H. *Encyclopedia of Food Microbiology* **2004**, 2154-2158.
174. Garciagaribay, M.; Marshall, V. M. E. *Journal of Applied Bacteriology* **1991**, *70*, 325-328.
175. Dobois, M.; Gilles, K. A.; Hamilton, J. K.; Rebers, P. A.; Smith, F. *Analytical Chemistry* **1956**, *28*, 350-356.
176. Bradford, M. M. *Analytical Biochemistry* **1976**, *72*, 248-254.
177. Laws, A. P.; Chadha, M. J.; Chacon-Romero, M.; Marshall, V. M.; Maqsood, M. *Carbohydrate Research* **2008**, *343*, 301-307.
178. Shankar, P. N.; Kumar, M. *Proceedings of the Royal Society of London Series a-Mathematical Physical and Engineering Sciences* **1994**, *444*, 573-581.
179. Paradossi, G.; Chiessi, E.; Barbiroli, A.; Fessas, D. *Biomacromolecules* **2002**, *3*, 498-504.

180. van Kranenburg, R.; Kleerebezem, M.; de Vos, W. M. *Plasmid* **2000**, *43*, 130-136.
181. Cerning, J. *Fems Microbiology Reviews* **1990**, *87*, 113-130.
182. Chacon-Romero, M., University of Huddersfield, 2005.
183. Tuinier, R.; Zoon, P.; Olieman, C.; Stuart, M. A. C.; Fleer, G. J.; de Kruif, C. G. *Biopolymers* **1999**, *49*, 1-9.
184. Zor, T.; Seliger, Z. *Analytical Biochemistry* **1996**, *236*, 302-308.
185. Dinter, C.; Schuetz, A.; Blume, T.; Weinmann, H.; Harre, M.; Neh, H. *Journal of the Association for Laboratory Automation* **2005**, *10*, 408-411.
186. Agrawal, P. K. *Phytochemistry* **1992**, *31*, 3307-3330.
187. Lazaridou, A.; Biliaderis, C. G.; Roukas, T.; Izydorczyk, M. *Applied Biochemistry and Biotechnology* **2002**, *97*, 1-22.
188. Meyer, M. V. *Journal of Chromatographic Science* **1995**, *33*, 26-33.
189. Shu, C. H.; Lung, M. Y. *Process Biochemistry* **2004**, *39*, 931-937.
190. Atlas, R. M., Ed. *Principles of Microbiology*, 1st ed.; Mosby - Year Book Inc: St. Louis, **1995**
191. Degeest, B.; Vaningelgem, F.; De Vuyst, L. *International Dairy Journal* **2001**, *11*, 747-757.
192. Vaningelgem, F.; Zamfir, M.; Adriany, T.; De Vuyst, L. *Journal of Applied Microbiology* **2004**, *97*, 1257-1273.
193. Knoshaug, E. P.; Ahlgren, J. A.; Trempy, J. E. *Journal of Dairy Science* **2000**, *83*, 633-640.
194. Laws, A. P.; Leivers, S.; Chacon-Romero, M.; Chadha, M. J. *International Dairy Journal* **2009**, In Press, Accepted Manuscript.
195. Yang, F. C.; Liau, C. B. *Process Biochemistry* **1998**, *33*, 547-553.
196. Harrington, R. E.; Zimm, B. H. *Journal of Physical Chemistry* **1965**, *69*, 161-175.
197. Frenkel, J. *Acta Physicochem. URSS* **1944**, *14*, 51-76.
198. Szu, S. C.; Zon, G.; Schneerson, R.; Robbins, J. B. *Carbohydrate Research* **1986**, *152*, 7-20.
199. Atkins, P.; de Paula, J., Eds. *Atkins' Physical Chemistry*, 8th ed.; Oxford University Press: Oxford, **2006**
200. Chen, R. H.; Chang, J. R.; Shyur, J. S. *Carbohydrate Research* **1997**, *299*, 287-294.
201. Pala, H.; Mota, M.; Gama, F. M. *Carbohydrate Polymers* **2007**, *68*, 101-108.
202. Gibbons, R. A.; Dixon, S. N.; Pocock, D. H. *Biochemical Journal* **1973**, *135*, 649-653.
203. Iida, Y.; Tuziuti, T.; Yasui, K.; Towata, A.; Kozuka, T. *Innovative Food Science & Emerging Technologies* **2008**, *9*, 140-146.
204. Fry, S. C. *Biochemical Journal* **1998**, *332*, 507-515.
205. Schweikert, C.; Liskay, A.; Schopfer, P. *Phytochemistry* **2000**, *53*, 565-570.
206. Nie, M.; Wang, Q.; Qiu, G. H. *Ultrasonics Sonochemistry* **2008**, *15*, 222-226.
207. Basedow, A. M.; Ebert, K. H. *Advances in Polymer Science* **1977**, *22*, 83-148.
208. Henglein, A.; Gutierrez, M. *Journal of Physical Chemistry* **1988**, *92*, 3705-3707.
209. Malhotra, S. L. *Journal of Macromolecular Science-Chemistry* **1982**, *A17*, 601-636.
210. Price, G. J.; West, P. J.; Smith, P. F. *Ultrasonics Sonochemistry* **1994**, *1*, S51-S57.
211. Friebolin, H., Ed. *Basic one- and two-dimensional NMR spectroscopy*, 4th ed.; Wiley-VCH: Weinheim, **2005**

212. Young; Lovell, Eds. *Introduction to polymers*; Nelson Thornes Ltd: Kingston-on-Thames, UK 1991.
213. Ma, X. D.; Pawlik, M. *Carbohydrate Polymers* **2007**, *70*, 15-24.
214. Morris, G. A.; de al Torre, J. G.; Ortega, A.; Castile, J.; Smith, A.; Harding, S. E. *Food Hydrocolloids* **2008**, *22*, 1435-1442.
215. Navarini, L.; Bertocchi, C.; Cesaro, A.; Lapasin, R.; Crescenzi, V. *Carbohydrate Polymers* **1990**, *12*, 169-187.
216. Casas, J. A.; Santos, V. E.; Garcia-Ochoa, F. *Enzyme and Microbial Technology* **2000**, *26*, 282-291.
217. Khouryieh, H. A.; Herald, T. J.; Aramouni, F.; Alavi, S. *Food Research International* **2007**, *40*, 883-893.
218. Domon, B.; Costello, C. E. *Glycoconjugate Journal* **1988**, *5*, 397-409.
219. Cheng, H. L.; Pai, P. J.; Her, G. R. *Journal of the American Society for Mass Spectrometry* **2007**, *18*, 248-259.
220. Reinhold, V. N.; Reinhold, B. B.; Costello, C. E. *Analytical Chemistry* **1995**, *67*, 1772-1784.
221. Reinhold, V. N.; Reinhold, B. B.; Chan, S. In *High Resolution Separation and Analysis of Biological Macromolecules, Pt B*; Academic Press Inc: San Diego, **1996**; pp. 377-402.
222. Commission, B. P., Ed. *British pharmacopoeia*; Stationery Office: London, **2009**
223. EMEA. EMEA: London, **1994**; p. 15.
224. Mischnick, P. *Abstracts of Papers of the American Chemical Society* **1996**, *212*, 44-Cell.
225. Mischnick, P.; Kuhn, G. *Carbohydrate Research* **1996**, *290*, 199-207.
226. Price, N. P. J. *Applied Biochemistry and Biotechnology* **2008**, *148*, 271-276.
227. Keller, B. O.; Suj, J.; Young, A. B.; Whittal, R. M. *Analytica Chimica Acta* **2008**, *627*, 71-81.

8. PUBLICATIONS